

Massive MIMO Based Smart Antenna Systems Design for 5G Wireless Networks

Thesis Submitted for the Award of the Degree of

DOCTOR OF PHILOSOPHY

in

Electronics & Communication Engineering

By

Suvarna Sengar

Registration Number: 41800200

Supervised By:

Dr. Praveen Kumar Malik (23314)

Embedded System domain (Professor)

Lovely Professional University (LPU),

Phagwara, Punjab.

Co-Supervised by:

Dr. Sudipta Das

**Electronics and Communication
Engineering (Associate Professor)**

**IMPS college of Engineering and
Technology**



LOVELY PROFESSIONAL UNIVERSITY, PUNJAB

2024

DECLARATION

I hereby declare that this research work “**Massive MIMO Based Smart Antenna Systems Design for 5G Wireless Networks**” has been composed solely by myself and has not been submitted anywhere. It was carried out by me for the degree of Doctor of Philosophy in Electrical Engineering under the guidance and supervision of **Prof. & Dr. Praveen Kumar Malik**, Lovely Professional University, Phagwara Punjab, India and under the co-supervision of **Dr. Sudipta Das**, Associate Professor-IMPS college of Engineering and Technology, West Bengal.

The interpretations put forth are based on my reading and understanding of the original texts and they are not published anywhere in the form of books, monographs or articles. The other books, articles and websites, which I have made use of are acknowledged at the respective place in the text.

I certify that

- The work contained in this thesis is original and has been done by me under the guidance of my supervisor (s).
- The work has not been submitted to any other Institute for the reward of any other degree or diploma.
- I have followed the guidelines provided by the Institute in preparing the thesis.
- Whenever I used materials (data, theoretical analysis, figures and text) from other sources, I have given due credit to them by citing them in the text of the thesis and giving their details in the references.

Date: 27/09/2024

Suverna Sengar (41800200)

CERTIFICATE

This is to certify that the thesis entitled “**Massive MIMO Based Smart Antenna Systems Design for 5G Wireless Networks**” being submitted by **Suvarna Sengar** for the degree of Doctor of Philosophy in Engineering from Lovely Professional University, Jalandhar is a record of bonafide research work carried out by her under my supervision at the School of Electrical and Electronics Engineering. In our opinion, this is an authentic piece of work for submission for the degree of Doctor of Philosophy. To the best of our knowledge, the work has not been submitted to any other University or Institute for the award of any degree or diploma.

Supervisor

Dr. Praveen Kumar Malik, Professor

School of Electrical and Electronics Engineering
Lovely Professional University, Phagwara,
Punjab-144111

E-mail id: praveen.23314@lpu.co.in

Phone No: +91-9719437711

Co-Supervisor



Dr. Sudipta Das, Associate Professor
Electronics and Communication
Engineering , IMPS college of Engineering
and Technology.

Email: Sudipta.das1985@gmail.com

Phone N0: +91-9647764962

ABSTRACT

In response to the increasing growth of user expectations in wireless communication applications, new criteria for developing single-layer or multi-layer integrated devices have emerged, with a significant emphasis on achieving higher compactness, low profiles, and cost-effectiveness, among other things. An antenna is required for wireless signal transmission because it converts electrical impulses to electromagnetic waves and serves as a transducer at both the transmitter and reception ends. Antenna miniaturization is critical for optimizing designs for handheld wireless communication devices, reducing overall circuit or board dimensions for RF (Radio Frequency) components, and meeting the growing demand for compact size while maintaining excellent gain and bandwidth characteristics. In this regard, microstrip patch antennas based on PCB technology have gained a lot of interest.

Furthermore, wireless devices such as phones, laptops, and tablets use a range of technologies such as ISM band, Bluetooth, Zigbee, Wi-Fi, Wi-MAX, GSM, and CDMA, among others. Typically, conventional antennas operate in a single frequency band. Nonetheless, there is currently a desire for multiband antennas that can resonate on different frequencies, eliminating the need for several antennas in a single device. In order to obtain high data transmission rates, it is important to meet the FCC's minimum band criteria for each wireless standard.

In this context, the Microstrip patch antenna has established itself as a reliable and trusted solution for wireless communication applications. Its lightweight nature, low-profile design, smooth integration with microwave circuits, and cost-effectiveness when

manufactured using Printed Circuit Board (PCB-technology) are all compatible with the needs of wireless communication devices. Nonetheless, certain constraints, like as gain and bandwidth, must be addressed.

Every wireless communication equipment in today's world must have attributes such as a high data rate, a large channel capacity, lots of bandwidth, good quality of service, enhanced reliability, and low power consumption. To meet these requirements, multiple input multiple output (MIMO) systems and ultra-wide band technology (UWB) are used. Multiple antennas at the reception and transmitter ends can help to prevent multipath fading. While building many antennas is not difficult in and of itself, strategically positioning them within tight places is the actual issue. Less sophisticated strategies, such as polarization, spatial, or pattern variety, can also be utilized to tackle the fading problem. Despite its relevance in MIMO design, mutual coupling issues develop when numerous antennas are contained in a compact region, decreasing the antenna's overall performance.

The primary goal of this work is to create a small MIMO antenna with high isolation. Originally, the design consisted of a single radiating element on the top side of the substrate and a partially grounded structure on the bottom. The design was later changed to include four orthogonal antennas on the top side of the substrate, which significantly improves isolation without the need of decoupling structures/networks or other isolation methods. Another motivation for employing orthogonal layouts is to improve the diversity of polarization. The design was further improved by using various isolation techniques, such as the use of an X-shaped decoupling device on top of the substrate

between the four antenna elements. This change was discovered to channel the current in a new direction, resulting in a considerable reduction in mutual coupling.

In the final step, a Modified-Ground Structure (MGS) was built to the bottom side to strengthen isolation even further. Each design was simulated with the HFSS simulator, and a prototype was constructed. A Vector Network Analyzer (VNA) was used to compare simulated to actual readings. The radiation properties were tested in an anechoic chamber (a device that prevents sound or electromagnetic wave reflections or echoes). Finally, the observed matching provides strong support for this endeavor. Based on the results, we may conclude that the design suits MIMO applications.

ACKNOWLEDGEMENT

I would like to express my heartfelt appreciation to the people and organizations that helped me finish this dissertation. First and foremost, I want to thank my supervisor and co-supervisor, Prof. Dr. Praveen Kumar Malik, and Dr. Sudipta Das, for providing me with the opportunity, support, and independence to conduct this research. Throughout the past four years, their consistent encouragement, valuable guidance, and steadfast mentorship have been instrumental in shaping both my growth as a researcher and as an individual. I especially admire their unwavering dedication to their students' education and success.

I am grateful to Lovely Professional University's Chancellor, Pro-Chancellor, Vice Chancellor, and successive Deans for their inspiration and support in my research endeavor, as well as for ensuring the provision of necessary infrastructure and resources. The School of Electrical and Electronics Engineering is especially grateful for their facilities. I am grateful for the collaborative support and timely guidance on norms and guidelines provided by the Head of the School, the School of Electronics and Communication Engineering, as well as the faculty, staff members, and the Lovely Professional University Research Department. I would like to express my gratitude to the IIT Delhi staff for their technical assistance in the CIER Departments of IIT-Delhi and IIT-Roorkee in India.

Last but not least, I want to express my gratitude to my husband Mr. Prashant Kumar, and my family and second special thanks to my colleague Mr. Mohommad Asif Iqbal for their love sacrifices, and moral support, without which this work would not have been possible. Thank you so much to "Shrihaan Chauhan," my son, for his patience and understanding.

CONTENTS

Declaration	II
Certificate	III
Abstract	IV
Acknowledgments	VII
Table of Contents	VIII
List of Figures	XII
List of Tables	XVI
Acronyms and Abbreviations	XVIII
List of Symbols	XXI

Table of Contents

CHAPTER-1	1-16
INTRODUCTION	1
1.1 INTRODUCTION TO 5G (5th -GENERATION)	2
1.2 INTRODUCTION TO UWB-MIMO TECHNOLOGY	4
1.2.1 Evolution of 5G Massive MIMO Antenna Technology	7
1.3 MIMO ANTENNA DIVERSITY PARAMETER	8
1.3.1 Envelope Correlation Coefficient (ECC)	8
1.3.2 Diversity Gain (DG)	9
1.3.3 Mean Effective Gain (MEG)	10
1.3.4 Channel Capacity Loss (CCL)	11
1.3.5 Total Active Reflection Coefficient-(TARC)	11
1.4 RESEARCH MOTIVATION	13
1.5 STATEMENT OF PROBLEM	13
1.6 SCOPE OF PRESENT WORK	13
1.7 RESEARCH OBJECTIVE	14
1.8 THESIS ORGANIZATION	14

1.9	SUMMARY	16
	CHAPTER-2	17-35
	LITERATURE REVIEW	17
2.1	INTRODUCTION	17
2.2	LITERATURE REVIEW ON SINGLE ELEMEMENT MICROSTRIP PATCH ANTENNA	18
2.3	LITERATURE REVIEW ON UWB MIMO ANTENNA	21
2.4	SUMMARY	35
	CHAPTER-3	36-55
	DESIGN A SINGLE ELEMENT UWB MICROSTRIP PATCH ANTENNA FOR 5G MILLIMETER WAVE APPLICATIONS	36
3.1	INTRODUCTION	36
3.2	ANTENNA DESIGN PROCEDURE AND METHODOLOGY	38
3.3	SOFTWARE USED FOR SIMULATION	45
	3.3.1 High Frequency Structure Simulator (Ansys HFSS)	45
	3.3.1.1 Structure Designing Process	46
	3.3.1.2 Antenna Design steps	47
3.4	ANETNNA SIMULATION RESULTS	47
3.5	PERFORMANCE COMPARISON	54
3.6	SUMMARY	55
	CHAPTER-4	56-82
	DESIGN ACOMPACT QUAD-PORT UWB MIMO ANTENNA FOR 5G MILLIMETER WAVE APPLICATIONS	56
4.1	INTRODUCTION	56
4.2	MOTIVATION FOR UWB ANTENNA DESIGN	59
4.3	DESIGN PROCEDURE FOR QUAD PORT MIMO ANTENNA	61
4.4	ANTENNA SIMULATION AND RESULTS	63
4.5	RADIATION PATTERN, GAIN, AND EFFICIENCY	67
4.6	ANTENNA MEASUREMENT RESULTS	74

4.7	ANALYSIS OF MIMO DIVERSITY PARAMETERS	77
4.7.1	ECC (Envelope Correlation Coefficient)	78
4.7.2	Diversity Gain (DG)	78
4.7.3	TARC (Total Active Reflection Coefficient)	79
4.8	SUMMARY	82
CHAPTER-5		83-112
DESIGN AND ANALYSIS OF MIMO ANTENNA WITH DIFFERENT ISOLATION TECHNIQUES		83
5.1	INTRODUCTION	83
5.2	ANTENNA GEOMETRY AND DESIGN	87
5.3	ISOLATION TECHNIQUES	87
5.3.1	Self-Isolation Techniques	88
5.3.2	Modified the Partially Ground Structure	91
5.3.3	Decoupling Structure	94
5.3.4	Defected Ground Structure	97
5.3.5	Hybrid Isolation Technique	100
5.3.5.1	Hybrid Model 1 (Decoupling technique + DGS)	100
5.3.5.2	Hybrid Model 2 (DGS + MGS)	103
5.3.5.3	Hybrid Model 3 (Decoupling + Defected Ground + Modified Ground)	105
5.4	MEASUREMENT RESULTS FOR COMBINED ISOLATION TECHNIQUE	108
5.5	SUMMARY	112
CHAPTER-6		113-138
RESULTS AND DISCUSSIONS		113
6.1	INTRODUCTION	113
6.2	ANTENNA DESIGN AND ANALYSIS	113
6.3	SIMULATED RESULTS AND DISCUSSIONS	118
6.4	MEASUREMENT RESULTS AND DISCUSSION	126

6.5	DIVERSITY PARAMETERS	130
6.5.1	Envelope correlation coefficient (ECC)	130
6.5.2	Diversity Gain (DG)	131
6.5.3	Mean effective gain (MEG)	132
6.5.4	Total Active Reflection Coefficient (TARC)	134
6.5.5	Channel Capacity Loss (CCL)	134
6.6	SUMMARY	138
	CHAPTER-7	139-142
	CONCLUSION AND FUTURE SCOPE	139
7.1	INTRODUCTION	139
7.2	FUTURE SCOPE	142
	Research Publications	144-145
	Bibliography	146-156

List of Figures

Figure 1.1 Shows the frequency bands for Microwave, Millimetre waves and Terahertz wave band	2
Figure 1.2 Shows the 5G different User Cases	3
Figure 1.3 Comparison power spectral density (PSD) of UWB system with other systems	5
Figure 1.4 General Outline of Multiple Input Multiple Output System	6
Figure 1.5 Evolution of 5G Massive MIMO Technology	7
Figure 3.1 Flow chart for designing steps of proposed UWB Antenna	40
Figure 3.2 Steps development procedure of the Single cell UWB Antenna	42
Figure 3.3 Simulated results in terms of Reflection coefficient (S11) (a) step wise (b) effect of ground plane (c) effect of substrate height and (d) effect of feed line for Capsule shaped Single element UWB antenna	44
Figure 3.4 Unit Cell UWB Antenna design with dimensions	44
Figure 3.5 Simulated reflection coefficient (S11) performance for Capsule shaped UWB antenna	48
Figure 3.6 VSWR vs. Frequency Plot for Capsule shaped UWB antenna	49
Figure 3.7 Simulated Gain vs. frequency performance of proposed UWB antenna	49
Figure 3.8 Simulated 2D Gain of the proposed UWB antenna at different frequencies (a) 24 GHz (b) 26 GHz (c) 28 GHz and (d) directivity plot at 27GHz	51
Figure 3.9 The radiation pattern Plot of the proposed UWB antenna in 3D (a) 24 GHz, (b) 26 GHz, and (c) 28 GHz	52
Figure 3.10 HFSS Simulation E-field and H-field current distribution of proposed antenna at 27GHz frequency	53
Figure 3.11 HFSS Simulation E-field and H-field vector current distribution of suggested antenna at 27GHz frequency	53
Figure 4.1 Mutual-coupling reduction/ Isolation enhancement techniques for 5G massive-	58

MIMO antennas	
Figure 4.2 Different shapes of planar UWB antennas	60
Figure 4.3 UWB PCB or printed antenna designs	60
Figure 4.4 Geometry of Quad-port UWB MIMO antenna	62
Figure 4.5 Quad port UWB MIMO antenna performance simulation for Reflection Coefficient (S_{11}) in dB	63
Figure 4.6 Simulated VSWR Plot for quad port UWB MIMO antenna	64
Figure 4.7 Simulated Isolation plots for quad port UWB MIMO antenna	66
Figure 4.8 Simulated Gain vs. frequency plot for quad port UWB MIMO antenna	67
Figure 4.9 Simulated gain for proposed quad port MIMO antenna's in 3D and 2D radiation pattern	69
Figure 4.10 3D and 2D Directivity Plot at 27 GHz frequency	70
Figure 4.11 Proposed quad port MIMO antenna's (a) E-field, (b) H-field, and (c) surface current distribution at 26 GHz	72
Figure 4.12: Simulated Total Gain plot at 27GHz for quad port UWB MIMO antenna	73
Figure 4.13 Photograph of fabricated capsule shaped 4 x 4 UWB-MIMO antennas: (a) Top and (b) Bottom views	74
Figure 4.14 Measured S-Parameter (S_{11}) Reflection coefficient in dB	75
Figure 4.15 Measured Isolation of MIMO antenna (S_{21}) in dB with Frequency	75
Figure 4.16 Measurement Setup for Reflection coefficient (S_{11} in dB) and Isolation (S_{12}) for Proposed MIMO antenna	76
Figure 4.17 MIMO antenna measurement setup inside an Anechoic Chamber	77
Figure 4.18 Envelope correlation coefficient (ECC) with frequency	78
Figure 4.19 Simulated Diversity Gain (DG) with frequency	79
Figure 4.20 Simulated Total Active Reflection Coefficient (TARC) with frequency	80
Figure 5.1 Self-Isolated MIMO antenna design (a) Top view & (b) Bottom view	88
Figure 5.2 Dimensions of Self-Isolated MIMO antenna	89
Figure 5.3 Simulation Results of self-isolated MIMO Antenna design: (a) Reflection	90

coefficient , (b) VSWR, (c) Gain, and (d) Isolation	
Figure 5.4 MIMO antenna with Modified Ground Structure (MGS): (a) Top view, (b) Bottom view	91
Figure 5.5 Simulation Results of quad port MIMO Antenna design with Modified Ground Structure (MGS): (a) Reflection coefficient , (b) VSWR, (c) Gain, and (d) Isolation	92
Figure 5.6 Simulation Results of quad port MIMO Antenna design with Modified Ground Structure (MGS): (a) Reflection coefficient , (b) VSWR, (c) Gain, and (d) Isolation	93
Figure 5.7 MIMO antenna with Decoupling structure (a)Top view (b) Bottom view	94
Figure 5.8 Dimensions of Quad Port MIMO antenna with decoupling (X-shaped wall) structure	95
Figure 5.9 Simulation Results of quad port MIMO Antenna design with introducing X- shaped decoupling structure: (a) Reflection coefficient , (b) VSWR, (c) Gain, and (d) Isolation	96
Figure 5.10 MIMO antenna with Defected Ground Structure (DGS): (a)Top view and (b) Bottom view	97
Figure 5.11 Dimensions of Quad Port MIMO antenna with Defected Ground Structure (DGS)	98
Figure 5.12 Simulation Results of quad port MIMO Antenna design with Defected Ground Structure (DGS): (a) Reflection coefficient , (b) VSWR, (c) Gain, and (d) Isolation	99
Figure 5.13 MIMO antenna with Hybrid Model 1 (a)Top view (b) Bottom view	100
Figure 5.14 Dimensions of Quad Port MIMO antenna with combination of Decoupling and Defected Ground Structure	101
Figure 5.15 Simulation Results of quad port MIMO Antenna design with hybrid model 1: (a) Reflection coefficient , (b) VSWR, (c) Gain, and (d) Isolation	102
Figure 5.16 MIMO antenna with Hybrid Model 2 (a)Top view (b) Bottom view	103
Figure 5.17 Simulation Results of quad port MIMO Antenna design with hybrid model 2: (a) Reflection coefficient , (b) VSWR, (c) Gain, and (d) Isolation	104
Figure 5.18 MIMO antenna with Hybrid Model 3 (a)Top view (b) Bottom view	105
Figure 5.19 Simulation Results of quad port MIMO Antenna design with hybrid model 3: (a) Reflection coefficient , (b) VSWR, (c) Gain, and (d) Isolation	106

Figure 5.20 Fabricated prototype (a) Top View (b) Bottom View	108
Figure 5.21 Measurement setup with VNA (a), and Anechoic Chamber (b)	109
Figure 5.22 Simulated and measured S11 in dB	109
Figure 5.23 Simulated and measured S12 in dB	110
Figure 6.1 The proposed antenna layout (a) Top View and (b) Bottom View	116
Figure 6.2 Dimensions of the proposed MIMO antenna with decoupling Structure	117
Figure 6.3 Simulated Reflection coefficient (S(1,1) dB) of the proposed antenna	119
Figure 6.4 Simulated VSWR Plot of the proposed antenna	119
Figure 6.5 Simulated Isolation between each Port	120
Figure 6.6 Different Gain plots for the proposed antenna	121
Figure 6.7 Total Efficiency in percentage(%) Verses gain plot	122
Figure 6.8 2D Gain, Directivity and Radiation Efficiency (E-Plane and H-Plane plots)	123
Figure 6.9 3D Gain and Directivity plots at 24 GHz, 26 GHz and 27 GHz frequencies	125
Figure 6.10 Surface Current Distribution of the proposed UWB MIMO antenna	125
Figure 6.11 Fabricated prototype (a) Top View (b) Bottom View	126
Figure 6.12 Measurement setup with VNA (a), (b)	127
Figure 6.13 Measurement setup inside anechoic chamber	127
Figure 6.14 Simulated and measured (a) Only S11 in dB and (b) Reflection coefficient (or reflection coefficient)	128
Figure 6.15 Simulated and measured isolation parameter	128
Figure 6.16 Measured Gain Plot in dBi	130
Figure 6.17 Simulated and measured ECC Plots	131
Figure 6.18 Simulated and measured DG Plots	132
Figure 6.19 Simulated MEG Plots	134
Figure 6.20 Simulated TARC and CCL Plots	134

List of Tables

Table 2.1 Some more Literature survey on single element antenna with different shape and design	20
Table 2.2 Comparison of various antenna Designs	25
Table 3.1 Dimensions of proposed capsule shaped UWB antenna	45
Table 3.2 A comparison between the suggested UWB antenna and earlier works	54
Table 4.1 UWB MIMO antenna geometrical specifications	62
Table 4.2 Reflection coefficient values at different frequencies	64
Table 4.3 VSWR values at different frequencies	65
Table 4.4 Isolation of all port at different frequencies	66
Table 4.5 Gain value at different frequencies	67
Table 4.6 The suggested UWB MIMO antenna simulation results in terms of S11, VSWR, Isolation and Gain	67
Table 4.7 Comparisons with other MIMO Antennas	80
Table 5.1 State of the Art comparison with Isolation Techniques	85
Table 5.2 Optimal values of the self-isolated MIMO antenna dimensions (all in mm)	89
Table 5.3 Optimal values of the proposed antenna dimensions for MGS (all in mm)	92
Table 5.4 Optimal values of the proposed antenna dimensions for Decoupling structure (all in mm)	95
Table 5.5 Optimal values of the proposed antenna dimensions for DGS (all in mm)	98

Table 5.6 Optimal values of the proposed antenna dimensions for DGS (all in mm)	101
Table 5.7 Comparison table of all simulated results for Isolation Techniques	107
Table 5.8 Comparison table of existing work with proposed work	111
Table 6.1 Optimal values of the proposed antenna dimensions (all in mm)	117
Table 6.2 The performance comparison in relation to prior studies published literature	135

Acronyms and Abbreviations

Acronyms	Description
2D	Two Dimensional
2G	2nd Generation
3D	Three Dimensional
3GPP	3 rd Generation Partnership Project
4G	4 th generation
5G	5 th generation
AF	Audio Frequency
AR	Axial Ratio
ARBW	Axial Ratio Bandwidth
AUT	Antenna Under Test
BPF	Band Pass Filter
BW	Bandwidth
CP	Circular Polarization
CPW	Coplanar Waveguide
CST	Computer Simulation Technology
DGS	Defected Ground Structures
DUT	Device Under Test
EBG	Electromagnetic Band gap
ETSI	European Telecommunications Standards Institute
FDGS	Fractal Defected Ground Structure
FHSS	Frequency Hopping Spread Spectrum
FR4	Flame Retardant 4

GPA	Ground plane aperture
GPS	Global Positioning System
GSM	Global System for Mobile
GUI	Graphical User Interface
HA	Hybrid Antenna
HFSS	High Frequency Structure Simulator
HIPERMAN	High Performance Radio Metropolitan Area Network
HPBW	Half Power Beam Width
IE3D	Integral Equation Three-Dimensional
IEEE	Institute of Electrical and Electronics Engineers
IFS	Iterated Function System
IoT	Internet of Things
ISM	Industrial Scientific and Medical
LTE	Long Term Evolution
M2M	Machine 2 Machine
MAC	Media Access Control
MIMO	Multiple input Multiple Output
MM	Metamaterial
MPA	Microstrip Patch Antenna
MS	Meta Surface
MTA	Microwave Transition Analyzer
PCB	Printed Circuit Board
PIFA	Planar Inverted F-Antenna
PMPA	Planer Microstrip Patch Antenna
RADAR	Radio Detection and Ranging

RCR	Cherenkov radiation
RF	Radio frequency
RFID	Radio Frequency Identification
RHCP	Right-Hand Circular Polarized
RL	Reflection coefficient
SRR	Split Ring Resonator
TL	Total Loss
TV	Television
UHF	Ultra-High Frequency
UMTS	Universal Mobile Telecommunications System
VNA	Vector Network Analyzer
VSWR	Voltage Standing Wave Ratio
Wi-Fi	Wireless Fidelity
Wi-Max	Worldwide Interoperability for Microwave Access
WLAN	Wireless Local Area Network

List of Symbols

Symbol	Description
H	Efficiency
Γ	reflection coefficient
ϵ_r	relative permittivity
$\tan \delta$	loss tangent
λ	Wavelength
c	speed of light
f_r	resonating frequency
Z_0	Characteristics Impedance
λ_g	Guided Wave length

CHAPTER-1

INTRODUCTION

1.1. INTRODUCTION TO 5G (5th -GENERATION)

As the world's population grows by the day, hence now a day's there is a high traffic demands which is being faced by communication networks. To overcome this, network of cellular system are being installed in short range distance i.e., a few hundred of meter and also almost everywhere there is installation of WLAN i.e., wireless local area networks. As the mobile based broadband services have increased/increasing hence new technologies like IOT i.e., internet of things and M2M i.e., machine to machine communication are further adding up for increasing the wireless traffic. Further, as the cellular base services are getting deployed globally, the mobile phone users are able to use the cellular data enormously for supporting their day to day tasks like video calling, playing online games, social medial platform and sharing contents and information. Hence, there is a requirement of the new era of networks communication which is intended to offer lower latency, high data rate, ultra high speed and reliability [1]. Furthermore, to obtain the desired area throughput, the main problem with the evolution of the wireless network is depending either on increasing bandwidth (spectrum) or on densifying the cells and soon these schemes are going to be saturated very soon along with increasing cost of the hardware and with high latency. Further, there is another factor which is having high possibilities for improving the area throughput is the spectral efficiency which is still untouched and less explored during the fast evaluation of the wireless network. Hence there is a need of an efficient wireless access technology which is going to increase the area throughput of wireless network without densifying the cells or increasing the bandwidth so as to achieve the on-going requirement.

Therefore scientists and engineers are working on 5G network communication to meet the demand. To full fill the requirement of 5G wireless communication system, there is a need of different frequency bands with specific properties to be embedded. For the bands having low frequency, obtainability of spectrum-resources is less. But availability of wealthy spectrum-

resources can be fulfilled in the millimeter wave frequency bands i.e., mm-Wave frequency bands which is having a huge possibility for data transmission at high rate.

That's why, to meet the demand of 5G and future communication networks, MIMO (Multiple-input Multiple-output technology promises to revolutionize wireless network communication. For improving the area throughput and spectral efficiency, MIMO utilize larger number of antennas. MIMO is having potential for bringing antennas, radios and spectrum together so as to achieve high capacity along with high speed for the 5G technology [2]. Moreover, scope of using massive MIMO so as to increase the area throughput along with efficiency of spectra has designated it, a significant tool for the upcoming wireless standards [3] so as to achieve considerable array gain by utilizing large amount of antennas together [4].

Presently, the 5G-spectrum may subdivided into sub-6GHz and mm-Wave frequency bands. The millimeter waves are waves having frequencies b/w 30-GHz to 300-GHz and are called millimeter-waves as their lengths changes in between 1mm to 10mm as compared to the radio waves having length tens of centimeters and which are being used currently for mobile communication network. Further, frequency beyond M-wave frequency band i.e., from 300GHz to 3 THz abbreviated as Terahertz frequency band. Figure 1.1 shows the frequency band for microwave, millimeter wave and terahertz band.

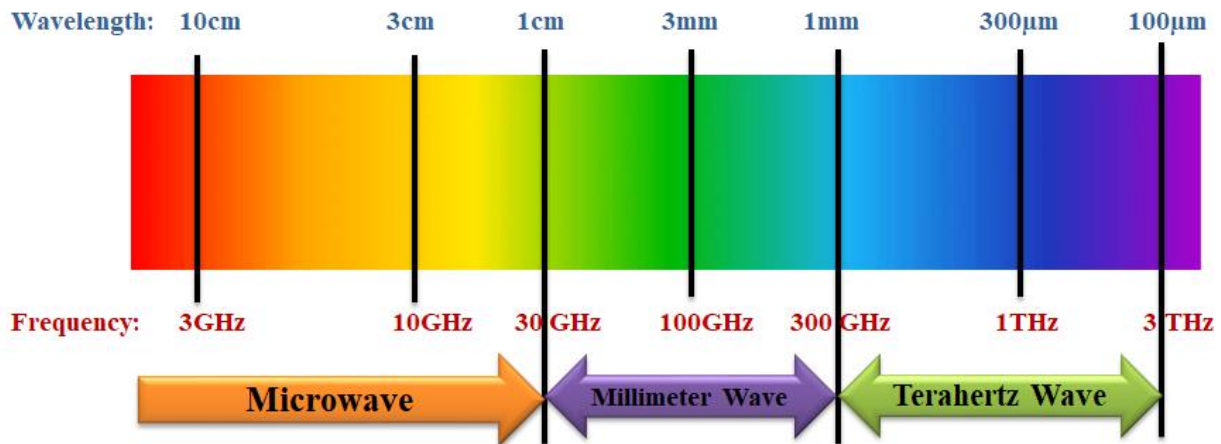


Figure1.1: Shows the frequency bands for Microwave, Millimetre waves and Terahertz wave band [5]

For upcoming 5G technologies in the frequency spectrum of 3400-3600MHz, World Radio Communication Conference in 2015 has initiated the research on the MIMO technology. MIMO technology allows for a linear increase in channel capacity by growing the number of transmitter and receiver antennas. It is also critical to improve the frequency spectrum and transmitted power. However, the integration of multiple antennas for multiple functions in a smart device is required, limiting the available space for a practical 5G MIMO array. As a result, addressing the required isolation and envelope correlation coefficient (ECC) within these confined spaces is a difficult task.

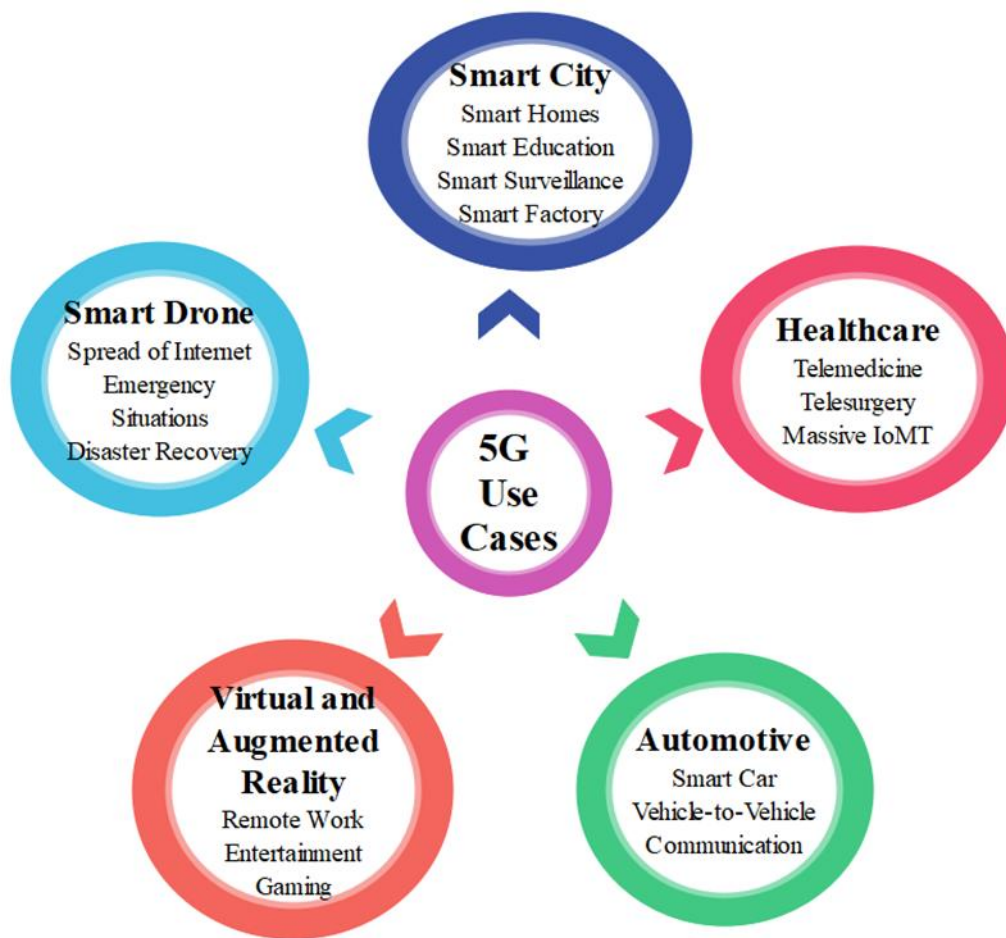


Figure 1.2: Shows the 5G different User Cases [5]

MIMO is a requirement for networks like 5G as it is the primary air interface for 5G and 4G broadband distant communications. Over the last few years, there has been an enormous rise in the amount of remote devices and adaptive users.

1.2. INTRODUCTION TO UWB-MIMO TECHNOLOGY

5G is a digital cellular network technology that is in its fifth generation. The 5G frequency spectrum is divided into three main bands. Millimetre waves, which range in frequency from 24 to 40 GHz, have the highest speed but a smaller coverage area. The mid band, also known as the sub-6 GHz band, operates between 1 GHz to 6 GHz frequencies. The low-band (less than 1 GHz) has a wider coverage but slower speeds [6-7]. The rapid expansion of 5G technology necessitates antennas with a continuous radiation pattern, low path loss, and low latency, all of which are required to meet fundamental technological requirements. The 5G UWB microstrip patch antenna's improved performance is expected to benefit the next generation of wireless communication systems. Faster transmission rates, increased reliability, very high data rates, improved spectral efficiency, reduced latency, and the ability to connect more wireless devices to networks are among the key benefits of 5G technology. The 5G UWB microstrip patch antenna is set to be a game changer, increasing capacity while increasing spectral efficiency by 50 times over a standard antenna [8].

Microstrip patch antennas can now meet the majority of requirements. It is made up of a dielectric substrate, a patch-connected feed, a radiating patch, and a metallic ground [9]. Microstrip patch antennas are small and low-profile, but they have a narrow bandwidth, low Reflection coefficient, and poor strength, among other drawbacks [10]. Current criteria for portable system antenna designs call for size reduction without sacrificing performance.

The wireless sector has shown keen interest in Ultra-wide band (UWB) technology ever since the United State FCC (Federal Communication Commission) authorized the profit-oriented utilization of unlicensed frequencies spanning from 3.1 to 10.6 GHz in 2002. [11]. The Ultra-wide band communication systems provide a number of advantages, including high precision, low cost, low complexity, fast data rate, and great power efficiency [12]. Nonetheless, multipath fading effects occur in these systems due to signal reflection and diffraction [13]. The most likely technology for high-speed, short-range indoor data transmission is ultra-wide band (UWB). Figure 1.3 compares the power spectrum density of UWB systems to that of all other radio communication technologies.

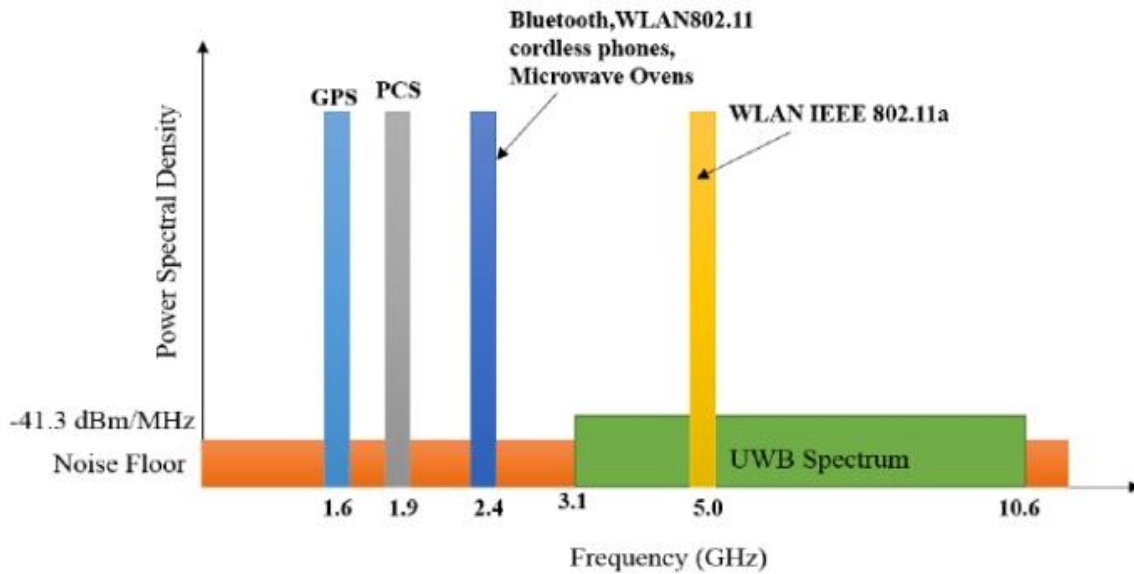


Figure 1.3: Comparison power spectral density (PSD) of UWB system with other systems [13]

Generally speaking, UWB antennas should be small and reasonably priced while still offering suitable wide-band performance for a range of industrial applications [14]. Determining the optimal bandwidth, efficiency, and low profile within the restricted dimensions is thus a major challenge in the design of UWB antennas. To improve the properties of UWB antennas, the geometry of the radiating patch can be altered. The patch can be whatever shape you choose, including heart-shaped, rectangular, elliptical, and spherical.

In single antenna system multipath fading and co-channel interference are the common issue. This can be reduced by associating MIMO technology, because of placing multiple numbers of antenna elements on receiver and transmitter side as depicted in Figure 1.4. The data rates, channel capacity and coverage area are very well enhanced, just by adding MIMO system. The good thing about MIMO is that it can provide all said points without any additional increment in power and frequency spectrum. Depending upon the arrangement of antenna in transmitter and receiver side, usually there are four types of configuration possible. In conventional radio communication system, single antenna present on both transmitter and receiver side which is commonly known as single input single output (SISO) configuration. This configuration is very simple and does not require any additional processing. But SISO system has more chances of receiving interference and fading with limited amount of bandwidth. In the Multiple-Input and

Single-Output (MISO) setup, several antennas are positioned on the transmitter (Tx) end, while only one antenna is located on the receiver (Rx) end. In this configuration same data is transmitted from multiple antennas and the receiver will receive optimum signal thereafter it would extract the required data [15].

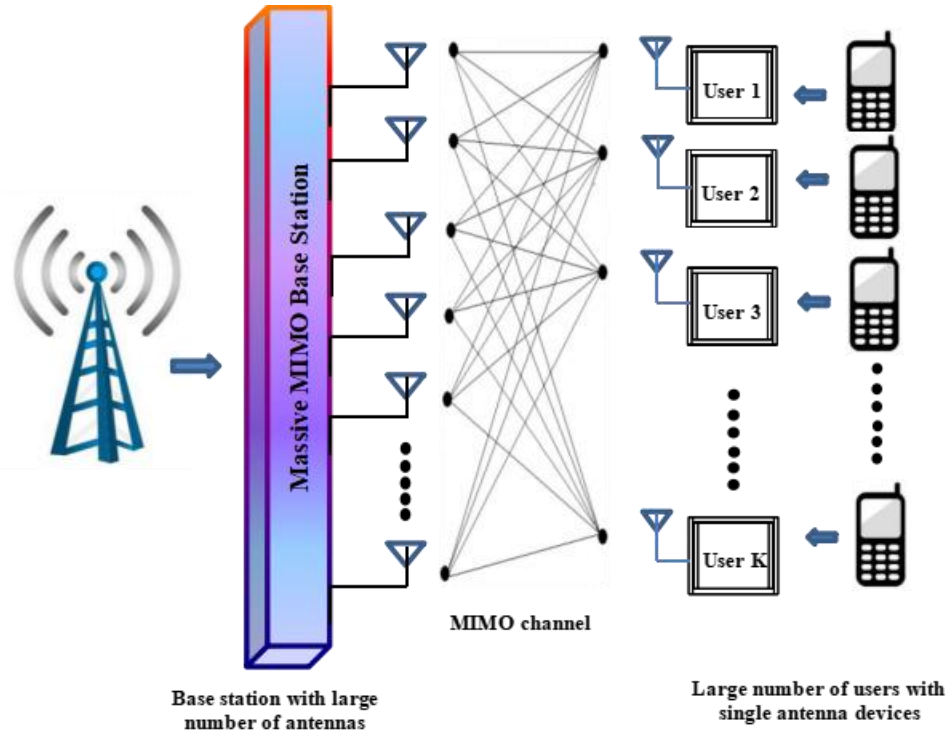


Figure 1.4: A General Overview of Multiple Input Multiple Output (MIMO) Systems

According to Shannon-Harley capacity theorem, SISO system's capacity of the a channel that is free from error is given by:

$$C = B \log_2(1 + \text{SNR}) \tag{1.1}$$

Where, C represents the channel capacity in bits per second (bps), B represents the channel's bandwidth in Hz, and SNR = signal-to-noise ratio (a unit less ratio).

MIMO systems increase capacity by using multiple independent channels (spatial streams) between the transmitter and receiver. A MIMO system's capacity can be calculated as:

$$C_{MIMO} = B \sum_{i=1}^{\min(N_t, N_r)} \log_2 \left(1 + \frac{P_i \lambda_i}{N_0 B} \right) \tag{1.2}$$

Where, N_t - number of transmit antennas, N_r - number of receive antennas, λ_i - eigenvalues of the channel matrix, P_i - power allocated to the i^{th} spatial stream, and N_0 - noise power spectral density.

1.2.1. Evolution of 5G Massive MIMO Antenna Technology:

Designers of antenna have advanced the techniques so as to develop the wireless networks with improved speeds for data transfer and yearly evolution of the antenna design technology have been occurred to fulfil the necessity of the efficient transmission of data. Figure 1.5: shows the evolution of the massive MIMO technology for 5G network communication [16].

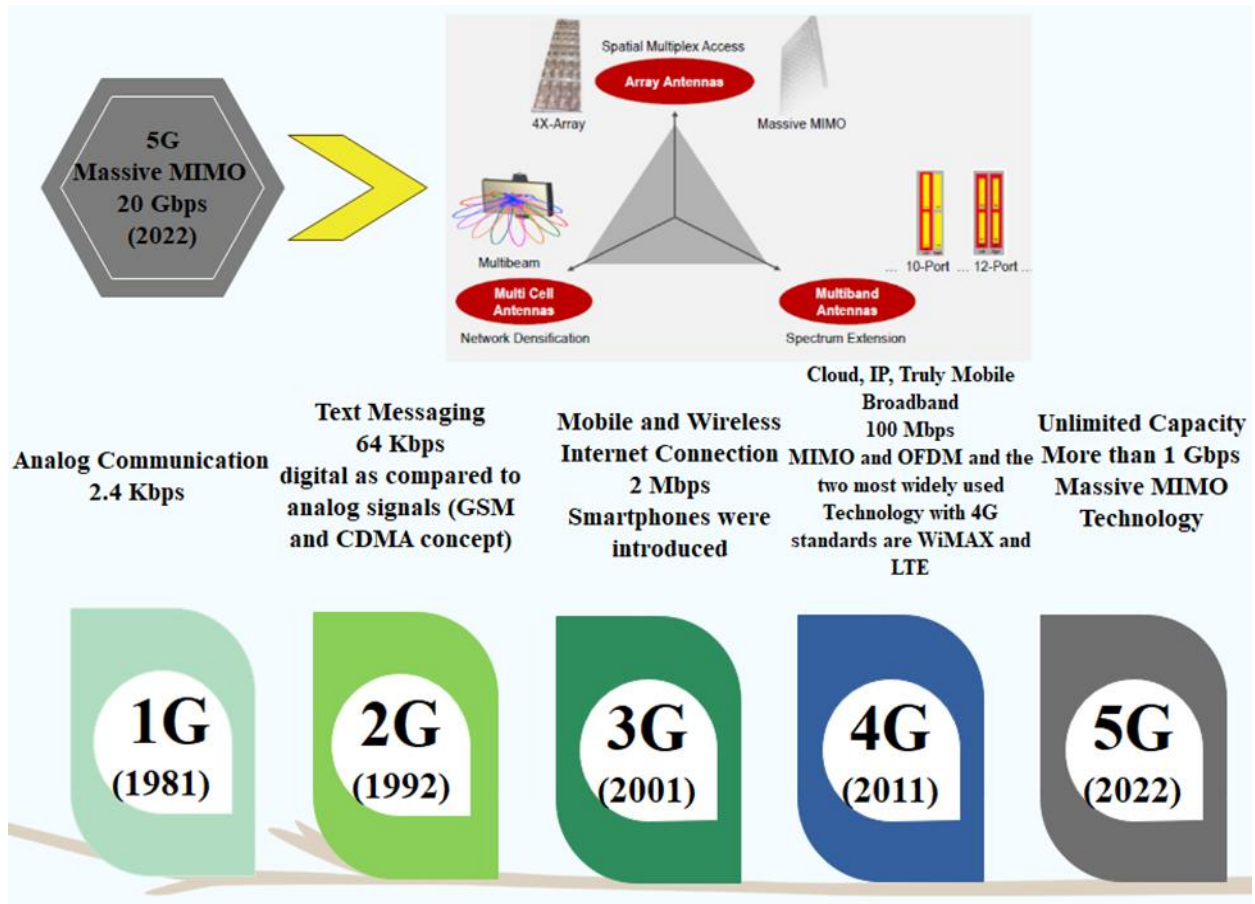


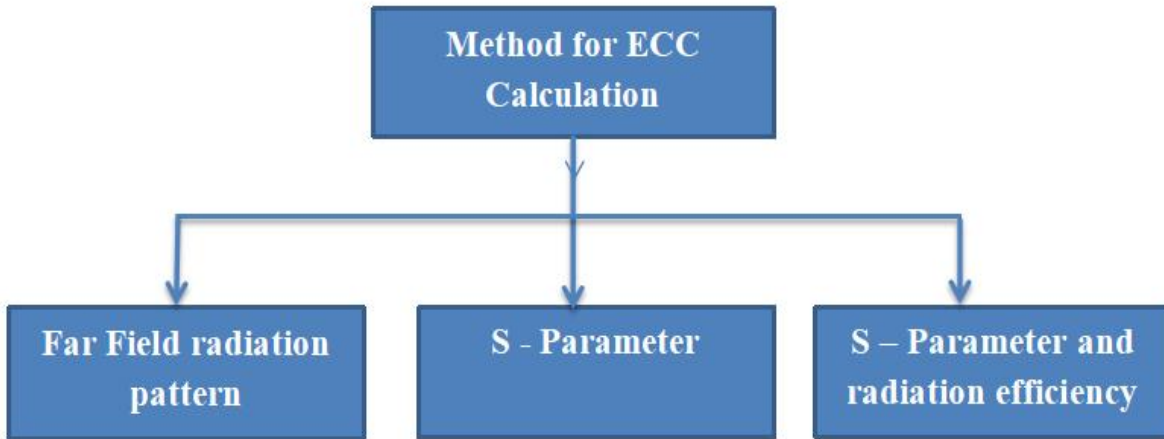
Figure 1.5: Evolution of 5G Massive MIMO Technology [17]

1.3. MIMO ANTENNA DIVERSITY PARAMETER

In this section, describe the various diversity parameters which decide the effective performance of MIMO antenna [31-37].

1.3.1. Envelope Correlation Coefficient (ECC):

The MIMO system's capacity in a multipath environment is determined by the number of antenna elements. When a large number of antennas are placed close together, there is a greater chance of coupling between the antenna parts, reducing the capacity of the MIMO antenna system and antenna efficiency. There are three way to calculate ECC parameter [31].



Method-1: From Far-Field pattern of radiation

Far-field is used [32] to calculate the ECC value. During the measurement of ECC, all the ports of antenna are terminated except on port that is excited by a load impedance of 50 ohm. This method uses both the elevation and azimuth radiation field pattern for calculating ECC value between i^{th} and j^{th} elements.

$$\rho_e(i, j) = \frac{\left| \iint_{4\pi} \vec{\beta}_i(\theta, \phi) \times \vec{\beta}_j(\theta, \phi) d\Omega \right|^2}{\left[\iint_{4\pi} |\vec{\beta}_i(\theta, \phi)|^2 d\Omega \right] \left[\iint_{4\pi} |\vec{\beta}_j(\theta, \phi)|^2 d\Omega \right]} \quad (1.3)$$

Where β_i and β_j are field radiation pattern of two radiating elements.

The ECC calculation from this method is very tedious in terms of calculation, measurement, time consuming and more expensive but this method is more accurate and exact. In this method anechoic chamber is used to extract the parameters.

Method-2: From Scattering parameter

There is another simplest, easy and fast way to evaluate ECC value directly from S-parameter value [33]. The scattering parameters are extracted from each port with the help of vector network analyzer (VNA). The envelope correlation coefficient between i^{th} and j^{th} element for N number of antenna element is evaluated as follows [34].

$$\rho_e(i, j, N) = \frac{|\sum_{n=1}^N S_{ij}^* S_{nj}|^2}{\pi_{k=i,j} [1 - \sum_{n=1}^N S_{kn}^* S_{nk}]} \quad (1.4)$$

Method-3: S- parameter and radiation efficiency

This method is suitable for correct measurement of lossy antenna system. It is very complex method and not suitable for pattern shape and tilt beam for ECC calculation. In this method for ECC calculation, it requires radiation efficiency of each radiating element and reliable for high efficiency. The ECC value for the multi-port MIMO antenna is computed as follows [35],

$$\rho_e(i, j, N) = \frac{\sum_{n=1}^N S_{ij}^* S_{nj}}{\sqrt{(1 - \sum_{n=1}^N |S_{ni}|^2)(1 - \sum_{n=1}^N |S_{nj}|^2)} \eta_{rad,i} \eta_{rad,j}} + \sqrt{\left(\frac{1}{\eta_{rad,i}} - 1\right) \left(\frac{1}{\eta_{rad,j}} - 1\right)} \quad (1.5)$$

Where $\eta_{rad,i}$ and $\eta_{rad,j}$ are radiation efficiency for i^{th} and j^{th} elements.

1.3.2. Diversity Gain (DG):

It is achieved when a transmitter and receiver send or receive numerous signals on a multiple channel path at the same time. The diversity of whole communication system is decided by diversity gain. The ideal theoretical value for uncorrelated antenna is -9.95 dB. The higher is the value of diversity gain better is the performance of MIMO system. It describes how a MIMO

system boosts combined signal gain in relation to time average SNR. The diversity gain is evaluated as follows [36].

$$G_{DG} = 10 \times \sqrt{1 - |\rho_e|^2} \quad (1.6)$$

1.3.3. Mean Effective Gain (MEG):

The MEG, denoted by G_e , is defined as the fraction of the P_r , which is the mean power received by the antenna under test, to the P_{ref} , which is the average power received by an isotropic antenna under identical conditions [35].

$$G_e = \frac{P_r}{P_{ref}} \quad (1.7)$$

For MIMO system, MEG can be evaluate as follows [36],

$$MEG = \int_0^{2\pi} \int_0^\pi \left\{ \frac{XPR}{1+XPR} G_\theta(\theta, \phi) P_\theta(\theta, \phi) + \frac{XPR}{1+XPR} G_\phi(\theta, \phi) P_\phi(\theta, \phi) \right\} \sin\theta \, d\theta \, d\phi \quad (1.8)$$

Where $G_\theta(\theta, \phi)$ represents the θ part of the antenna power gain, $P_\theta(\theta, \phi)$ represents the θ component of angular density function, $P_\phi(\theta, \phi)$ illustrates the ϕ component of angular density function and XPR denotes the cross polarization coupling.

$$XPR \text{ (cross polarization coupling)} = \frac{P_1}{P_2}$$

In which P_1 and P_2 are mean received power of vertically polarized and horizontally polarized isotropic antenna respectively.

The MEG can also be calculated from the knowledge of scattering parameter [37].

$$MEG_i = 0.5 \left[1 - \sum_{j=1}^N |S_{i,j}|^2 \right] \quad (1.9)$$

In order for a MIMO antenna to operate effectively, it is essential that the mean effective gain of each antenna element remains below -3 dB, and the variance in mean effective gain between any two components remains within a 3 dB range.

1.3.4. Channel Capacity Loss (CCL):

The CCL is defined as the maximum reliable data transmission over transmission channel. The practical acceptable limit in a MIMO system is less than 0.4 bits/s/Hz across the whole operating frequency band. Following formula is used for evaluating CCL.[33].

$$C_{Loss} = -\log_2 \det(\varphi^R) \quad (1.10)$$

Where φ^R is the receiving antenna's correlation matrix.. For the multi-port MIMO system, the process of computing it mentioned below.

$$\varphi^R = \begin{bmatrix} \varphi_{11} & \varphi_{12} & \cdots & \varphi_{1N} \\ \varphi_{21} & \varphi_{22} & \cdots & \varphi_{2N} \\ \varphi_{31} & \varphi_{32} & \cdots & \varphi_{3N} \\ \vdots & \vdots & \cdots & \vdots \\ \varphi_{N1} & \varphi_{N2} & \cdots & \varphi_{NN} \end{bmatrix} \quad (1.11)$$

$$\varphi_{nm} = 1 - \sum_{n=1}^4 |S_{nm}|^2 \quad (1.12)$$

$$\varphi_{nm} = -(S_{nn}^* S_{nm} + S_{mn}^* S_{nm}) \quad (1.13)$$

1.3.5. Total Active Reflection Coefficient-(TARC):

For the MIMO systems, TARC is very essential parameter to measure radiation characteristics and bandwidth for different polarization operation. It involves taking the square root of the disparity between the total available powers of all excitation and the radiated power, divided by the available power [34].

$$\Gamma_a^t = \sqrt{\frac{\text{available power} - \text{radiated power}}{\text{available power}}} = \sqrt{\frac{P_a - P_r}{P_a}} \quad (1.14)$$

The TARC is a real number and its value normally ranges between zero and one. If all the delivered power radiated by antenna element then it will be zero and one if completely reflected back. TARC is generally expressed in decibel scale. The practically acceptable value for effective performance is less than -10 decibels across the full working spectrum. For multi-port

MIMO system, if i^{th} port of antenna is excited and remaining ports are at matched loads, TARC can be calculated directly from the scattering matrix using equation 1.18.

$$\Gamma_a^t = \sqrt{1 - P_{ri}} = \sqrt{\sum_{j=1}^N |S_{ij}|^2} \quad i=1, 2, \dots, N \quad (1.15)$$

It is defined as the ratio of the square root of overall reflected power to the square root of total incident power [35].

$$\Gamma_a^t = \frac{\sqrt{\sum_{i=1}^N |b_i|^2}}{\sqrt{\sum_{i=1}^N |a_i|^2}} \quad (1.16)$$

Where b_i indicates the power of reflection and a_i denotes the power of incidence. The scattering matrix for the $N \times N$ MIMO antennas is shown below:

$$\begin{bmatrix} b_1 \\ b_2 \\ \vdots \\ b_N \end{bmatrix} = \begin{bmatrix} S_{11} & S_{12} \cdots & S_{1N} \\ S_{21} & S_{22} \cdots & S_{2N} \\ \vdots & \vdots & \vdots \\ S_{N1} & S_{N2} \cdots & S_{NN} \end{bmatrix} \begin{bmatrix} a_1 \\ a_2 \\ \vdots \\ a_N \end{bmatrix} \quad (1.17)$$

If the magnitude of reflected signal assumed to be unity but phase is varying at different angle. Following is the formula for calculating the TARC for N-port MIMO at different phase angle [36-37],

$$\Gamma_{ai}^t = \sqrt{\frac{|S_{11} + S_{12}e^{j\theta_1} + \dots + S_{1N}e^{j\theta_{N-1}}|^2 + |S_{21} + S_{22}e^{j\theta_1} + \dots + S_{2N}e^{j\theta_{N-1}}|^2 + \dots + |S_{N1} + S_{N2}e^{j\theta_1} + \dots + S_{NN}e^{j\theta_{N-1}}|^2}{N}} \quad (1.18)$$

TARC analysis is critical for evaluating and optimizing MIMO and UWB antenna performance. TARC aids in the design of efficient, wide-band, high-performance antennas by providing a thorough understanding of the reflection and coupling properties when all ports are active. Lower TARC values over the operational bandwidth demonstrate that the antenna system successfully reduces power loss and interference, making it appropriate for high-capacity, high-speed applications like 5G.

1.4. RESEARCH MOTIVATION

Today everyone demands of high data rates, large bandwidth, low cost with low power consumption and size of every wireless device becoming small, so antenna placed inside these devices also need to be compact. From the last few years UWB technology has greatly enhanced the high frequency of operation and data rates with low power spectral density. But this technology is suitable for short distance communication and very high chance of multipath fading occurs. As a result, UWB technology is used with MIMO technology to achieve great diversity and channel capacity. However, there are certain drawbacks to installing several antennas in a limited space since it increases mutual coupling. The primary goal of this project is to design and build a compact MIMO antenna with good isolation and wide bandwidth for usage in UWB applications.

1.5. STATEMENT OF PROBLEM

A examination of the literature reveals that several approaches have been proposed to increase antenna bandwidth while reducing mutual interaction between radiating parts. These methods encompass alterations to ground planes, the inclusion of meandered shorting strips, modifications to feeding structures, the incorporation of parasitic elements, and the utilization of isolation techniques. Antennas exhibit diverse shapes, including ellipses, circles, triangles, dipoles, and various other geometries. Various methods for feeding, including coaxial, strip line, proximity-coupling, aperture-coupling approaches, are utilized. Each type of antenna possesses its unique advantages and drawbacks when applied to wireless communication applications. The primary shortcomings commonly associated with antennas include limited bandwidth, modest gain, and larger physical dimensions.

1.6. SCOPE OF PRESENT WORK

The current study focuses on to develop and create a small sized multi-band patch antenna for wireless communication. The HFSS simulation software is used to fine-tune antenna parameters such resonance Reflection coefficient , frequency, bandwidth, voltage standing waves ratio, Gain, and Directivity for the proposed antenna. The following steps are done in the design of a UWB MIMO antenna:

1. Employing and analyzing existing antennas with different parameters.
2. Developing and fine-tuning the proposed antenna for wireless applications, taking into account factors such as gain, bandwidth, and Reflection coefficient .
3. Fabrication, testing, simulations and validation of presented antenna.
4. Comparing the presented antenna's simulated and experimental results to those of existing antennas designed for wireless applications.

1.7. RESEARCH OBJECTIVE

Based on the finding of the research survey following would be the research objectives:

1. Analysis and synthesis of existing massive MIMO smart antenna design for 5G communication.
2. Design of the massive MIMO smart antenna with enhanced antenna performance parameters.
3. To optimize the results of the designed massive MIMO 5G antenna in terms of the parameters like efficiency, gain, ECC, Isolation/mutual coupling and VSWR etc.
4. A prototype will be designed for the comparing the measured and simulated antenna parameters entities.

1.8. THESIS ORZANIZATION

The thesis report has organized as following chapters.

Chapter-1: Introduction

This chapter provides the brief introduction of UWB and MIMO technology, MIMO performance parameter, various techniques for isolation improvement and antenna miniaturization techniques, motivation of research and thesis organization presented.

Chapter-2: Literature Review

This chapter provides the brief literature survey of various UWB antenna and MIMO antenna for various applications and different approaches used for isolation enhancement.

Chapter-3: Design a Single element UWB Microstrip Patch Antenna For 5G millimeter Wave Applications

This chapter provides four port MIMO antenna which are orthogonally placed. One of the standout features of this antenna is its remarkable isolation, which ensures minimal interference between multiple input and output channels. This isolation is crucial for improving the reliability and efficiency of wireless communication systems, especially in UWB applications where a wide spectrum of frequencies is utilized.

Chapter-4: Design a Compact Quad Port UWB MIMO Antenna for 5G mm-wave Applications.

This chapter provides the very compact four element MIMO antenna which is orthogonally placed for isolation improvement without using any decoupling structure. It also describe the effect of different housing material on Reflection coefficient and isolation parameter.

Chapter-5: Design and Analysis of MIMO Antenna with Different Isolation Techniques

In this chapter, four antenna elements placed in the parallel orientation and isolation significantly improved due to hybrid model structure including decoupling structure used on top plane with defected ground structure used on the ground plane. The antenna is quite suitable for various UWB portable devices as well as for mobile communication systems.

Chapter-6: Result and Discussions

In this chapter, a MIMO antenna developed and mutual coupling is reduced by introducing by with X shaped decoupling structure on the top plane with partial ground plane and this is the

final design of the antenna in this thesis that we are discussing all the simulated and fabricated results in this chapter.

Chapter-7: Conclusion and Future Scope

This chapter provides the summary of research work done in the thesis and some future scope main points were discussed.

1.9. SUMMARY

This chapter discusses the role of MIMO (Multiple Input Multiple Output) and UWB (Ultra-Wide band) technology in millimeter-wave applications. It begins by examining the growing demand for high-speed wireless communication networks, which is driven by the rapid expansion of data-intensive applications and the introduction of 5G technology. The chapter then emphasizes the importance of antennas in enabling these modern communication systems, notably in terms of high data rates, increased capacity, and greater dependability.

The introduction also discusses the difficulties of developing antennas for millimeter-wave frequencies, such as the necessity for high bandwidth, small size, and efficient radiation performance. It emphasizes the relevance of MIMO technology in improving system performance through spatial diversity and multiplexing, which are critical for overcoming the limits of millimeter-wave transmission. The chapter concludes by outlining the structure of the thesis and summarizing the main topics that will be explored in subsequent chapters.

CHAPTER-2

LITERATURE REVIEW

2.1. INTRODUCTION

Due to consumer needs and technological advancement, wireless communication networks have significantly advanced in everyday life. Over the course of the 1G–5G evolution [38-39], the field of wireless network communication has expanded significantly. Multiple applications, access technologies, and a variety of user and traffic kinds must all be supported by wireless communication systems. Though these applications have a wide range of needs and requirements, 5G wireless communication technologies may encourage ideas like smart power-grids, smart cities, smart parking, smart libraries, and e-health. The bit rate at which wireless data traffic may send and receive is one of the most crucial factors to consider.

$$\text{Throughput (bits/s)} = \text{Bandwidth (Hz)} \times \text{Spectral efficiency (bits Sec}^{-1}\text{Hz}^{-1}) \quad (2.1)$$

Thus, expanding bandwidth has drawbacks, such as reducing the signal-to-noise ratio (SNR) by a hertz while maintaining the same transmitted power, which is in line with current studies that concentrate on spectral efficiency techniques. It is a well-known technique to increase spectral efficiency at the transceivers by employing multiple antennas [40]. It keeps the servicing quality at a minimum while enabling greater gearbox. How efficient the spectrum is has also grown in importance as the necessity for wireless technology has increased.

One of the most interesting developments in antenna and electromagnetic history is the advent of microstrip antenna, also commonly called patch antenna. It is most likely the most adaptable answer to the needs of the modern wireless system. It supports both linear and circular polarization, is lightweight, easy to fabricate, has strong radiation control, is inexpensive to produce, and integrates well with microwave monolithic integrated circuits, among its many other benefits. It comes in a range of forms, including square, triangular, circular, and rectangular etc.

Microstrip antennas can handle power, but they have several limitations, including low gain, low efficiency, and a narrow bandwidth. In recent years, many scholars have used UWB technology

to improve the bandwidth and other properties of microstrip antennas. Nonetheless, multipath fading and channel capacity continue to be the main issues facing modern wireless communication technologies. In order to address these problems further, MIMO design and UWB technologies are coupled. Numerous studies on MIMO antennas are still being conducted in an effort to increase different diversity factors.

2.2. LITERATURE REVIEW ON SINGLE ELEMENT MICROSTRIP PATCH ANTENNA

A lot of antennas are overly big and too complicated for portable wireless devices that are small in size. An I-shaped monopole antenna was printed on a 28 mm \times 29 mm patch [41]. An H-shaped slotted multiband antenna measuring 60 mm \times 60 mm was on display [42]. The writer presents a dual-polarized antenna in this context that features broad bandwidth, low cross-polarization, and effective isolation. A reflector ground plane and two orthogonal planar printed dipoles are used to create the two linear polarization. Openings are created at the dipole corners, and short links are established between the perpendicular dipoles to enhance both cross-polarization and isolation, as documented in reference [43]. A printed elliptical patch antenna with a 5 GHz band-notch frequency band and a UWB operational bandwidth was suggested by the work's author. By inserting the antenna into a U-shaped slot, the band-notching function is carried out. Except for the band rejection, this configuration generates a satisfactory radiation pattern, a rejection band spanning from 4.90 to 5.86 with a -10 dB reflection coefficient, and bandwidth (BW) ranging from 2.97 GHz to 15.09 GHz. The gain remains consistently even across the entire Ultra-Wide band (UWB) frequency spectrum, as indicated in reference [44]. This article suggests an impressive antipodal Vivaldi antenna designed for ultra-wide band (UWB) applications, showcasing outstanding impedance matching and gain. An elliptical-shaped director is inserted into the tapered slot to maximize gain at the high-frequency band, and two symmetrical sets of rectangular slits are implanted around the slot to increase impedance matching at the low-frequency band [45]. The writer proposed a compact dual-band antenna featuring a rectangular ground plane slot and an unconventional patch design inspired by the Fibonacci sequence. To create a UWB antenna, join circular sectors and an L-shaped strip to the rectangular slot, increasing the ellipse's bandwidth. To regulate the antenna's circular polarization, the ground plane additionally features a strip in the shape of “#” [46]. Here, the author presented

a low-cost UWB elliptic antenna. Mounted on FR4 dielectric material, the antenna measures only $(21 \times 27 \times 1.6) \text{ mm}^3$. Its impedance bandwidth is 16.26 GHz and its maximum gain is 6 dBi [47]. A tiny $(15 \times 25 \times 1.6) \text{ mm}^3$ elliptic monopole antenna has been provided by the author. The antenna design makes use of a basic FR4 dielectric material. The antenna performs best in the range of 3.1 GHz to 10.6 GHz frequencies, where R_L (reflection coefficient) is ($<$) less than -10 dB. Furthermore, the antenna has a range of 2.5 dBi (minimum gain) to 9 dBi (maximum gain) in the UWB [48]. The author of this article describes a tiny $(17 \times 14 \times 1.6) \text{ mm}^3$ elliptical antenna made of FR-4 material that is appropriate for mobile use. The suggested antenna operates at 24 gigahertz with a gain of 6.8 dBi [49]. This article describes an ultra-wide band CPW-fed elliptic antenna of $18.3 \times 23 \times 1.6 \text{ mm}^3$ with an operational bandwidth of 3.7 gigahertz to 11.3 gigahertz made of FR-4 materials. This antenna's uni planar form and modest size make it unique and easy to fabricate at a low cost [50]. The author suggested using a wide band antenna with a 7.5 GHz resonance. The suggested design has a polygonal shape, and extra stubs are added to improve the antenna's operational characteristics. The optimized antenna had a gain of 3.0393 dBi and worked at frequencies ranging from 2.8 to 9.4 GHz. The $(23 \times 18 \times 1.6) \text{ mm}^3$ antenna is built on a low-cost FR4 substrate [51]. This study looks at a small dual band antenna suited for several Sub-6 GHz applications. Two resonance loops and two additional feeding loops power the antenna's two resonance loops. To improve the lower operating band, metal frames have been added to the antenna system's ground. The antenna measures $(50 \times 30) \text{ mm}^2$ and has two resonant frequencies of 2.46GHz and 0.93GHz [52]. An ultra-thin slot monopole antenna with a co-planar wave guide feed was designed and built by the author. The fabrication process uses the thin E- strate of $\epsilon_r=2.2$ from the ENrG. The ink jet printing method and elector-textile technique are used to fabricate the CPW - fed antenna. The $66 \times 62 \times 0.04 \text{ mm}^3$ ultra-thin, flexible antenna resonates at 2.75 gigahertz and 5.8 gigahertz frequencies [53] with a gain of 4.52 dB and 5.19 dB. A dual-slot antenna array system on a thin substrate and a thick substrate is designed and studied in this work. For both scenarios, the differences in gain and bandwidth were examined. The antenna measures $50 \times 54 \text{ mm}^2$ and has a resonance frequency of 5.8 GHz. Constructed on a thin substrate, it boasts a 617 MHz bandwidth, 6.7 dBi gain, and 94% efficiency. The same antenna structure operating on a thick substrate demonstrated a 455 MHz bandwidth, 7.23 dBi gain, and 92% efficiency [54].

Table 2.1: Some more Literature survey on single element antenna with different shape and design [38-42]

Ref. No	Authors	Year	Work Done	Findings	Application
[38]	Kiran Raheel, Ahsan Altaf, Arbab Waheed, Saad Hassan Kiani, Daniyal Ali Sehrai, Faisal Tubbal and Raad Raad	2021	A self-decoupled small dual-band mm-wave MIMO antenna array featuring E-shaped and H-slotted elements was designed here self-decoupled small dual-band mm-wave MIMO antenna array featuring E-shaped and H-slotted elements was designed. Size of the antenna: 20 x 24 x 0.508 mm ³ . Dielectric material: Rogers-5880	Working Frequency: 27.6 - 28.6 GHz and 37.4 - 38.6 GHz Gain = 7.9 dB Isolation = 28 dB ECC < 0.001 Efficiency = 85%	mm-wave for 5G Technology
[39]	Laurent Canale, Mustapha El Halaoui, Georges Zissis, Adel Asselman, and	2021	The author developed a 28/38 gigahertz Dual-Band Inverted-F Array Design Antenna System for cellular phones (Handsets). Size of Antenna: 5.5 × 04 × 0.2 mm ³ Substrate: FR4, $\epsilon_r = 4.4$	Working Frequency Range: 27.94 - 28.83 GHz and 37.97 - 38.96 GHz Acheived Gains: 15.35 dB at 38.49 GHz 16.52 dB at 28.38 GHz, and Mutual Coupling is < -35dB	Used in both 4G and 5G Mobile Applications
[40]	Hijab Zahra, Wahaj	2021	Here, an end-fire broadband antenna with a	Working Frequency Range: 26.25 GHz to	Used in Pattern Diversity

	Abbas Awan, Wael Abd Ellatif Ali, and Niamat Hussain, Syed Muzahir		grounded-CPW feed and T-shaped helical inspiration was designed. Size of antenna: $15 \times 25 \times 0.203 \text{ mm}^3$ Substrate: Rogers-5880, $\epsilon_r = 3.38$	30.14 GHz Gain is 5.83 dB, Mutual Coupling: < - 30 dB ECC is < 0.005	Applications
[41]	Son Xuat Ta, Hosung Choo, and Ikmo Park	2017	Here, an 8-element linear array and a broadband printed-dipole antenna were created. Substrate Used: Rogers RT/Duroid™ -5880, $\epsilon_r = 2.2$	Working Frequency Range: 26.5GHz - 38.2 GHz Gain = 4.5 - 5.8 dBi, Mutual coupling is less then < -20 dB	Used in the 5G wireless cellular network applications.
[42]	Ajay Kumar Dwivedi, Akhilesh Kumar Pandey, Anand Sharma, Vivek Singh	2021	A 2-port wide-band circularly polarised (CP) small size MIMO antenna array was created in this case. Substrate Used: FR4, $\epsilon_r = 4.4$	Working Frequency Range: 3.3GHz - 4.2 GHz ECC is < 0.10 dB Isolation is >15 dB TARC: $\leq -15 \text{ dB}$ DG: > 9.94 dB Efficiency: 95%	Used in the sub-6 GHz applications.

2.3. LITERATURE REVIEW ON UWB MIMO ANTENNA

In January 2018, Zhao et al. [43], presented two UWB antenna placed opposite edge of ground plane. The antenna based on theory of characteristic mode (TCM) in which one behaves as electric source and other behave as magnetic source at lower frequency band. The antenna achieved high isolation without any decoupling structure and measured efficiency more than

70%. Morsy et al. [44] published a two-element MIMO antenna for the long-term evolution (LTE) and universal mobile telecommunications service (UMTS) bands in January 2018. The antenna consists of two meander type radiator which is separated by ground plane (Bottom side). A T-shaped slit/slot etched between antenna elements for isolation improvement. The antenna's overall dimension is 110 mm × 150 mm, with tested total efficiency ranging from 59-71% and an ECC value less than 0.085. In April 2018, Chandel et al. [45] proposed a UWB MIMO antenna which consists of two circular monopole antenna in which eye shaped slot etched on radiator. The designed antenna has operating bandwidth 2.8-20 GHz with compact size 18 mm × 36 mm. In April 2018, Jehangir et al. [46], reported two element MIMO antenna in which miniaturization achieved due to small loop meandered line. For improving end fire radiation pattern multiple slits etched on partial ground plane. The antenna worked in telemetry L-band and LTE band with overall size 120 mm x 50 mm. The measured gain more than 5 dB with total efficiency of each element 85 and 78 % respectively.

In June 2019, Prabhu and Malarvizhi [47] reported double sided UWB MIMO antenna. The antenna consists of polygon shaped radiator used on bottom and top of the substrate. The mutual coupling was decreased by employing an EBG structure with bandwidth ranging from 3.1 gigahertz to 11 gigahertz, with a peak gain ranging from 2.5 to 6.8 dB. Suriya and Anbazhagan [48] suggested a UWB-MIMO antenna with band-notch features in 2019. The antenna is made out of an inverted A-shaped radiator that is orthogonally positioned to promote isolation. The dimension of antenna is 38.5mm x 38.5 mm with operating bandwidth 3.1-10.6 GHz. The fractional bandwidth 109.48 % achieved with low ECC value. In July 2019, Babu and Anuradha et al. [49] proposed two port MIMO antennas for UWB system with overall size 65 × 35 mm². The antenna consists of a rectangle patch, half of a circle shape etched from each corner of the radiator, and a semi-arc shape cut from the ground plane. The antenna's impedance bandwidth ranged from 3 Gigahertz to 10 Gigahertz with an ECC value of less than (<) 0.25. S.Chouhan et al. [50] claimed in August 2019 that a two-port MIMO antenna worked for multiband (WiFi/WiMax/Bluetooth/C-bands) applications, with multiband achieved by the arm of a spider-shaped radiator. The antenna is 37 mm x 56 mm in total, with a Y-shaped stub on the ground plane for increased isolation. In the first band, the measured gain was above (>) 2 dB and the efficiency was greater than 73 percentage.

Pannu and Sharma [51] presented a four-port MIMO antenna with two notch bands in May 2020. The antenna consists of four identical elliptical shaped radiator has orthogonally placed and for bandwidth improved defected ground structure is used in which square slot and half ring etched. The antenna's overall size is 45 mm × 45 mm with operating band from 2 -16.8 GHz. The dual band notch achieved due to H-shaped and C- shaped slot etched on radiator. In 2020, Tang et al. [52] reported UWB MIMO antenna in which DGS, u-shaped branch on ground and window shaped patch along with folded feed line. The size of proposed antenna 80 mm × 35 mm with 2.57-12.2 GHz bandwidth. The antenna gain ranged from 3.06 to 4.669 dB, with isolation less than (<) -15 dB and no need for any decoupling structure. In 2020, Roy et. Al [53] presented a MIMO antenna by using textile substrate. For improving diversity performance meander type structure used between radiator on top surface and on ground plane. The diversity performance has measured in terms of ECC < 0.1 , DG > 9.8 and MEG lies between +3 dB to -3 dB. The prototype antenna were analyzed in human body and found to be low ECC.

2021, Chattha et al.,[54] discussed a 4-element and octa port MIMO for different 5G applications. Ground dimensions of the antenna are 60 ×120 mm² and antennas occupy the crooks of the ground portion. Slots engraved on to the ground, aids in the reduction of mutual coupling. Operational bandwidth for this antenna is 2.4 GHz – 3.8 GHz and covers all the 5G frequencies below 6 GHz. The gain ranges from 3.2 to 5 dB over the entire operational frequency band. Wani and Kumar, in [55], designed and investigated a 4-element UWB MIMO of size 35mm × 35mm. The ground plane stubs, together with the perpendicular orientation of the antenna components, provide more than (> 15 dB) fifteen decibels of isolation between radiating elements. This antenna is proposed for use in UWB MIMO applications. All diversity metrics were found to be within the intended range.

2022, Khurshid et al., [56] designed a low-profile MIMO antenna of super wide band, (2.3-23) GHz, for IoT applications. The quad-element antenna is of size 60 × 55 × 1.2 mm³. The elements are orthogonally arranged to attain an isolation of over 20 dB. Nagendra and Swarnalatha, in [57], designed and fabricated a four-port MIMO antenna for multiband IoT applications. The three working resonant frequencies are 1.44, 2.3, and 4.1 Gigahertz. The meandered design of radiating element claims to achieve good gain and the SRR provides good isolation. Antenna Design for MIMO UWB Systems. Designing MIMO UWB antennas for 5G, especially at mm-

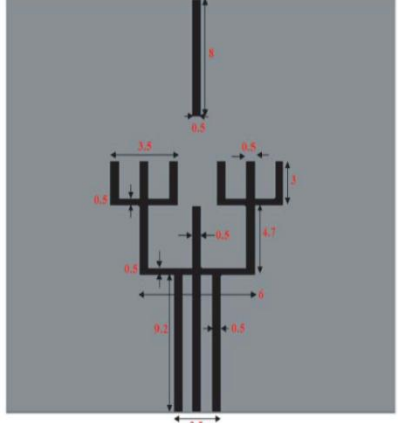
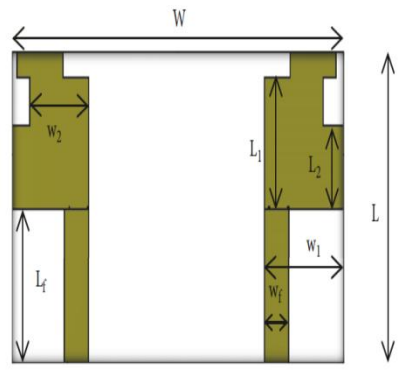
wave frequencies, presents several challenges, such as maintaining wide-band performance while ensuring a compact form factor. Recent studies have focused on various antenna structures that cater to these requirements. For example, 2022, Li et al., [58] discussed the development of compact MIMO UWB antennas using planar monopole and slot designs, which offer extensive bandwidth and are conducive to integration in dense antenna arrays. These designs also focus on minimizing mutual coupling between antenna elements, which is crucial for maintaining high performance in MIMO configurations.

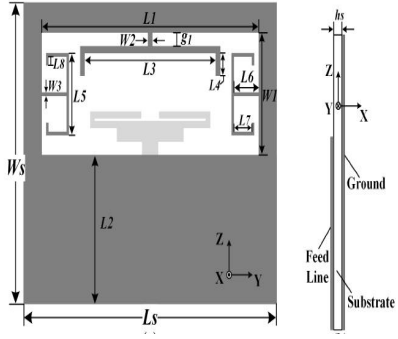
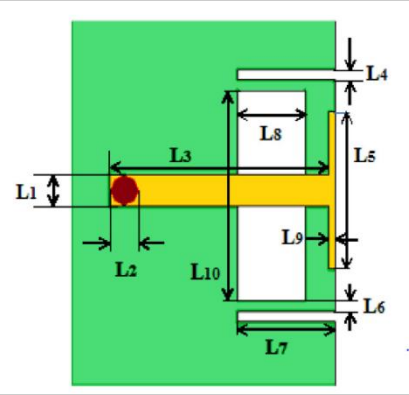
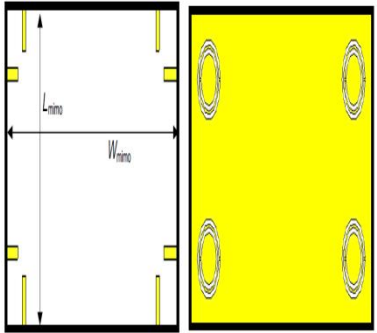
Furthermore, advancements in materials, such as the use of meta materials and re-configurable antenna designs, have been pivotal. 2023, Wang et al., [59] explored how meta materials can be utilized to create antennas with tunable properties, enabling dynamic adaptation to various frequency bands and environments. This adaptability is particularly beneficial for 5G mm-wave applications, where the propagation environment can vary significantly.

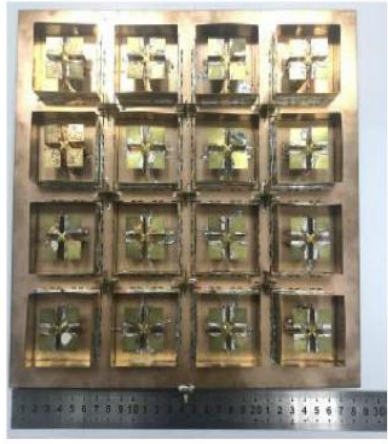
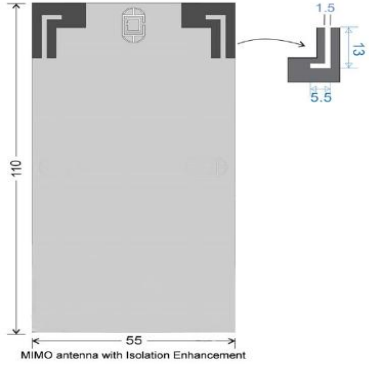
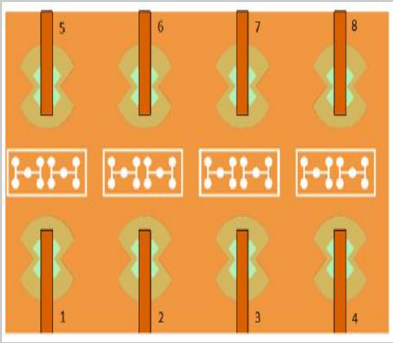
Designing MIMO UWB antennas for 5G, particularly for mm-wave frequencies, poses significant challenges, such as achieving wide band performance while maintaining a compact size. Recent research continues to refine these designs. For instance, 2024, Zhang et al., [60] introduced a novel dual-polarized MIMO UWB antenna that significantly reduces mutual coupling through a modified ground structure, enhancing isolation and overall system performance. This design is particularly advantageous for densely packed antenna arrays in 5G devices. In another 2024 study, Lee et al., [61] explored the use of advanced metamaterial in the design of re-configurable UWB antennas. These antennas can dynamically adapt to varying frequency bands and propagation environments, a critical feature for mm-wave 5G applications. The study highlights the potential of these materials to further miniaturize antenna structures while maintaining high performance, making them ideal for integration into compact 5G devices. Some more literature survey is shown in the Table 2.2.

Table 2.2: The Comparison of various antenna Designs

References	Work Done	Findings	Topology	Application
[62]	<p>The author was designed a coplanar wave guide (CPW) fed stub-loaded slot-antenna array with 10 multiple input multiple output (MIMO) elements.</p> <p>Antenna Size: 32 x 80 mm²</p> <p>Dielectric Substrate: FR4, $\epsilon_r = 4.4$</p>	<p>Frequency band: 22.9-28.8 GHz</p> <p>Isolation is < -20 dB</p> <p>Bandwidth: 22.8%</p> <p>ECC is < 0.0004</p> <p>CCL: 0.1 bps/Hz</p> <p>Antenna gain is 1.46 - 3.32 dBi</p> <p>Front-to-Back ratio (FBR) is 8.9 - 17.9 dB</p>		mm-wave in 5G communication
[63]	<p>2 x 2 MIMO dome-shaped monopole radiating elements are used to design</p> <p>Antenna Size: 20 x 34 x 1.6 mm³</p> <p>Dielectric Substrate: FR4, $\epsilon_r = 4.4$</p>	<p>Frequency bands: 2.11- 4.19 GHz and 4.98 - 6.81 GHz</p> <p>Isolation is >21</p> <p>ECC is <0.004</p>		<p>LTE, Wi-Fi, W-LAN, Bluetooth, and Wi-MAX etc.</p>
[64]	<p>Spider-shaped multiband MIMO antenna.</p> <p>Antenna size: 37 x 56 x 1.6 mm³</p> <p>Dielectric Substrate: FR4</p>	<p>Frequency Band used: 2.24 – 2.50 GHz, 3.60 – 3.99 GHz, 4.40 – 4.60 GHz, and 5.71 – 5.90 GHz</p> <p>Isolation is < 10 dB</p> <p>ECC is < 0.08</p>		<p>Wi-Fi, Wi-MAX, Bluetooth, C-Band etc.</p>

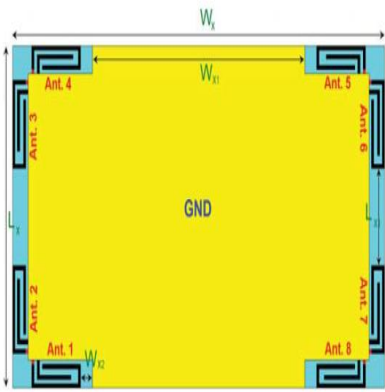
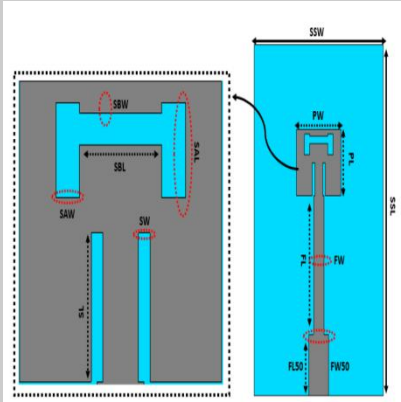
		<p>Antenna Gain: > 2 dBi</p>		
<p>[65]</p>	<p>The author developed a hexagonal-shaped multiple input, multiple output (MIMO) patch or printed antenna.</p> <p>Antenna Size: 48 x 48 mm²</p> <p>Dielectric Substrate: FR4, $\epsilon_r = 4.4$</p>	<p>Frequency Bands:</p> <p>2 - 4 GHz, 3.1 - 10.6 GHz and 8 - 12 GHz</p> <p>Isolation: 20dB</p> <p>ECC is < 0.04</p> <p>TARC: < -10 dB</p> <p>DG: > 9.985</p> <p>Radiation efficiency : 78–94%</p> <p>peak gain: 1.4 - 6.6 dB</p>		<p>S-Band, X-Band WLAN, UWB etc.</p> <p>Applications</p>
<p>[66]</p>	<p>The author was designed a novel compact 2 x 2 planar MIMO antenna array system with ultra wide band (UWB) capacities.</p> <p>Antenna Size: 13 x 25 x 0.254 mm³</p> <p>Dielectric Substrate: Rogers-5880, $\epsilon_r = 2.2$</p>	<p>Frequency Band:</p> <p>2 - 12 GHz for IEEE-802.11 a/ b/ g/ n/ & ac.</p> <p>Reflection coefficient : -10dB</p> <p>Mutual Coupling is less then -20dB</p> <p>Antenna Gain : 4.8 dB</p> <p>ECC: 0.009</p> <p>DG: 9.8 dB</p>		<p>Wi-Fi operation in mobile devices</p>

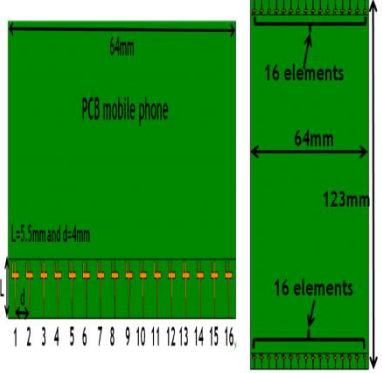
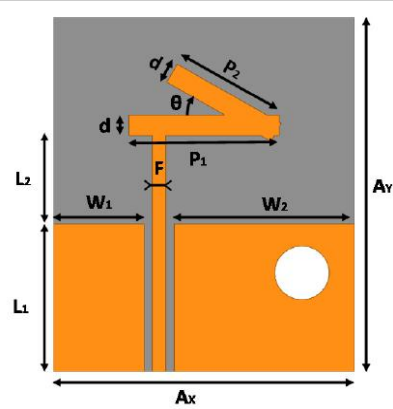
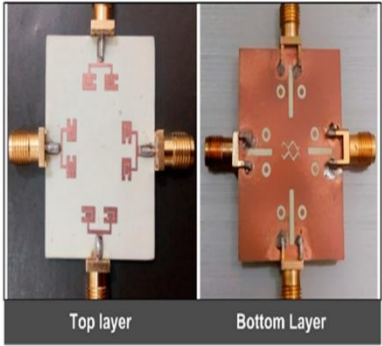
<p>[67]</p>	<p>A four-band slot antenna was designed.</p> <p>Antenna Size: 0.44 x 0.35 mm²</p> <p>Substrate: FR4,</p> <p>$\epsilon_r = 3.5$</p>	<p>Frequency Bands:</p> <p>1.575 - 1.665 GHz,</p> <p>2.4 - 2.545 GHz,</p> <p>3.27 - 3.97 GHz and</p> <p>5.17 - 5.93 GHz</p> <p>Antenna Gains:</p> <p>3.55 dBi, 3.93 dBi, 5.02 dBi, and 4.86 dBi</p>		<p>GPS,</p> <p>Wi-MAX,</p> <p>WLAN etc.</p>
<p>[68]</p>	<p>Design an 18 element antenna system.</p> <p>Antenna Size: 150 x 80 x 1.6 mm³,</p> <p>Substrate: FR4,</p> <p>$\epsilon_r = 4.4$</p>	<p>LTE band - 42: 3.4 - 3.6 GHz and</p> <p>LTE band - 43: 3.6 - 3.8 GHz.</p> <p>Reflection coefficient is greater than 20 dB</p> <p>Isolation is > 20 dB</p> <p>Total antenna efficiency improved by 87%</p> <p>ECC is < 0.01</p> <p>Antenna Gain is > 5.3 dBi</p>		<p>Used in both 4G and 5G</p> <p>6-inch smartphone applications</p>
<p>[69]</p>	<p>In this review a Complementary-Split Ring-Resonator (CSRR) based massive MIMO antenna system were designed.</p> <p>Antenna Size: 75 x 150 x 1.6 mm³</p> <p>Dielectric</p>	<p>Frequency Band are used:</p> <p>3.43 - 3.62 GHz, and</p> <p>4.78 - 5.04 GHz.</p> <p>ECC: < 0:15</p> <p>Isolation: > 15 dB</p>		<p>Mostly used application sub-6 GHz 5G Wireless smartphone</p>

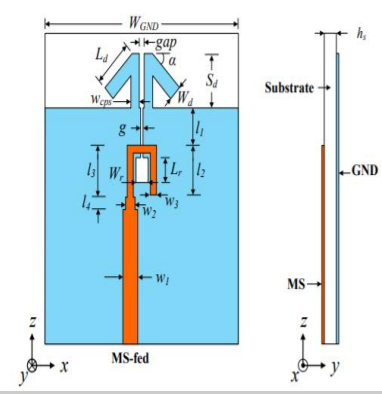
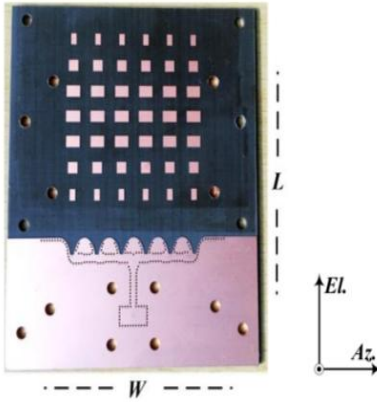
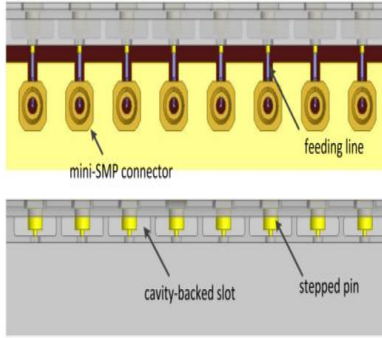
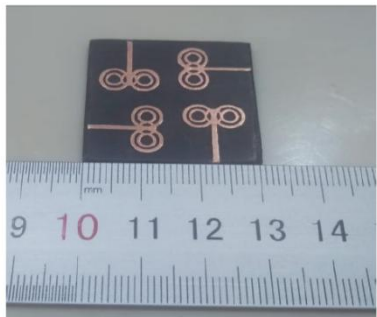
	Substrate: FR4			
[70]	<p>In the research paper the author were proposed a 5G array for massive MIMO communication system with a dual-polarized antenna.</p> <p>Substrate: FR4</p>	<p>Frequency Band: 3.3 - 5.1 GHz</p> <p>ECC is 0.004</p> <p>Antenna Gain is 17.3 dBi</p> <p>Front- to- back ratio (F/B): 22.7 dB</p> <p>Isolation is 27dB</p>		<p>Used in 5G array or</p> <p>Massive MIMO communication system applications.</p>
[71]	<p>In this research, the authors created a two-element MIMO antenna array with a planar inverted-F antenna (PIFA) structure as an antenna element for sub-6 GHz and mm-Wave 5G systems.</p>	<p>Frequency Bands: 3.5 GHz, 4.3 GHz, 28 GHz and 35 GHz</p> <p>Isolation is improved by 21dB</p> <p>Efficiency is greater than 65%</p>	 <p>MIMO antenna with Isolation Enhancement</p>	<p>Used in the 5G wireless device applications.</p>
[72]	<p>Author was designed- For public safety, a compact and low-cost MIMO Bowtie dielectric resonator antenna for two, four, and eight elements has been developed.</p> <p>Antenna Size for</p> <p>Unit Cell: 30 x 25.6 mm² and</p> <p>Eight elements: 120 x 51.2 mm²</p>	<p>Frequency Bands: 4.94 - 4.99 GHz and 5.15 - 5.35 GHz</p> <p>Antenna Gain for unit cell: 5.24 dBi, two elements: 5.49 dBi, four elements: 5.68 dBi, eight elements: 6.2 dBi.</p>		<p>Used in WLAN applications</p>

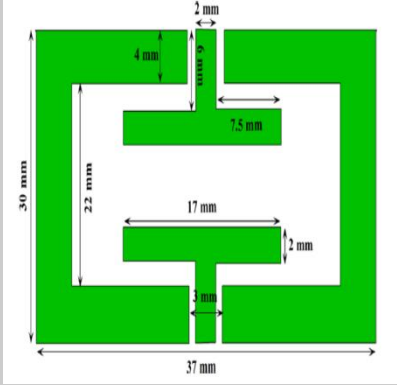
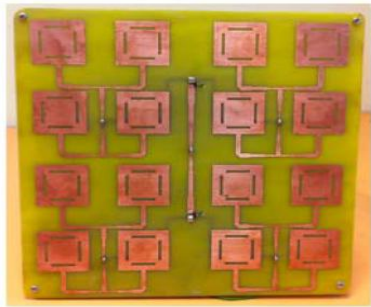
		<p>Isolation = 25 dB</p> <p>ECC = 0.04</p>		
[73]	<p>In this article the author was proposed an extremely compact MIMO antenna for portable wireless ultra-wide-band (UWB) devices.</p> <p>Antenna Size: 38 x 38 mm²</p> <p>Substrate: FR4</p>	<p>Frequency Band: 3 - 20 GHz</p> <p>Antenna Gain: 1.3 - 6.2 dBi</p> <p>Isolation is > 17 dB</p> <p>ECC is < 0.08</p> <p>Efficiency is improved by 75%</p> <p>DG: > 9.97 dB</p>		Used for UWB applications
[74]	<p>In this article the author was proposed a compact tree shape planar quad element MIMO antenna array for 5G communication system.</p> <p>Antenna Size: 80 x 80 x 1.57 mm³</p> <p>Substrate: FR4</p>	<p>Frequency Band: 3 - 300 GHz</p> <p>Antenna Gain: 12dB</p> <p>Isolation is > 20 dB</p> <p>Efficiency is improved by 70%</p> <p>ECC: < 0.0014</p>		<p>Used in millimeter-wave spectrum for</p> <p>Wi-Fi, Wi-MAX, Bluetooth,</p> <p>ISM, and mobile communication etc.</p>
[75]	<p>In this research, the author generated a unique super-wideband multiple-input multiple-output (SWB-MIMO) antenna array system.</p> <p>Antenna Size:</p>	<p>Frequency Band: 3.2 - 13.2 GHz</p> <p>Bandwidth: 2.9 - 40 GHz</p> <p>Antenna Gain: 4.3 - 13.5 dBi</p> <p>Isolation: < -17 dB</p>		Used in WLAN system application

	<p>58 x 58 x 1 mm³</p> <p>Substrate: FR4</p>	<p>ECC: < 0.04</p>		
[76]	<p>The author designed a dual-band, dual-polarized base-station antenna array for fifth-generation applications.</p> <p>Antenna Size: 250 x 250 mm²</p> <p>Dielectric Substrate: RF-30, $\epsilon_r=3.0$</p>	<p>Frequency Bands: 0.69 - 0.96 GHz and 3.5 - 4.9 GHz</p> <p>Isolation: > 25 dB</p> <p>Bandwidth: 43.8%</p> <p>VSWR: 2</p>		<p>Used in 5G applications</p>
[77]	<p>A dual-polarized slot antenna array with eight ports and four resonators designed for MIMO 5G mobile terminals.</p> <p>Antenna Size: 25 x 25 mm²</p> <p>Dielectric Substrate: FR-4, $\epsilon_r = 4.4$</p>	<p>Frequency Band: 3.4 to 3.8 GHz</p> <p>Antenna Gain is improved by 1.9 dB</p> <p>ECC is < 0.5</p> <p>Mutual coupling: < -15 dB</p> <p>Isolation: > -25 dB</p>		<p>Used in the 5G smartphone applications</p>
[78]	<p>The author designed a substrate-integrated magneto-electric (ME) dipole antenna with a meta-surface.</p> <p>Antenna Size: 60 x 60 x 7.92 mm³</p> <p>Dielectric Substrate: FR4,</p>	<p>Frequency Bands: 3.4 - 3.6 GHz, and 4.8 - 5 GHz</p> <p>Antenna Gain : 6.1 dBi - 9.1 dBi for lower band and 5.6 dBi - 9.2 dBi for upper band</p> <p>front- to- back ratio (FBR): > 18 dB</p>		<p>Used in the 5G Wi-MAX, WLAN and X-Band MIMO applications</p>

	$\epsilon_r = 2.2$	ECC: < 0.5		
[79]	<p>Here the author was proposed a modified planar-inverted-F antenna (PIFA) element designed for MIMO.</p> <p>Antenna Size: 20.5 x 6.5 mm²</p> <p>Substrate: FR4</p>	<p>Frequency ranges:</p> <p>2.5 - 2.7 GHz, 3.4 - 3.8 GHz, and 5.6 - 6 GHz</p> <p>TARC: < -20dB</p> <p>ECC: < 0.01</p> <p>Mutual coupling < -10dB</p> <p>Antenna Gain: 3-4.5 dBi</p>		Used in 5G Smart Phones
[80]	<p>Here, an E-Shaped and H-Slotted with Self-decoupled compact dual-band mm-wave MIMO antenna array were designed.</p> <p>Antenna Size: 20 x 24 x 0.508 mm³</p> <p>Dielectric substrate: Rogers-5880</p>	<p>Frequency bands:</p> <p>27.6 - 28.6 GHz and 37.4 - 38.6 GHz</p> <p>Antenna Gain is 7.9 dB</p> <p>Isolation is 28 dB</p> <p>ECC < 0.001</p> <p>Efficiency improved by 85%</p>		mm-wave for 5G Technology

<p>[81]</p>	<p>The author devised a 28/38 GHz Dual-Band Inverted-F Array Design Antenna System for Mobile Phones (Handsets).</p> <p>Antenna size: 5.5 x 4 x 0.2 mm³</p> <p>Substrate: FR4, $\epsilon_r = 4.4$</p>	<p>Frequency Bands: 27.94 - 28.83 GHz and 37.97 - 38.96 GHz</p> <p>Antenna Gains: 16.52 dB at 28.38 GHz, and 15.35 dB at 38.49 GHz</p> <p>Mutual Coupling: < -35dB</p>		<p>Used in both 4G and 5G Mobile Applications</p>
<p>[82]</p>	<p>Here, a grounded-CPW fed with T-shaped helical inspired broadband antenna with an end-fire radiation pattern was designed.</p> <p>Antenna Size: 15 x 25 x 0.203 mm³</p> <p>substrate: Rogers-5880, $\epsilon_r = 3.38$</p>	<p>Frequency Band: 26.25 GHz to 30.14 GHz</p> <p>Gain: 5.83 dB,</p> <p>Mutual Coupling is < -30 dB</p> <p>ECC: < 0.005</p>		<p>Used in Pattern Diversity Applications</p>
<p>[83]</p>	<p>Here, a 4-port MIMO antenna array was designed which operates on the mm-wave frequency band.</p> <p>Antenna Size: 30 x 35 x 0.76 mm³</p> <p>Substrate: FR4</p>	<p>Frequency Bands: 24.25 - 27.5 GHz and 27.5 - 28.35 GHz</p> <p>Antenna Gain: 8.3 dBi</p> <p>ECC: < 0.01,</p> <p>DG: > 9.96dB</p>		<p>Used mm-wave spectrum for 5G applications</p>

<p>[84]</p>	<p>Here, a broadband printed-dipole antenna and 8-element linear arrays were designed.</p> <p>Dielectric Substrate: Rogers RT/Duroid™ - 5880, $\epsilon_r = 2.2$</p>	<p>Frequency Band: 26.5 - 38.2 GHz</p> <p>Antenna Gain: 4.5 - 5.8 dBi</p> <p>Mutual coupling: < -20 dB</p>		<p>Used in the 5G wireless cellular network applications.</p>
<p>[85]</p>	<p>In the millimetre wave (mm-wave) range, a parasitic patch antenna with 42 elements has been designed.</p>	<p>Frequency Band: 27.5 GHz to 28.5 GHz</p> <p>Gain: > 21.4 dBi</p> <p>cross polarization: > -12 dB</p> <p>side lobe levels (SLLs): > -19.1 dB</p>		<p>5G mobile communication base stations</p>
<p>[86]</p>	<p>Here the author was proposed a novel design for 28 GHz beam steering phased array antenna.</p> <p>Dielectric Substrate: Rogers-5880, $\epsilon_r = 2.2$</p>	<p>Frequency Band: 27.5 - 28.35 GHz</p> <p>Antenna Gain: > 15 dBi</p>		<p>Used in the 5G mobile device applications</p>
<p>[87]</p>	<p>Here the author was proposed a novel design a single layer MIMO antenna array.</p> <p>Antenna Size: 30 x 30 mm²</p> <p>Substrate:</p>	<p>Frequency Band: 28 GHz</p> <p>Antenna Gain: 5.5 dBi</p> <p>ECC: < 0.16 dB</p> <p>Efficiency is improved by 92%</p>		<p>Used in the 5G mm-wave communication applications.</p>

	Rogers-5880, $\epsilon_r = 2.2$	Isolation: < -29 dB		
[88]	<p>Here, a compact size wide-band circularly polarized (CP) 2-port</p> <p>MIMO antenna array was designed.</p> <p>Substrate: FR4, $\epsilon_r = 4.4$</p>	<p>Frequency Band: 3.3 - 4.2 GHz</p> <p>ECC: < 0.10 dB</p> <p>Isolation: > 15 dB</p> <p>TARC ≤ -15 dB</p> <p>DG > 9.94 dB</p> <p>Efficiency is improved by 95%</p>		Used in the sub-6 GHz applications.
[89]	<p>Here, the author was proposed a re-configurable antenna system to improved data throughput limitations in MIMO.</p> <p>Substrate: FR4, $\epsilon_r = 4.7$</p>	<p>Frequency Band: 2.4 and 2.6 GHz</p> <p>Isolation is 15 dB</p> <p>Reflection coefficients: -24.3 dB</p>		Used in wireless communication systems like: WLAN and LTE.

From the above literature survey some of the important design parameters where we need to do more better improvements are as following:

This thesis addresses the aforementioned gaps by proposing innovative solutions that advance the state of the art in MIMO UWB antenna design for 5G mm-wave applications. The thesis introduces a novel antenna design that significantly enhances isolation between MIMO UWB elements using a simplified and compact structure. Also involves the different mutual coupling techniques which are already define by the others but in this thesis we make some Hybrid combination using different techniques in single design to further reduce the mutual coupling and improves the other parameters to fulfill the research gap. This design not only reduces mutual coupling but also maintains high bandwidth and gain, making it suitable for practical

deployment in compact 5G devices. With the addition of two elliptical slots to the capsule-shape UWB antenna, the total antenna size was reduced, and the radiation patch area was lowered overall by 38% compared to the others and an antenna-radiating structure has been developed for increasing the bandwidth that is suitable for use with 5G wireless communication applications. this research not only advances current knowledge but also provides practical solutions that can be directly applied to the development of next-generation 5G wireless systems.

2.4. SUMMARY

This chapter starts by providing an introduction to 5G wireless communication technologies employed across various frequency bands, emphasizing the essential bandwidth for effective communication. It then discusses the relevance of microstrip patch antennas in the context of 5G wireless applications. Also discussed about different number of research article on UWB antenna with different shaped and bandwidth enhancement technique has been presented. This chapter also presented various types of MIMO antenna, isolation enhancement technique and miniaturization technique from previous literature. It has been observed that the problem of miniaturization, isolation enhancement along with higher bandwidth is still required more attention. As a result, the research is chosen to develop and build a highly compact, high bandwidth, and high isolation UWB MIMO antenna for today's 5G wireless communication equipment. The next chapter describes the design and testing of compact Multiple-Input Multiple-Output (MIMO) antennas with enhanced isolation for Ultra-Wideband (UWB) applications.

CHAPTER-3

DESIGN A SINGLE ELEMENT UWB MICROSTRIP PATCH ANTENNA FOR 5G MILLIMETER WAVE APPLICATIONS

3.1. INTRODUCTION

The rapid evolution of wireless communication systems demands advanced antenna designs that can meet the stringent requirements of emerging technologies like 5G. One of the key enablers of 5G networks is the use of millimeter-wave (mm-Wave) frequencies, which offer significantly higher data rates, improved bandwidth, and enhanced capacity compared to traditional communication bands. However, designing antennas that operate efficiently at these higher frequencies presents several challenges, such as maintaining wide bandwidth, achieving compact size, and ensuring stable radiation patterns.

Ultra-Wide band (UWB) technology has gained prominence in addressing these challenges due to its capability to operate over a wide frequency range, offering high data rates and low power consumption. UWB antennas, particularly in the mm-Wave spectrum, are increasingly being considered for integration into 5G systems to support high-speed data transmission and low latency. The combination of UWB technology and microstrip patch antenna design has emerged as a promising approach for realizing efficient antennas in compact and portable form factors.

This research focuses on the design of a single-element UWB microstrip patch antenna specifically tailored for 5G mm-Wave applications. The antenna design aims to cover the frequency range required for 5G communication while maintaining a compact structure suitable for integration into various devices. The microstrip patch antenna's low-profile nature, ease of fabrication, and compatibility with printed circuit boards make it an ideal candidate for next-generation wireless communication systems.

By exploring various design parameters, including the shape of the radiating patch, substrate material, and the introduction of slits and slots, this study seeks to optimize the antenna's performance in terms of bandwidth, gain, and radiation efficiency. The goal is to develop a

robust antenna solution that meets the demands of 5G mm-Wave applications, contributing to the advancement of high-speed wireless communication technologies.

Antennas operating at high frequencies demand increased power and space. To address these challenges, an advanced antenna element design is crucial. The SHF spectrum is used in this study to construct a small UWB (Ultra-wide band) MSA (microstrip patch antenna) appropriate for millimeter-wave applications.

- The narrowband antenna bandwidth is usually less than 1% of the center frequency. GPS and traditional mobile communication are examples of technologies that target a certain frequency.
- Wide-band antenna bandwidth is usually between 10% and 20% of the center frequency. Suitable for systems that require frequency coverage but are not as extensive as UWB, such as Wi-Fi or certain wireless communication systems.
- UWB antennas having more than 500 MHz of bandwidth or a fractional bandwidth greater than 20%. Ideal for high-speed data transmission, radar, and imaging devices, particularly in 5G networks.

The Federal Communication Commission (FCC) has formally allocated the frequency spectrum from 3.1 GHz to 10.6 GHz for commercial UWB communication applications. UWB band-pass filters are one example. UWB is a radio transmission technology that uses a reasonably broad bandwidth of at least 500 MHz above the center frequency, or at least 20% of the center frequency. This technology has created curiosity since it has the potential to be a game changer for wireless communication over short distances and with high bandwidth. UWB allows real-time accurate distance measurements without interfering with traditional narrowband and carrier wave communications in the same frequency ranges. It also resists noise and reflection, making it safe and useful for various applications.

The FCC of numerous nations has recommended a bandwidth definition for Ultra-Wide band (UWB). The allocation of the UWB spectrum varies across regions. In the United States, UWB operates within the 3.1 to 10.6 GHz frequency band. Europe designates a low band of 3.1 GHz to 4.8 GHz and a high band of 6 GHz to 8.5 GHz for UWB. Japan divides its UWB spectrum into a low band of 3.4 GHz to 4.8 GHz and a high band of 7.25 GHz to 10.25 GHz. Meanwhile, Malaysia uses a single UWB band from 3.1 GHz to 10.6 GHz [90].

The developed UWB MSA, with dimensions of $(15 \times 12 \times 0.8)$ mm³, exhibits simplicity, high frequency, and improved microwave circuit features, such as enhanced isolation, current distribution, and reduced bandwidth. The proposed antenna is placed on a Rogers RT/Duroid 5880 substrate, operates in the 24–28 gigahertz frequency range. The inclusion of elliptical slots to the radiating patch alters current distribution, which improves radiation performance. The proposed antenna design has an operating frequency range from 24 to 28 gigahertz and a wide bandwidth of ten gigahertz, making it ideal for higher frequencies. Simulation results validate the appropriateness of the antenna model, showing improvements in Reflection coefficient, gain, and VSWR compared to older versions. Utilizing Ansoft HFSS v.15.0, comprehensive simulations and comparative analyses are conducted, confirming good impedance matching and resonance between 24 GHz and 28 GHz. Within the intended frequency band, the measured VSWR is less than two, and the gain ranges from 3.6 to 5 dB. The proposed antenna resonates at millimeter-wave frequencies, proves beneficial for 5G applications, offering resonance frequencies of 4 to 5 dB.

This chapter introduces a microstrip line-fed patch antenna characterized by a compact, capsule-shaped design, tailored for deployment in both 5G and UWB applications. The proposed antenna design main purpose is to provide insights into advanced 5G technologies that operate in the 24 gigahertz to 28 gigahertz frequency spectrum. The proposed design consists of a capsule-shaped patch, a portion of the ground plane, and a line-stripe microstrip feed line. To attain the required results, the ground plane is calibrated. The simulation outputs include the antenna's reflection coefficient is less -10 dB, VSWR (< 2), surface current distributions, gain, radiation patterns and radiation efficiency. This chapter introduces a compact UWB antenna characterized by a broad bandwidth exceeding 24 GHz, coupled with enhanced gain performance suitable for contemporary 5G wireless applications.

3.2. ANTENNA DESIGN PROCEDURE AND METHODOLOGY

In a MPA (microstrip patch antenna), An isolation of dielectric substrate is positioned between two layers: a top layer referred to as a patch and a bottom layer known as a ground layer. These MPAs can be created by etching different shapes, including squares, circles, ellipses, E, H, S, and others, a double-sided copper layers on printed circuit board. The bottom layer of the PCB functions as the ground plane and may have either a smooth or uneven surface, while the top

patch layer serves the dual purpose of being both a radiator for transmitting signals and a receiver for capturing them [91].

To achieve resonant frequency ranges tailored for specific applications, patch antennas can adopt various shapes. Presently, elliptical patch antennas are gaining significant attention for their circularly polarized properties in patch configuration or geometry [92]. Capitalizing on the properties of elliptical patch antennas, we developed a similar shape referred to as a capsule. This design includes a rectangular patch antenna with two semi-circular ends, which meets the requirements of modern wireless communication systems, such as broadband capability and numerous features.

Designing UWB patch antennas involves a complex interplay of various physical phenomena and design techniques to achieve wide-band performance. The key formulas related to resonant frequency, impedance matching, radiation pattern stability, and ground plane effects provide a theoretical foundation for understanding and optimizing UWB antenna designs. The choice of materials, ground plane configurations, and feed structures all play critical roles in creating an antenna that can perform efficiently across a wide range of frequencies. These design principles allow UWB patch antennas to meet the stringent requirements of modern communication systems, including 5G and other high-data-rate applications. We also state that if the frequency bandwidth is between 3.6 GHz and 10.6 GHz, it is a UWB. The proposed antenna has a bandwidth of 7.3 GHz, which falls within the above-defined range, hence we may conclude that this antenna is best suited for UWB.

The following conclusion may be drawn from the proposed antenna's design steps:

Step 1: By adjusting the characteristics of the exponentially-shaped, 50 micro strip line, create a capsule-shaped UWB antenna with a realized gain at 24-28 GHz.

Step 2: In order to achieve appropriate impedance matching at 24-28 GHz, embed two sets of elliptical slots/slits from the radiating patch antenna.

Step 3: To enhance the bandwidth and gain at 24-28 GHz, elliptical slits should be inserted into the radiating patch.

Step 4: Obtain the final design that satisfies all parametric requirements.

A flowchart outlining, the suggested work is shown in Figure 3.1. Initially, an ultra-wide band antenna is created using a straightforward slit/slots loading approach to function over the band of 24-28 GHz. The designed structure is then simulated to see if the antenna delivers the promised results. After that a parametric analysis is completed to create the antenna's optimal version.

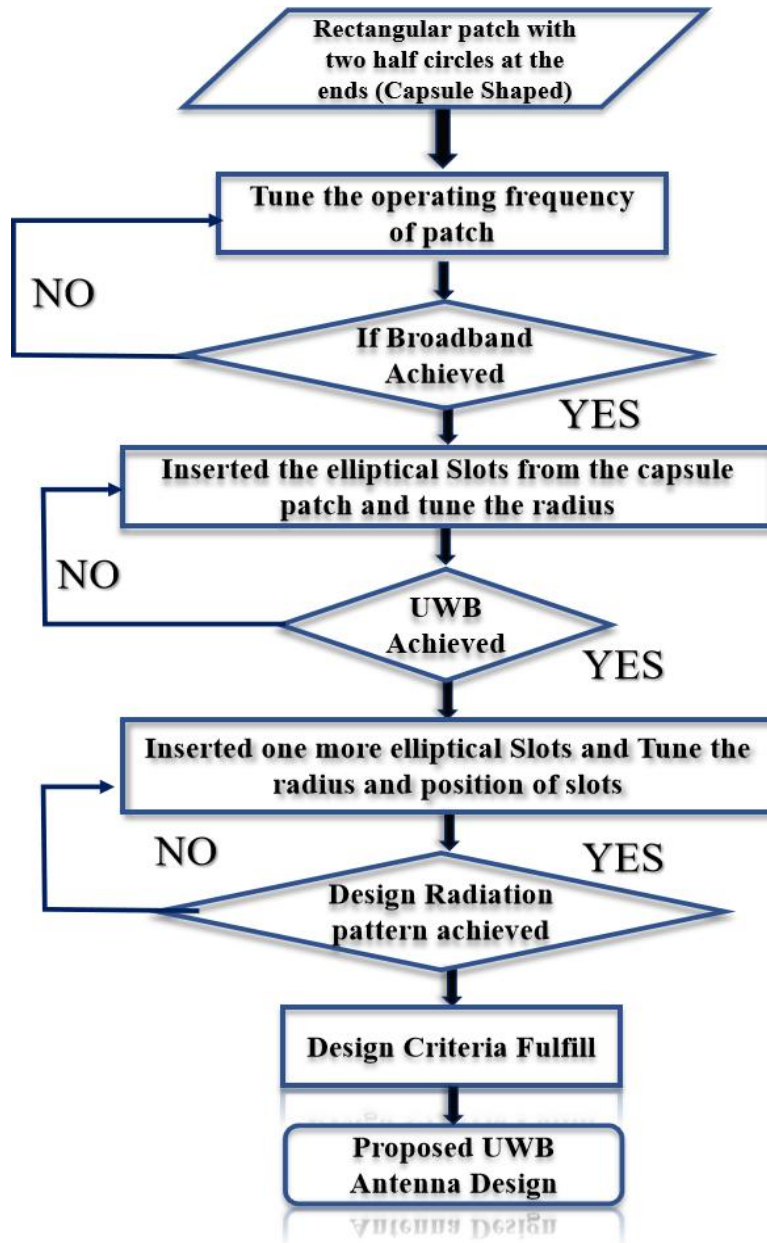


Figure 3.1: Flow chart for designing steps of proposed UWB Antenna

To get the width (W) and length (L) of the antenna, use the condensed formula from the transmission line model that is given below.

The suggested antenna's width (W) is determined using the formula below [93].

$$W = \frac{c}{2f_r \sqrt{\frac{(\epsilon_r+1)}{2}}} \quad (3.1)$$

Where, c is the speed of light in the air ($c = 3 \times 10^8$ meter/second), ϵ_r is the substrate material permittivity (given as $\epsilon_r = 2.2$), f_r is the resonant frequency, and The equation can be obtained as follows to determine the substrate's effective permittivity [94]:

$$\epsilon_{eff} = \left(\frac{\epsilon_r+1}{2}\right) + \left\{ \left(\frac{\epsilon_r-1}{2}\right) \times \left(1 + 12 \frac{h}{W}\right)^{-\frac{1}{2}} \right\} \quad (3.2)$$

Where, h is the thickness of substrate. The length (L) can be calculated as:

$$L = \frac{c}{2f_r \sqrt{\epsilon_{eff}}} - (2 \times \Delta L) \quad (3.3)$$

Where,

$$\Delta L = 0.412 \times h \left\{ \frac{(\epsilon_{eff}+0.3) \left(\frac{w}{h}+0.264\right)}{(\epsilon_{eff}-0.258) \left(\frac{w}{h}+0.8\right)} \right\}$$

Elliptical geometry:

$$e = \sqrt{1 - \left(\frac{b}{a}\right)^2} \quad (3.4)$$

In an elliptical patch, the major axis is represented by "a," the minor axis is represented by "b," and the eccentricity is represented by "e,"

The equation of Resonance frequency calculation for dual band elliptical slots [95-97]:

$$f_{11}^{e,0} = \frac{15}{\pi e(a_{eff})} \sqrt{\frac{Q_{11}^{e,0}}{\epsilon_r}} \text{ GHz} \quad (3.5)$$

$$a_{eff} = a \sqrt{\left[1 + \frac{2h}{\pi \epsilon_r a} \left\{ \ln\left(\frac{a}{2h}\right) + (1.41\epsilon_r + 1.77) + \frac{h}{a} (0.268\epsilon_r + 1.65) \right\}\right]} \quad (3.5a),$$

$$Q_{11}^e = -0.0049e + 3.788e^2 - 0.7228e^3 + 2.2314e^4 \quad (3.5b),$$

$$Q_{11}^0 = -0.0063e + 3.832e^2 - 1.1351e^3 + 5.2229e^4 \quad (3.5c)$$

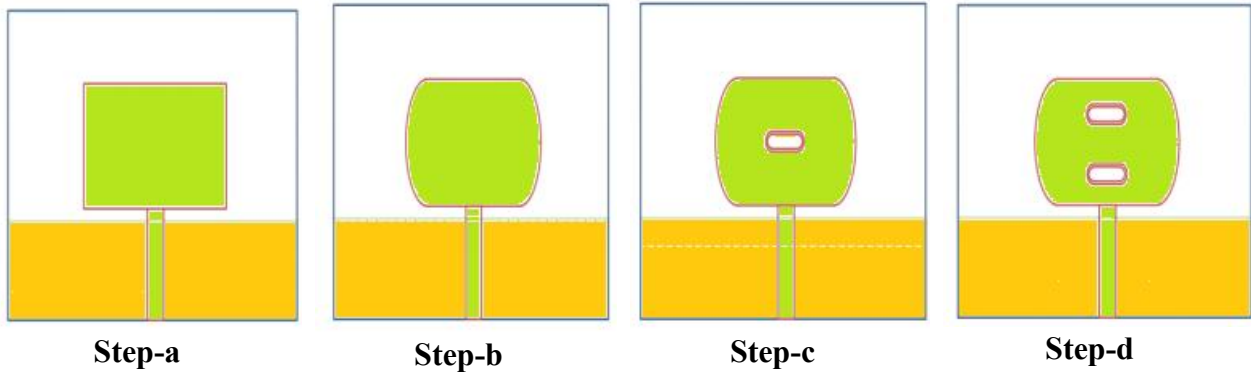
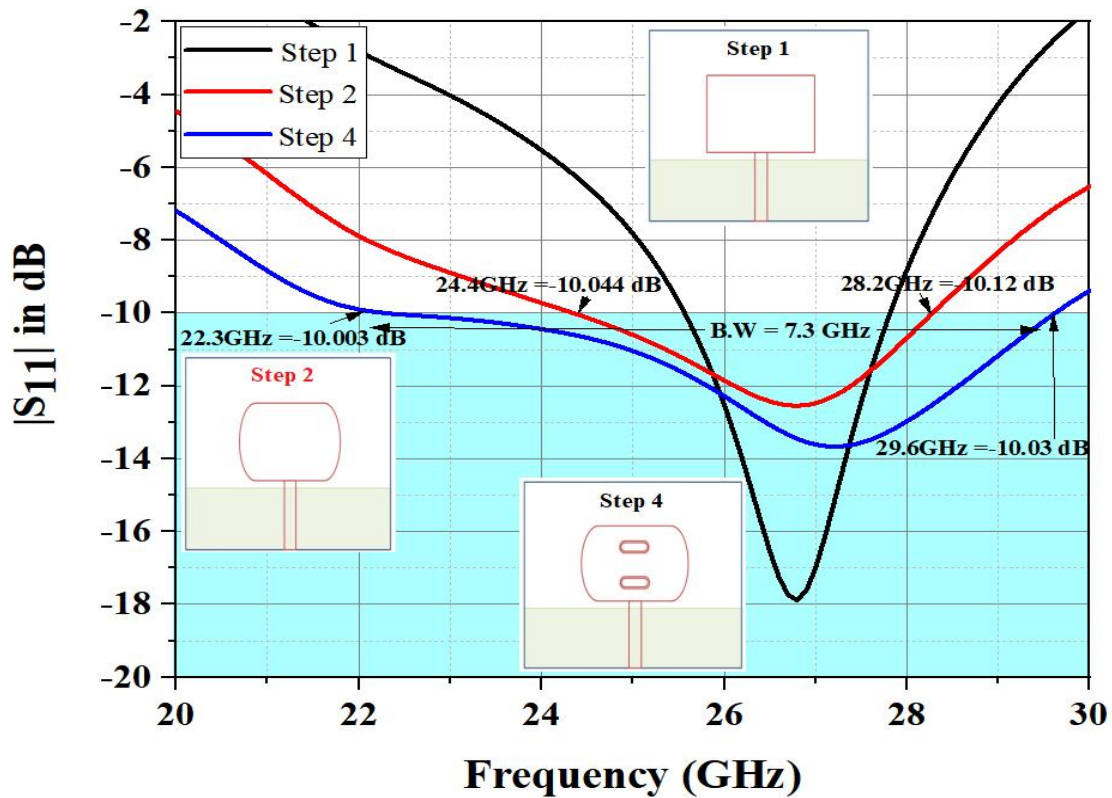
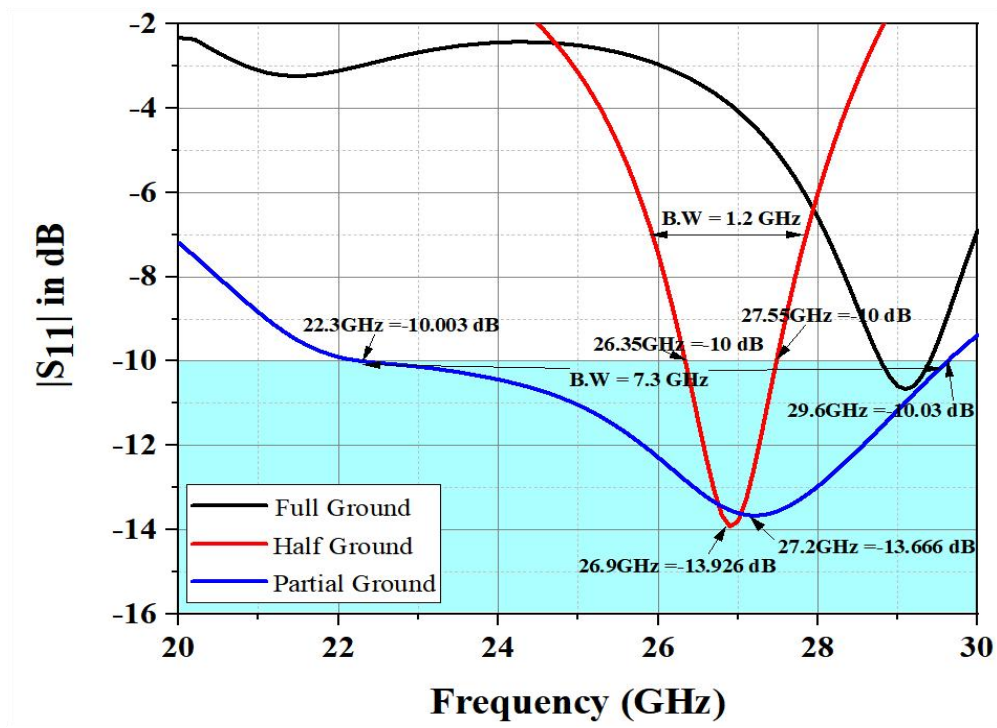


Figure 3.2: Steps development procedure of the Single cell UWB Antenna

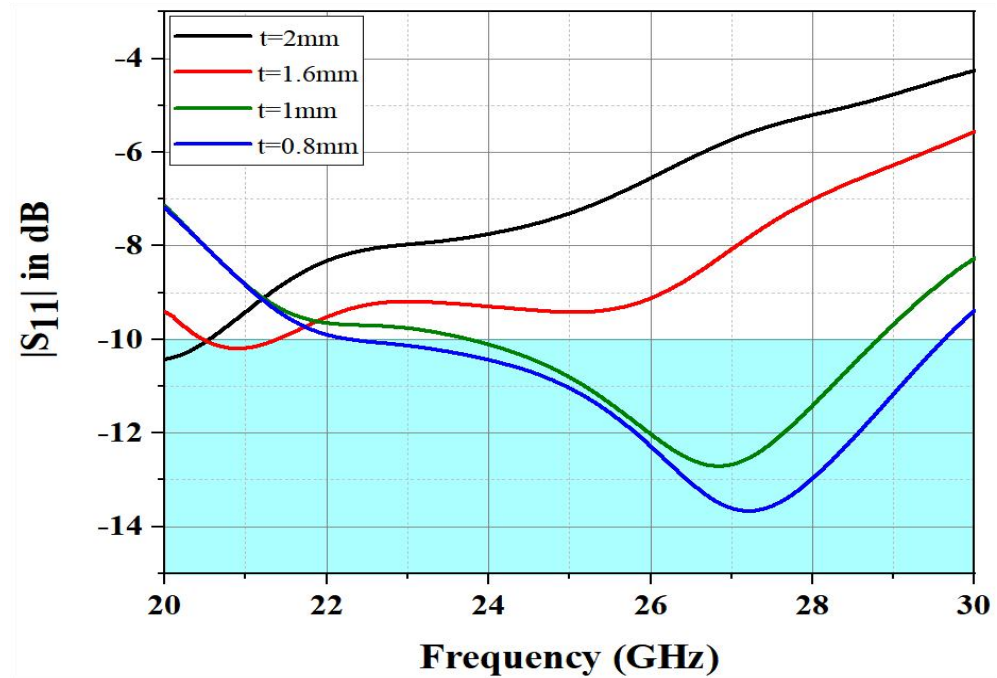
Figure 3.2 shows the steps development procedure of proposed UWB antenna as first started with basic rectangular patch but did not achieved the proper parameters then improved the design with added two half circles at the end of rectangle now achieved the parametric results but did not achieved the required bandwidth then cut the two elliptical slots from the radiating patch then achieved all the parametric results with good bandwidth as shown in Figure 3.3.



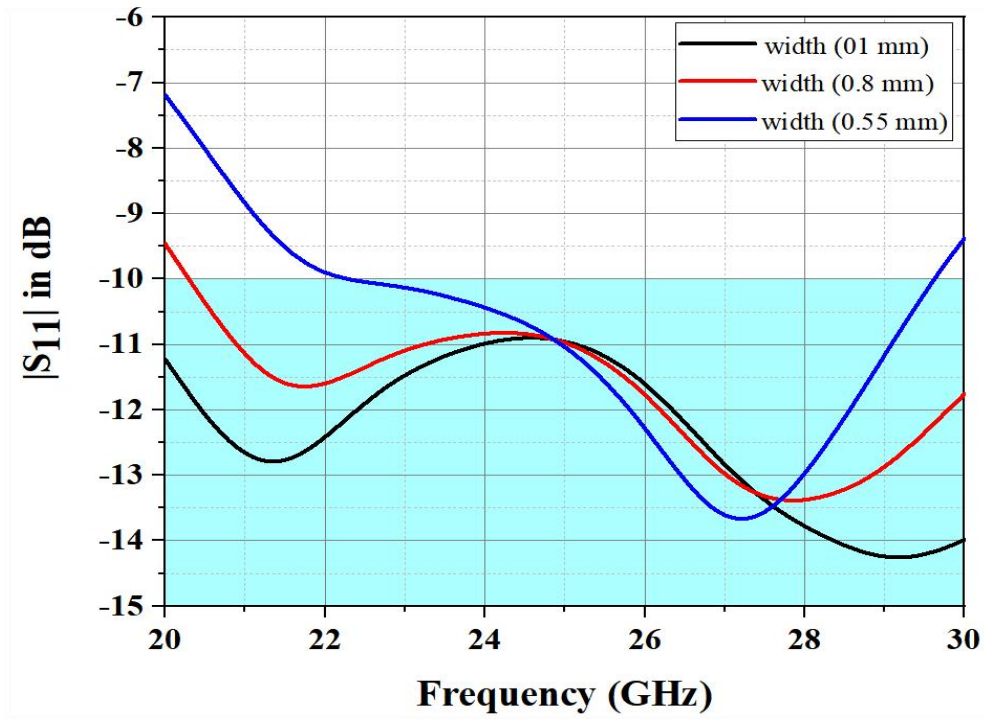
(a)



(b)



(c)



(d)

Figure 3.3: Simulated results in terms of Reflection coefficient (S_{11}) (a) step wise (b) The effect of ground plane (c) The effect of substrate height and (d) effect of feed line for Capsule shaped Single element UWB antenna

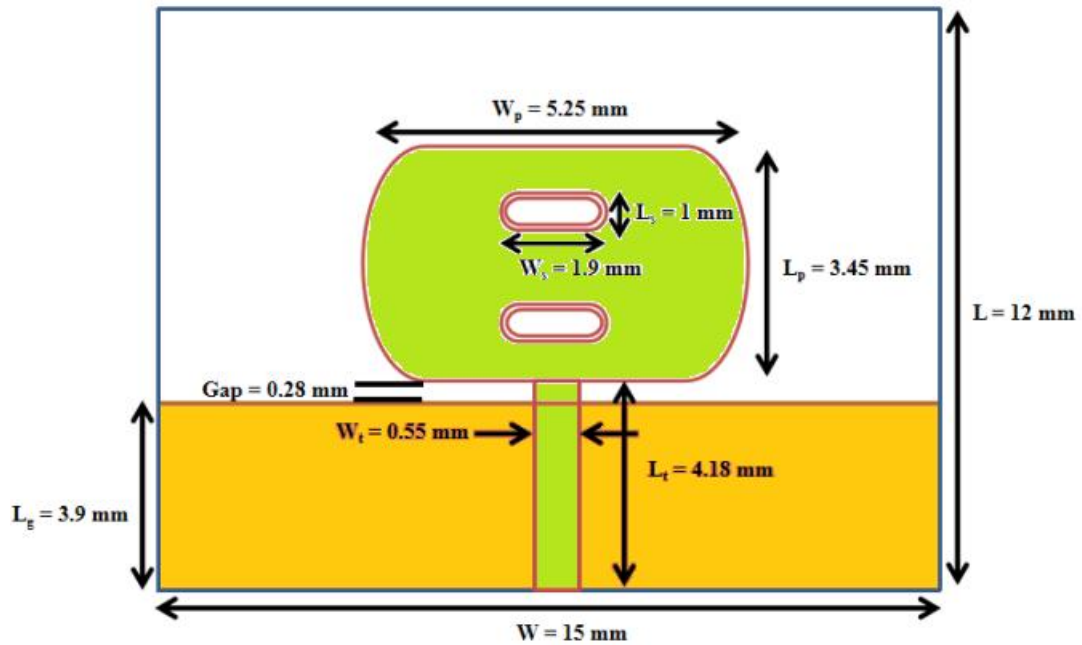


Figure 3.4: Unit Cell UWB Antenna design with dimensions

Figure 3.4 displays the diagram of the Ultra-Wide band (UWB) antenna. The capsule patch was etched on a partially grounded Roger RT/Duroid 5880 laminate of $3.9 \times 15 \text{ mm}^2$, with a thickness of 0.8 mm, permittivity of 2.2, and tangent loss of 0.0009. The patch has a radius of 1.725 mm and is coupled to a 4.18 mm feed transmission line. The Ansys High-Frequency Structure Simulator (HFSS) was used to simulate the proposed antenna.

Table 3.1: Dimensions of proposed capsule shaped UWB antenna

Antenna Parameters	Dimensions (mm)
Dielectric constant (ϵ_r)	2.2
Dielectric Substrate	Roger RT/Duroid 5880
Thickness of Substrate (h)	0.8
Length of Substrate (L_s)	12
Width of Substrate (W_s)	15
Transmission line length (L_t)	4.18
Transmission line Width (W_t)	0.55
Ground Length (L_g)	3.9
Ground Width (W_g)	15
Capsule patch length (L_p)	3.45
Capsule patch width (W_p)	5.25
Elliptical Slots (E_1 and E_2) length (L_s)	1
Elliptical Slots (E_1 and E_2) width (W_s)	1.9

Table 3.1 outlines the dimensions relevant to the antenna design specifications. It is important to note that the suggested antenna is compact in size, enabling for smooth integration into a variety of 5G wireless equipment. The proposed antenna demonstrates outstanding performance by achieving maximum bandwidth within the smallest achievable size.

3.3. SOFTWARE USED FOR SIMULATION

3.3.1. High Frequency Structure Simulator (Ansys HFSS):

Ansys HFSS 15 proves valuable in the design and simulation of high-frequency electronic structures, including antennas, filters, microwave and RF components, printed circuit boards, and connections. The software includes a variety of solutions and a user-friendly Graphical User Interface (GUI). HFSS allows interaction with fluid dynamics tools, structural, Ansys thermal,

and to verify thermal and structural reliability of electronic components. Widely adopted in research and development as a primary electromagnetic tool, it aids in the virtual prototype design process. HFSS has established itself as the industry standard for 3D modeling in high-frequency design, with its origins dating back to its initial development by Professor Zoltan Cendes and his students at Carnegie Mellon University in 1990 [98].

To achieve optimal performance, the programme integrates visualization, simulation, solid modelling, and automation, utilizing the Finite Element Method (FEM), advanced meshing and graphics techniques. Users have the freedom to select the solver that best meets their individual design needs.

3.3.1.1. Structure Designing Process:

The systematic process of creating and evaluating antenna designs using the HFSS tool follows a structured approach. It commences with the selection of the designer's model type, enabling the creation of a geometric model. The antenna construction is then outfitted with a suitable dielectric material, like FR4 Epoxy or Rogers RT Duroid 5880, as well as the specified dielectric constant and thickness.

Following this, the pivotal stage involves assigning sources, which may take the form of either lumped port lines or wave ports, and setting up boundary conditions. These conditions encompass perfect-E conditions for patches, grounding, and radiation, oriented towards a radiation box. After specifying boundary constraints for all solids and sheets in the HFSS simulation software, a port - whether wave or lumped - is inserted to stimulate the antenna construction.

The configuration for the solution setup is established once the structure has been properly modeled and confirmed. This includes defining the solution frequency and implementing a frequency sweep to generate data across the desired frequency range. In the last steps a far-field setup is used to determine critical far-field characteristics such as radiation patterns and antenna gain. Following that, the design is analysed to provide performance parameters such as VSWR, Directivity, 2D and 3D radiation patterns, S11, and Gain. To assist a thorough review, these parameters are displayed in Smith chart or tabular, graphical formats.

3.3.1.2. Antenna Design Steps:

The dielectric material used is critical in achieving the best radiation performance for the antenna. The dielectric material must have small dielectric loss and small dielectric constant. The material used for dielectric constants is determined by the application. Materials with low dielectric constant and thick substrates result in increased antenna efficiency and bandwidth, but larger structures. Materials those are having a high value of dielectric constant, on the other hand, cause increased surface waves and reduced bandwidth. To boost antenna efficiency, the proposed antenna design used Rogers RT Duroid as the dielectric substrate, which has a dielectric constant of 2.2 and a thickness of 0.8mm. Although RT Duroid is available in a variety of thicknesses, due to its high loss, the commonly used FR-4 Epoxy is avoided, making Rogers RT Duroid the preferred material for antenna fabrication. The chosen PCB board is a double layer with 0.35-micrometer-thick copper layers on both sides.

The performance of the designed antenna, produced utilizing PCB fabrication method, is evaluated in real-world assessments of antennas based on parameters such as Reflection coefficient , VSWR, Gain, and Radiation Patterns. The use of a Vector Network Analyzer (VNA) makes measuring Antenna Reflection coefficient and VSWR easier.

3.4. ANETNNA SIMULATION RESULTS

The performance of any antenna can be evaluated through its radiation and Reflection coefficient characteristics. The scattering and reflection properties of an antenna play a crucial role in its ability to transmit and receive electrical signals. The radiative features of an antenna, including directivity, gain, and power density within its resonant frequency bands, determine its effectiveness. These parameters can be visually depicted through 2D radiation patterns. The Ansys HFSS simulator is used to simulate antenna performance in the frequency range beginning at 20 gigahertz and ending at 30 gigahertz (GHz). An antenna's performance is measured using Reflection coefficient , bandwidth, voltage standing waves ratio, gain, and radiation pattern. Figure 3.5 illustrates the S-parameter (S11) for the suggested prototype antenna. The antenna exhibits resonance at a frequency of 27.20 GHz, with a reflection coefficient of approximately -13.66 dB at this resonant point. The reflection coefficient is less than (< -10 dB), indicating that the antenna has a broad bandwidth ranging from 24 gigahertz to 28 gigahertz.

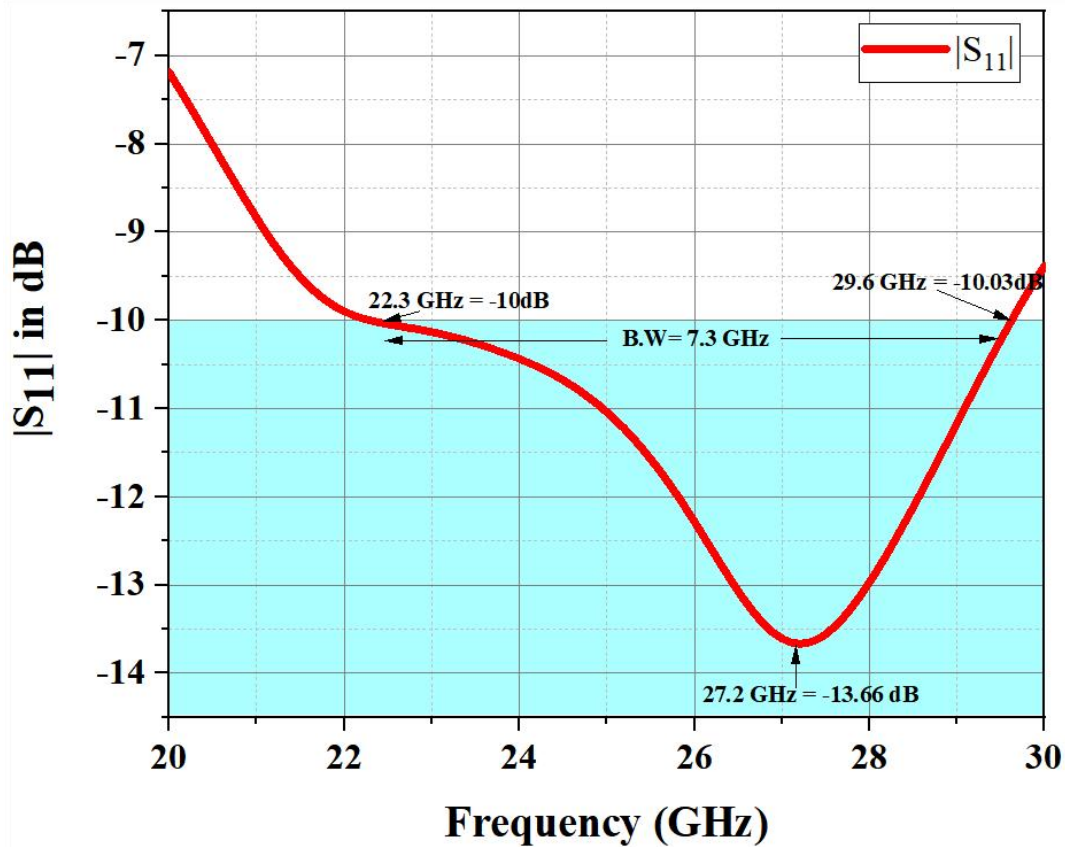


Figure 3.5: Simulated reflection coefficient (S_{11}) performance for Capsule shaped UWB antenna

Figure 3.6 depicts the VSWR value of the same design as a function of frequency. The VSWR value of 1.52 (less than 2) indicates that the recommended capsule-shaped patch antenna provides adequate impedance matching at 27.20 GHz. The suggested antenna is smaller than a number of recently reported antennas for similar applications. The slits and slots in the radiating patch were removed, enhancing the antenna's bandwidth. Employing the slotted antenna technique enhances the gain at the central operating frequency while also offering a broader bandwidth.

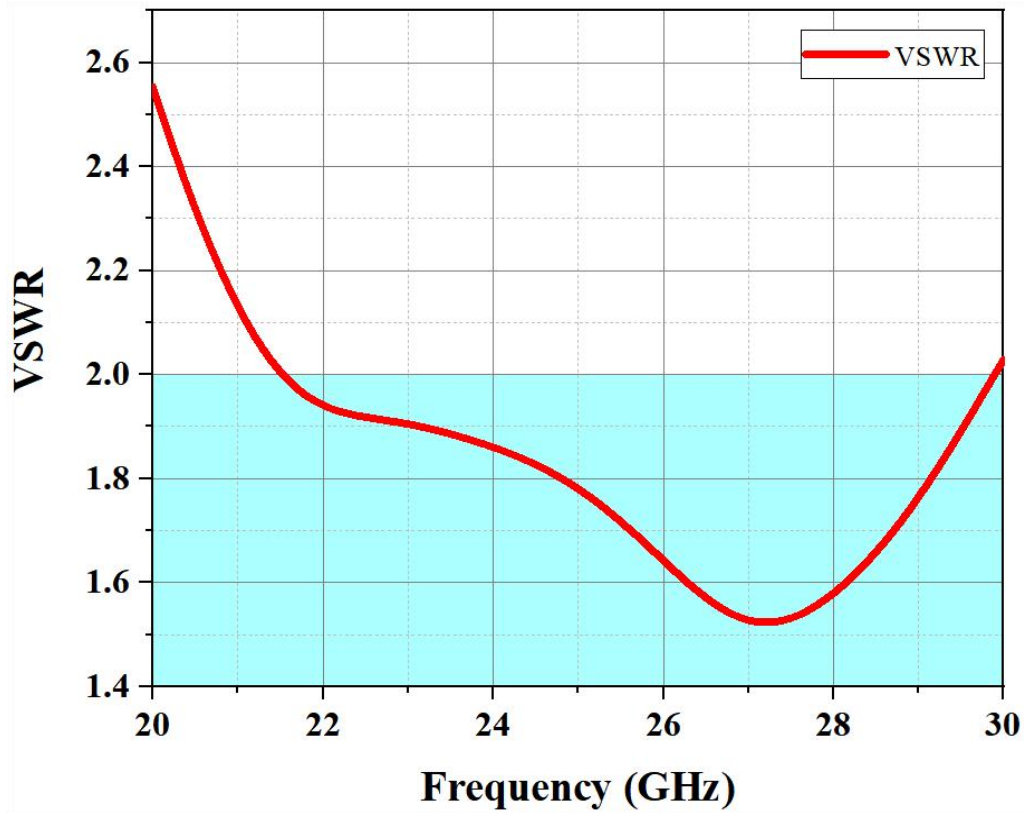


Figure 3.6: VSWR vs. Frequency Plot for Capsule shaped UWB antenna

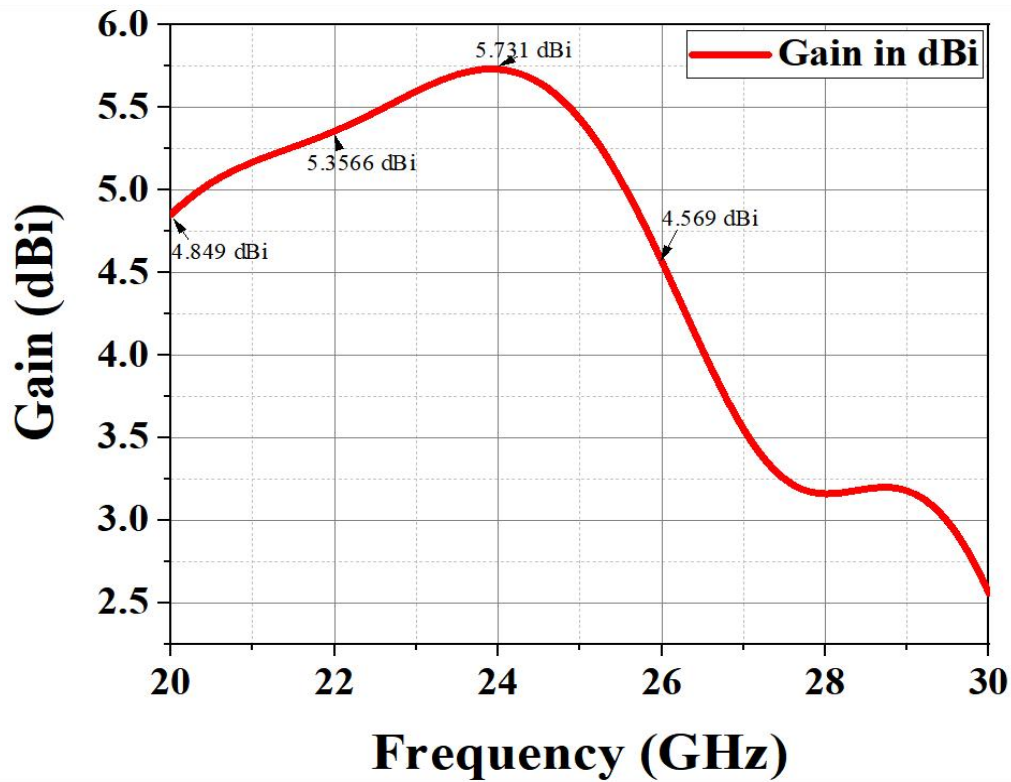
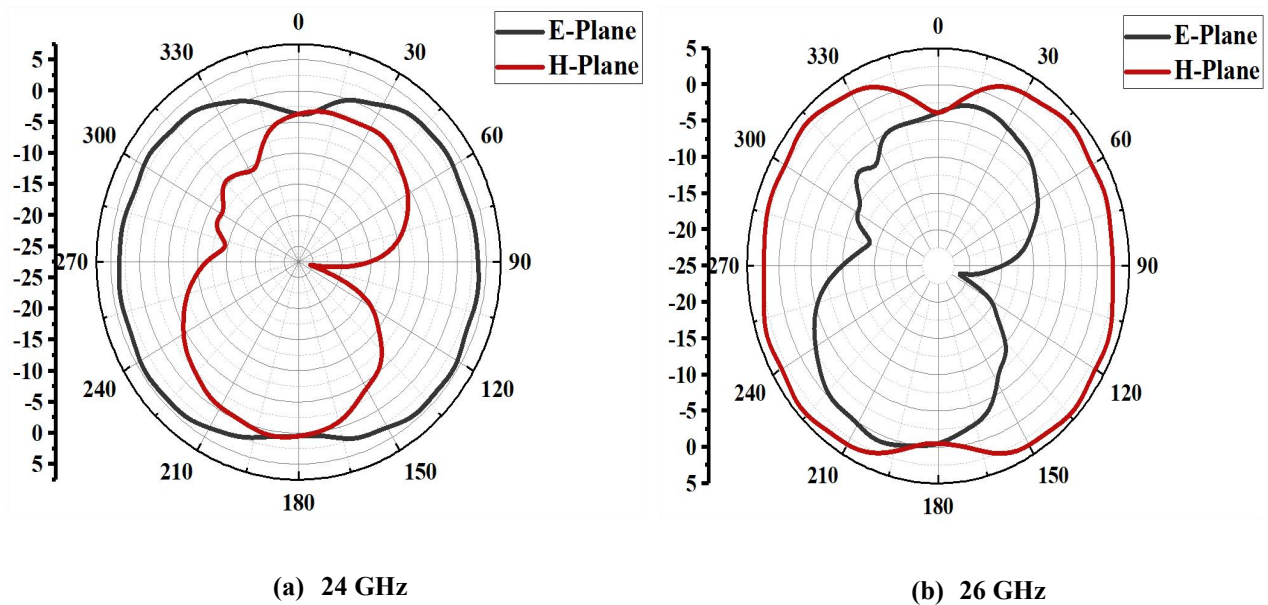
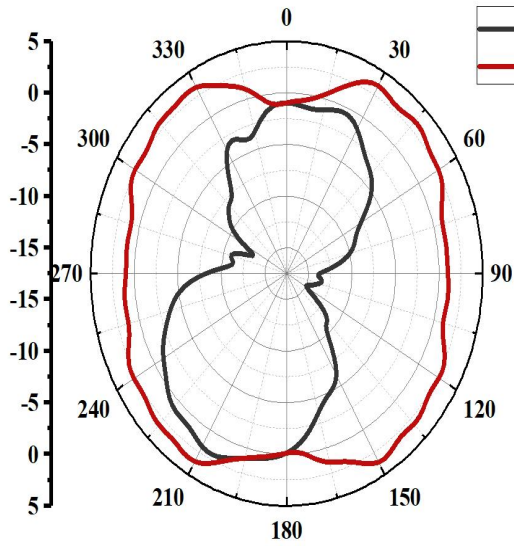


Figure 3.7: The Simulated Gain in dBi of proposed UWB single antenna

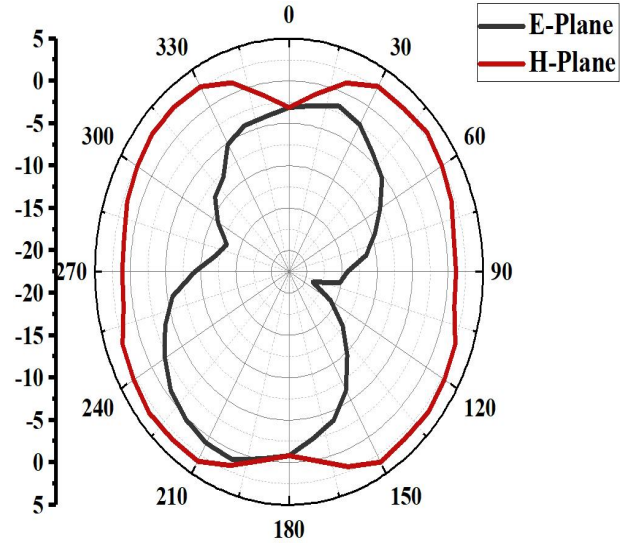
Figure 3.7 illustrates the frequency-dependent gain of the proposed design. The proposed antenna provides gains of 3.588 decibels at 24 gigahertz and 1.35 decibels at 27.20 gigahertz which are appropriate for the operational frequency band.

Figure 3.8 depicts the 2D gain radiation pattern of the produced UWB at various frequencies, emphasizing the XZ (E-plane) elevation plane and the YZ (H-plane) azimuth plane, which correspond to the characteristics of a UWB antenna. At 24 GHz, the gain is 5.02 dBi, 5.05 dBi at 26 GHz, and 4.53 dBi at 28 GHz. As a result, at 26 GHz, the maximum gain was reached. The figure-eight form pattern in the XZ - plane ($\phi = 0^\circ$) and an essentially omnidirectional pattern in the YZ - plane ($\phi = 90^\circ$) are clearly visible in the 2D directivity radiation pattern plot at 24, 26, and 28 GHz for the UWB antenna, which has a resonance frequency of 27 GHz. These findings unambiguously demonstrate that the UWB bandwidth radiation patterns are appropriate. At $\phi = 90^\circ$, the suggested antenna directivity is omnidirectional, while at $\phi = 0^\circ$, it is concentrated between 0° and 180° . All directions have the same level of directivity.



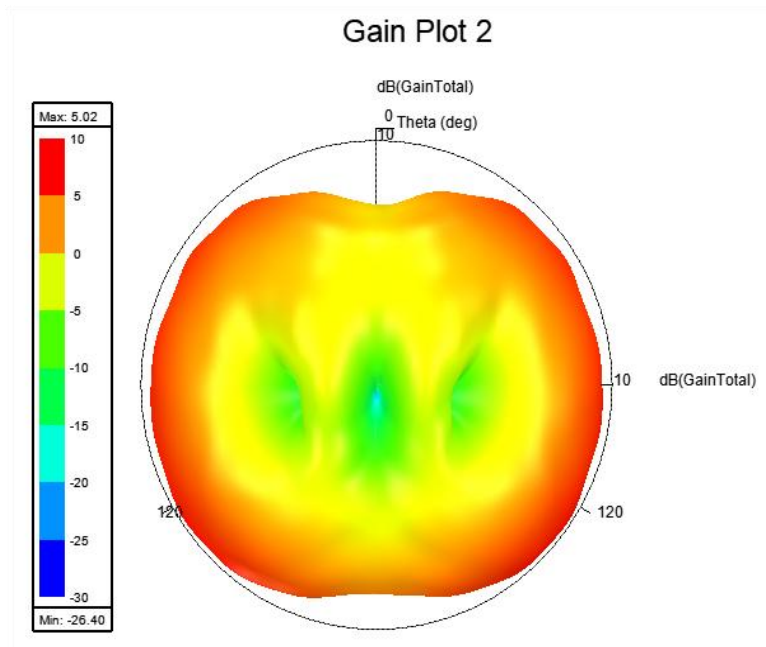


(c) 28 GHz

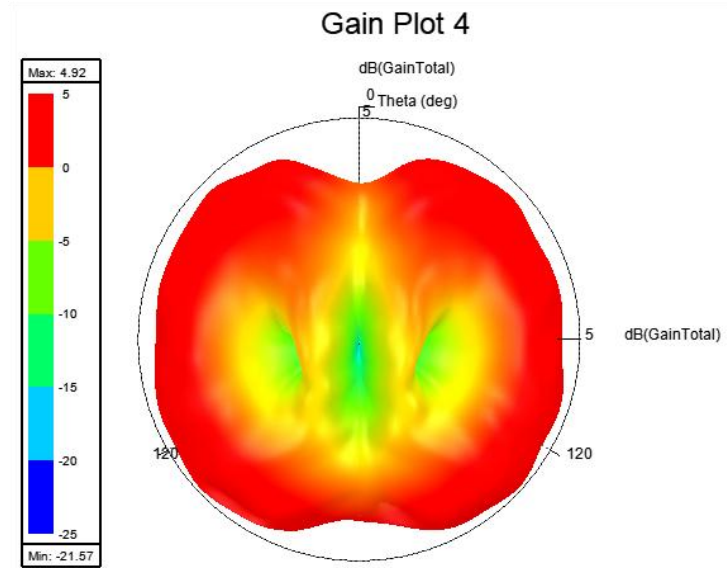


(d) Directivity at 27 GHz

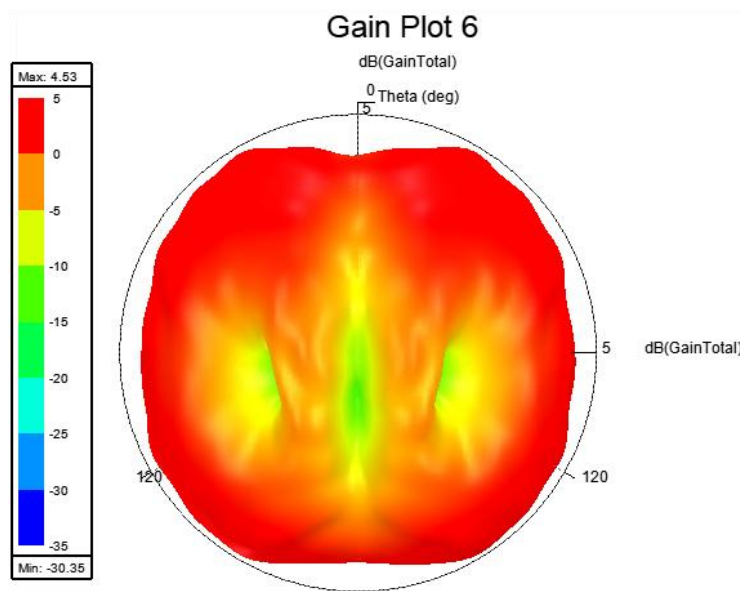
Figure 3.8: Simulated 2D Gain of proposed UWB antenna at different frequencies (a) 24 GHz (b) 26 GHz (c) 28 GHz and (d) directivity plot at 27 GHz



(a)



(b)



(c)

Figure 3.9: The radiation pattern Plot of the proposed UWB antenna in 3D
(a) 24 GHz, (b) 26 GHz, and (c) 28 GHz

Figure 3.9 displays the proposed UWB antenna's 3D gain radiation patterns at various frequencies, including the XZ (E-plane) elevation plane and the YZ (H-plane) azimuth plane, both of which are compatible with UWB antenna properties. At 24 GHz, the gain is 5.02 dBi, 5.05 dBi at 26 GHz, and 4.53 dBi at 28 GHz. As a result, the maximum gain was obtained at 26 gigahertz (GHz). To analyse the Reflection coefficient behaviour of the proposed structure, utilize the HFSS simulator to analyse electric current distribution density and antenna current

distribution at various operating frequencies and phi and theta values. Figures 3.10 and 3.11 show graphs of the proposed antenna's electric and magnetic field densities at resonance. The largest concentration of current is detected near the feed line borders and at the periphery of the capsule patch, contributing to the proposed antenna's wide bandwidth. In addition, the current is dispersed uniformly throughout the surface of the capsule patch. The current distribution along the patch's borders extends the electrical length of the feed line, causing the antenna to resonate with a low Reflection coefficient .

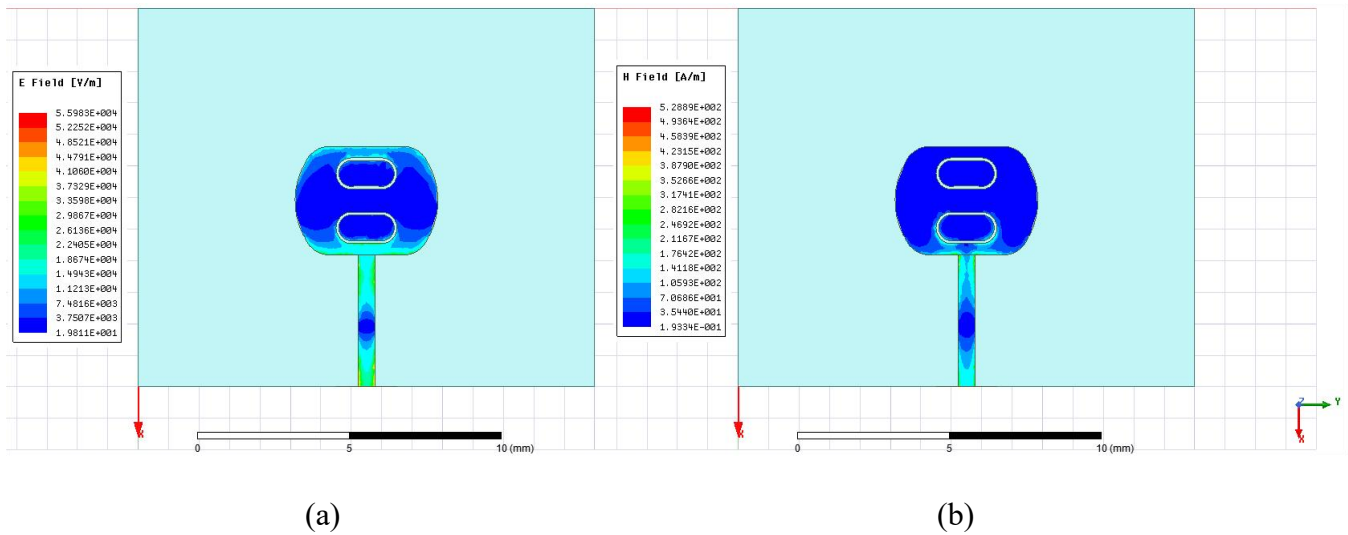


Figure 3.10: HFSS Simulation E-field and H-field current distribution of proposed antenna at 27GHz frequency

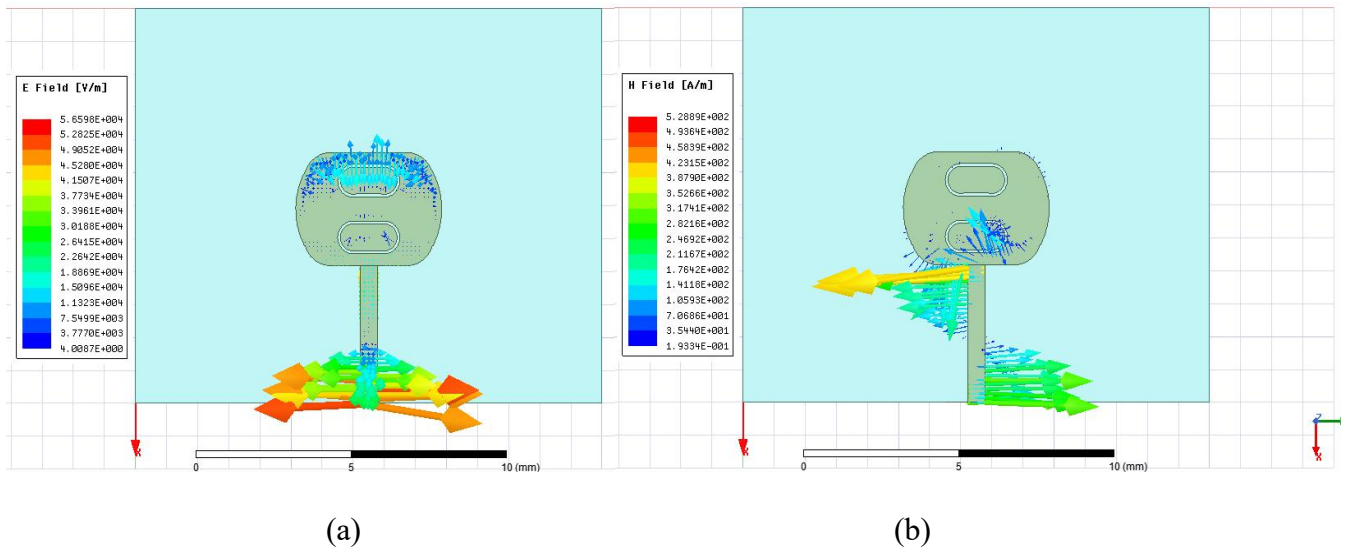


Figure 3.11: HFSS Simulation E-field and H-field vector current distribution of suggested antenna at 27GHz frequency

The capsule radiating element's edge has the largest current density, as can be observed. Additionally, the current spread is made constantly throughout the finite ground plane, with an immediate increase in current strength due to electromagnetic coupling effects with the ground at the bottom of the capsule patch.

3.5. PERFORMANCE COMPARISON

Table 3.2 compares the proposed UWB antenna's performance, including size, frequency band, gain, and VSWR, to previously published results. According to the chart, the proposed MIMO antenna has the smallest dimensions and resonant frequencies. The suggested antenna also has a broad frequency range and produces high gain. As a result, the suggested UWB antenna performs similarly to previous experiments.

Table 3.2: Comparison of the proposed UWB antenna with previous works

Ref. No.	Size (mm ³)	Substrate Used	Frequency Rang (GHz)	Gain (dB)	Reflection Coefficient (S ₁₁)	VSWR
[99]	25×25×1.45	FR4-epoxy	3.1 to 16.24	4.56	Not Present	Not Present
[100]	20×20×1.5	FR4	3 to 15 (3.3, 4.6, 9.2)	2.95, 4.15, 4.30	<-25dB	Not Present
[101]	38×40×1	FR4	5.15–5.825	Not Present	<-40dB	Not Present
[102]	20×33×1.6	FR4	2.70–10.15	– 2–1.5	Not Present	< 2
[103]	41.95×21.2 × 1.27	Rogers 5880 LZ	2.5 to 10.5	5.2	<-25	Not Present
[104]	18×17×1.605	FR4	24 to 31	3.53	-22	1.16
[105]	50×41×1.75	Rogers RT Duroid 5880	3 to 11.4 GHz	5.27	< -10	< 2
[106]	30×35 ×0.9	FR4	3.1 to 10.6 GHz	Not Present	<-10dB	< 2
[107]	13×12 ×1.6	FR4	11.2 GHz	3.21 and 1.2	-37	< 2

				dB _i		
Proposed Antenna	12×15 ×0.8	Rogers RT duroid 5880	24 to 28 GHz	3.5	-13.66	1.57 (< 2)

When compared to all the antenna designs outlined in Table 3.2, the suggested antenna is compact in size and fulfills all criteria, including gain, VSWR, and reflection Coefficient, among others. As a result, the proposed architecture is an excellent fit for high-frequency, 5G wireless, and UWB applications.

3.6. SUMMARY

A novel microstrip patch antenna, featuring a simple capsule-shaped design with a slot-loading technique, has been created specifically for 5G applications operating at millimeter-wave frequencies. The compact nature of the antenna ensures its seamless integration into confined spaces around microwave electronics, particularly at higher frequencies. To enhance the antenna design, two elliptical slots have been incorporated, resulting in increased current density. The suggested antenna boasts optimal dimensions of $(15 \times 12 \times 0.8)$ mm³, underscoring its compact and straightforward design.

This proposed design offers several advantages over other UWB microstrip antennas, including reduced radiation loss, lower dispersion, a novel configuration, and commendable gain without the need for additional techniques. The antenna exhibits favorable characteristics, including a low VSWR (< 2), a broad bandwidth (10 GHz spanning from 20 to 30 GHz), and satisfactory gain (3.53 dB). Furthermore, the study describes radiation patterns in the E and H planes at different frequencies.

The introduction of a capsule-shaped UWB antenna with elliptical slots is proposed to achieve high bandwidth in the SHF range. A key highlight of this design is its miniaturization, making it particularly suitable for both 5G and UWB applications at millimeter-wave frequencies, owing to its appropriate geometry and straightforward structure.

CHAPTER-4

DESIGN A COMPACT QUAD-PORT UWB MIMO ANTENNA FOR 5G MILLIMETER WAVE APPLICATIONS

4.1. INTRODUCTION

The anticipated 5th generation (5G) wireless communication system aims to utilize the millimeter-wave frequency range, known for its abundant spectrum, to tackle the existing bandwidth challenges in contemporary wireless networks. [108]. Modern wireless communication technologies necessitate a system capable of rapidly exchanging substantial volumes of data while enhancing capacity, reliability, and security with minimal complexity.

As a result, the Fifth Generation (5th G) technology is now being developed. The majority of nations have now standardized 5G after conducting in-depth studies to handle the demand for increased bandwidth and data rates, which is a difficult problem [109]. In recent years, MIMO technology has received a lot of interest as a solution to this problem. The researchers propose using Multiple-Input Multiple-Output (MIMO) technology to improve throughput, data rates, and bandwidth utilization. When creating the fifth generation of MIMO antennas, three key mm-wave spectrum requirements must be considered: high bandwidth, high gain, and ultimately, a unique design and structure to enable simple integration into a MIMO system [110]. A feasible technology to satisfy the 5G requirements is the many antenna systems (MIMO Technology), which improves spectral efficiency with increased channel capacity. However, the task of developing a MIMO antenna system with outstanding element isolation poses a significant difficulty. With data rates reaching several Gigabits per second (Gbps) and expanded bandwidth, 5G technology has primarily focused on the wave spectrum (3-300 GHz) of millimeter and centimeter [111]. Many wireless networks and applications, such as Wi-Fi, Wi-MAX, mobile communication, Bluetooth, and Industrial, Scientific, and Medical (ISM), utilize the lower segment of the spectrum. On the other hand, the higher part of the spectrum, which is open to 5G technologies [112], is mostly unused.

Keeping an eye on the higher spectrum causes certain challenges for this 5G technology, though. As signals at lower frequencies can easily penetrate large buildings and trees and travel distances exceeding tens of kilometers, a challenge arises in the free space propagation of these

frequencies. Nevertheless, due to their limited range and challenges in penetrating dense obstacles, signals in higher frequency bands exhibit a smaller coverage area [113].

The incorporation of small cell base stations like Pico-cells and femto-cells can enhance frequency reuse by leveraging propagation losses. Another challenge for wireless communication at higher frequencies arises from adverse weather conditions, particularly rain, which renders these frequencies impractical [114]. In plenty of other words, meteorological conditions like rain, snow, fog, etc. have a big impact on these frequencies. Electro-Magnetic (EM) waves experience significant quality losses in the signal and intensity as a result of these atmospheric attenuation, among other things [115]. This issue can be fixed, though, by creating an antenna using a high gain and good directivity [116].

Results from a previous study suggest that the MIMO antenna system has the potential to meet the UWB system's specifications. Because different antenna systems offer additional performance standards, it is a difficulty to build such an antenna. To prevent channel capacity loss, antenna elements' mutual coupling or isolation, one of the critical performance factors, should be as low as practical [117]. The two main problems that MIMO antennas face are the antenna's dimensions and its constituents' mutual coupling. Isolation between antenna elements refers to the ability of an antenna system to prevent energy from one antenna element from coupling into adjacent elements. Good isolation is crucial in multi-antenna systems like MIMO (Multiple-Input, Multiple-Output) to ensure that each element operates independently without interference. This isolation directly impacts the system's performance, influencing parameters like capacity, efficiency, and signal quality.

One way to do this is to scale back the MIMO antenna for the same devices that are placed adjacent to one another. Due to this design, there is mutual coupling.

One effective technique in order to scale down the MIMO antenna system is utilizing polarization and angle diversity. When compared to a spatially separated MIMO, orthogonal polarization has shown to offer good isolation with little space needs. Similar to this, angle diversity uses antennas that radiate at various angles to create a variety of radiation patterns. For optimal diversity performance, nearby elements should be kept at a low mutual coupling. Another is the antenna placement and orientation [118],

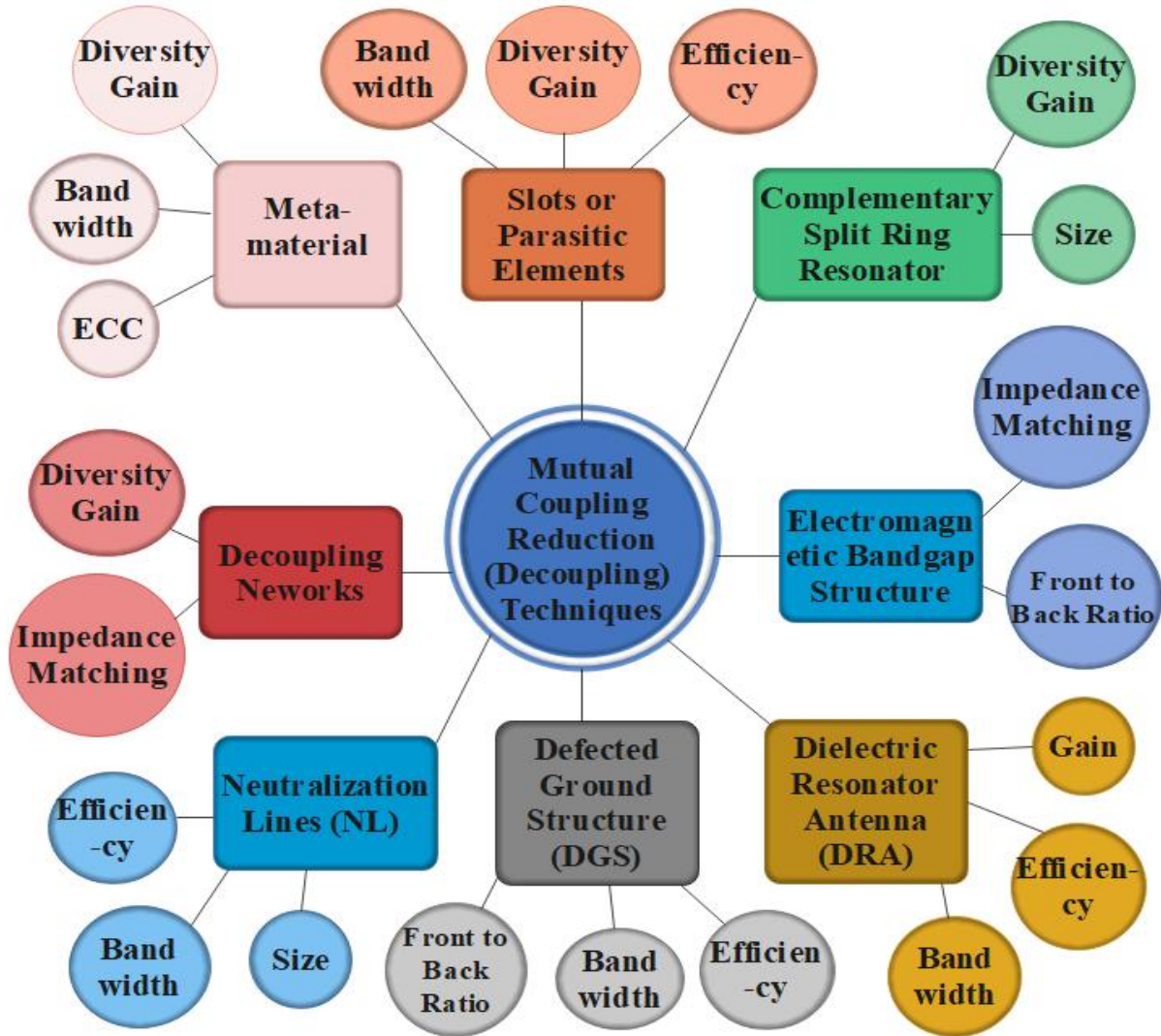


Figure 4.1: Mutual-coupling reduction/ Isolation enhancement techniques for 5G massive- MIMO antennas

There have been several techniques to minimize coupling between antenna elements like decouple network, parasitic element, defected ground structure (DGS), neutralization line (NL), meta-material structure, etc. are a few examples of isolation approaches that minimize mutual coupling as shown in Figure 4.1.

Ultra-wide band (UWB) technology can be employed to meet these requirements. Given that the UWB technique allows for an economical infrastructure to deliver high data rates, it can find applications in various wireless communication systems. The conventional UWB technology is affected by multipath propagation and it is able for short-distance transmission.

MIMO (Multiple-Input Multiple-Output) technology will boost UWB system data throughput and reliability while slightly reducing power and bandwidth. Due to its exceptional performance, MIMO technology is hence widely sought-after and in demand. The MIMO technology has three requirements. To avoid multipath fading, sufficient isolation between the radiating elements must first be found. Second, the overall antenna size needs to be smaller due to the limitations of space in handheld devices. Finally, and most significantly, the UWB system requires some form of the science of filtration since, when other narrowband systems like WLAN, Wi-Fi, and Wi-Max are present in the UWB area; it has a tendency to interfere with the intended UWB spectrum.

UWB antennas have the following key characteristics: wide impedance bandwidth, constant gain in the desired direction, constant polarization, high radiation efficiency, linear phase response, small size, low profile, embedded, low cost, and minimal complexity (installation, fabrication, materials, and maintenance). Low-power UWB systems transmit data, and channel capacity varies with bandwidth (i.e., data transfer rates up to several Gbps or hundreds of Mbps). UWB signals do not considerably interfere with the other wireless networks. UWB provides extremely trustworthy and safe communication solutions.

4.2. MOTIVATION FOR UWB ANTENNA DESIGN

Numerous researchers, scientists, and engineers consider Ultra-Wide band (UWB) technology as an intriguing and promising option for achieving higher speed, elevated data rates, and short-range indoor wireless communications. The approval by the US FCC in 2002 for UWB radio applications in the frequency band between 3.1 GHz and 10.6 GHz further underscores its potential [119]. Both academic research and the business world are currently very interested in the development and deployment of UWB systems. The increasing use of UWB systems has led to several improvements in design of UWB antennas. Among the numerous difficulties facing the installation of a UWB system is the creation of an adequate antenna that can function across the whole UWB spectrum. This is because the antenna makes a substantial impact to the UWB system's overall performance. In recent years, UWB systems have adopted a range of antenna designs, including the spiral antenna, bi-conical antenna, Vivaldi antenna, log periodic antenna, and so on, to achieve broad bandwidth.

A Vivaldi antenna's directional radiation pattern makes it unsuitable for use with either of these applications because mobile/portable devices and indoor wireless communication both need omnidirectional radiation patterns make it easier and more efficient for transmitters and receivers to communicate with one another in all directions. The usage of these devices is constrained by the 16 enormous physical characteristics of single- and double-conical antennas [120] difficult designs. Academics are showing more interest in mobile/portable devices and UWB indoor wireless communications that can address all of these issues. The planar or printed antenna is a different option. Widely shaped printed antennas, including elliptical, circular, rectangular, and trapezoidal ones, have been proposed and are depicted in Figures 4.2 and Figure 4.3, respectively, for use in UWB applications.

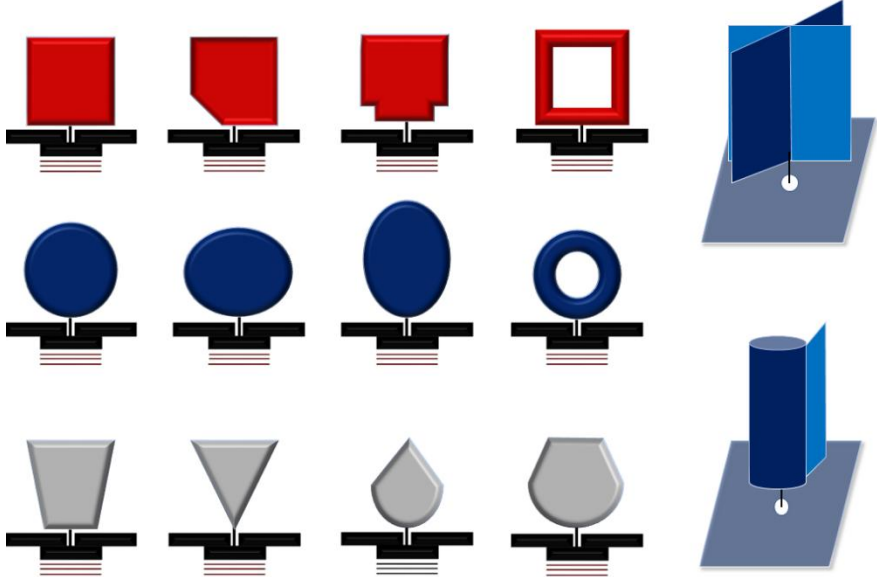


Figure 4.2: Different shapes of planar UWB antennas [114]

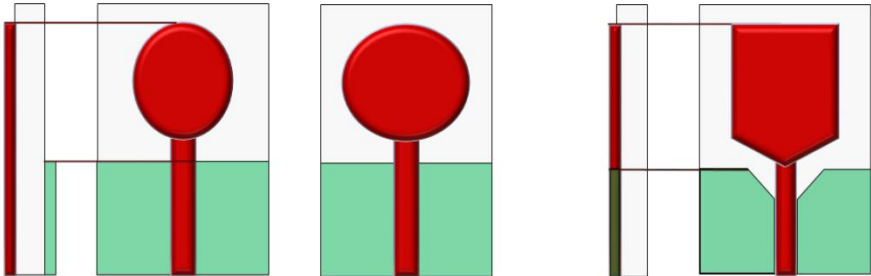


Figure 4.3: UWB PCB or printed antenna designs [114]

Recent years have seen a lot of research into conventional antenna design for ultra-wide band wireless communication. Numerous aspects of antennas are common among them, and it's important to note that each design aims an increased perfectly matched impedance spectrum without losing a radiation pattern that is omnidirectional. The creation of UWB in antennas is achieved by leveraging design strategies that support multiple resonances, broadband impedance matching, dispersion radiation mechanisms, and careful manipulation of the current distribution and electromagnetic fields. By optimizing these physical factors, the antenna can efficiently radiate across a wide frequency range, which is the hallmark of UWB technology.

4.3. DESIGN PROCEDURE FOR QUAD PORT MIMO ANTENNA

The antenna assembly consists of four resonant patches, each of which is a metalized capsule-shaped patch that is fed through a 50-Ohm microstrip line at the bottom centre. The four radiating elements are positioned along the periphery of a metallic ground plane in a capsule shape, aiming to minimize the mutual coupling among them. The ground plane is shaped in a capsule form to attain symmetrical patterns of radiation for the MIMO antenna. The suggested unique design for a compact size quad port MIMO antenna is conceptually based on a simple and efficient approach that employs Resonant Patch Antenna elements as radiating elements. Figure 4.3 illustrates the configuration and measurements of a 4×4 quad port UWB-MIMO antenna. Feeding portion of the antenna is constructed such that it is further apart from the ground plane. This minimizes the interactions between the ports while maintaining the desired input impedance values for each port.

Selecting the first dimensions of a microstrip line is essential for quality performance.

The equation that describes the relation between characteristic impedance Z_0^{MPA} and the width of a microstrip line is quite straightforward [121].

Where, W is width of the microstrip line which is around 0.55 mm and h is the height which is 0.8 mm and $Z_0^{MPAfeed} = 50\Omega$.

$$Z_0^{MPA} = \frac{120 \pi}{\sqrt{\epsilon_r \left[\left(\frac{w}{h} \right) + 1.393 + 0.667 \ln \left(\left(\frac{w}{h} \right) + 1.444 \right) \right]}} \quad (4.1)$$

The small size and wide band requirements may be fully meet by this innovative UWB MIMO antenna design without sacrificing aspects like the radiation pattern, gain, efficiency, and mutual

coupling. A compact 4×4 UWB MIMO antenna designed for 5G wireless devices operates in the 22 gigahertz to 30 gigahertz frequency spectrum, with an impressive 8 GHz bandwidth.

Table 4.1: UWB MIMO antenna geometrical specifications

Parameters	W	W_f	W_G	W_P	W_S	L	L_f	L_g	L_p	L_s
Unit (mm)	36	0.55	15	5.25	1.9	24	4.18	3.9	3.45	1

Table 4.1 details the dimensions relevant to the antenna design specifications. It is important to highlight that the recommended antenna features a compact and miniature layout shown in Figure 4.4, facilitating its integration into various 5G wireless devices. Notably, the proposed antenna demonstrates outstanding performance by achieving the maximum possible bandwidth within the smallest achievable size.

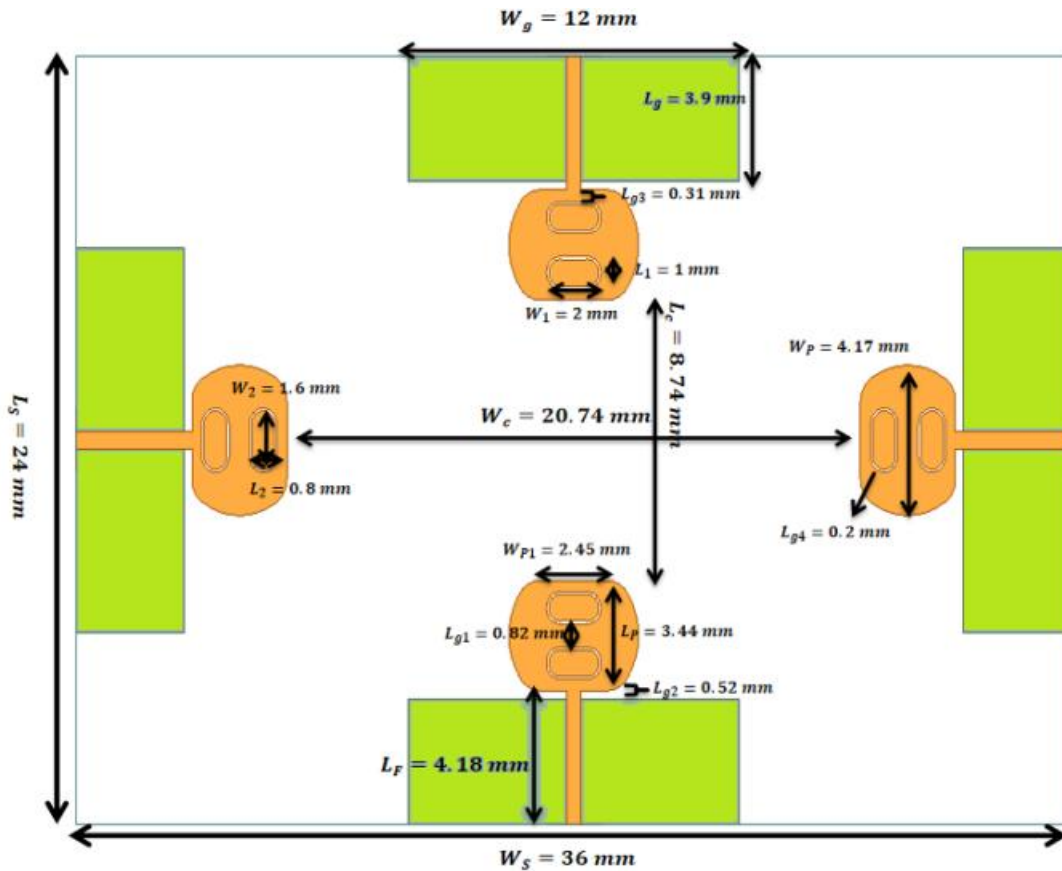


Figure 4.4: Geometry of Quad-port UWB MIMO antenna

4.3. ANTENNA SIMULATION AND RESULTS

This antenna features two elliptically shaped slot structures and a capsule patch, as well as four ports with reflection coefficients below -10 dB from 22 to 30 GHz, an ultra-broadband with a BW of 8 GHz. Isolation parameters S_{12} , S_{13} , and S_{14} are significantly enhanced due to the elliptical slots cutting from the radiating patch at the correct position, allowing enhanced isolation without the need for a separate decoupling network. Furthermore, improved isolation is attained by setting up the antenna components orthogonally in the suggested arrangement.

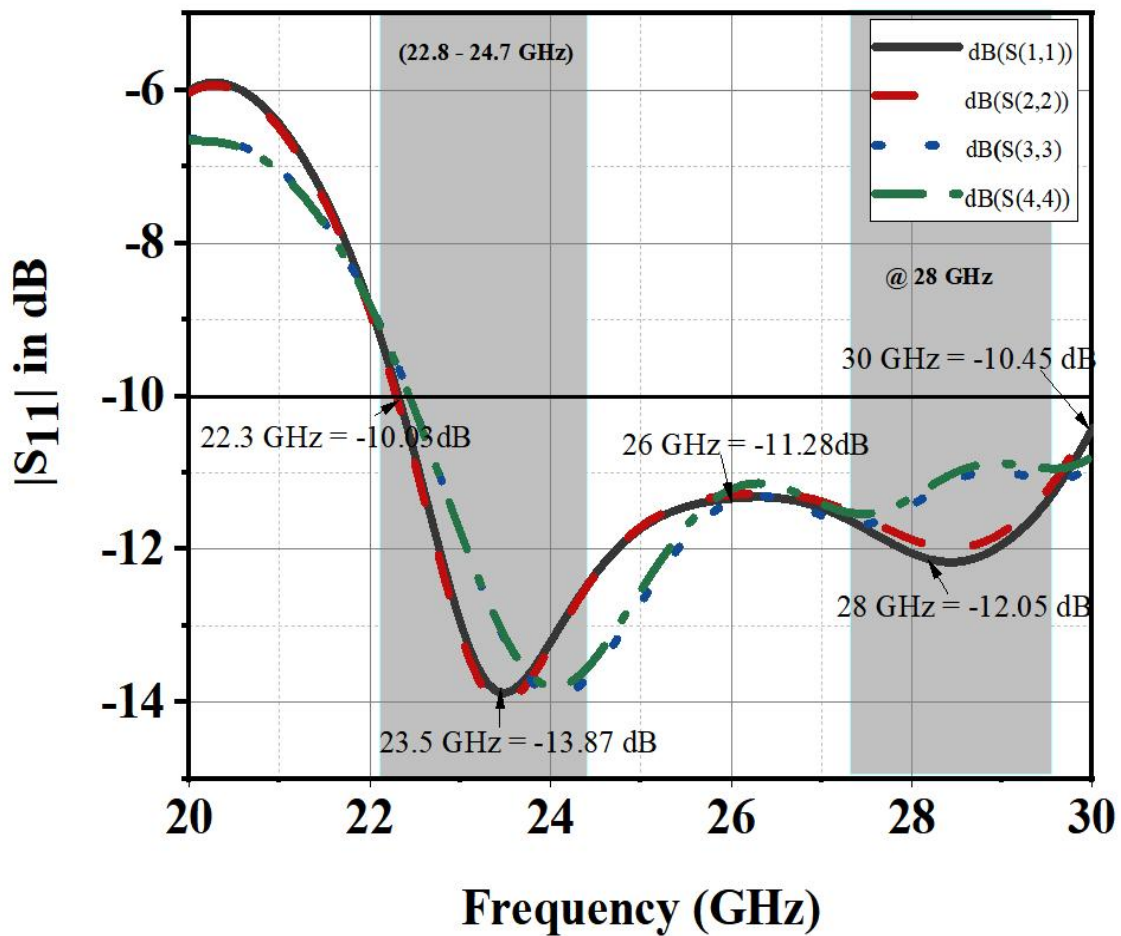


Figure 4.5: Quad port UWB MIMO antenna performance simulation for Reflection Coefficient (S_{11}) in dB.

Figure 4.5 depicts the overall performance of the proposed antenna in terms of its reflection coefficient. The chart shows the suggested antenna's wide impedance bandwidth, which

resonates across the operational frequency range of 22 gigahertz to 30 gigahertz, with an average Reflection coefficient of around -12 decibels.

Table 4.2: Reflection Coefficient values at different frequencies

Freq. (GHz)	dB(S _{1,1})	dB(S _{2,2})	dB(S _{3,3})	dB(S _{4,4})
24	-13.2147	-13.2724	-13.8944	-13.7957
25	-11.727	-11.7049	-12.6975	-12.5384
26	-11.3345	-11.2873	-11.3729	-11.2137
27	-11.4625	-11.3743	-11.5553	-11.4017
28	-12.052	-11.8727	-11.424	-11.3204

It has been concluded from the above Table 4.2 that it has a good Reflection coefficient because all the values are below -10dB.

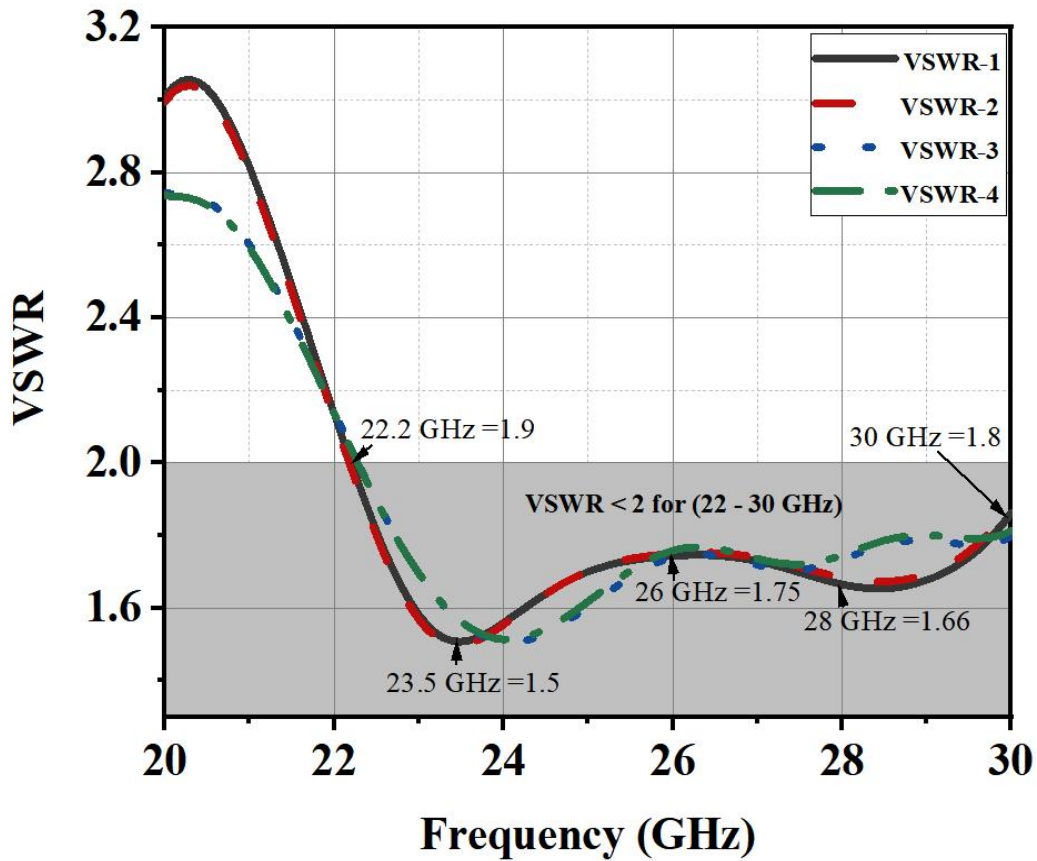


Figure 4.6: Simulated VSWR Plot for quad port UWB MIMO antenna

Figure 4.6 shows a plot of the Voltage Standing Waves Ratio against frequency. The reflection coefficient, depicting the power reflected from the antenna, is a function of VSWR. The VSWR quantifies the disparity between the peak and minimum amplitudes of a standing wave. A good VSWR for an antenna is one between 1 and 2. According to Table 4.3, it is 1.55 at 24 GHz, 1.65 at 25 GHz, 1.73 at 26 GHz, etc. It is satisfied that the VSWR performance is less than 2, while it should be between 1 and 2.

Table 4.3: VSWR values at different frequencies

Freq. (GHz)	VSWR(1)	VSWR(2)	VSWR(3)	VSWR(4)
24	1.558876	1.554149	1.506162	1.513428
25	1.699819	1.70222	1.603508	1.618118
26	1.744203	1.749775	1.739706	1.758572
27	1.729343	1.739543	1.718809	1.736359
28	1.665563	1.684193	1.73377	1.745867

Using the antenna elements' structural characteristics, isolation is utilized to determine the degree to which the adjacent antenna parts are connected electrically. Figure 4.7 shows the S-parameters for the simulated configurations when ports are excited, as well as an isolation map of the recommended quad port UWB MIMO antenna. Table 4.4 displays the antenna's operational frequency range and isolation parameter values. The table clearly shows that it has the broadest bandwidth and the average isolation -21.92dB- S(1,2), -24.70dB- S(1,3), -24.72dB- S(1,4), -24.74dB- S(2,3), -24.73dB- S(2,4), and -38.73dB- S(3,4) over the 22 to 30 GHz frequency range.

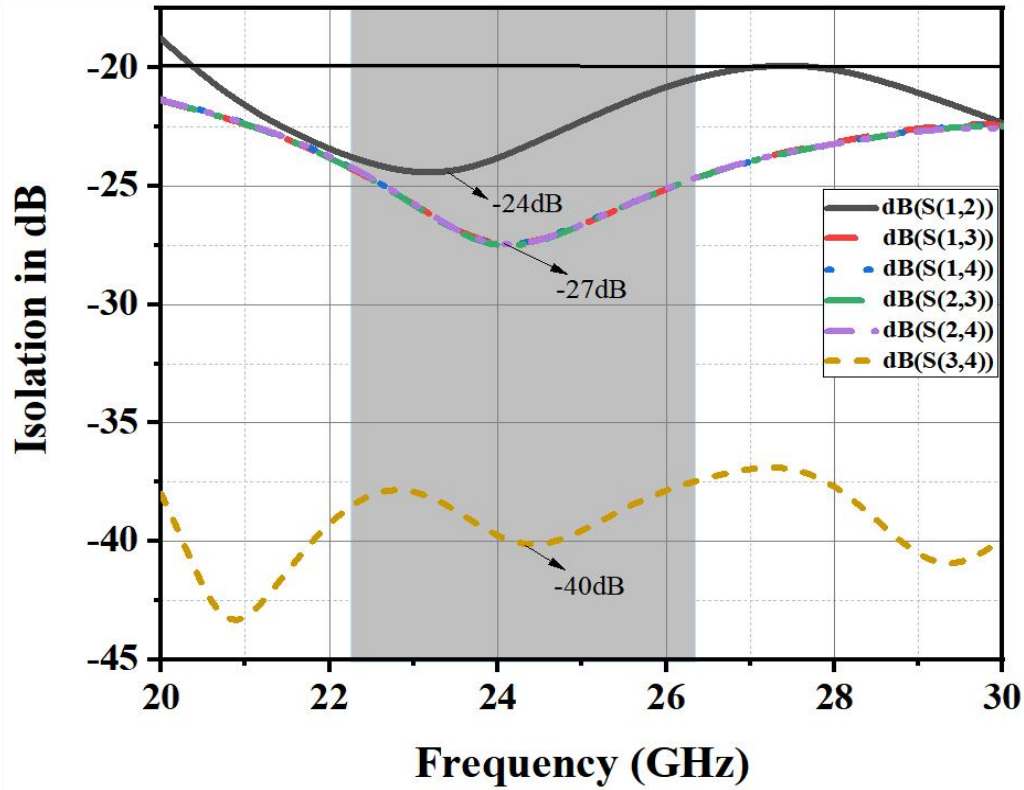


Figure 4.7: Simulated Isolation plots for quad port UWB MIMO antenna

Table 4.4: Isolation of all port at different frequencies

Freq. (GHz)	dB(S ₁₂)	dB(S ₁₃)	dB(S ₁₄)	dB(S ₂₃)	dB(S ₂₄)	dB(S ₃₄)
24	-23.8106	-27.4036	-27.4342	-27.4795	-27.4421	-39.762
25	-22.2565	-26.6299	-26.5797	-26.6366	-26.6167	-39.5513
26	-20.8196	-25.1316	-25.1332	-25.1236	-25.1114	-37.8659
27	-20.0087	-23.9274	-23.9776	-23.9583	-23.937	-36.9539
28	-20.0916	-23.158	-23.2209	-23.2279	-23.2164	-37.6987

Figure 4.8 illustrates the simulated gain characteristics of the proposed antenna. The antenna's gain spans from 1.47 dB to 4.06 dB across frequencies ranging from 24 GHz to 28 GHz, with an average gain of 3.0 dB. Notably, 27 GHz exhibits the highest gain value of 4.06 dB. All the gain values with corresponding frequencies are detailed in Table 4.5.

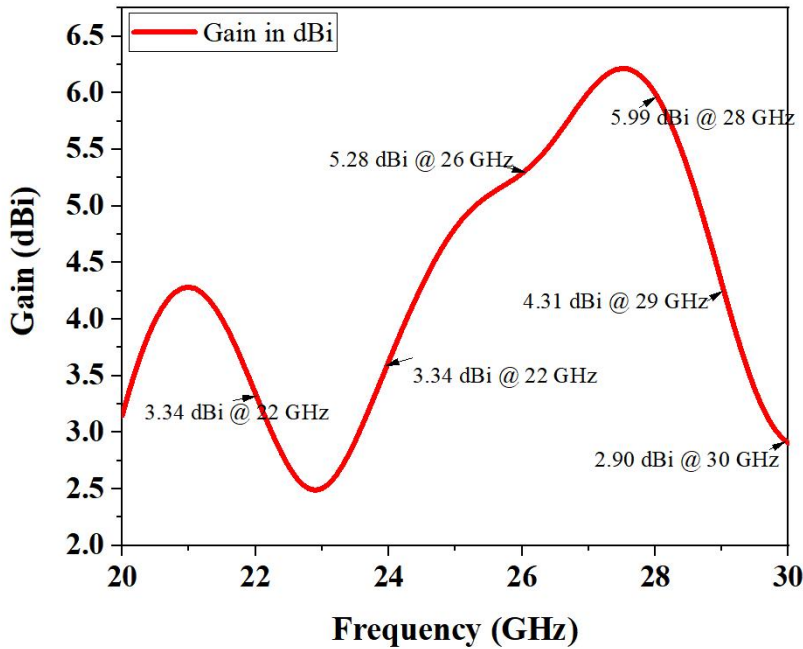


Table 4.5: Gain value at different frequencies

Freq. [GHz]	Gain (dB)	Gain (dBi)
24	1.4777	3.977
25	2.6670	5.1670
26	3.3033	5.8033
27	4.0682	6.5682
28	3.6253	6.1253

Figure 4.8: Simulated Gain vs. frequency plot for quad port UWB MIMO antenna

Table 4.6: The suggested UWB MIMO antenna simulation results in terms of S_{11} , VSWR, Isolation and Gain

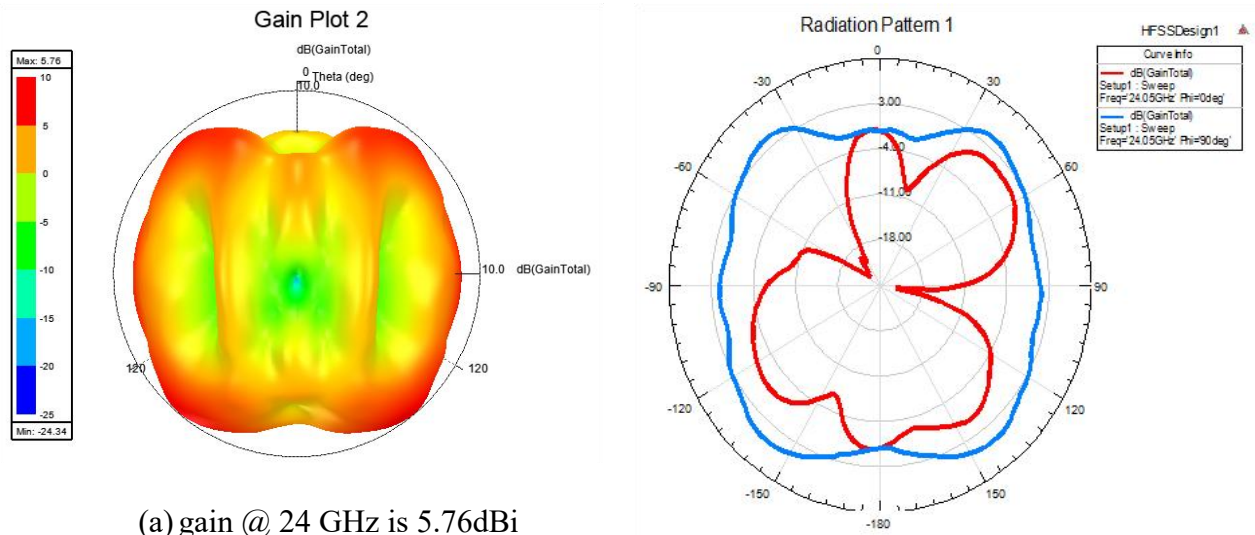
Freq. (GHz)	Reflection coefficient (dB)	VSWR	Isolation	Gain (dB)
24	-13.214	1.558	-23.810	1.477
25	-11.727	1.699	-22.256	2.667
26	-11.334	1.744	-20.819	3.303
27	-11.462	1.729	-20.008	4.068
28	-12.052	1.665	-20.091	3.625

In Table 4.6 it has all parametric values given for Reflection coefficient , VSWR, isolation and gain at respected frequencies.

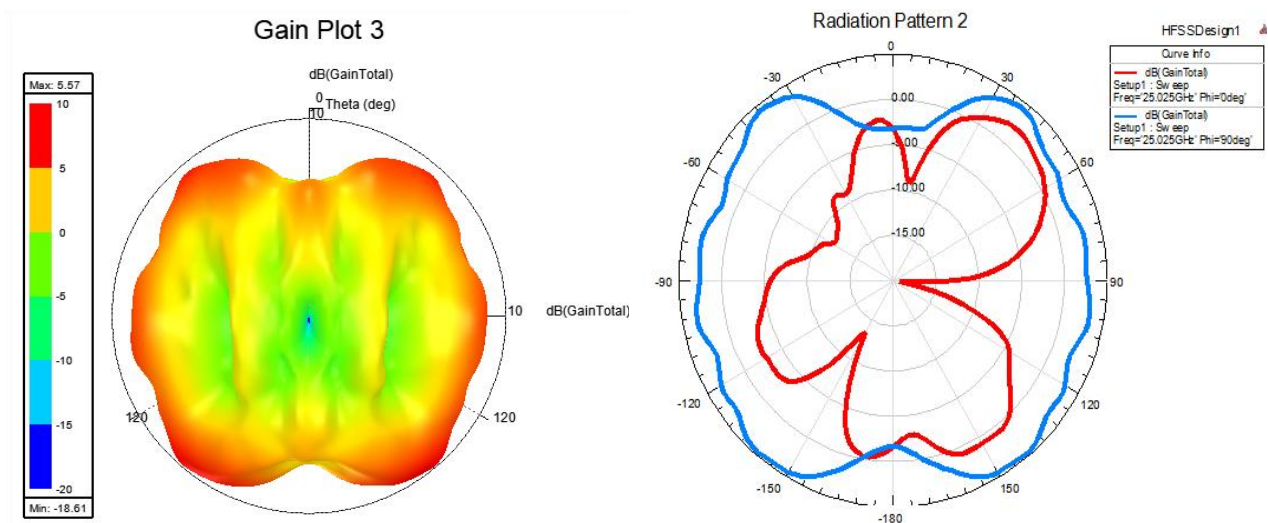
4.4. RADIATION PATTERN, GAIN, & EFFICIENCY

Antenna gain signifies the power directed from an isotropic source toward the direction of peak radiation. The far-field radiation patterns for the recommended MIMO antenna are presented through 3D and 2D gain plots within the resonant frequency band spanning from 24 GHz to 28

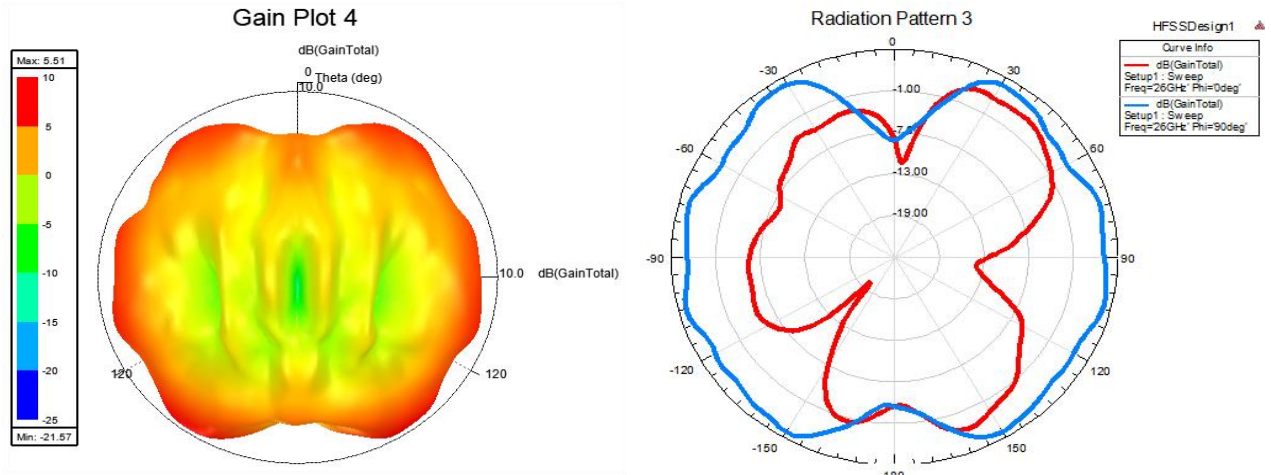
GHz. The antenna demonstrates a substantial gain of 6 and 5 dBi at these operational frequencies, with an average gain of 5 dBi. A radiation pattern illustrates the power variation radiated by an antenna concerning distance or angle from the antenna. In the far field, this power variation is observable as a function of the arrival angle. Figure 4.9 portrays the 3D and 2D radiation patterns of the proposed antenna at Phi (E-plane) and Phi (H-plane) across the frequency band of 24 GHz to 28 GHz. At 27 GHz frequency, the radiation pattern is essentially omnidirectional for Phi, emitting energy in all directions at lower frequencies with a gain of 5 dBi. The main lobes appear at theta 0° and 180°, with smaller lobes at the ends. Figure 4.9 presents the 3D and 2D directivity plots at 27 GHz frequency.



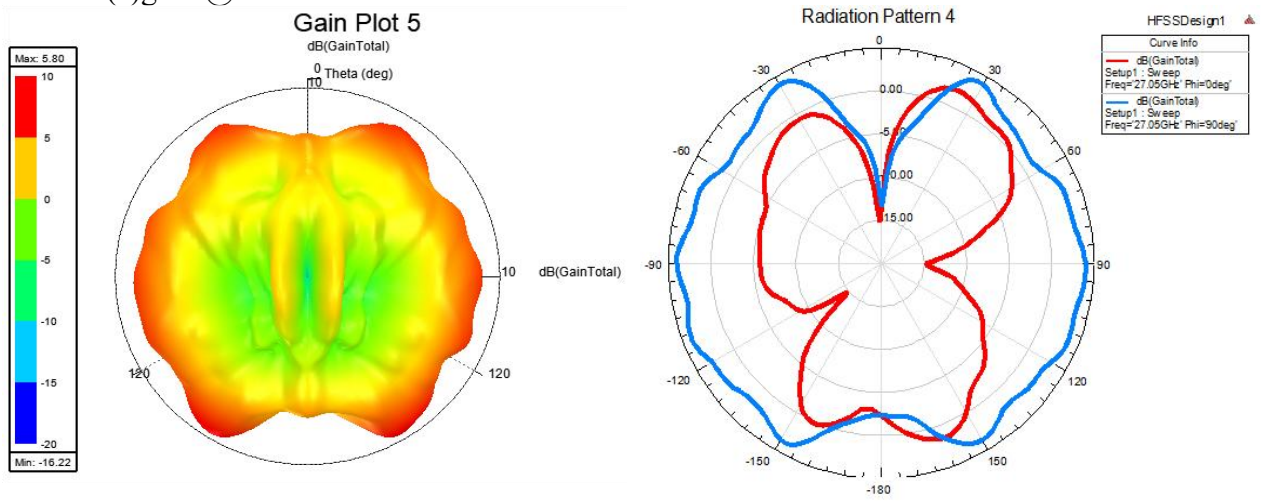
(a) gain @ 24 GHz is 5.76dBi



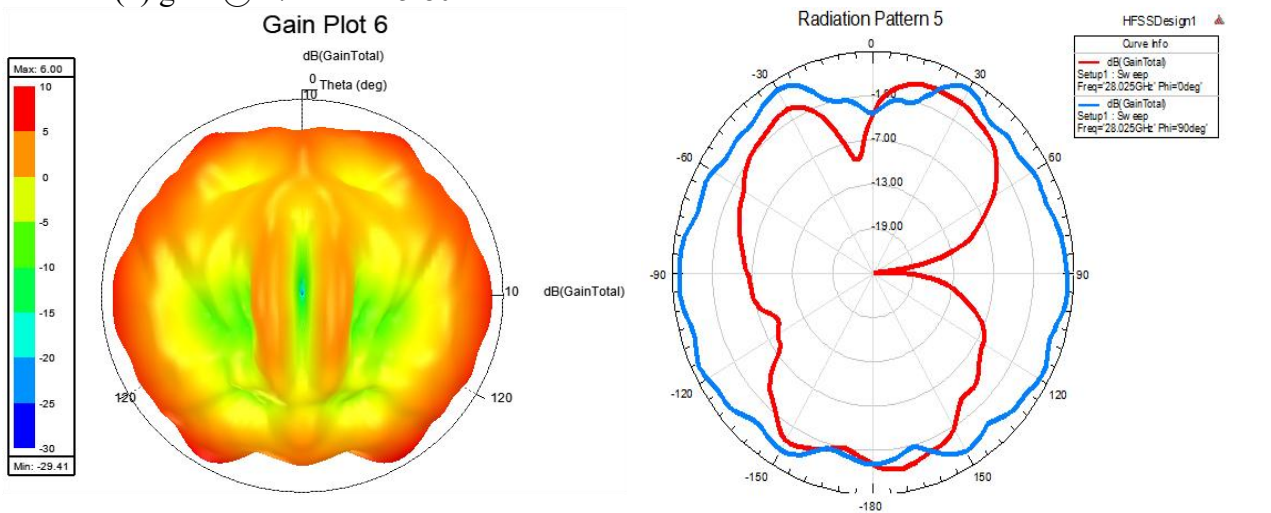
(b) gain @ 25 GHz is 5.57dBi



(c) gain @ 26 GHz is 5.51dBi



(d) gain @ 27 GHz is 5.80dBi



(e) gain @ 28 GHz is 6dBi

Figure 4.9: Simulated gain for proposed quad port MIMO antenna's in 3D and 2D radiation pattern

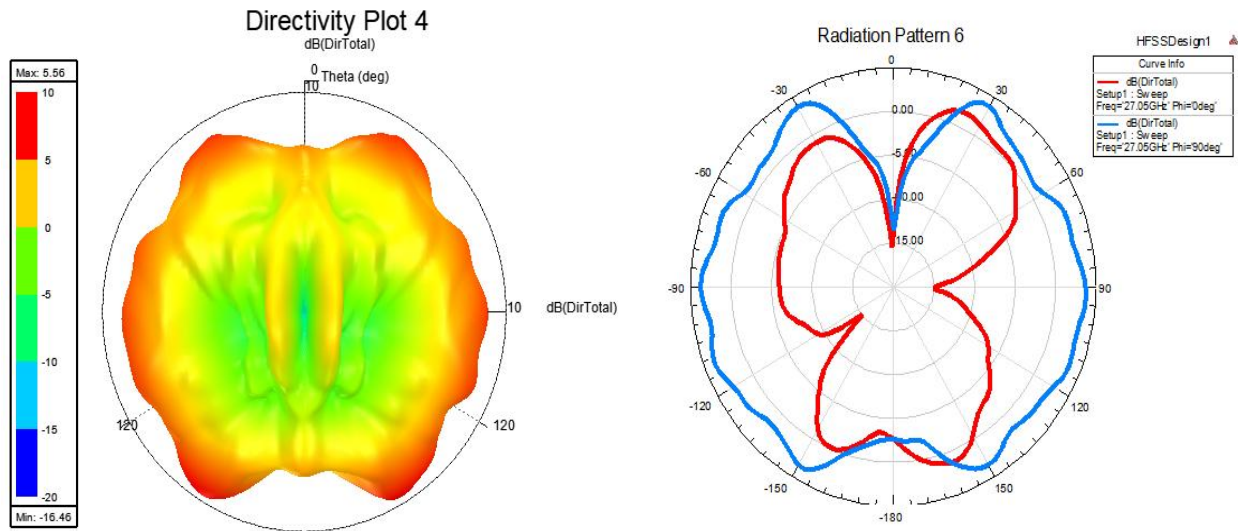


Figure 4.10: 3D and 2D Directivity Plot at 27 GHz frequency

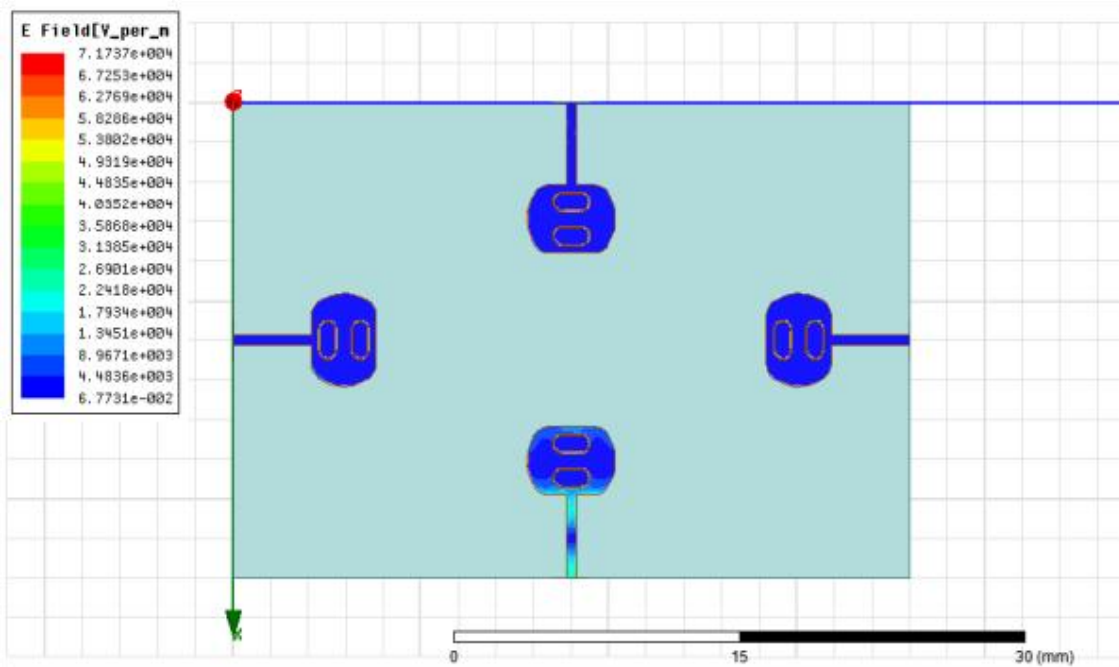
The HFSS simulator can examine the Reflection coefficient behaviour of an antenna configuration by displaying surface current distribution and electric current distribution density at different operating frequencies and phi/theta values. Figure 4.11 displays the proposed antenna's electric and magnetic field density graphs at resonant frequencies.

The physics behind isolation primarily revolves around minimizing the interaction between the electromagnetic fields generated by closely spaced antenna elements. These interactions can be described through surface currents and near-field power flow etc.

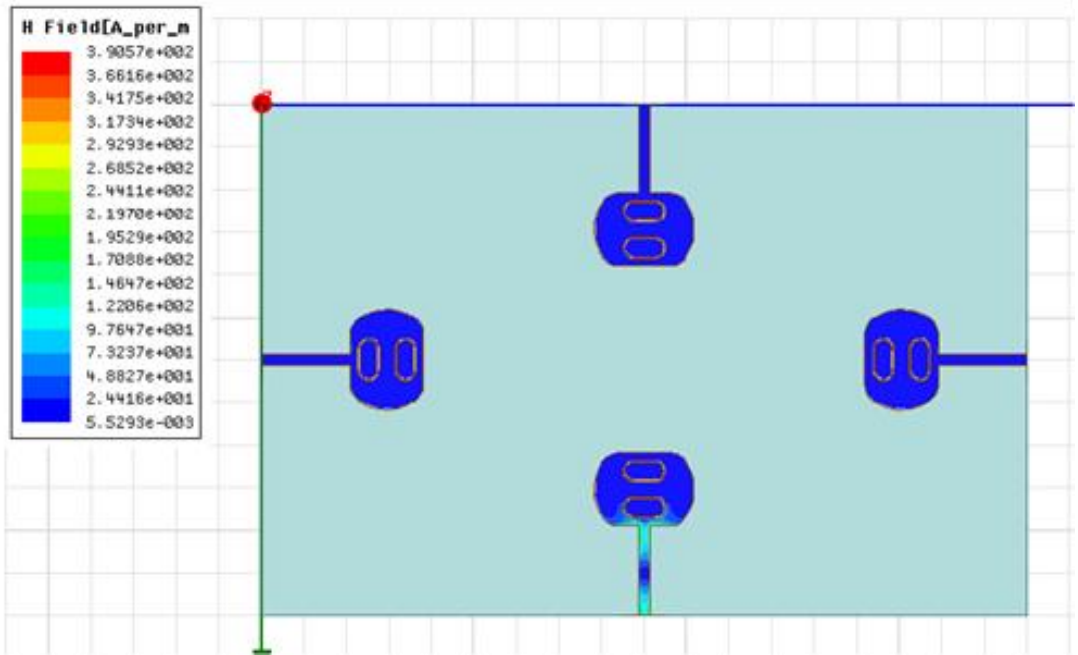
1. When one antenna element radiates, it induces surface currents not only on itself but also on nearby elements. This is known as mutual coupling and is a major cause of poor isolation. The electromagnetic fields generated by these surface currents can transfer energy from one antenna to another, leading to signal interference. By disrupting the path of these surface currents, mutual coupling can be reduced. This can be achieved through various techniques such as introducing slots, slits, or decoupling elements on the antenna structure, or modifying the ground plane. These methods alter the current distribution, effectively confining the currents to the radiating element and preventing them from inducing unwanted currents in neighboring elements.
2. In the near-field region (closer to the antenna where reactive fields dominate), power can couple between antennas through capacitive or inductive means. This near-field coupling can lead to significant interference between closely placed antennas. Near-field coupling can

be mitigated by altering the local environment around the antennas. Techniques such as the use of electromagnetic band gap (EBG) materials, metasurface, or defected ground structures (DGS) can help control and confine the power flow in the near-field region, preventing it from affecting nearby antenna elements.

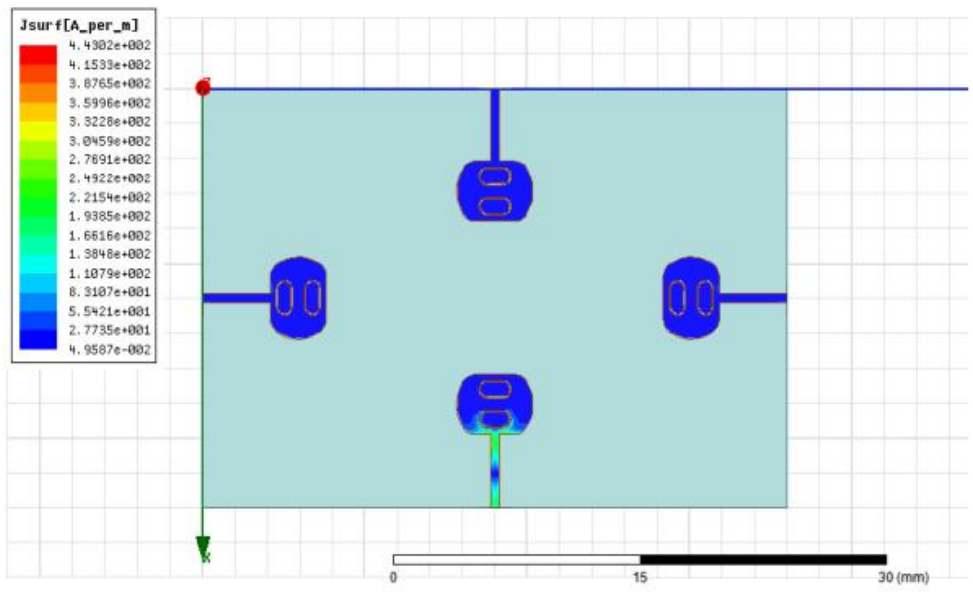
The extensive bandwidth attributes of the proposed antenna result from the concentration of maximum current along the feed-line borders and the edges of the capsule patch structure. Additionally, there is a uniform distribution of current across the surface of the capsule patch. The current distribution along the patch's edges lengthens the feed-line electrically, which causes the antenna to resonate with an acceptable Reflection coefficient value.



(a)



(b)



(c)

Figure 4.11: Proposed quad port MIMO antenna's (a) E-field, (b) H-field, and (c) surface current distribution at 26 GHz

Antenna 1 and the other three elements of the antenna display unstable connections, notably influenced by elliptical slots that confine the current primarily to the area of the excited element. The elliptical slots lead to self-isolation among antenna elements, as the current flow from port 1

to other components is weak. The symmetric design ensures similar current distribution among the other antenna elements when excited. Except for the stimulated port operating between 22 and 30 GHz, all prototype ports terminate to 50 broadband-matched loads. The protruding ground, parasitic elements, and active elements are all contained within the current's boundaries, with currents in the nearby ports not particularly strong. The distribution of boundary currents demonstrates excellent isolation. The proposed structure maintains crucial radiation characteristics, ensuring minimal loss, achieving good gain, and directional patterns. The Total ECC, DG, and TARC of the MIMO antenna were examined to assess MIMO performance. The results depicts that the recommended MIMO antenna design stands as a robust candidate for 5G mm-wave wireless communication systems.

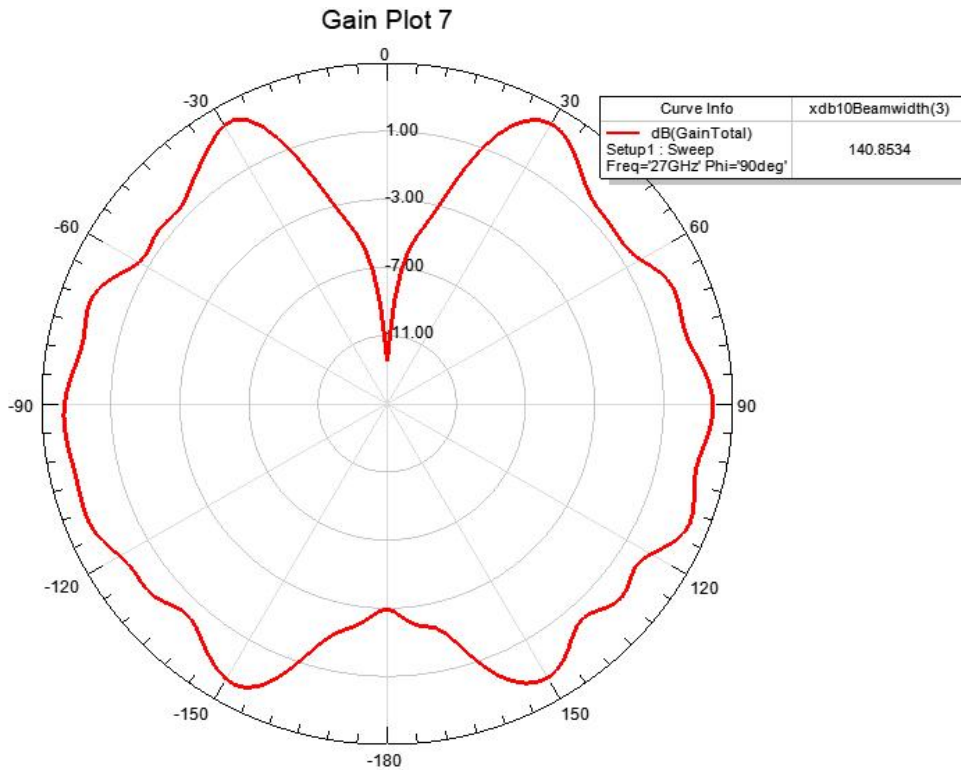
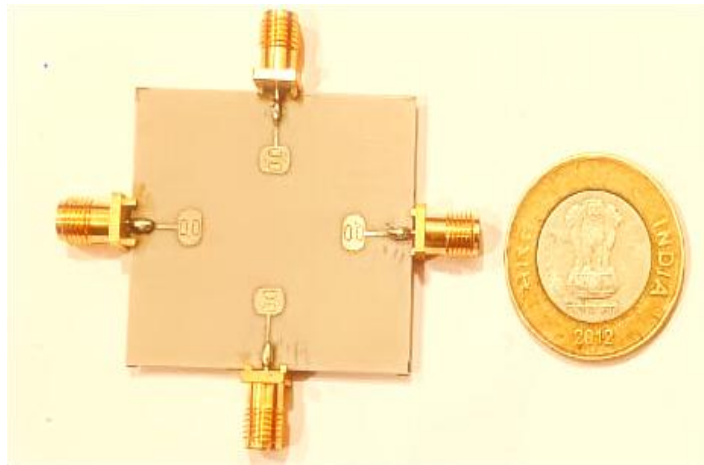


Figure 4.12: Simulated Total Gain plot at 27GHz for quad port UWB MIMO antenna

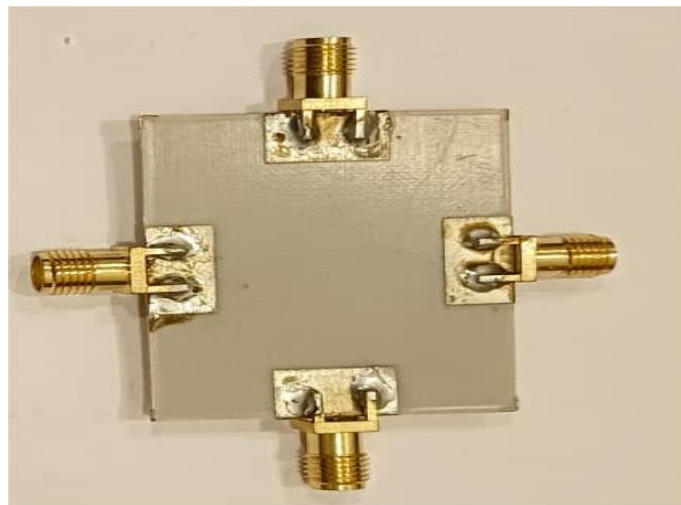
In Figure 4.12 shows the antenna's 2D radiation pattern is being analyzed in the $\phi = 90^\circ$ plane, which is the vertical Y-Z plane. The main lobe of the radiation pattern spans a beam width of 140.85°, meaning that the antenna radiates most of its power within this angular range in the Y-Z plane. The total gain in this direction reflects how effectively the antenna radiates energy in this plane compared to an ideal isotropic radiator.

4.5. ANTENNA MEASUREMENT RESULTS

Upon concluding all simulations and validating the results in HFSS, the proposed antenna was designed on a Rogers RT Duroid 5880 PCB with copper measuring 0.35 millimeters (mm) in thickness. The final product's front and back views are depicted in Figure 4.13. The manufactured antenna is fed through a microstrip feed-line, utilizing a 4-hole flange SMA connector constructed from brass with gold plating, possessing a resistance of 50 ohms, and exhibiting a temperature tolerance range from $-55\text{ }^{\circ}\text{C}$ to $+155\text{ }^{\circ}\text{C}$. SMA connections are sub-miniature, semi-precision devices that deliver superior electrical performance. They are exceptionally mechanically durable high-performance connectors that are small and compact size.



(a)



(b)

Figure 4.13: The Photograph of fabricated capsule shaped 4×4 quad port UWB-MIMO antennas: (a) Top and (b) Bottom views

Figure 4.14 displays the measured Reflection coefficient, which is superior to the calculated Reflection coefficient because the resonating band was relocated to a higher frequency (26.33 GHz - 32.15 GHz instead of 22 GHz - 30 GHz), yielding positive and substantial outcomes for real-world applications.

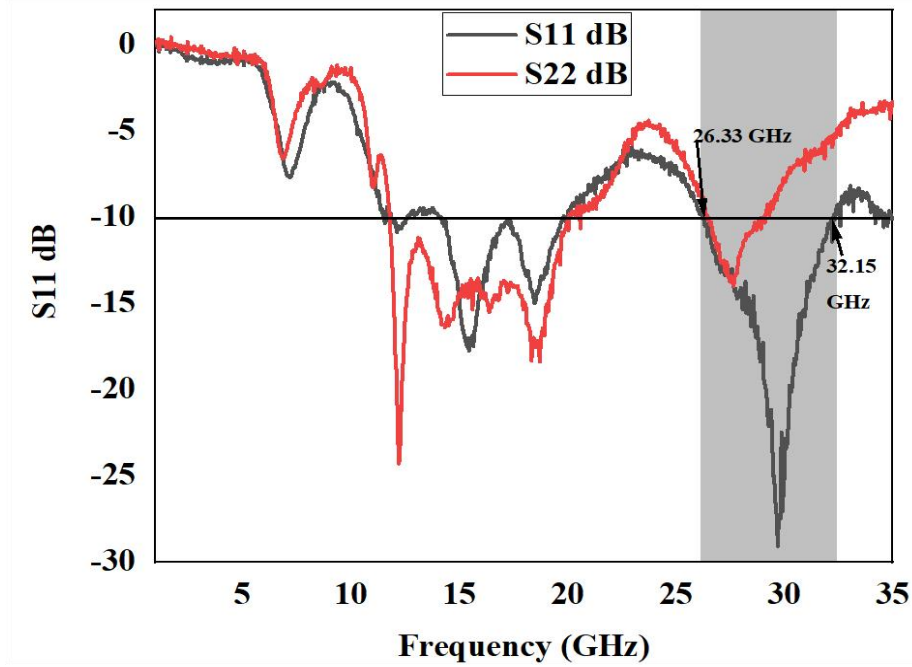


Figure 4.14: Measured S-Parameter (S_{11}) Reflection coefficient in dB

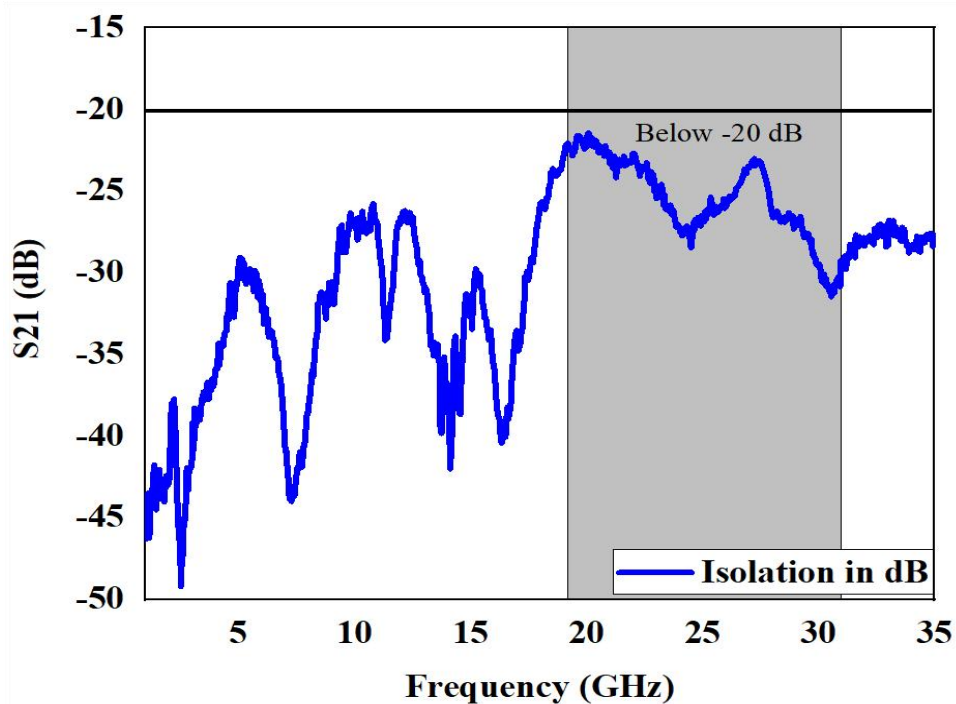


Figure 4.15: Measured Isolation of MIMO antenna (S_{21}) in dB with Frequency

The recorded return-loss values indicate a minor fluctuation within the frequency range. The measured Reflection coefficient, however, was better than the calculated Reflection coefficient because the constructed antenna radiated at a higher frequency at 28 GHz. Figure 4.15 indicates that the proposed UWB MIMO antenna has an average observed isolation of -26.27 dB between the first and second ports in the frequency range (22 GHz - 32 GHz). The measured values are superior based on a comparison of the observed and simulated isolation findings for the same frequency range (22 GHz - 30 GHz).

The Reflection coefficient and VSWR (Voltage Standing Wave Ratio) of the created antenna are assessed using a VNA (Vector Network Analyzer) having specification ZNB-40 operating within the frequency span of 10^{-4} GHz to 40 GHz. Prior to measuring the Reflection coefficient, the VNA undergoes calibration using the calibration kit. Figure 4.16 illustrates the setup required for the antenna measurement in order to determining Reflection coefficient.

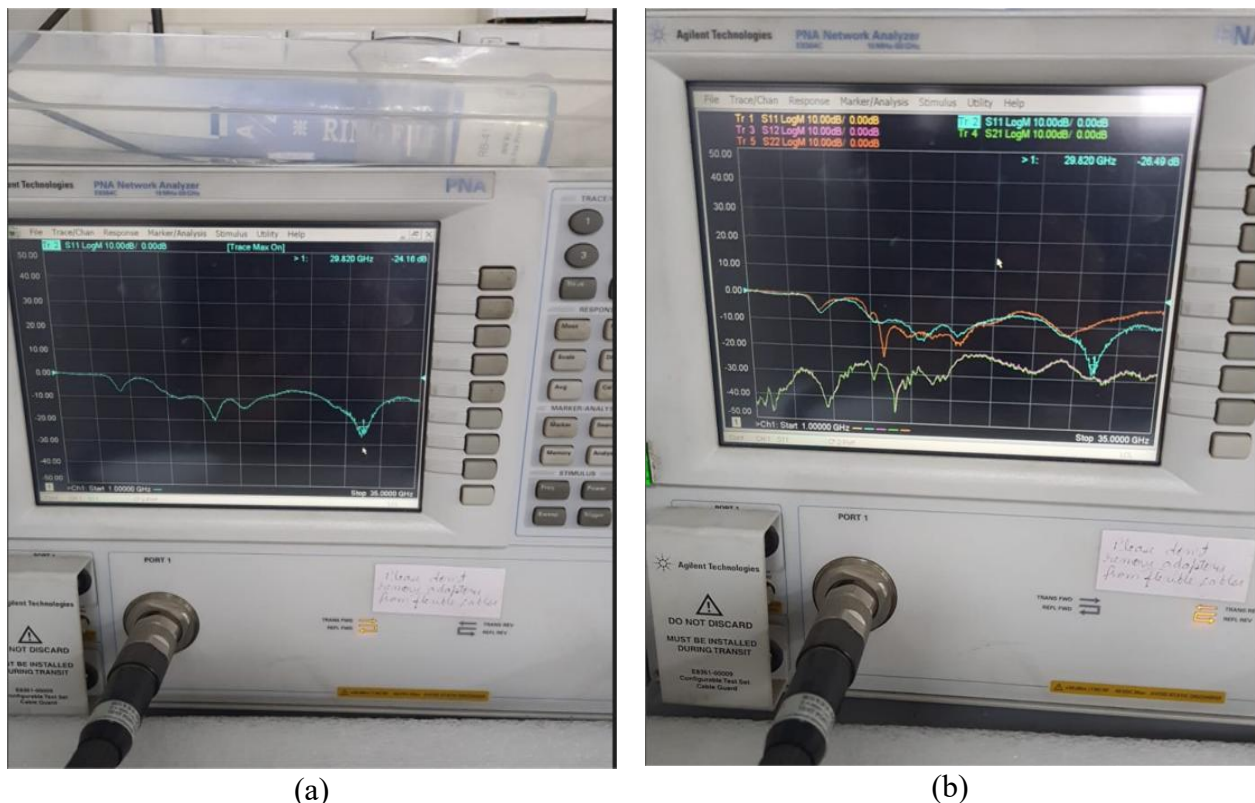


Figure 4.16: Measurement Setup for Reflection coefficient (S11 in dB) and Isolation (S12) for Proposed MIMO antenna

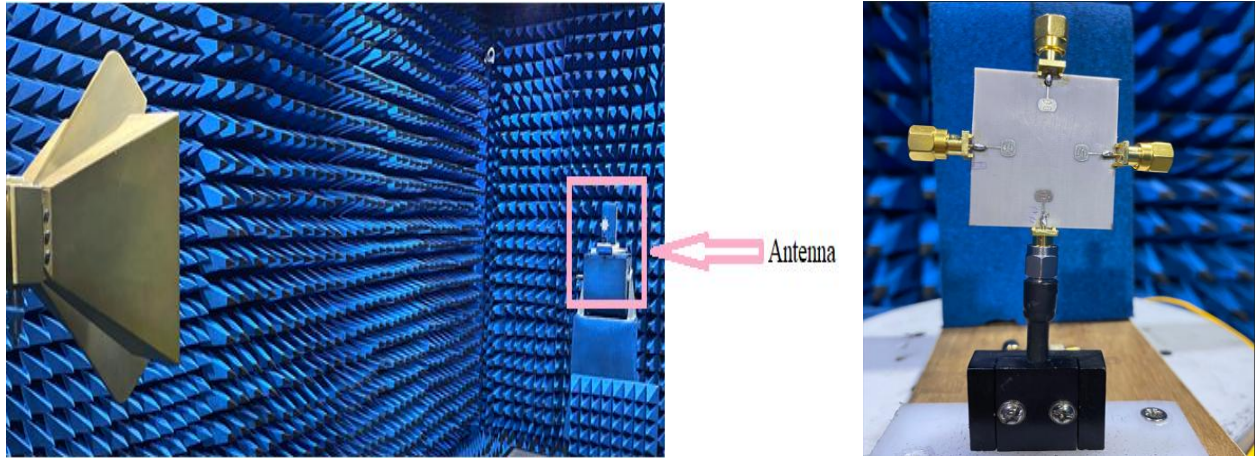


Figure 4.17: MIMO antenna measurement setup inside an Anechoic Chamber

Figure 4.17 illustrates the measurement environment by providing the measurement scenarios for the suggested antenna. The testing arrangement for the anechoic antenna includes an RF transmitter system, antenna under test, a receiver system, a reference antenna, and a positioning system. Anechoic chambers are screened spaces that are entirely or partially covered in electromagnetic absorbers that completely suppress outside emissions.

4.6. ANALYSIS OF MIMO DIFFERENT DIVERSITY PARAMETERS

MIMO systems leverage different diversity parameters to enhance wireless communication performance. Spatial diversity improves signal reliability by using multiple antennas placed apart to experience independent fading. Frequency diversity mitigates frequency-selective fading by transmitting across different frequency bands. Polarization diversity reduces polarization-dependent fading and interference by utilizing antennas with different polarization. Pattern diversity enhances signal reception by employing antennas with various radiation patterns that cover multiple directions. Lastly, time diversity combats fast fading by transmitting signals at different time intervals, making it useful in rapidly changing environments. Together, these diversity techniques significantly boost MIMO system performance.

When evaluating the performance of the MIMO system, major considerations include ECC and Diversity Gain (DG), and TARC etc contributes to the evaluation of the MIMO antenna's diversity performance.

4.6.1. ECC (Envelope Correlation Coefficient):

It's a vital diversity metric used to characterize the mutual connection between antenna components. Figure 4.18 shows the Envelope Correlation Coefficient (ECC) of the MIMO antenna in respect to the frequency plot. The simulated ECC value is less than 0.007 across the whole frequency spectrum, showing that the MIMO antenna performs exceptionally well in terms of diversity.

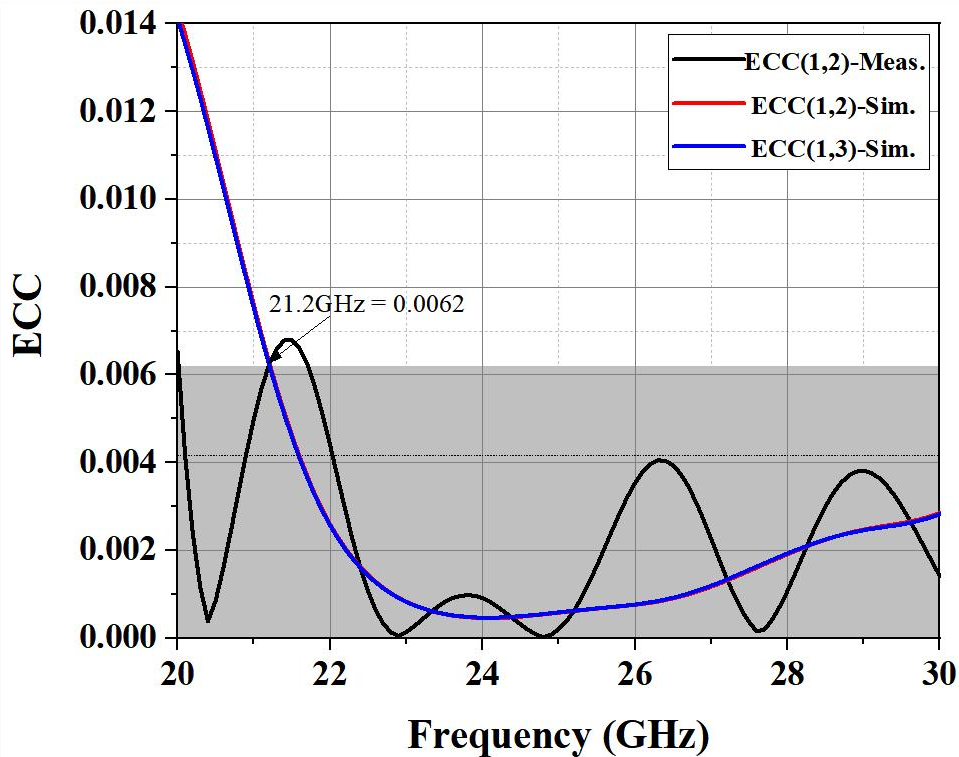


Figure 4.18: Envelope correlation coefficient (ECC) with frequency

4.6.2. Diversity Gain (DG):

A well-known measurement used to assess the effectiveness of diversity is the antenna Diversity gain (DG). For the MIMO antenna to function properly, the diversity gain, which can be calculated directly from the ECC value, should be closer to 10 dB. Figure 4.19 displays the diversity gain while terminating all the port except port 1. The DG value, which is seen to be 10 dB, is higher than the generally recognized value of 9.9 dB.

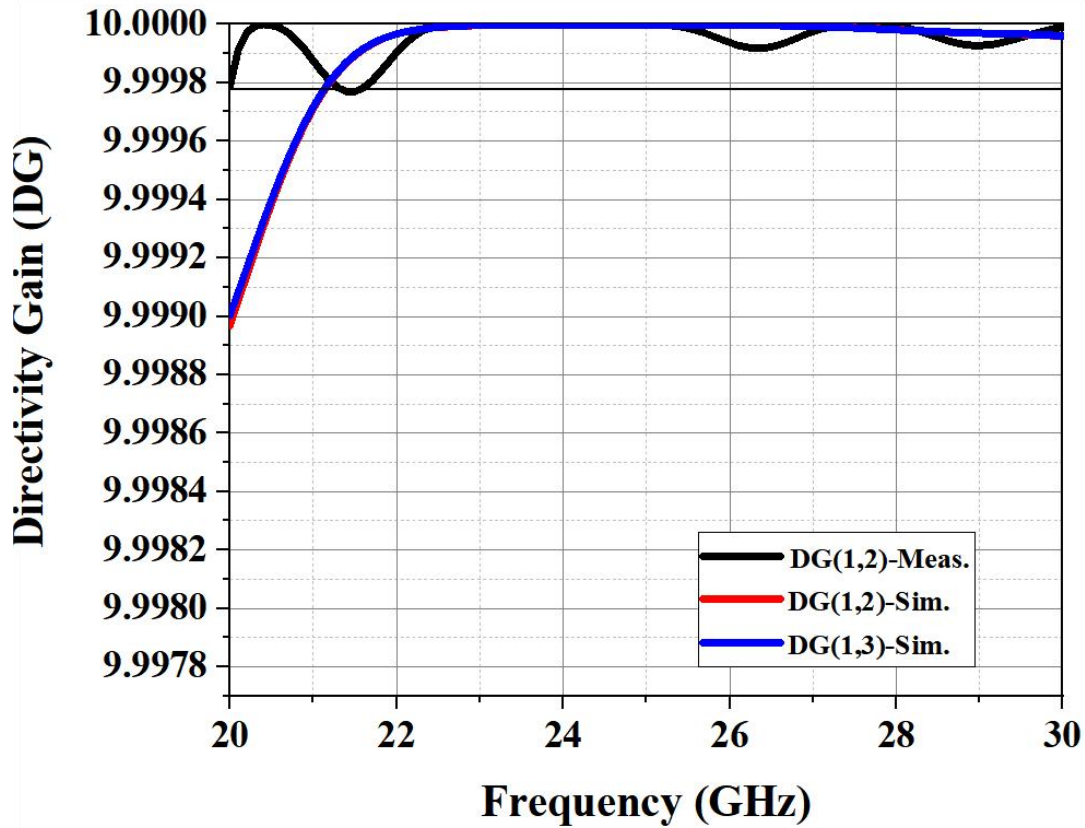


Figure 4.19: Simulated Diversity Gain (DG) with frequency

In the 22-30 gigahertz frequency spectrum, the ECC is less than ($<$) 0.007 and the DG is greater than ($>$) 9.9 dB.

4.6.3. TARC (Total Active Reflection Coefficient):

The operating bandwidth and the efficiency in the MIMO system will be impacted when all antenna elements are active at once. As a result, S-parametric data are insufficient to determine how effective the antenna is, thus we used TARC, another crucial parameter, to assess the antenna's performance. Given the assumption that all incoming signals at every port possess identical amplitude and phase (0° phase difference) in the recommended MIMO antenna.

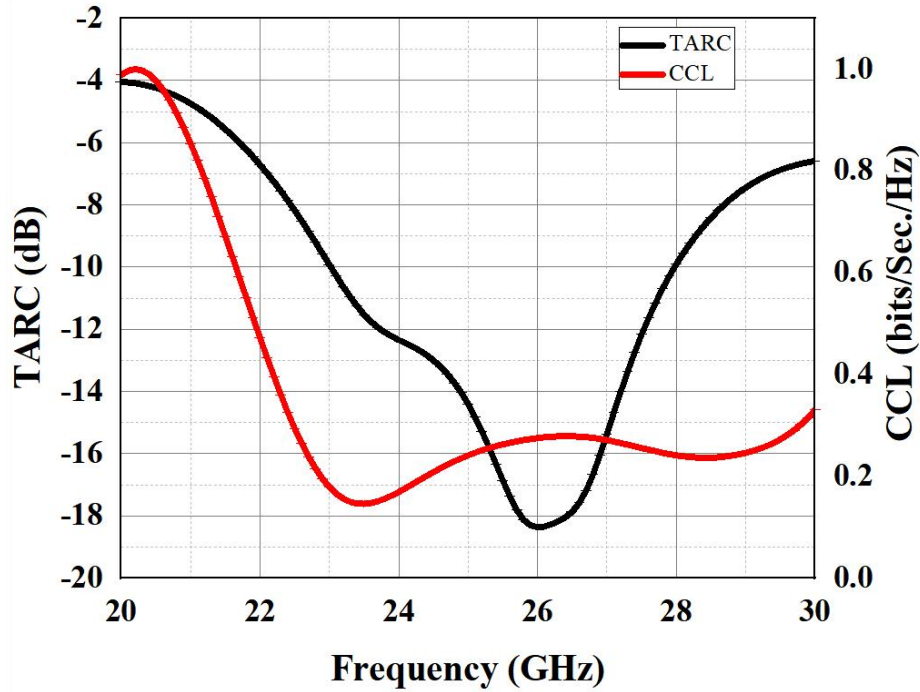


Figure 4.20: Simulated TARC and CCL versus frequency plot

Figure 4.20 shows that the TARC value is below -10 decibels over the whole frequency span, approaching the authorized limit of 0 decibels. Given all of the aforementioned findings, the suggested MIMO antenna is a promising alternative for UWB and 5G use cases.

Table 4.7: Comparisons with other MIMO Antennas

Reference	No. of elements	Substrate Used	Size of Antenna (mm ³)	Frequency Range (GHz)	Isolation (dB)	Antenna Gain (dBi)	ECC
[122]	4	Rogers 5880	24 × 24 × 0.8	24.8 - 44.45	>20	8.6	<0.008
[123]	4	Rogers 5880	50.8 × 12 × 0.8	25.1 - 37.5	>20	10.6	<0.1
[124]	4	Rogers 5880	30 × 35 × 0.787	27.5 - 28.5	>40	12	<0.003
[125]	4	Rogers 5880	28 × 28 × 0.78	26.5 - 31.5, 36 - 41.7	>40	9.5, 11.5	<0.001
[126]	4	RO4003C $\epsilon_r = 3.55$	33 × 33 × 0.233	25 - 50	>10	---	<0.005

[127]	4	Rogers 5880	$80 \times 80 \times 1.57$	23 - 40	>20	12	<0.0014
[128]	4	R04350B $\epsilon_r = 3.66$	$30 \times 35 \times 0.76$	25.5 - 29.6	>10	8.3	<0.01
[129]	4	Rogers 5880	$30 \times 30 \times 1.575$	26.16 - 29.72	>30	7.1	<0.0005
[130]	4	Rogers 5880	$55 \times 110 \times 0.508$	28.044 & 38.04	>26	7.95, 8.27	---
[131]	4	FR4	$36 \times 36 \times 1.6$	39 - 75	>24.539	4.82 - 9.3	<0.00075
[132]	4	Roger RT/Duroid 6002	$27 \times 27 \times 1.52$	26.5 - 43.7	>40	8.4	<0.001
[133]	4	Rogers RT 5880	$75 \times 100 \times 0.508$	28, 38	>36	7.6, 8.12	<0.5
[134]	4	FR4	$40 \times 40 \times 1.6$	5 - 39	>19	---	<0.038
[135]	4	RO5880	$48 \times 12 \times 0.254$	23 - 33, 37.75 - 41	>20	5.7	<0.00015
[136]	4	Rogers RT-5880	$47.4 \times 32.5 \times 0.51$	36.83 - 40.0	>45	6.5	<0.001
Proposed work	4	Rogers RT-5880	$36 \times 24 \times 0.8$	22 - 30	> 21	5	<0.007

This comparison shows that in terms of isolation, compact size, and diversity gain favorable ECC, the suggested antenna design compares effectively with the other designs shown in Table 4. The recommended antenna is noticeably smaller than the other antennas specified in Table 8. It is ideal for compact and highly isolated operation at higher frequencies, with a low ECC value (0.007), superior isolation, and attainable gain. These qualities together make the suggested antenna a strong contender for 5G wireless communication systems.

4.7. SUMMARY

The presented study entails creating and fabricating a compact quad-port ($36 \times 24 \times 0.8$) mm³ UWB MIMO antenna on an RT Duroid 5880 substrate. This is accomplished with specific sub-values for the dielectric constant, thickness ($h=0.8$ mm), and loss tangent (0.0009). Notably, the design avoids the incorporation of any external decoupling structure, a choice made to prevent unnecessary increases in antenna complexity and size. By aligning four similar antenna elements in a capsule shape on the radiator with two elliptical slits which are useful in achieving a significant level of isolation, interference is decreased via diversity. Elliptical slots are created in the ground plane to adjust surface electrical dispersion and increase antenna bandwidth. The prototype antenna is ideal for modern 5G wireless systems, notably indoor UWB-MIMO devices. Its notable features include an extensive bandwidth ranging from 22 to 30 GHz, high isolation, enhanced gain, and favorable metrics such as ECC, DG, and TARC, all contributing to the antenna's commendable MIMO performance. The suggested work is then compared to the most recent works for connected applications. By offering compact size and high-performance MIMO antenna specifications, the comparison shows that the suggested antenna outperformed related attempts.

CHAPTER-5

DESIGN AND ANALYSIS OF MIMO ANTENNA WITH DIFFERENT ISOLATION TECHNIQUES

5.1. INTRODUCTION

Recent progress in affordable millimeter-wave (mm-wave) RF integrated circuits and devices has made it possible to apply MIMO techniques at frequencies reaching up to 24 GHz. This development holds particular significance in meeting the substantial bandwidth needs of emerging 5G wireless cellular networks and the progress of the IoT [137]. The ITU known as International Telecommunication Union has mandated that 5G networks have a channel capacity of approximately 20 Gbps. In order to address the continually rising need for higher data speeds, it is critical to combine the wide bandwidth available in mm-wave bands with the increased channel throughput achieved by MIMO techniques. This synergy enables higher data rates and better performance in future wireless networks [138].

Mutual coupling (MC) has a significant impact on MIMO antenna performance and the propagation channel in the 24 GHz band. This influences the radiation pattern of the array, the level of side lobes, gain, impedance matching, and channel capacity [139]. Maintaining a low MC level of at least -25 dB is critical in certain applications. High levels of isolation between radiating elements are required in MIMO systems to ensure a low envelope correlation coefficient [140]. As a result, considering antenna element isolation during the design phase of MIMO systems is critical for achieving antenna diversity schemes.

Previous research has shown that mutual coupling between antennas has a negative impact on channel correlation and radiation efficiency in diversity antenna solutions [141]. As a result, minimizing the correlation between antenna ports is critical for achieving high diversity gain [142]. The advent of 5G wireless systems brought forth Massive MIMO technology as a highly promising solution, markedly augmenting channel capacity in comparison to conventional MIMO systems, particularly in realistic propagation scenarios. On the other hand, Compact

MIMO antennas, are preferred in mobile terminals and base stations. Since antenna elements are close enough, it is difficult to avoid electromagnetic mutual coupling. The mutual coupling has the potential to impact the input impedance, radiation patterns and reflection coefficients of the array elements. Consequently, it is crucial to devise strategies for mitigating the influences of mutual coupling in antenna design. To address this issue, several approaches have been developed, including DGS, polarization diversity, EBG, and the incorporation of parasitic elements between antennas. To counter coupling in MIMO antennas for Ultra-Wide band (UWB) applications, additional methods are used [143]. These techniques include the use of spatial, pattern, polarization, and decoupling structures, as well as meta-materials. Surface wave occurrence is eliminated by integrating EBG structures, resulting in a reduction in the in-phase reflection coefficient and associated coupling. CSRR (Complimentary Split-Ring Resonators) are used to filter and improve isolation via a series of extended metal strips [144].

Different isolation techniques in MIMO antenna design play a crucial role in minimizing mutual coupling between antenna elements, which directly impacts the performance and efficiency of the system. By employing methods such as decoupling networks, defected ground structures (DGS), electromagnetic band gap (EBG) materials, and parasitic elements, isolation can be enhanced, leading to improved signal quality and reduced interference. These techniques help maintain the independence of each antenna element, which is vital for maximizing the MIMO system's capacity and reliability. However, while these techniques reduce coupling, they can also introduce trade-offs, such as increased design complexity, larger physical size, and potential reductions in bandwidth and radiation efficiency. Therefore, careful consideration is needed to balance isolation improvements with overall antenna performance and system requirements. Following research looks into spatial, polarization, and pattern models, as well as strategies for reducing mutual coupling such as parasitic approaches, neutralization lines, slot/slit etching, meta-materials, and coupling/decoupling networks [145-147].

Table 5.1: State of the Art comparison with Isolation Techniques

Ref. No.	No. of Elements	Size (mm^3)	Substrate	Operating Frequency (GHz)	Gain (dBi)	Isolation (dB)	Isolation Technique	Applications
[130]	4	25 × 12 × 0.381	Roger RT/Duroid 5880	1.8-2.6 25-40	7.2	≥ 17	tapered slot	Integrated 5G/4G in Same Structure, mm-wave
[131]	4	Diameter = 30.6 mm with 2 mm height	FR4	3.3 to 4.2	6.21	>9.7	----	5G-applications
[132]	2	48 × 35 × 1.6	FR4-epoxy	2.1 - 18	2- 8	>20	Meta-materials (SRR)	UWB applications
[133]	4	60 × 60 × 1.6	FR4	3 – 16.2	10.55	>17.5	EGB	Modern wireless communication systems
[134]	2	50 × 30 × 1.6	FR4	2.5- 14.5	7.4	>20	F-shaped stubs	UWB applications
[135]	4	80 × 80 × 1.6	FR4	- 20	5.8	>25	H and U-slots	WiMAX and military/radar applications
[136]	4	48 × 52 × 1.6	FR4	2.7 - 11	3.5	>20	asymmetric coplanar strip (ACS) feed	WiMAX applications

[137]	4	18 × 16 × 1.57	RT/Duroid 5870	5.6-6.05	7.98	>24	DNG Meta- material Superstrate	WLAN applications
[138]	4	36.2 × 36.2 × 5	Rogers RT 4003	36.6 – 39.5	10	>25	FSS	5G communicati ons
[139]	4	24 × 20 × 1.85	Transparen t conductive sheet AgHT-8	24.10 - 27.18; 33 - 44.13	3	>16	undivided ground plane	n low profile smart devices at mm-wave 5G applications
[140]	4	80 × 80 × 1.57	Rogers- 5880	23 - 40	12	>20	---	5G mm- wave applications
[141]	4	30 × 35 × 0.76	RogersR04 350B	25.5–29.6	8.3	>10	zig- zagshaped DGS	5G mm- wave applications
[142]	4	---	Rogers RT/Duroid 5880	22.5 - 32	8.2 - 9.6	>20	substrate integrated waveguide (SIW)	multi- channel millimeter- wave transceivers
[143]	2 × 2	41.3 × 46 × 0.508	Rogers RT/Duroid 5880	27.5–31.44	13.1	>23	U-slots	mm-wave applications

In this chapter explains the design process of a miniaturized quad port MIMO antenna with a board size of $(40 \times 40) \text{ mm}^2$ and placed on Rogers RT Duroid 5880 substrate is utilized, featuring a 0.8 mm thickness and a loss tangent ($\delta = 0.0009$) and dielectric constant ($\epsilon_r = 2.2$).

Isolation techniques such as modified ground structure (MGS), Decoupling (Parasitic element) Structure, and Defected Ground Structure (DGS) were applied respectively. Further, parameters like VSWR, S-parameters, total Gain, and Radiation efficiency etc. were simulated with the software Ansys HFSS. The results showed that the decoupling technique achieved the highest isolation in the entire band of frequency range among the applied techniques. Thus, the quad port MIMO antenna design would benefit most from the decoupling isolation technique.

This chapter is organized as follows: The Introduction and comparative studies are discussed in Section-I, and the antenna geometry and design discuss in Section-II, different Isolation techniques are covered with the effects of varying resonant frequencies and antenna characteristics on the outcomes of the research are described in the Section-III, and also presents the comparison of the proposed design with different isolation techniques, and last Section-IV having overall conclusion of the study.

5.2. ANTENNA GEOMETRY AND DESIGN

The antenna design for 5G wireless applications should have MIMO capabilities. The antenna should be capable to support a wide frequency range from 20 GHz to 30 GHz for MIMO applications in 5G wireless applications. The antenna should have high directivity and high gain in order to maximize connectivity between wireless devices. The antenna should also have wide beam width coverage and low side lobe levels in order to reduce interference and crosstalk in an area with a high density of users. To further enhance the signal and data transmission capacity of the antenna, polarization diversity should be considered. The impedance should be matched with 50 ohms with the lowest possible VSWR to ensure efficient data transmission. The design should also incorporate high isolation between each antenna element to avoid any interference and crosstalk [144].

5.3. ISOLATION TECHNIQUES

There are lots of isolation techniques but here we are going to show only few of them and compared there simulated results and based on the results explain that which isolation technique provided the beat results for this proposed MIMO antenna.

5.3.1. Self-Isolation Techniques:

In this approach, the separation between the radiating elements is increased from $\lambda/4$ to $\lambda/2$. The increase in distance results in improved separation among the radiating components. The MIMO antenna configuration depicted in Figure 5.1 has been modeled and simulated using HFSS. An RT Duroid-5880 substrate is selected for the construction of the antenna due to its low dielectric losses. The substrate possesses other values as 2.2, 0.0009, 0.8 mm dielectric constant, a loss tangent, and a thickness of respectively. The substrate dimensions are denoted as $L \times W$ mm². The four antenna elements, labeled Ant-1 to Ant- 4, are printed on the four sides of the substrate. The top layer of the substrate is utilized for positioning the microstrip feeding lines, while a section of the ground plane on the bottom layer is etched.

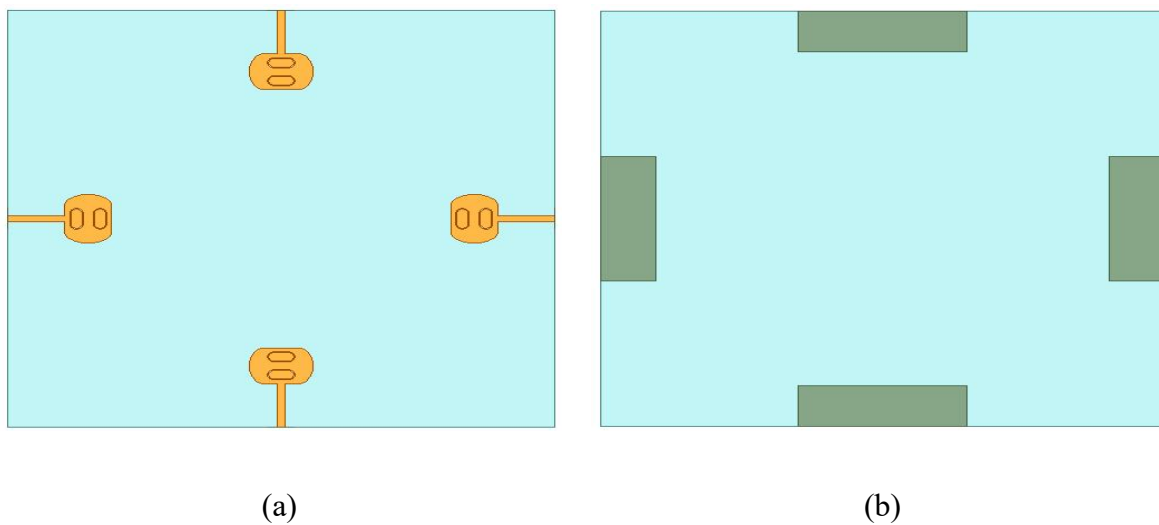


Figure 5.1: Self-Isolated MIMO antenna design (a) Top view & (b) Bottom view

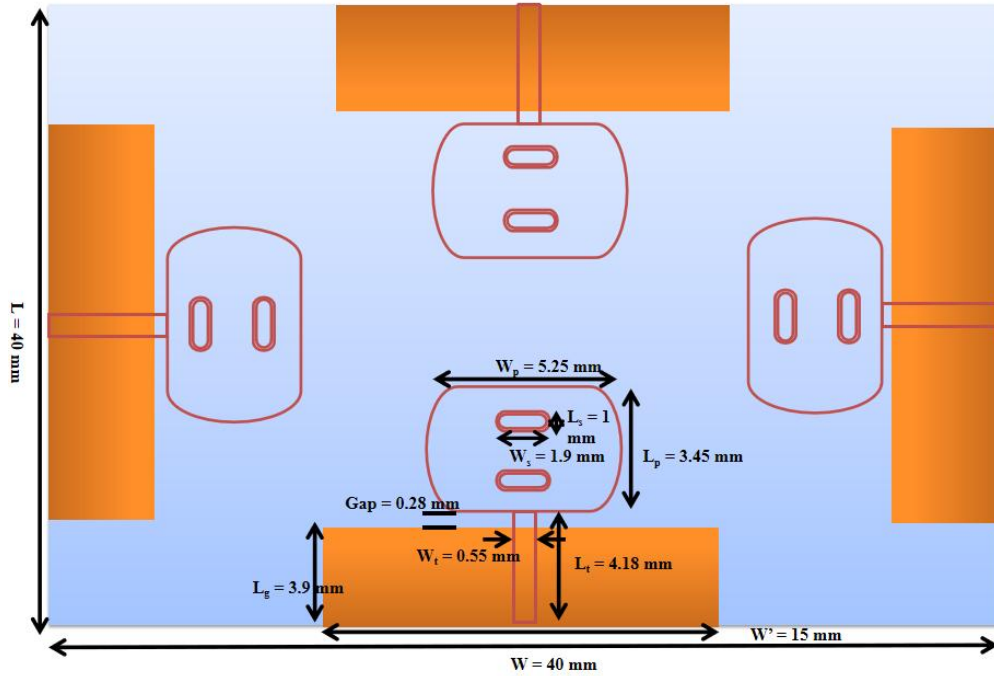
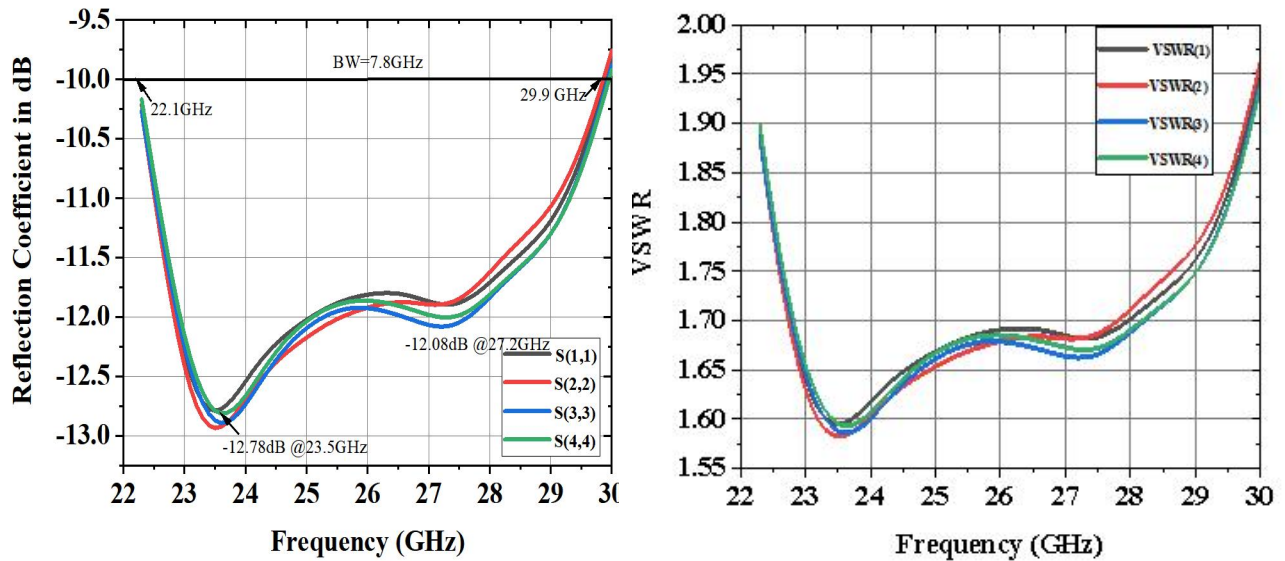


Figure 5.2: Dimensions of Self-Isolated MIMO antenna

Table 5.1: Optimal values of the self-isolated MIMO antenna dimensions (all in mm)

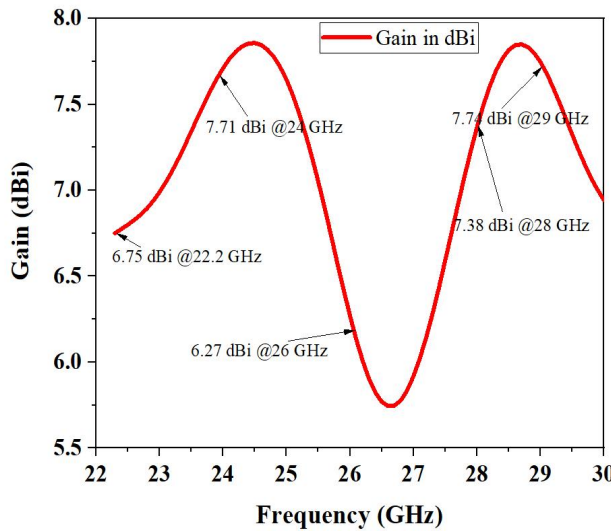
Parameters	Values (mm)	Parameters	Values (mm)
W_S	40	W_2	1.6
L_S	40	L_2	0.8
H_S	0.8	W_3	0.25
W_P	4.17	L_3	0.25
L_P	3.44	W_a	14
W_F	0.525	W_b	19.72
L_F	4.18	W_c	24.82
W_g	12	L_{g1}	0.82
L_g	3.9	L_{g2}	0.52
W_1	2	L_{g3}	0.31
L_1	1	L_{g4}	0.2

In Figure 5.2 is showing the dimensions of the self-isolated MIMO antenna. All dimensions are defined in mm values with respective of parameters in Table 5.2.

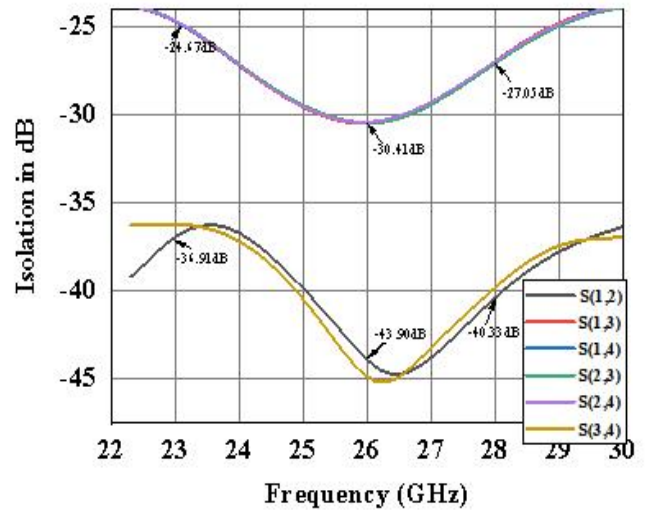


(a) Reflection coefficient vs. Frequency Plot

(b) VSWR vs. Frequency Plot



(c) Gain vs. Frequency Plot



(d) Isolation vs. Frequency Plot

Figure 5.3: Simulation Results of self-isolated MIMO Antenna design: (a) Reflection coefficient , (b) VSWR, (c) Gain, and (d) Isolation

In Figure 5.3 shows the simulation results of self-isolated MIMO antenna first figure is shown Reflection coefficient (S_{11}) the maximum Reflection coefficient is -12.88 dB at 23.7 GHz frequency with ultra wide band of 7.8 GHz. Second figure shows the VSWR which less than 2,

the overall gain of the antenna with in the entire band is greater than 3.7 dB or greater than 5.85 dBi and isolation is greater than > -23 dB.

5.3.2. Modified the Partially Ground Structure:

In this method, we made adjustments to both the ground and the two rectangular slots, altering their locations while maintaining identical dimensions. These modifications include open-source ground cuts, contributing to the enhancement of antenna bandwidth and gain. The microstrip feeding lines for the same antenna are positioned on the top layer of the substrate, while a section of the altered ground plane on the bottom layer is etched. The modified ground structure of the antenna design is depicted in both top and bottom views in Figure 5.4. The measurements of the proposed MIMO antenna incorporating MGS (Modified Ground Structure) are illustrated in Figure 5.5, with all measurements specified in millimeters and corresponding parameters detailed in Table 5.3.

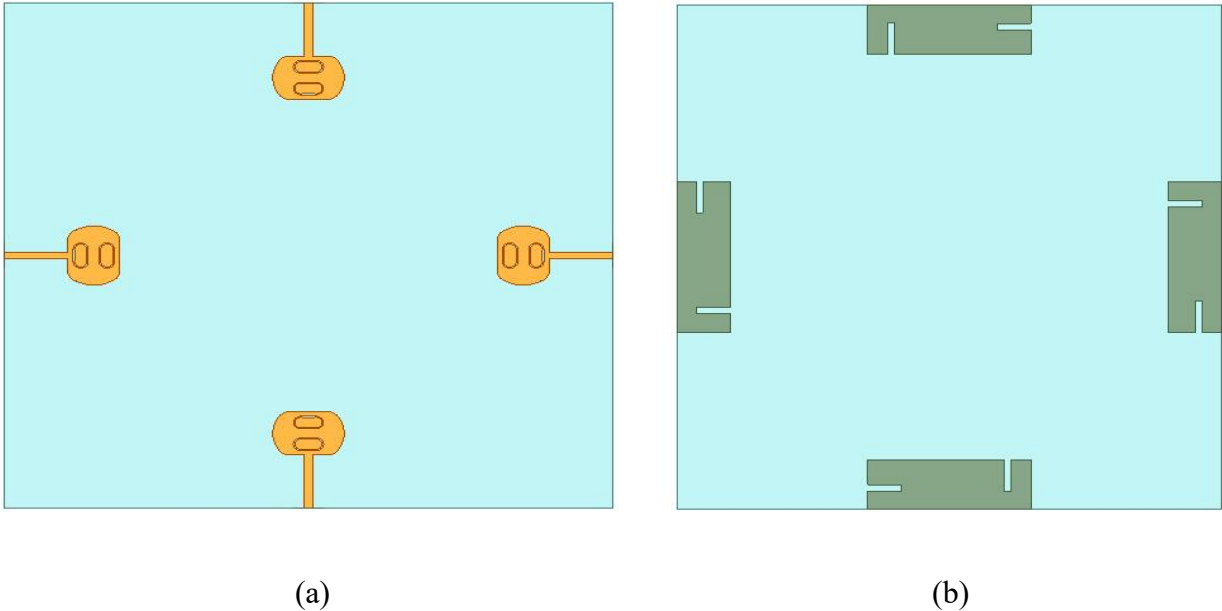


Figure 5.4: MIMO antenna with Modified Ground Structure (MGS): (a) Top view & (b) Bottom view

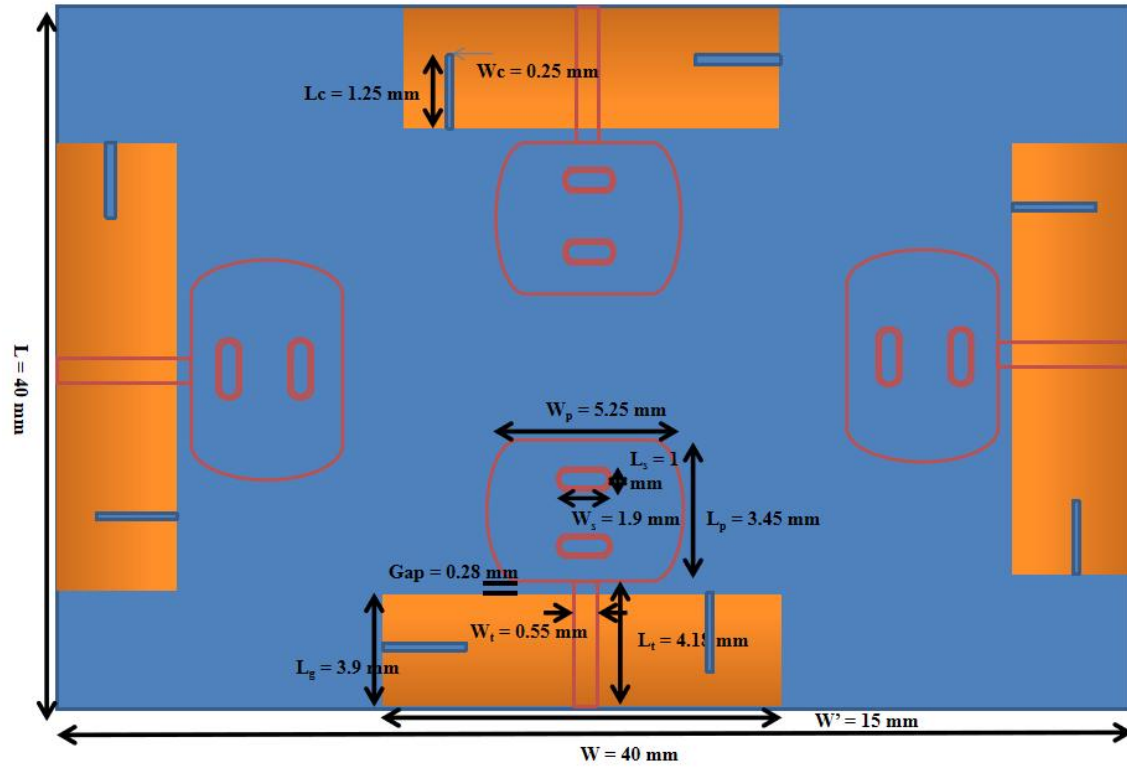
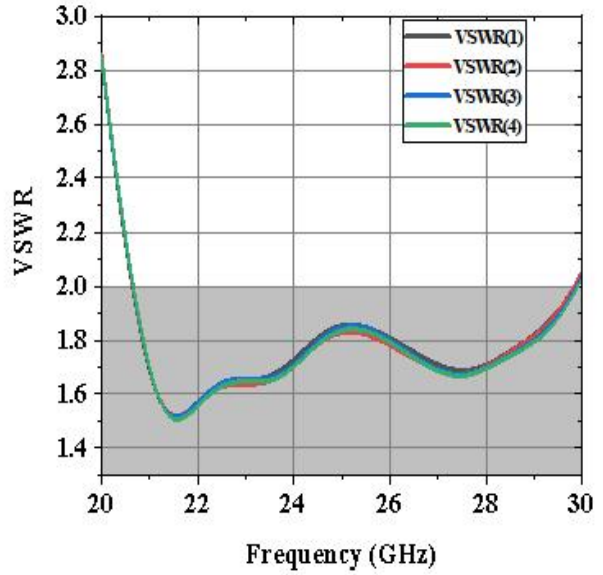
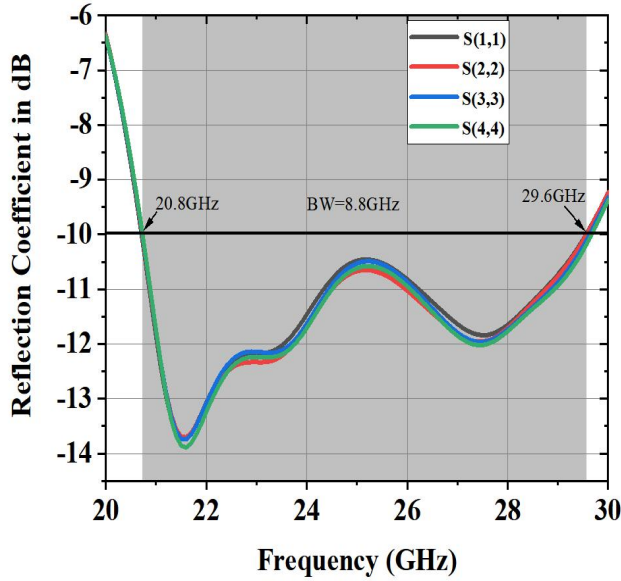


Figure 5.5: Dimensions of Quad Port MIMO antenna with Modified Ground Structure

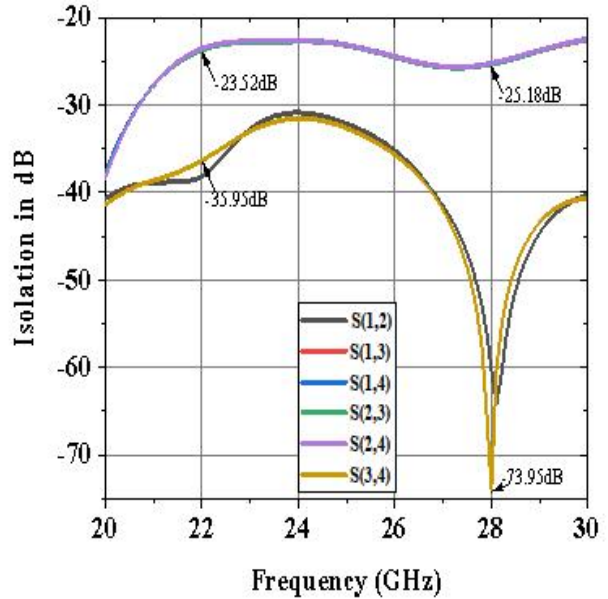
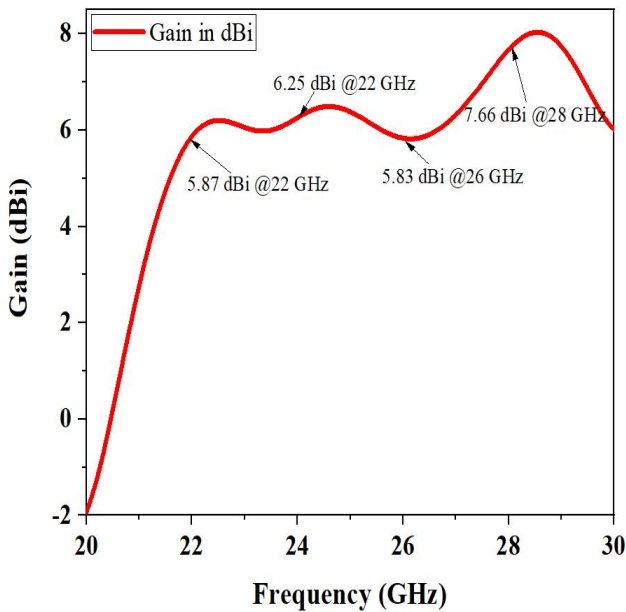
Table 5.3: Optimal values of the proposed antenna dimensions for MGS (all in mm)

Parameters	Values (mm)
W	40
L	40
H_S	0.8
W_c	0.5
L_c	2.25
W_b	0.5
L_b	2.25



(a) Reflection coefficient vs. Frequency Plot

(b) VSWR vs. Frequency Plot



(c) Gain vs. Frequency Plot

(d) Isolation vs. Frequency Plot

Figure 5.6: Simulation Results of quad port MIMO Antenna design with Modified Ground Structure (MGS): (a) Reflection coefficient, (b) VSWR, (c) Gain, and (d) Isolation

In Figure 5.6 shows the all simulated results of MIMO antenna with modified ground structure first figure is shown Reflection coefficient (S11) the maximum Reflection coefficient is -14 at 21.5 GHz frequency with ultra wide band of 8.8 GHz. Second figure shows the VSWR which

less than 2, the overall gain of the antenna with in the entire band is greater than 3.71 dB or greater than 5.86 dBi and isolation is greater than -23 dB. In this technique the bandwidth is increased very much, so to modify the ground means to modify the bandwidth.

5.3.3. Decoupling Structure:

The MIMO antenna structure featuring four ports and employing the proposed isolation techniques is developed and simulated using the Ansys HFSS software. This design is employed on an RT Duroid-5880 substrate, chosen for its minimal dielectric losses, with a dimension (L×W) mm², and other values as 2.2, 0.0009, 0.8 mm dielectric constant, a loss tangent, and a thickness of respectively. All four antenna elements (Ant-1 to Ant-4) are printed on the four sides of the substrate. The top layer of the substrate accommodates the placement of microstrip feeding lines, incorporating the X-shaped decoupling structure on the radiating patch, while a section of the ground plane on the bottom layer is etched. Figure 5.7 illustrates both top and bottom views of the the proposed antenna design featuring the Decoupling structure. In the subsequent Figure 5.8, the dimensions of the MIMO antenna incorporating the X-shaped decoupling structure are provided. All measurements are specified in millimeters, with corresponding parameters detailed in Table 5.4.

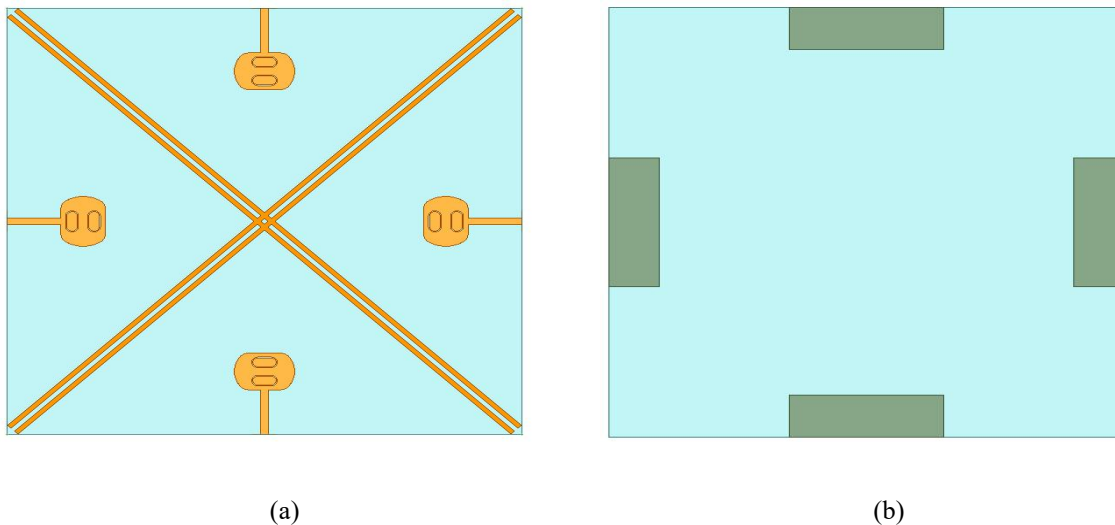


Figure 5.7: MIMO antenna with Decoupling structure: (a) Top view & (b) Bottom view

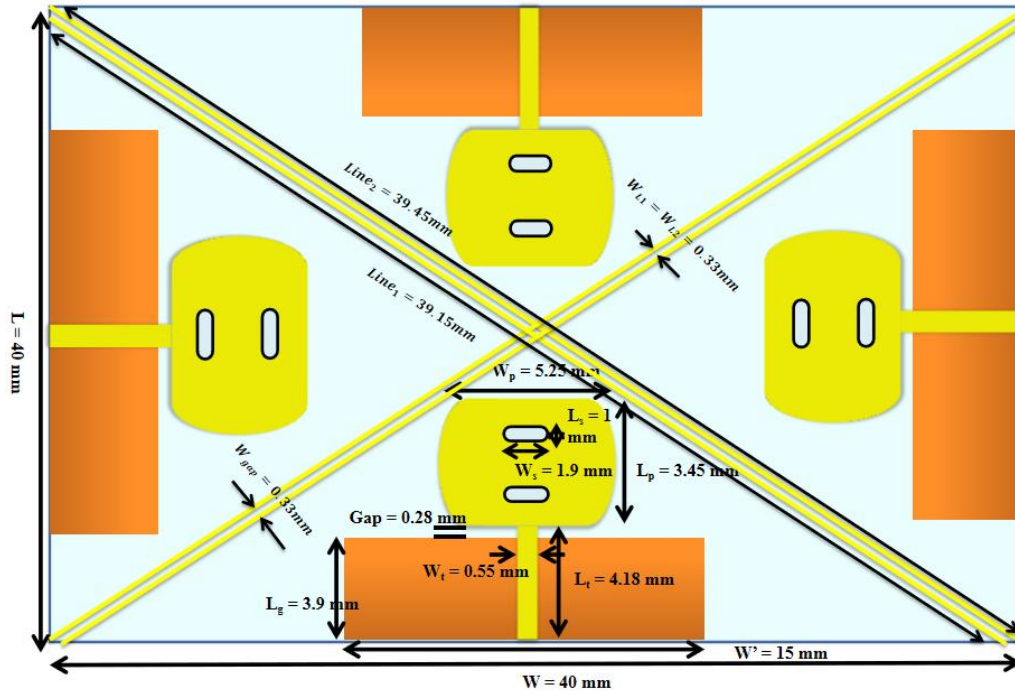
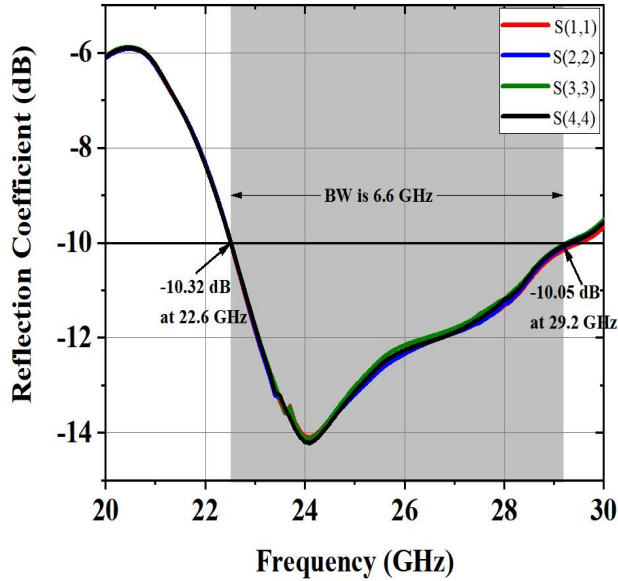


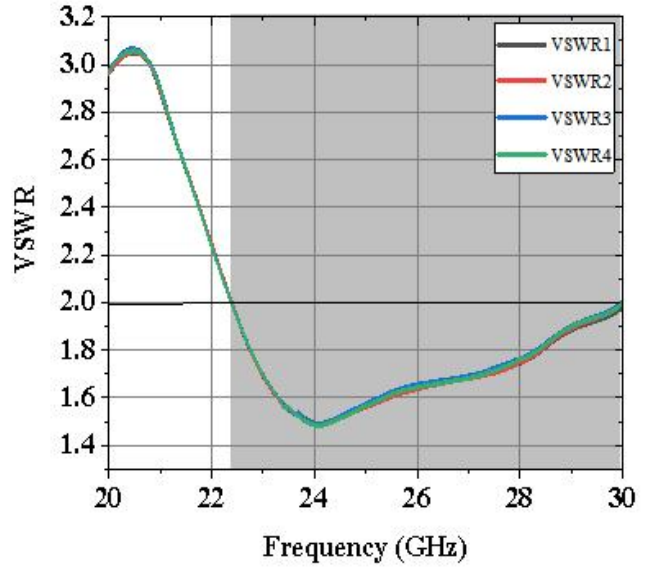
Figure 5.8: Dimensions of Quad Port MIMO antenna with decoupling (X-shaped wall) structure

Table 5.4: Optimal values of the proposed antenna dimensions for Decoupling structure (all in mm)

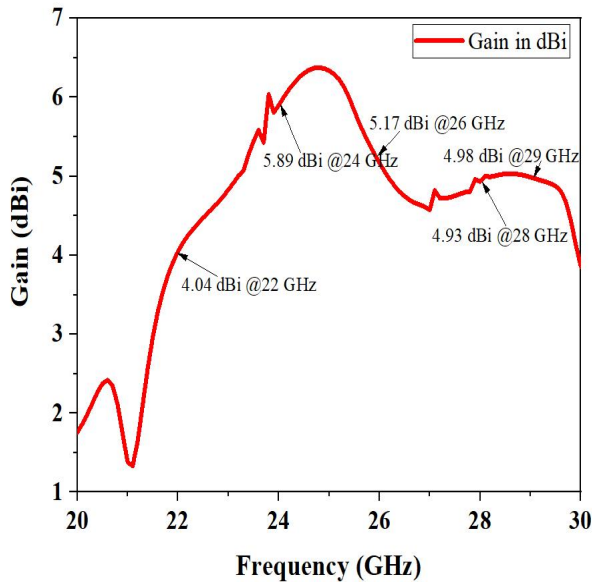
Parameters	Values (mm)
W_S	40
L_S	40
H_S	0.8
$Line_1$	39.15
$Line_2$	39.45
W_{gap}	0.33
W_{L1}	0.33
W_{L2}	0.33



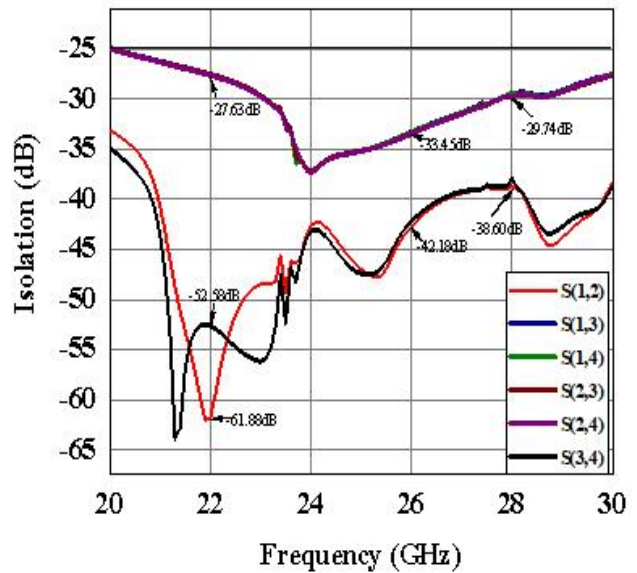
(a) Reflection coefficient vs. Frequency Plot



(b) VSWR vs. Frequency Plot



(c) Gain vs. Frequency Plot



(d) Isolation vs. Frequency Plot

Figure 5.9: Simulation Results of quad port MIMO Antenna design with introducing X-shaped decoupling structure:
 (a) Reflection coefficient , (b) VSWR, (c) Gain, and (d) Isolation

In Figure 5.9 shows the all simulated results of MIMO antenna with decoupling structure (introducing the X-shaped wall between the radiating elements) first figure is shown Reflection coefficient (S11) the maximum Reflection coefficient is -14.38 at 24 GHz frequency with wide band of 6.6 GHz. Second figure shows the VSWR which less than 2, the overall gain of the

antenna with in the entire band is greater than 2 dB or greater than 4.15 dBi and isolation is increased from -23 dB to -27.63 dB. In this technique the bandwidth is little bit decreased but isolation is improved so this technique is good for improving the isolation.

5.3.4. Defected Ground Structure:

The MIMO antenna structure with four ports and an isolation technique has been devised and simulated using Ansys HFSS software. The design is situated on an RT Duroid-5880 substrate, chosen for its low dielectric losses, featuring other values as 2.2, 0.0009, 0.8 mm dielectric constant, a loss tangent, and thickness respectively, and dimensions $L \times W$ mm². All four antenna elements (Ant-1 to Ant-4) are imprinted on the four sides of the substrate. The top layer of the substrate is utilized for positioning the microstrip feeding lines, while a section of the defected ground (incorporating a square mesh type defected ground structure) on the bottom layer is etched. Figure 5.10 presents both top and bottom views of the antenna design with the defected ground structure. In the subsequent Figure 5.11, the dimensions of the MIMO antenna with Defected Ground Structure (DGS) are delineated. All measurements are specified in millimeters, with corresponding parameters detailed in Table 5.5.

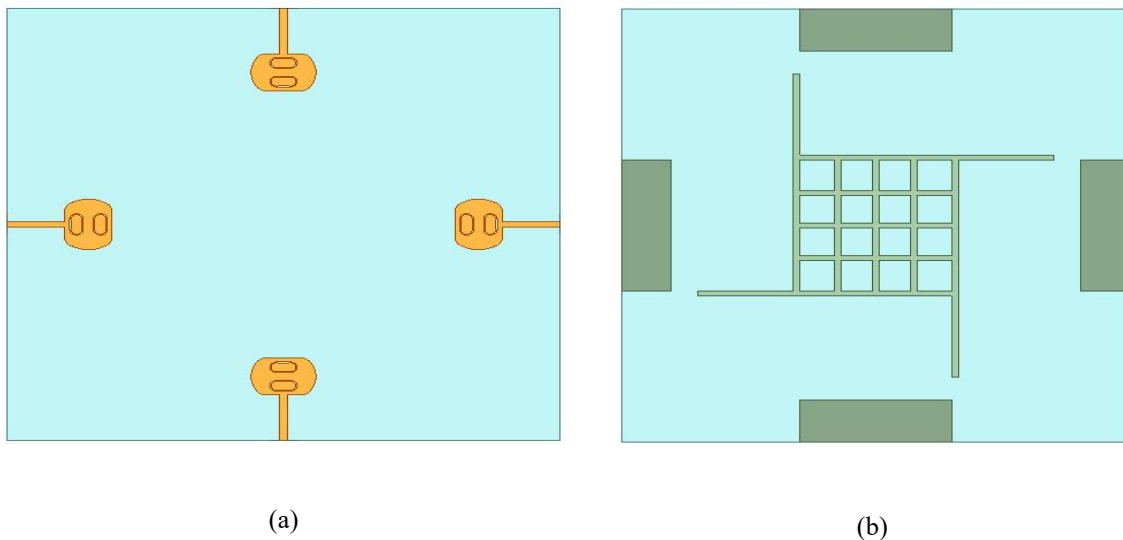


Figure 5.10: MIMO antenna with Defected Ground Structure (DGS): (a)Top view and (b) Bottom view

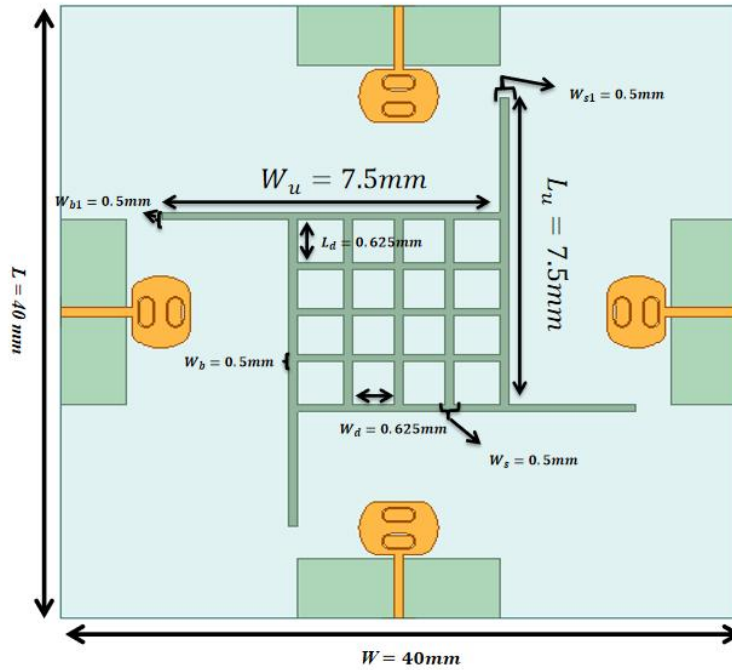
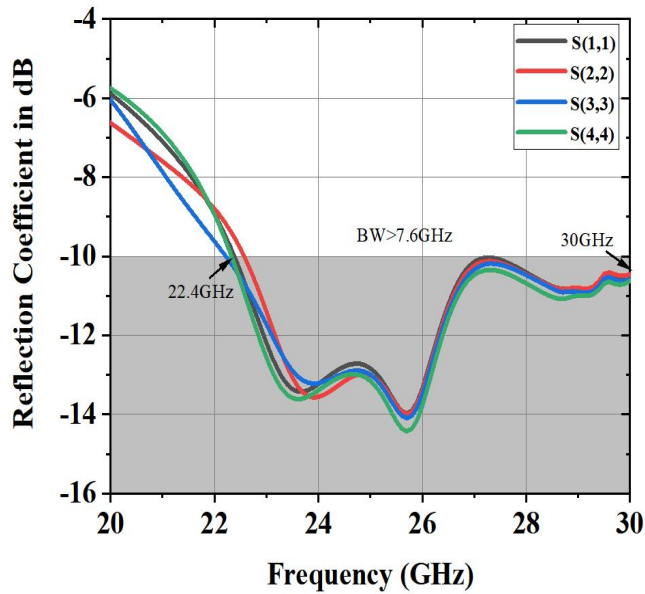


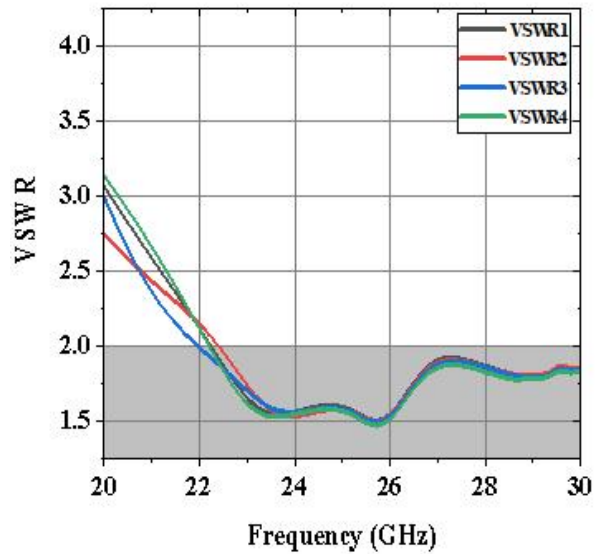
Figure 5.11: Dimensions of Quad Port MIMO antenna with Defected Ground Structure (DGS)

Table 5.5: Optimal values of the proposed antenna dimensions for DGS (all in mm)

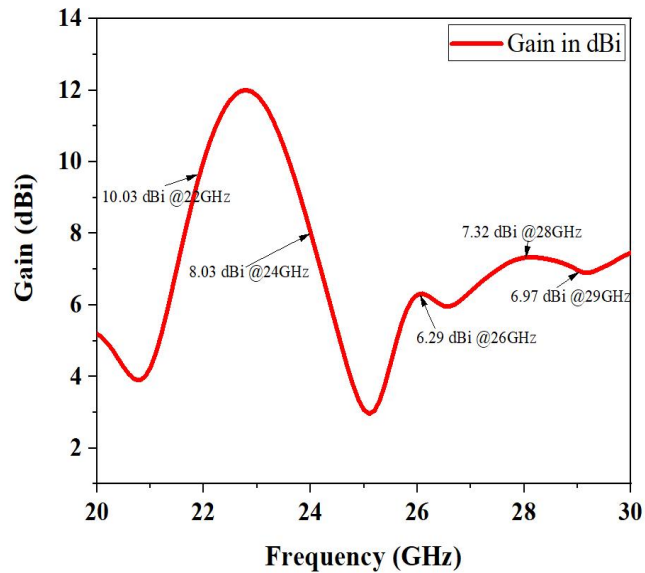
Parameters	Values (mm)
W	40
L	40
H_S	0.8
W_u	7.5
L_u	7.5
W_d	0.625
L_d	0.625
W_b	0.5
W_{b1}	0.5
W_s	0.5
W_{s1}	0.5



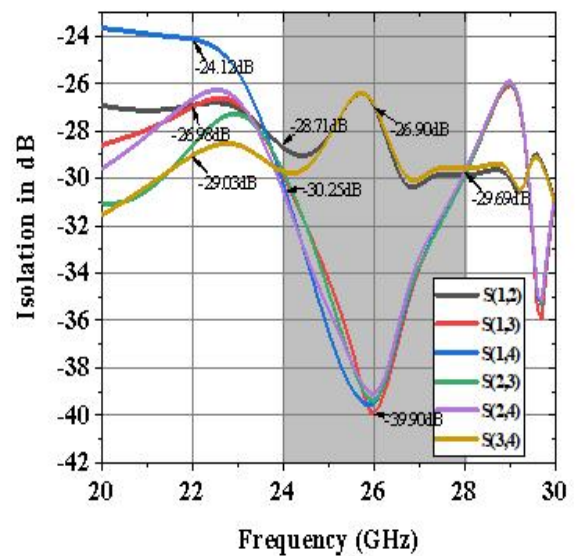
(a) Reflection coefficient vs. Frequency Plot



(b) VSWR vs. Frequency Plot



(c) Gain vs. Frequency Plot



(d) Isolation vs. Frequency Plot

Figure 5.12: Simulation Results of quad port MIMO Antenna design with Defected Ground Structure (DGS): (a) Reflection coefficient , (b) VSWR, (c) Gain, and (d) Isolation

In Figure 5.12 shows the all simulated results of MIMO antenna with defected ground structure first figure is shown Reflection coefficient (S11) the maximum Reflection coefficient is -14.73 at 25.8 GHz frequency with ultra wide band of 7.6 GHz. Second figure shows the VSWR which

less than 2, the overall gain of the antenna with in the entire band is greater than 4.14 dB or greater than 6.29 dBi and isolation is greater than -24 dB.

5.3.5. Hybrid Isolation Techniques:

Hybrid means combination of more then one or more techniques to make a new technique.

Following are some hybrid models proposed:

5.3.5.1. Hybrid Model 1 (Decoupling technique + DGS):

In this method, we integrate the decoupling technique with a Defected Ground Structure (DGS), resulting in an expansion of the bandwidth from 6.6 GHz to 7.5 GHz. Additionally, isolation is enhanced from -27 GHz to -28 GHz, and there is an improvement in Reflection coefficient from -14 dB to -16 dB, albeit with a trade-off in gain. Figure 5.13 provides front and bottom views of the antenna, while Figure 5.14 illustrates the dimensions of the MIMO antenna employing this hybrid technique. All measurements are specified in millimeters, with corresponding parameters detailed in Table 5.6.

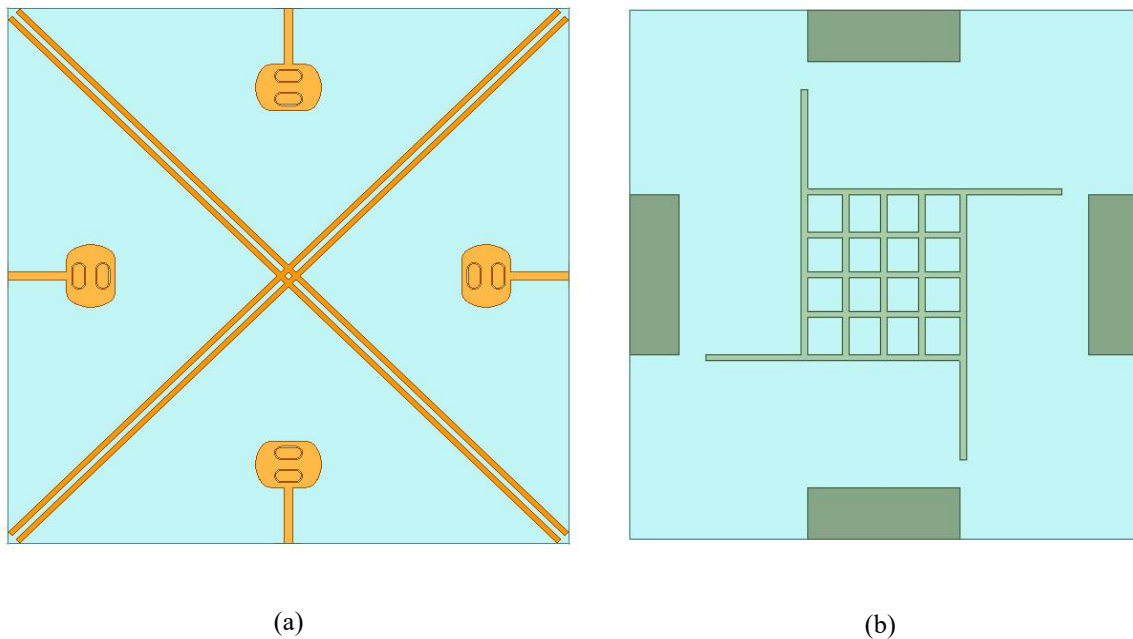


Figure 5.13: MIMO antenna with Hybrid Model 1 (a)Top view (b) Bottom view

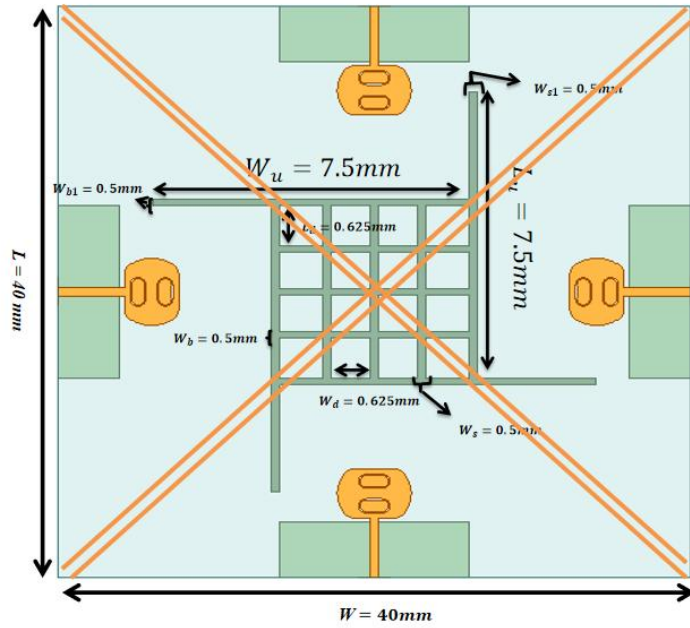
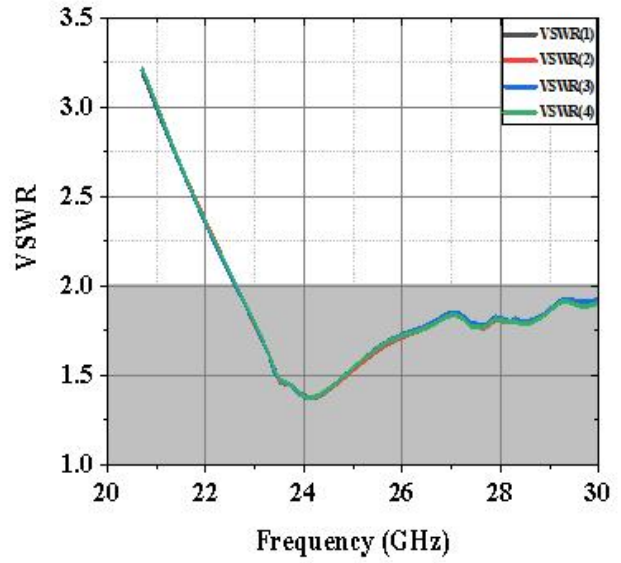
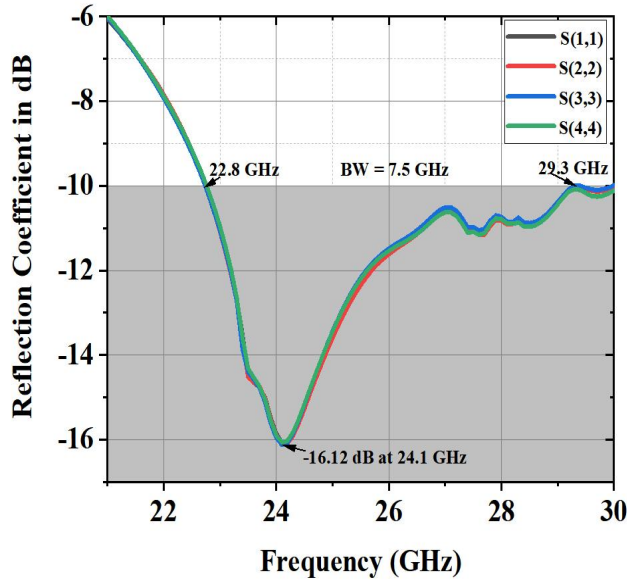


Figure 5.14: Dimensions of Quad Port MIMO antenna with Hybrid Model 1

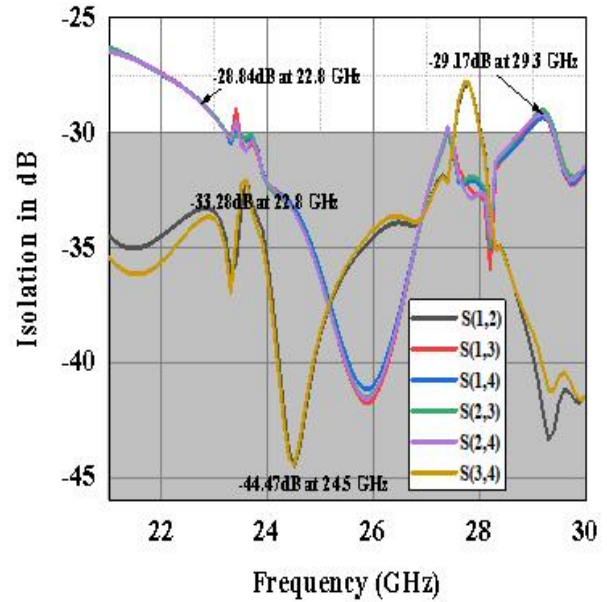
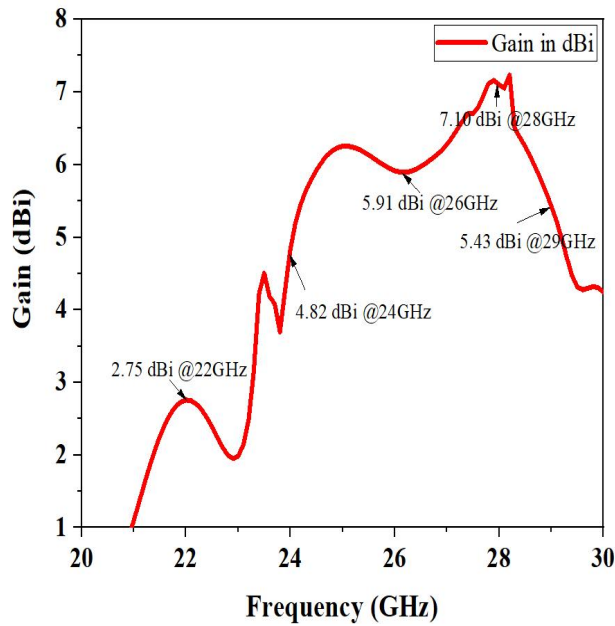
Table 5.6: Optimal values of the proposed antenna dimensions for Hybrid Model 1 (all in mm)

Parameters	Values (mm)
W_u	7.5
L_u	7.5
W_d	0.625
L_d	0.625
W_b	0.5
W_{b1}	0.5
W_s	0.5
W_{s1}	0.5
$Line_1$	39.15
$Line_2$	39.45
W_{gap}	0.33
W_{L1}	0.33
W_{L2}	0.33



(a) Reflection coefficient vs. Frequency Plot

(b) VSWR vs. Frequency Plot



(c) Gain vs. Frequency Plot

(d) Isolation vs. Frequency Plot

Figure 5.15: Simulation Results of quad port MIMO Antenna design with Hybrid Model 1: (a) Reflection coefficient, (b) VSWR, (c) Gain, and (d) Isolation

In Figure 5.15 shows the all simulated results of MIMO antenna with hybrid technique (combine two isolation technique like decoupling structure with defected ground structure) first figure is shown Reflection coefficient (S11) the maximum Reflection coefficient is -16.12 at 24.1 GHz frequency with ultra wide band of 7.5 GHz. Second figure shows the VSWR which less than 2, the overall gain of the antenna with in the entire band is maintained to 2 dB or greater than 4.15 dBi and isolation is improved from -23 dB to -28.84 dB. In this technique the bandwidth and gain both are maintained but isolation is increased. So for improving the isolation may use the hybrid technique.

5.3.5.2. Hybrid Model 2 (DGS + MGS):

In this method, we integrate the Modified Ground Structure (MGS) with a Defected Ground Structure (DGS), resulting in an expansion of the bandwidth from 7.5 GHz to 9.5 GHz (2 GHz increment). Additionally, isolation is decreased from -27 GHz to -23 GHz, and there is not improvement in Reflection coefficient from -14 dB to -13.012 dB, albeit with a trade-off in gain. Figure 5.16 provides front and bottom views of the antenna, due to these decrements in isolation and Reflection coefficient (in dB) and negative gain this prototype is not fit to our application although its provide the good bandwidth.

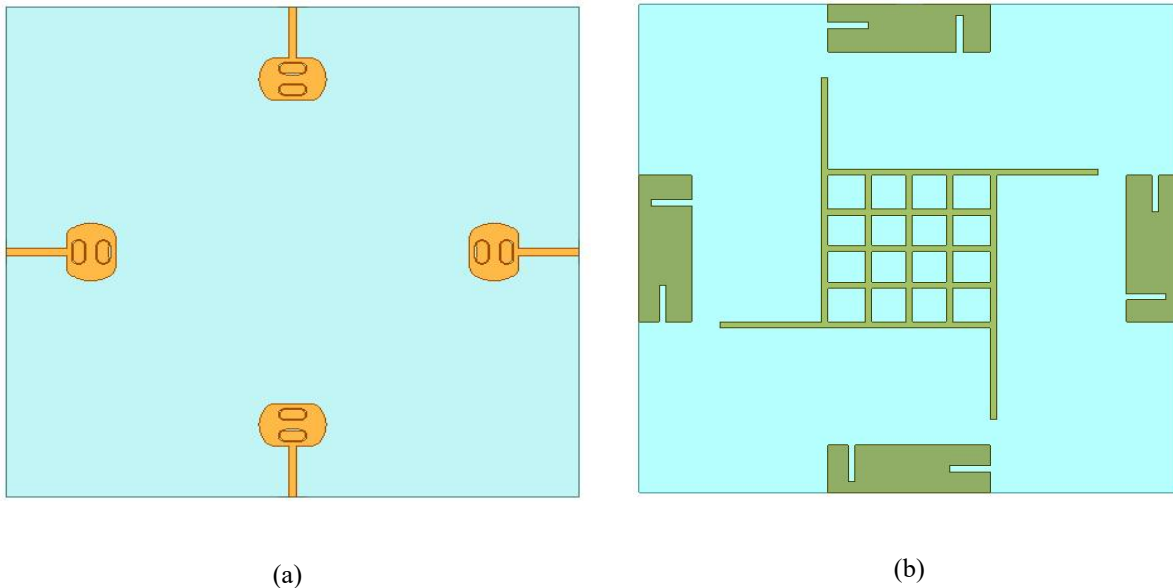
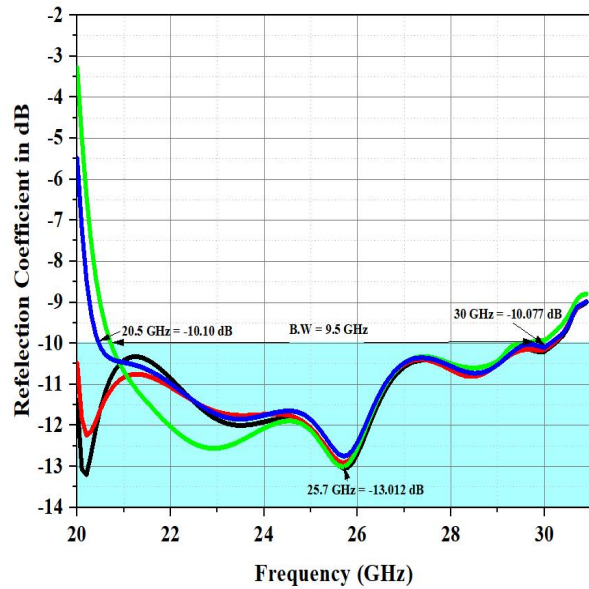
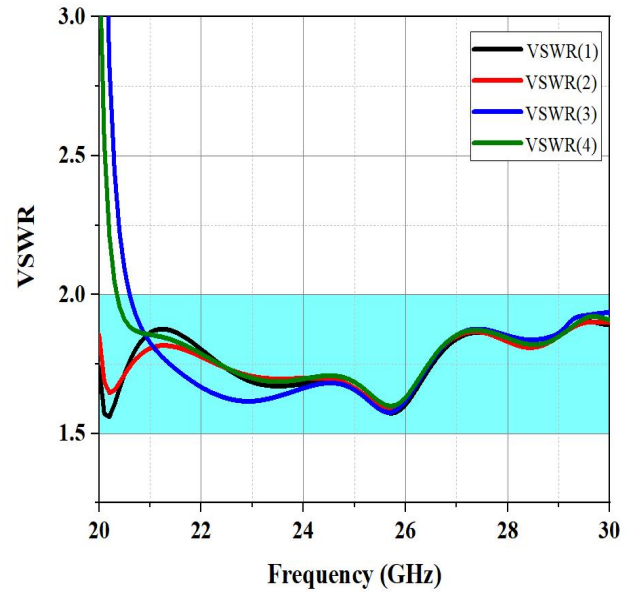


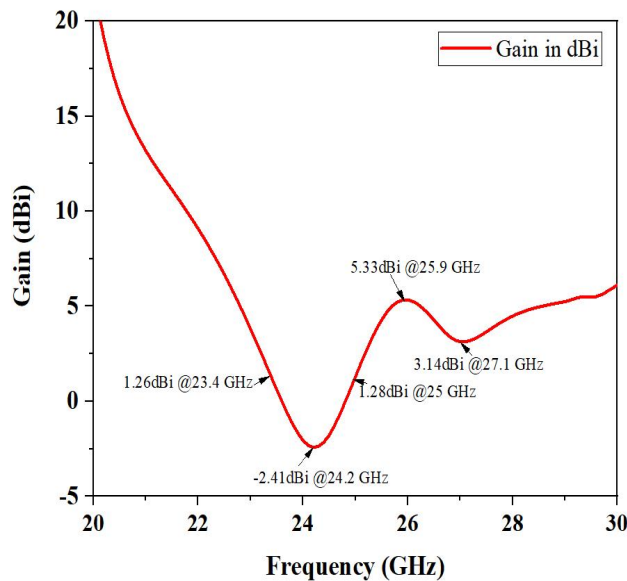
Figure 5.16: MIMO antenna with Hybrid Model 2 (a)Top view (b) Bottom view



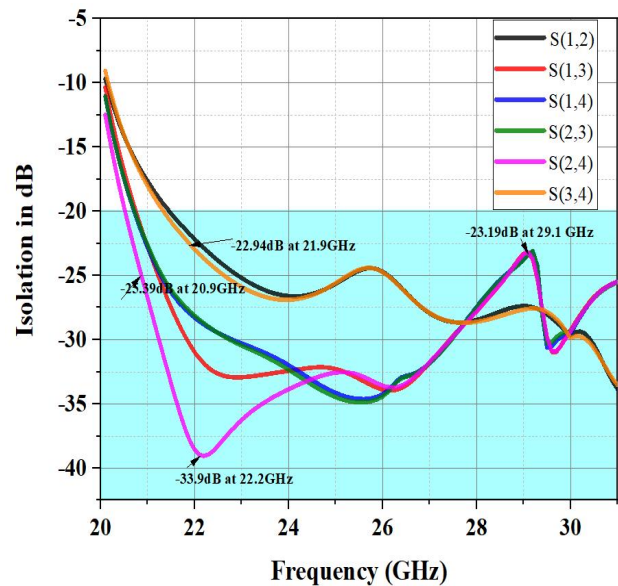
(a) Reflection coefficient vs. Frequency Plot



(b) VSWR vs. Frequency Plot



(c) Gain vs. Frequency Plot



(d) Isolation vs. Frequency Plot

Figure 5.17: Simulation Results of quad port MIMO Antenna design with Hybrid Model 2: (a) Reflection coefficient, (b) VSWR, (c) Gain, and (d) Isolation

In Figure 5.17 shows the all simulated results of MIMO antenna with hybrid technique 2 (combine two isolation technique like modified Ground structure with defected ground structure) first figure is shown Reflection coefficient (S_{11}) the maximum Reflection coefficient is -13.014 at 25.7 GHz frequency with ultra wide band of 9.5 GHz. Second figure shows the VSWR which

less than 2, due to these decrements in isolation and Reflection coefficient (in dB) and negative gain this prototype is not fit to our application although its provide the good bandwidth.

5.3.5.3. Hybrid Model 3 (Decoupling + Defected Ground + Modified Ground):

In this approach, we integrate the three isolation techniques like a Decoupling Structure, Defected Ground Structure (DGS) and Modified Ground Structure (MGS), resulting in an expansion of the bandwidth from 7.5 GHz to 8 GHz. Moreover, isolation is enhanced from -27 GHz to -28 GHz, and there is an improvement in Reflection coefficient from -13.014 dB to -14.57 dB, although there is a little bit compromisation with gain overall gain is 1.89dB or 4.04 dBi. Figure 5.18 displays the front and bottom views of the antenna, while Figure 5.17 provides the dimensions of the MIMO antenna using this hybrid technique 3. All measurements are specified in millimeters, with respective parameters detailed in Table 5.7.

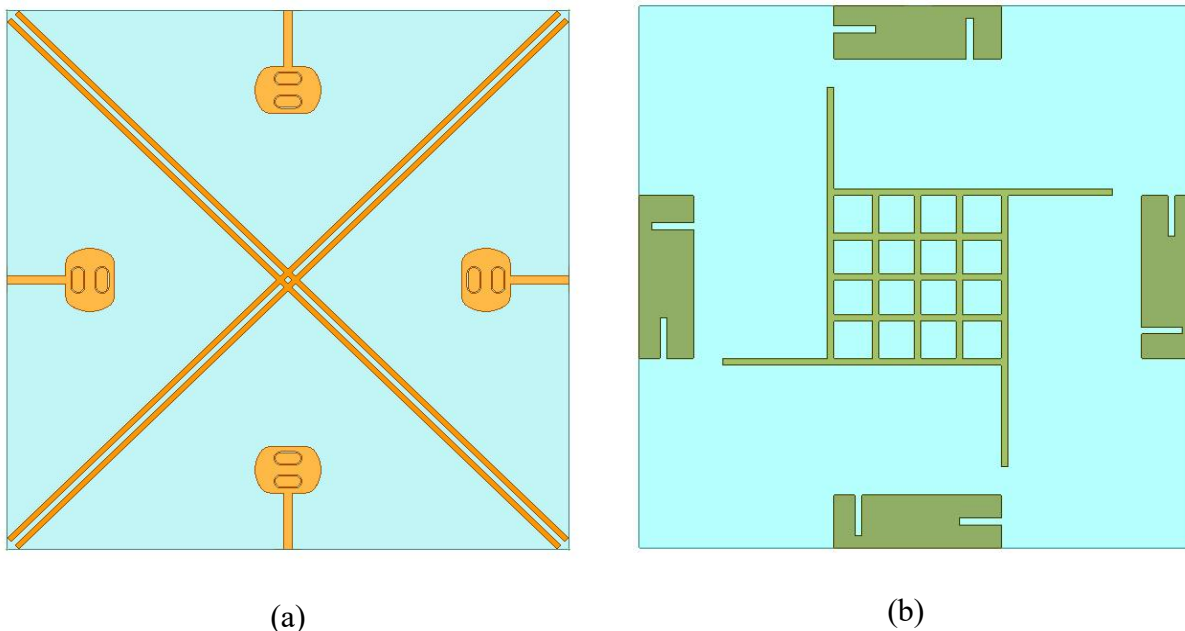
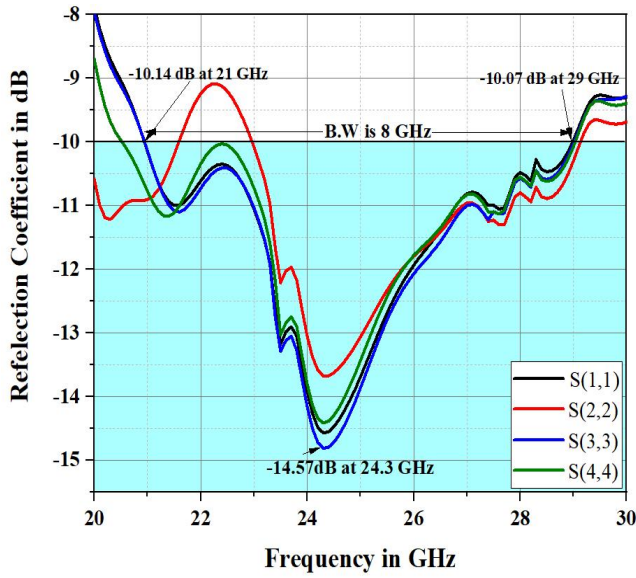
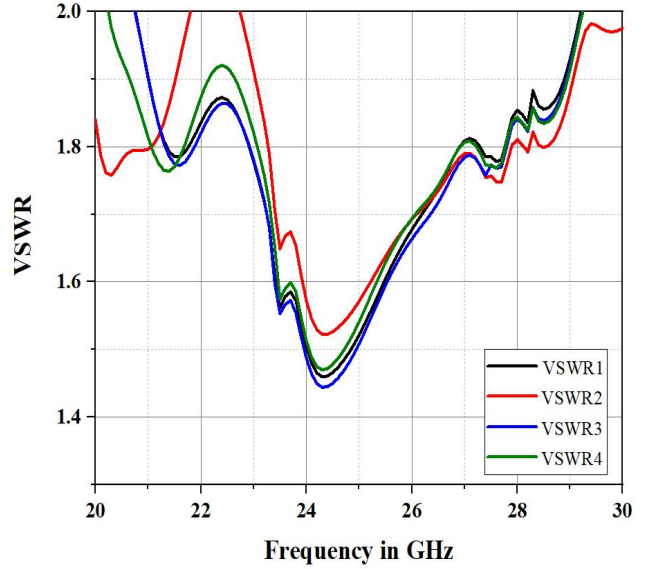


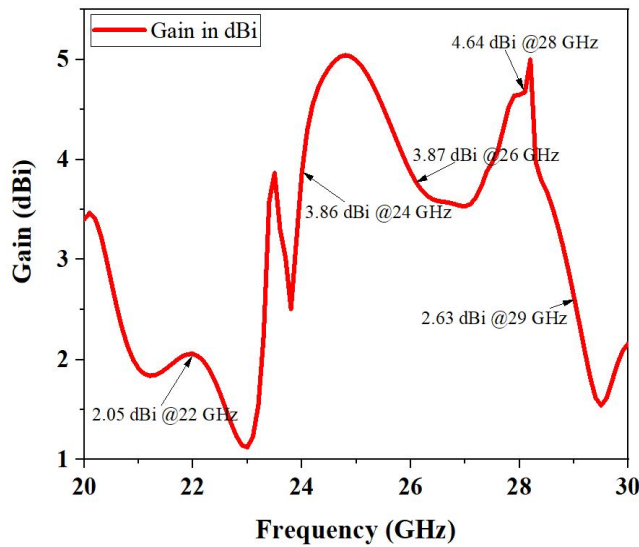
Figure 5.18: MIMO antenna with Hybrid Model 3 (a)Top view (b) Bottom view



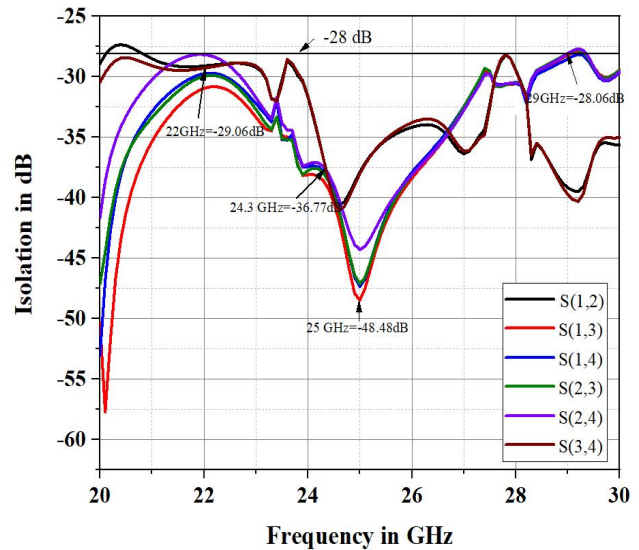
(a) Reflection coefficient vs. Frequency Plot



(b) VSWR vs. Frequency Plot



(c) Gain vs. Frequency Plot



(d) Isolation vs. Frequency Plot

Figure 5.19: Simulation Results of quad port MIMO Antenna design with Hybrid Model 3: (a) Reflection coefficient, (b) VSWR, (c) Gain, and (d) Isolation

In Figure 5.19 shows the all simulated results of MIMO antenna with hybrid technique 3 (combine three isolation techniques like decoupling structure, defected ground structure and modified ground structure) first figure is shown Reflection coefficient (S_{11}) the maximum Reflection coefficient is -14.57 at 24.3 GHz frequency with ultra wide band of 8 GHz (from 21 GHz to 29 GHz). Second figure shows the VSWR which less than 2, the overall gain of the

antenna with in the entire band is maintained to 1.89 dB or greater than 4.04 dBi and isolation is improved from -23 dB to -28 dB. In this technique the bandwidth and gain both are maintained but isolation is increased. So for improving the isolation may use the hybrid technique 3. Due to these improved features of the hybrid technique 3 (like improved isolation and Reflection coefficient (in dB) and maintaining the gain etc.) this prototype is fit to all 5G and millimeter wave applications although its provide the good bandwidth.

Table 5.7: Comparison table of all the simulated results

S. No.	Isolation Technique	Frequency range (GHz)	Bandwidth (BW GHz)	Reflection Coefficient (S11 dB)	Overall Gain (dBi)	Isolation (dB)
1.	MIMO (without isolation)	22.1 to 29.9	7.8	-13	> 5.85	> -23
2.	Modified Ground Structure (MGS)	20.8 to 29.6	8.8	-14	> 5.86	> -23.52
3.	Defected Ground Structure (DGS)	22.4 to 30	7.6	-14.73	> 6.29	> 24
4.	Decoupling structure	22.6 to 29.2	6.6	-14.34	> 4.15	> -27.63
5.	Hybrid Model 1 (Decoupling + DGS)	22.8 to 29.3	7.5	-16.12	maximum gain is 7.35 dBi	> -27 (with high variation)
6.	Hybrid Model 2 (DGS + MGS)	20.5 to 30	9.5	-13.012	Negative Gain	> -23
7.	Hybrid Model 3 (Decoupling + DGS + MGS)	21 to 29	8	-14.81 at 24.3 GHz	maximum gain is 5.35 dBi	> -28

The proposed MIMO antenna in this work has several notable features, as observed in Table 5.1 and Table 5.7. Firstly, it provides wide band coverage for high-frequency 5G wireless applications, surpassing the range of reference [130-143]. Secondly, maintaining a level above -

27 dB throughout the operating band. Additionally, the proposed antenna has smaller dimensions when compared to References [134-137]. Moreover, the proposed antenna does not rely on a three-dimensional structure, making it straightforward to fabricate and less intricate. Lastly, the newly designed MIMO antenna offers complete K-band coverage within a single ultra-wide band.

5.4. MEASUREMENT RESULTS FOR COMBINED ISOLATION TECHNIQUE

The experimental antenna showcased in this research was produced using the MITS-Eleven Lab printed circuit board machine, employing a Roger RT Duriod 5880 substrate. It features four antenna elements arranged on a compact substrate measuring 40 mm x 40 mm, as shown in Figure 5.20. The substrate had other values as 2.2, 0.0009, 0.8 mm dielectric constant, a loss tangent, and a thickness respectively. To validate the accuracy of the simulated results, measurements were conducted using an Agilent N5230A vector network analyzer (VNA). Additionally, radiation characteristics were assessed within an anechoic chamber, as depicted in Figure 5.21.

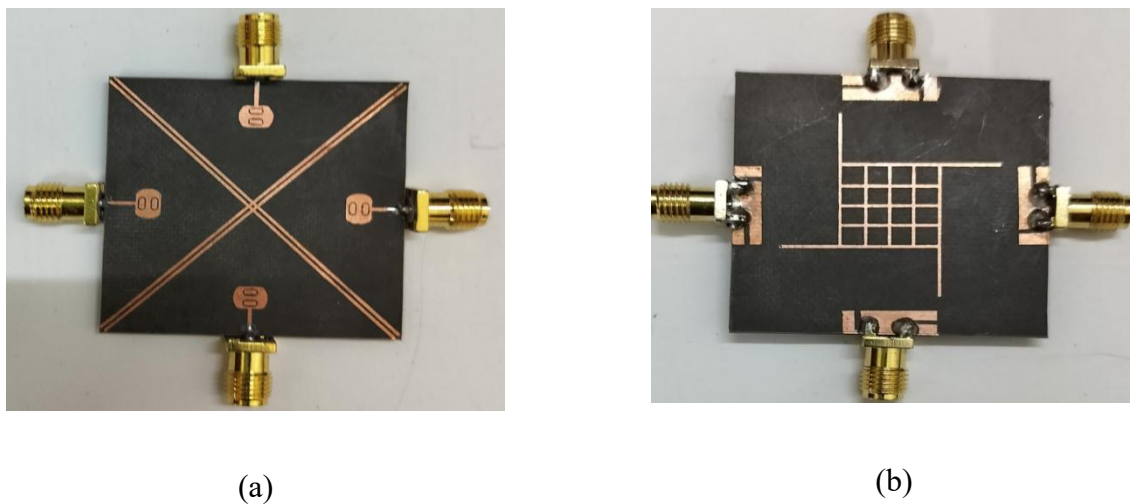
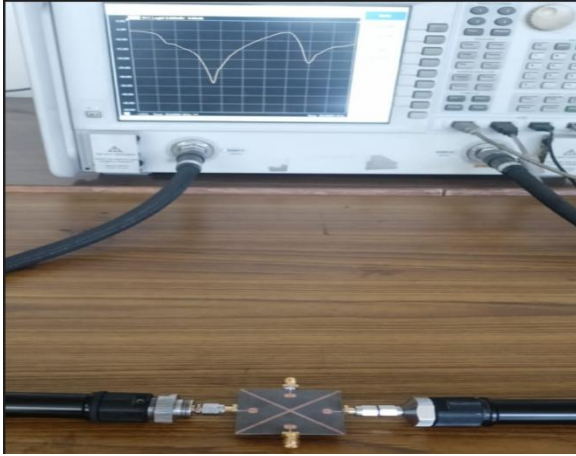
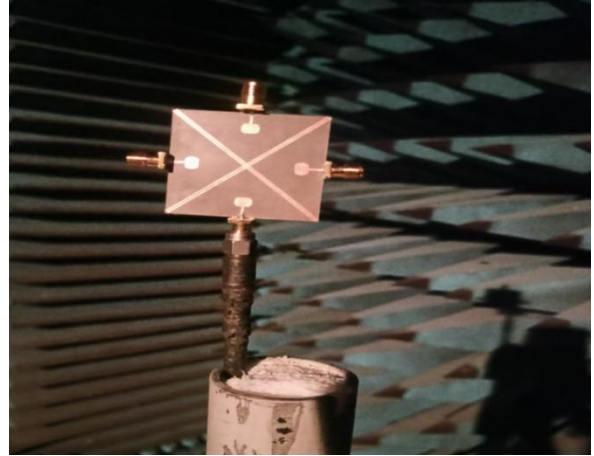


Figure 5.20: Fabricated prototype (a) Top View (b) Bottom View



(a)



(b)

Figure 5.21: Measurement setups (a) with VNA , and (b) in Anechoic Chamber

A comparison between the measured and simulated results is conducted to authenticate the antenna's performance. Figure 5.22 illustrates the S-parameter outcomes, offering a side-by-side comparison of the measured and simulated data. The measured Reflection coefficient indicated an impedance bandwidth spanning from 22 GHz to 29 GHz, meeting the UWB requirement stipulated by the FCC. The measured and simulated results from HFSS demonstrated robust agreement.

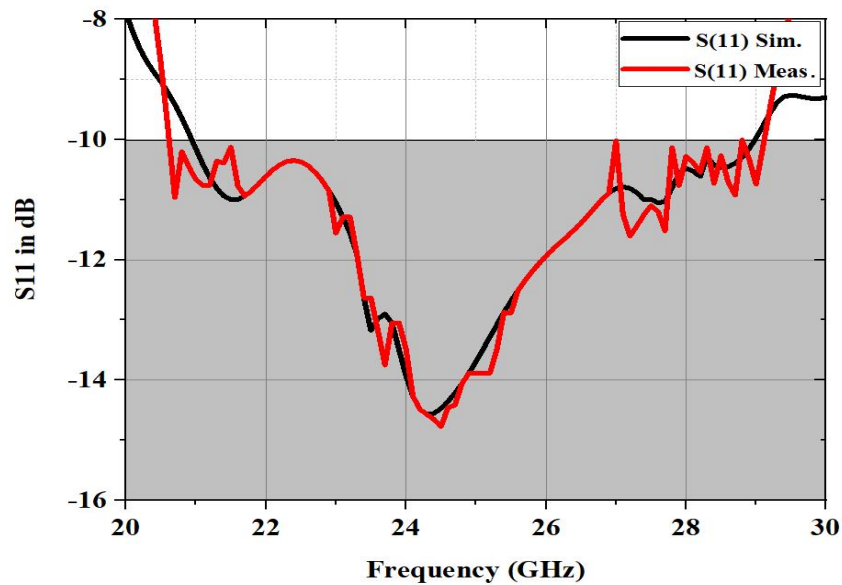


Figure 5.22: Simulated and measured S11 in dB

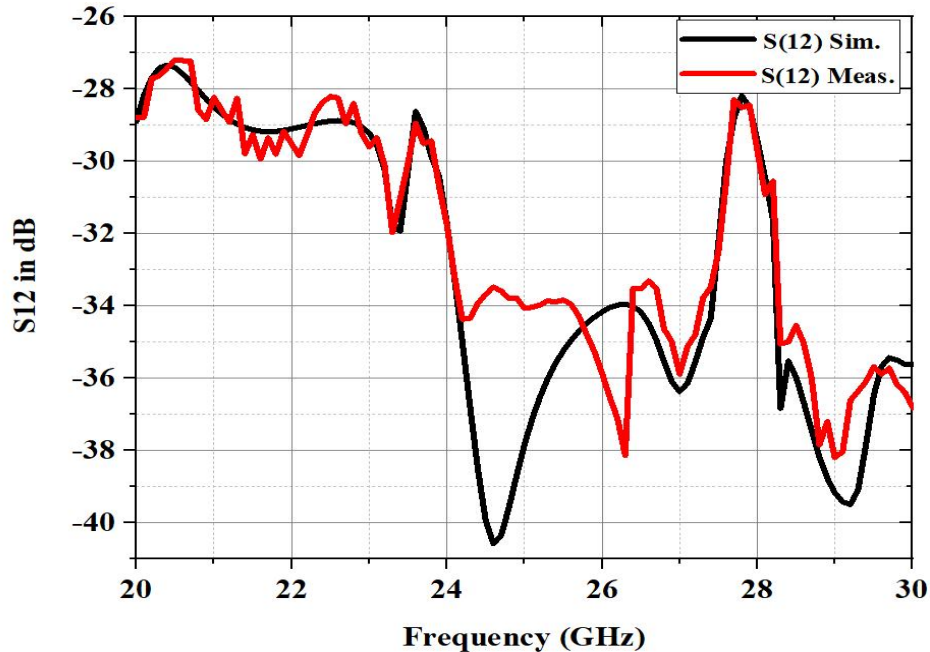


Figure 5.23: Simulated and measured S12 in dB

In Figure 5.23, the measurement and simulation results of the isolation parameters are depicted. The analysis reveals that the values for S_{12} , were consistently below -27 dB across the entire UWB range. This finding suggests that the proposed prototype exhibits minimal interference or coupling between its ports.

The performance analysis of the MIMO antenna design with high isolation techniques for 5G wireless systems yielded promising results. The proposed antenna design achieved high isolation between the antenna elements, ensuring minimal interference and improved overall system performance. Through extensive simulations and measurements, it was observed that the proposed antenna design achieved a high level of isolation, surpassing the requirements set by 5G communication standards. The significant isolation achieved between the antenna elements resulted in increased system capacity and network efficiency. Furthermore, the MIMO antenna design demonstrated excellent radiation pattern characteristics, ensuring consistent pattern stability across a wide range of frequency bands. This guarantee of consistent and reliable signal transmission reduced signal degradation and increased coverage area. The results also showed that the proposed antenna design significantly improved bandwidth, gain, and isolation. These advances in isolation and frequency bandwidth are crucial for 5G wireless systems.

Table 5.8: Comparison table of all the existing work with proposed work

Ref. No.	Year	Antenna Size (mm ²)	No. of Elements	Frequency (GHz)	BW (GHz)	Isolation (dB)	ECC	DG (dB)
[144]	2017	115 × 65 = 7475	4	28.5	1.22	12	0.1	---
[145]	2017	80 × 80 = 6400	4	30	23-30	20	0.0014	9.91
[146]	2017	60 × 100 = 6000	2	28	27.6-28.3	17	0.134	9.92
[147]	2018	31 × 48 = 1488	4	28	5	21	0.0015	---
[148]	2019	35 × 46 = 1610	4	28/38	2.55	20	<0.005	10
[149]	2019	55 × 110 = 6050	4	28.044 /38.04	10	26	---	--
[150]	2020	80 × 80 = 6400	4	28/38	17	20	<0.0014	---
[151]	2020	30 × 35 = 1050	4	28	4.1	17	<0.01	9.96
[152]	2020	60 × 100 =6000	2	28	1.7	20	---	---
[153]	2023	36.2 × 36.2 = 1310.44	4	38	2	25	<0.005	9.99
[154]	2023	45 × 45 = 2025	4	28	1.65	23.31	<0.002	9.99
This Work	2023	40 × 40 = 1600	4	24/28	8	>28	<0.006	9.999

Here, in Table 5.8 compared all designed antenna simulated results. The size of the antenna is $40 \times 40 \times 0.8 \text{ mm}^3$ and placed on the Rogers RT/ Duroid 5880 substrate. Its seem that decoupling structure improved the isolation but on the compromisation on other parameters like gain and bandwidth while the hybrid model (combination of decoupling and defected ground structure) improved the isolation as well as maintain the other parameters. Overall, the results of the performance analysis suggest that the MIMO antenna design with high isolation techniques is a promising solution for 5G wireless systems. Its ability to achieve high isolation, maintain stable radiation patterns, and enhance signal quality metrics makes it a valuable choice for future.

5.5. SUMMARY

When designing a MIMO antenna with various isolation techniques, it is crucial to thoroughly analyse the antenna type, design properties, and the desired level of isolation. This careful consideration is essential for optimizing the antenna's overall performance. Each type of isolation technique offers unique features that are suited to certain types of wireless communication systems, ranging from low-cost conventional methods to more complex signal cancellation techniques. As a result, the selection of the most suitable isolation technique for any given MIMO antenna design depends on the individual goals and requirements of the system. The suggested MIMO antenna comprises four elements, with decoupling structure (introducing the X-shaped wall between the radiating elements), is an effective solution for 5G communications. Operating at a frequency range between 22.5 GHz and 29.1 GHz, the antenna offers an isolation level of 27.63 dB and a gain enhancement of 6.39 dBi while the hybrid technique improved the isolation till 28.84 dB as well as improved the bandwidth from 6.6 GHz to 7.5 GHz with maintained gain. HFSS software simulations demonstrate excellent agreement between the expected results and the parameters observed, including Reflection coefficient, Voltage standing wave ratio (VSWR), isolation level, and Peak Gain, throughout the operating band. These outcomes affirm the antenna's dependable suitability for 5G communications. Here, Hybrid Technique is best suitable isolation technique for the proposed MIMO antenna design.

CHAPTER-6

RESULT AND DISCUSSIONS

6.1. INTRODUCTION

This Chapter introduces a newly designed four-element UWB MIMO antenna that exhibits improved performance and a wide impedance bandwidth. The design of the antenna is based on a symmetrical structure and incorporates an X-shaped decoupling structure, alongside multi-slit and multi-slot techniques. As a result of these enhancements, the antenna has a compact, low-profile structure measuring $40 \text{ mm} \times 40 \text{ mm} \times 0.8 \text{ mm}$, while delivering ultra-wide band performance. For evaluation purposes, the proposed antenna is constructed Employing Roger RT Duroid 5880, characterized by a dielectric constant of 2.2 and thickness (t_m) measuring 0.8 mm. Investigations reveal that the impedance bandwidth of antenna covers the frequency range of 22.5 GHz - 29.2 GHz, with isolation greater than -27 dB, a diversity gain of 10.0 dB, an envelope correlation coefficient (ECC) of 0.004, and an overall total effective reflection coefficient of -17 dB, accompanied by a gain of 4.38 dB. Notably, the proposed antenna strikes a balance between wide bandwidth, compact size, and excellent isolation. Moreover, its omnidirectional radiation characteristics make it particularly suitable for various emerging UWB-MIMO communication systems, including small scale wireless devices for satellite communication. The proposed MIMO antenna exhibits several advantageous features, especially when compared to recent UWB MIMO designs. These attributes position it as an appealing choice for 5G and future wireless communication systems.

6.2. ANTENNA DESIGN AND ANALYSIS

UWB (Ultra-Wide band) MIMO antenna design with a decoupling structure is aim to get maximum possible isolation in between the radiating antenna elements with enhanced performance of UWB-MIMO systems. MIMO technology is mostly used in modern wireless communication systems and devices to improve data transmission rates, spectral efficiency, and overall system capacity. Nonetheless, the close proximity of multiple antenna elements can cause

mutual coupling, affecting MIMO system performance [144]. A decoupling structure is introduced to address this coupling effect.

In some cases, an elliptical-shaped antenna outperforms rectangular and circular-shaped antennas. Here are some of the advantages of an elliptical design:

1. Elliptical antennas have wider bandwidths than rectangular and circular antennas. This is especially useful in Ultra-Wide band (UWB) communication systems, where a wide frequency range is required for high data rates and spectral efficiency.
2. In comparison to rectangular and circular antennas, the elliptical shape allows for better impedance matching over a wider frequency range. As a result, there are fewer signal reflections and better power transfer efficiency.
3. Circular antennas frequently exhibit higher levels of cross-polarization, resulting in increased interference and signal degradation. In polarization-sensitive applications, elliptical antennas typically exhibit superior cross-polarization characteristics, enhancing signal quality and reducing interference.

Impedance characteristic of the microstrip antenna's may calculated by using equation (6.1):

$$Z_0 = \frac{Z_{01}}{\sqrt{\epsilon_e}} \quad (6.1)$$

Where the microstrip line of impedance in free space is given by equation (6.2):

$$Z_{01} = Z_0 | (\epsilon_r=1) = 60 \ln \left[\frac{f_1 h}{w} + \sqrt{1 + \left(\frac{2h}{w} \right)^2} \right],$$

$$f_1 = 6 + (2\pi - 6) \exp\{-(30.66 * h/\omega) * 0.7528\} \quad (6.2)$$

The effective height and width of the antenna can be computed using the equations (6.3), (6.4), and (6.5):

$$W = w + \frac{t}{\pi} \left[\ln \left(\frac{2 \times h}{t} \right) + 1 \right]$$

$$\text{Here, } H = h - 2t \quad (6.3)$$

For $\frac{W}{H} < 1$

$$\epsilon_{\text{eff}} = \frac{\epsilon_r + 1}{2} + \frac{\epsilon_r - 1}{2} \left[\frac{1}{\sqrt{1 + 12 \left(\frac{H}{W}\right)}} + 0.04 \left(1 - \frac{W}{H}\right) \times 2 \right]$$

$$Z_0 = \frac{60}{\sqrt{\epsilon_{\text{eff}}}} \ln \left\{ 8 \left(\frac{H}{W}\right) + \frac{1}{4} \left(\frac{W}{H}\right) \right\} \Omega \quad (6.4)$$

Also,

$$\lambda = \frac{c}{f \sqrt{\epsilon_{\text{eff}}}} \quad \text{and} \quad \theta = \frac{2\pi}{\lambda}$$

For $\frac{W}{H} \geq 1$

$$\epsilon_{\text{eff}} = \frac{\epsilon_r + 1}{2} + \frac{\epsilon_r - 1}{2 \times \sqrt{1 + 12 \left(\frac{H}{W}\right)}}$$

$$Z_0 = \frac{120 \pi}{\sqrt{\epsilon_{\text{eff}} \left[\frac{W}{H} + 1.393 + \frac{2}{3} \ln \left(\frac{W}{H} + 1.444\right) \right]}} \Omega \quad (6.5)$$

The wavelength is determined using equation (6.6):

$$\lambda_g = \frac{c}{f \sqrt{\epsilon_r}} \quad (6.6)$$

To determine the size of the elliptical patch for both low and high cut-off frequencies, utilize the provided expression (6.7) to obtain the diameter.

$$f_L = \frac{72}{L + r + h} \quad (6.7)$$

Where L represents the diameter of the radiator, h is the substrate thickness, and r can be calculated using equation (6.8):

$$r = \frac{L}{2\pi} \quad (6.8)$$

Considering a substrate with a thickness of 0.8 mm and a dielectric permittivity of 2.2 and equation (6.1) to (6.8) belong to the reference [145].

Here, UWB MIMO antenna utilizing four elements and offering improved isolation is presented for 5G applications in the (22.6–29.2) GHz range. The radiating elements consist of microstrip feed rectangular patches with semi-circles at the bases and dual slots etched out, with a partial ground plane. Investing time into optimizing the antenna to resonate at 24 GHz delivered a wide impedance bandwidth ranging from 22.6 to 29.2 GHz (BW is 6.6 GHz). Moreover, introduction X-shaped walls placed between the antenna elements to enhance the isolation.

Figure 6.1 illustrates the antenna's geometry, structure, and layout, including the parameters, in both top view (incorporating X-shaped walls as a decoupling structure) and bottom view with partially grounded elements. The optimized parameters of the designed antenna are shown in Figure 6.2 and Table 6.1, achieved through analysis and optimization using the Ansys HFSS software. This section details the antenna's design process and development.

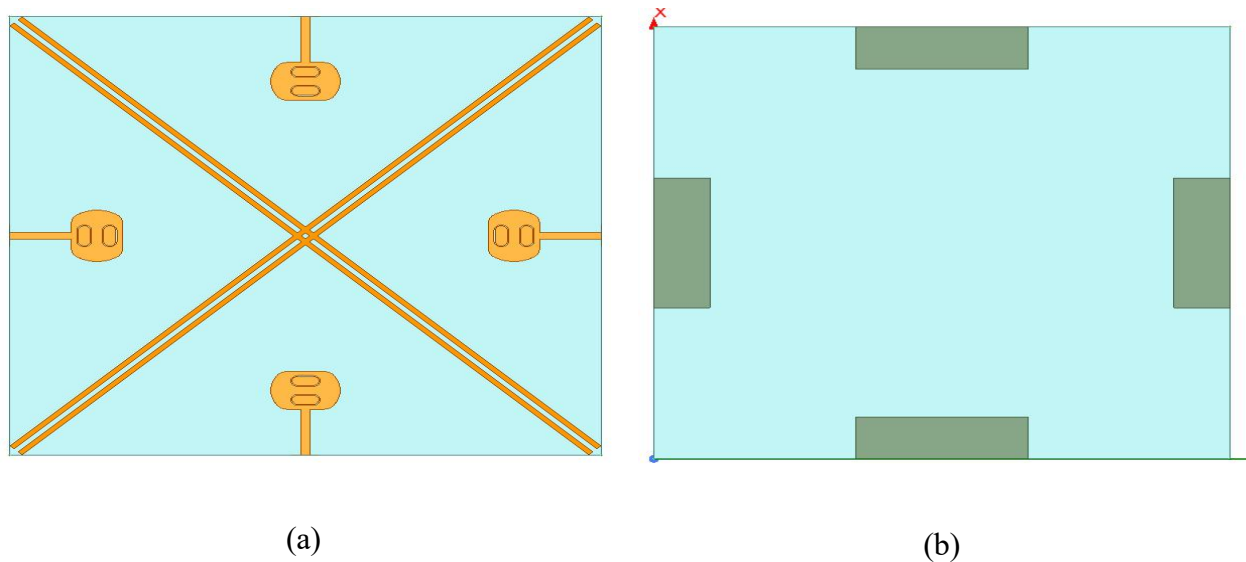


Figure 6.1: The proposed antenna layout (a) Top View and (b) Bottom View

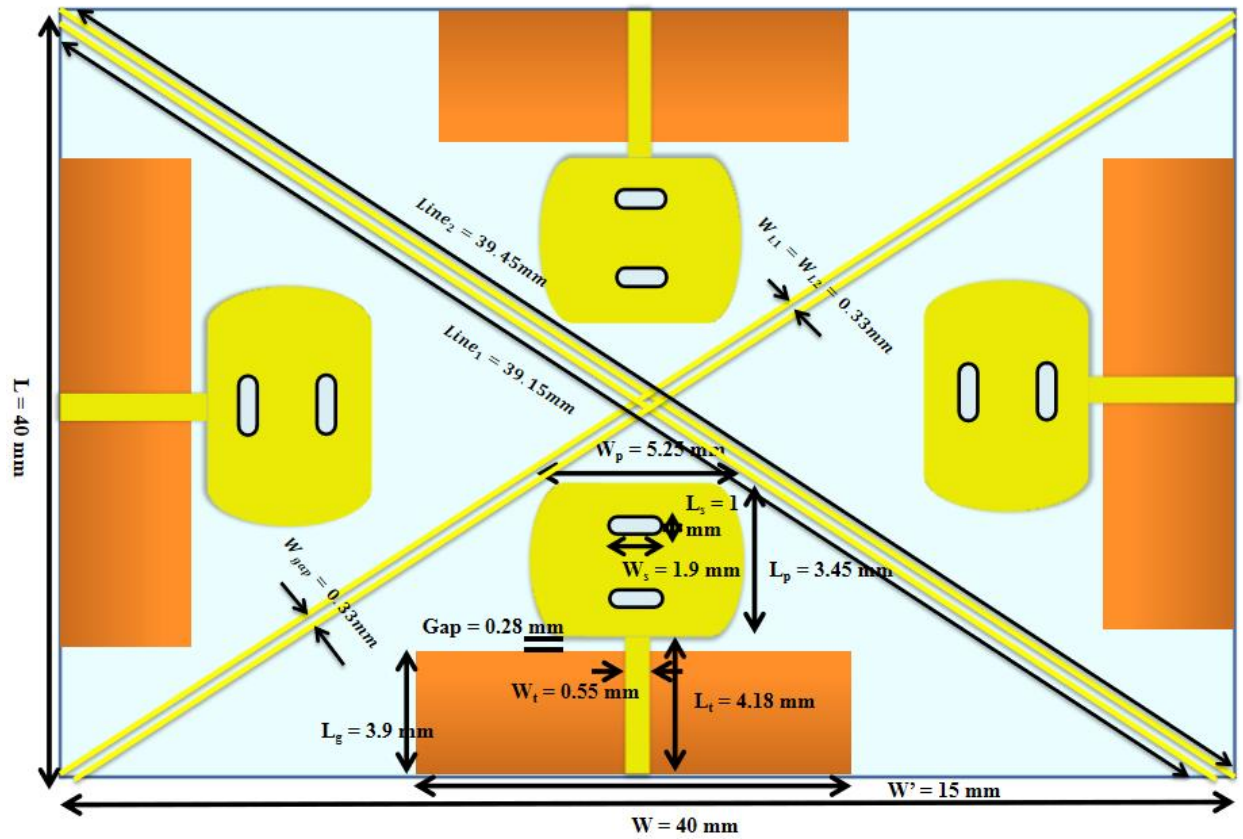


Figure 6.2: Dimensions of the proposed MIMO antenna with decoupling Structure

Table 6.1: Optimal values of the proposed antenna dimensions (all in mm)

Parameters	Values (mm)	Parameters	Values (mm)
W_S	40	W_3	0.25
L_S	40	L_3	0.25
H_S	0.8	W_a	14
W_P	4.17	W_b	19.72
L_P	3.44	W_c	24.82
W_F	0.525	L_{g1}	0.82

L_F	4.18	L_{g2}	0.52
W_g	12	L_{g3}	0.31
L_g	3.9	L_{g4}	0.2
W_1	2	$Line_1$	39.15
L_1	1	$Line_2$	39.45
W_2	1.6	$W_{L1} = W_{L2}$	0.33
L_2	0.8	W_{gap}	0.33

6.3. SIMULATED RESULTS AND DISCUSSIONS

In this section, we present the simulated results and discussions for the UWB MIMO antenna design, which incorporates a decoupling structure for high isolation. The UWB MIMO antenna, designed to cover a wide frequency range (22.6 to 29.2 GHz), enables superior data rates, increased spectral efficiency, and robust communication capabilities. The simulation results must be evaluated in order to assess the performance of the proposed UWB MIMO antenna design and compare it to existing configurations.

The proposed antenna design's Reflection coefficient, a critical parameter indicating the antenna's efficiency in power transfer from the transmitter to the receiver, was consistently less than -10 dB across the complete band of UWB frequency. In figure 6.3, this observation indicates excellent impedance matching and minimal signal reflection. This level of performance ensures that signals are transmitted and received with minimal energy loss. Furthermore, Figure 6.4 shows the Voltage Standing Wave Ratio (VSWR) remains less than < 2 throughout the entire UWB frequency band, confirming the antenna's efficient performance.

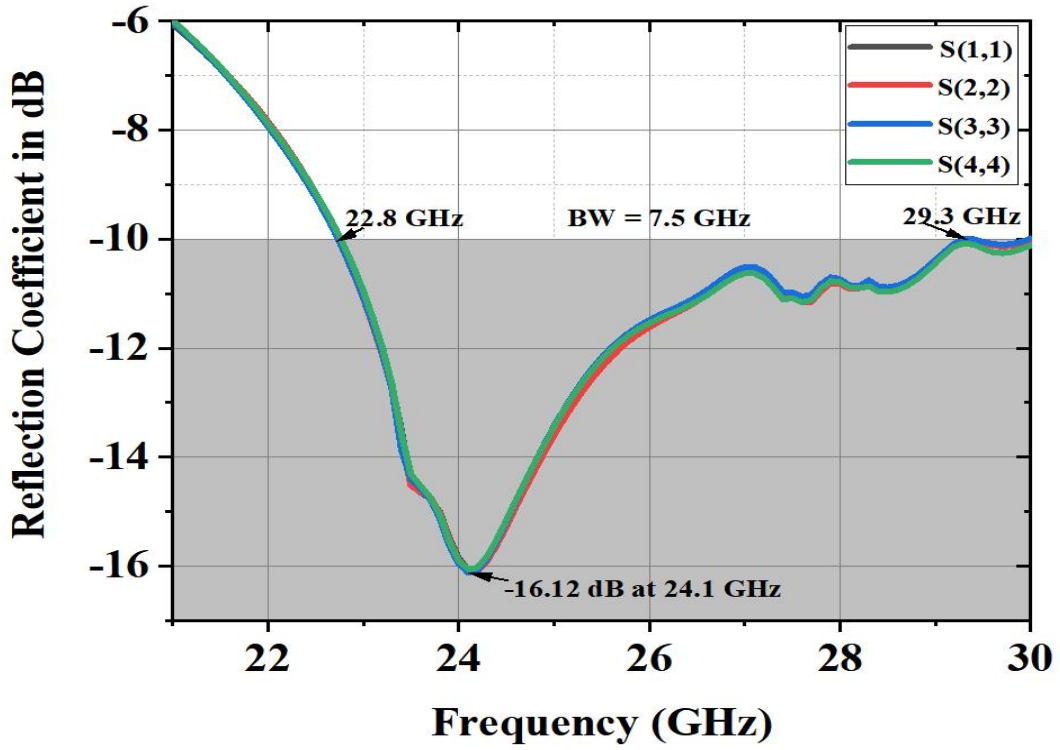


Figure 6.3: The Simulated Reflection coefficient ($S_{(1,1)}$ dB) of the proposed antenna

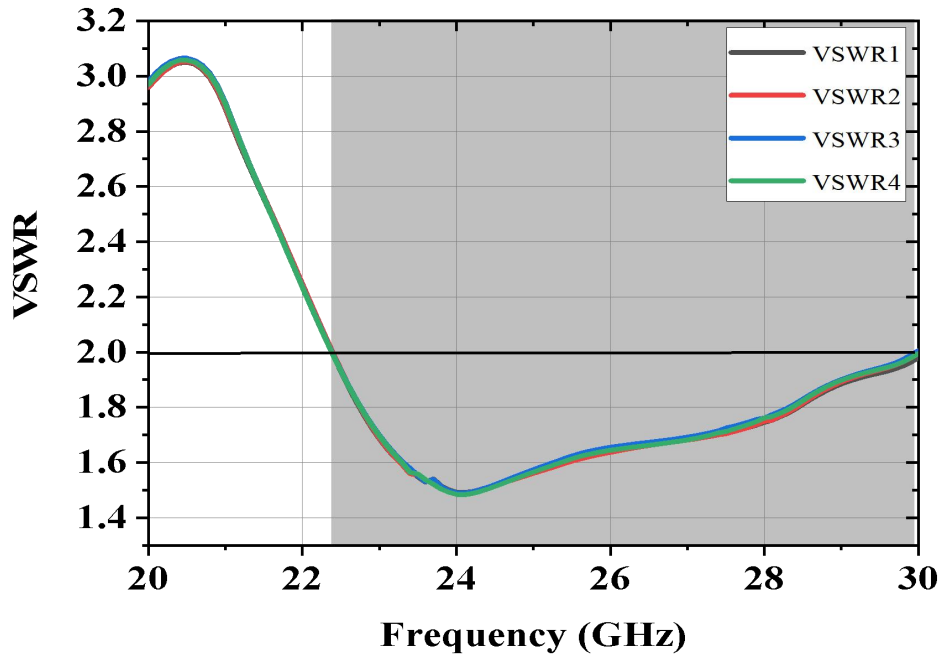


Figure 6.4: The Simulated VSWR Plot of the proposed antenna

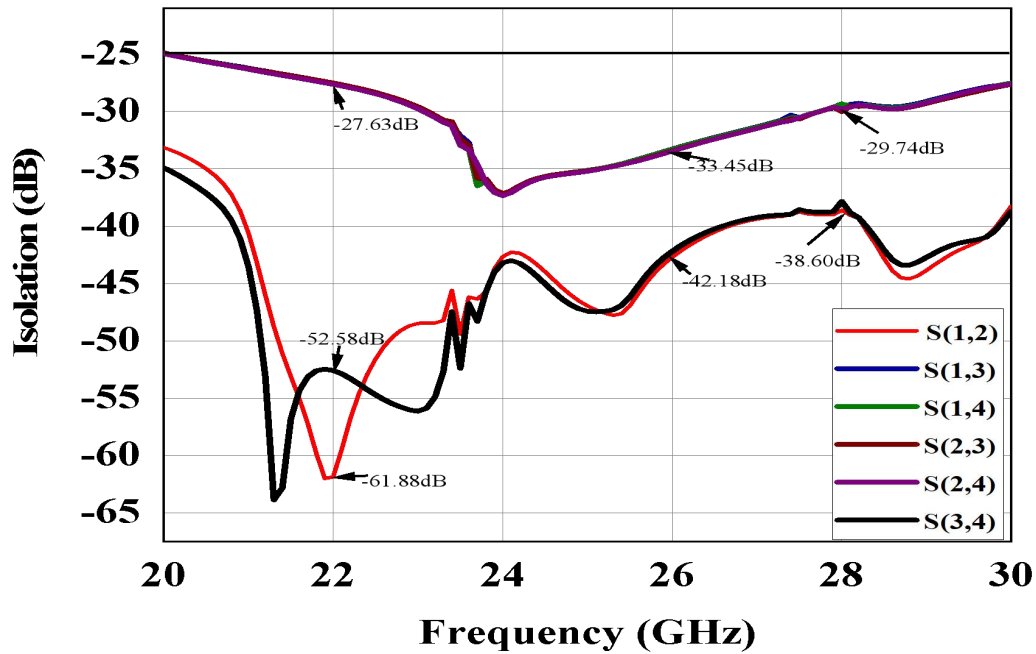
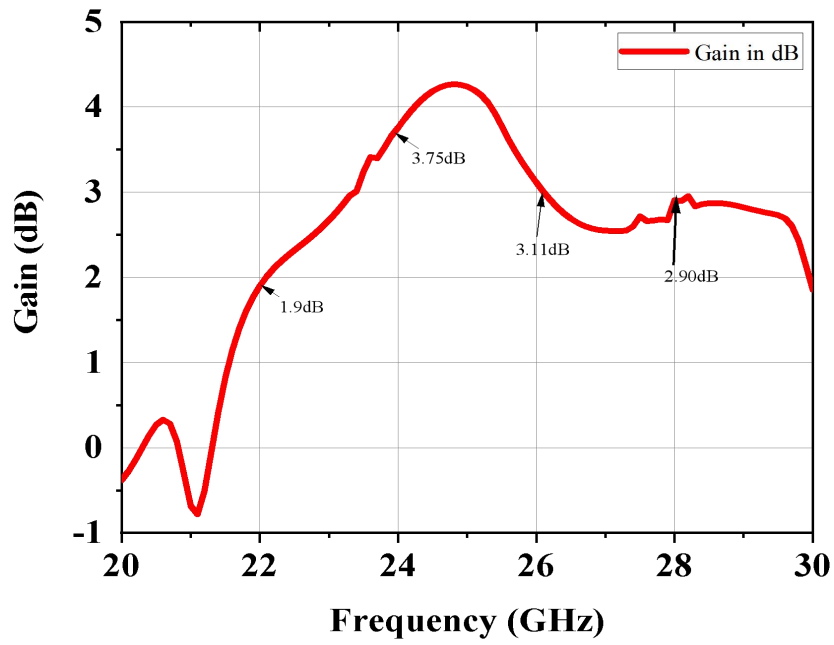
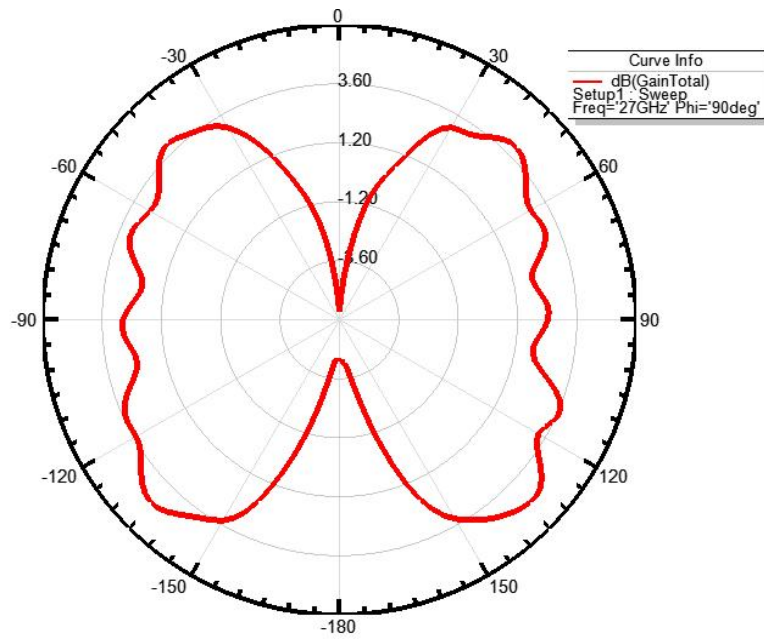


Figure 6.5: The Simulated Isolation between antenna Ports

Figure 6.5 illustrates the relation between isolation and frequency for the UWB MIMO antenna design. This graph offers valuable insights into the accomplishment of the antenna system across the frequency spectrum of the ultra-wide band. Notably, the measured and simulated isolation parameters at port 1 consistently remain below -27 dB in comparison to other ports throughout the entire operating band. By carefully analyzing and optimizing the isolation characteristics, designers can achieve a robust and reliable UWB-MIMO antenna system for high data transmission speed, multi streaming wireless communication applications. The range of gain is sustained between 1.9 to 4.8 dB (4.4 to 7.3 dBi) across a entire frequency range as depicted in the Figure 6.6. This level of gain is suitable for various short-distance communication applications, such as portable wireless devices and smart watches.



(a) Gain Plot in dB



(b) 2D gain Plot at 27 GHz of Frequency

Figure 6.6: Different gain Plots for the proposed Antenna

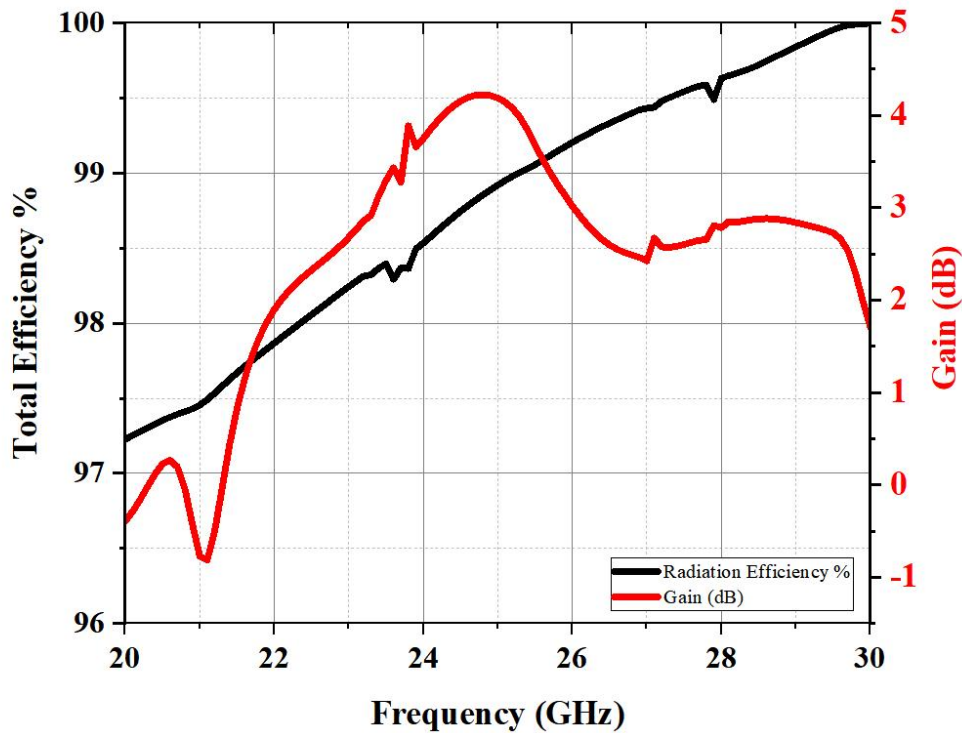
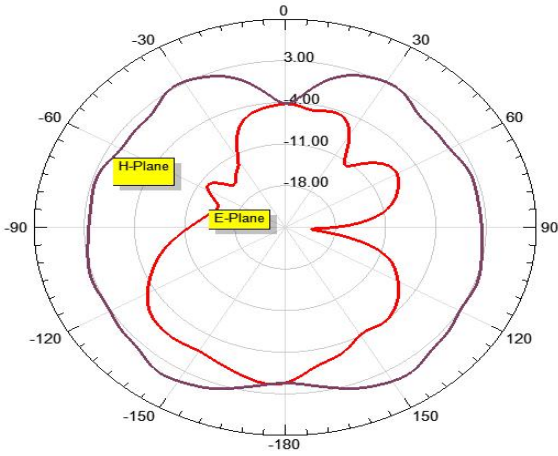


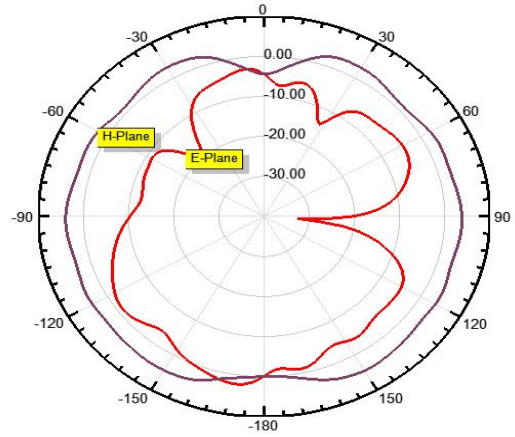
Figure 6.7: The Total Radiation Efficiency in percentage (%) Verses Gain in dB

Total efficiency is an important metric for determining an antenna's ability to efficiently radiate energy. The total efficiency of the UWB MIMO antenna was found to be greater than 97% across the entire UWB frequency range, as shown in Figure 6.7. This high efficiency ensures that most of the input power is radiated as electromagnetic waves, minimizing losses and improves the overall performance of the complete Eco system.

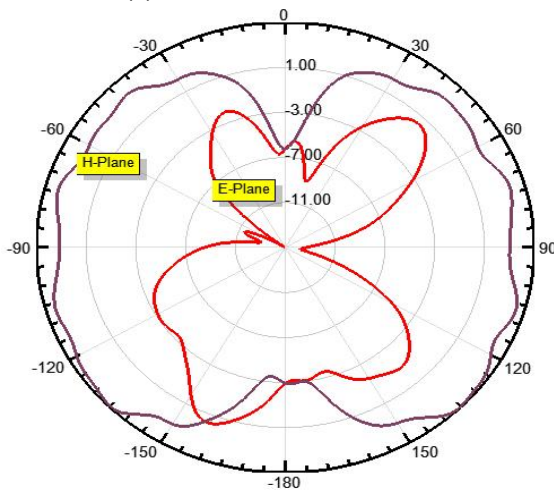
The radiation patterns of the proposed UWB-MIMO antenna, both in 2D and 3D were analyzed in the H-plane as well as in E-plane to assess the antenna's Omni-directional characteristics as shown in the Figure 6.8 and Figure 6.9 respectively at different frequencies. The simulation revealed that the antenna exhibits stable radiation patterns across the UWB frequency band, with consistent beam-width and minimal side lobes. This feature makes the UWB MIMO antenna suitable for communication systems that require stable and reliable signal coverage.



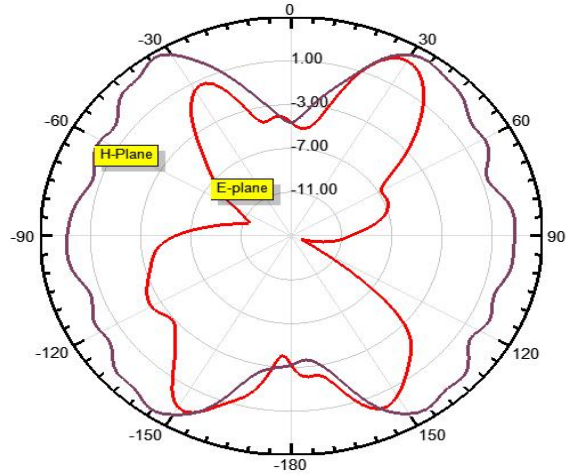
(a) Gain at 22.6 GHz



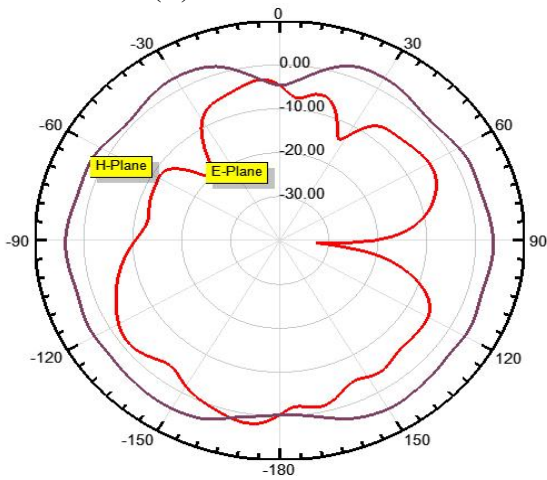
(b) Gain at 24 GHz



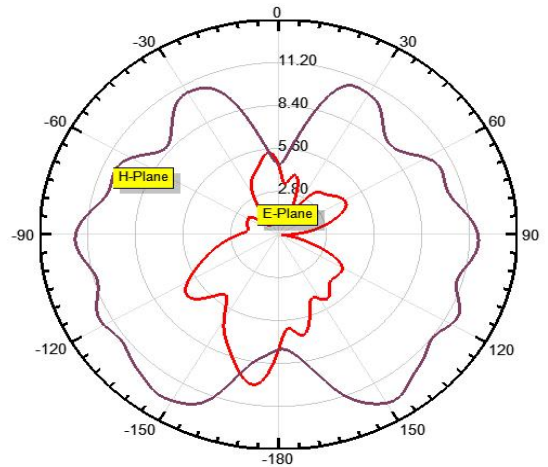
(c) Gain at 26 GHz



(d) Gain at 28 GHz

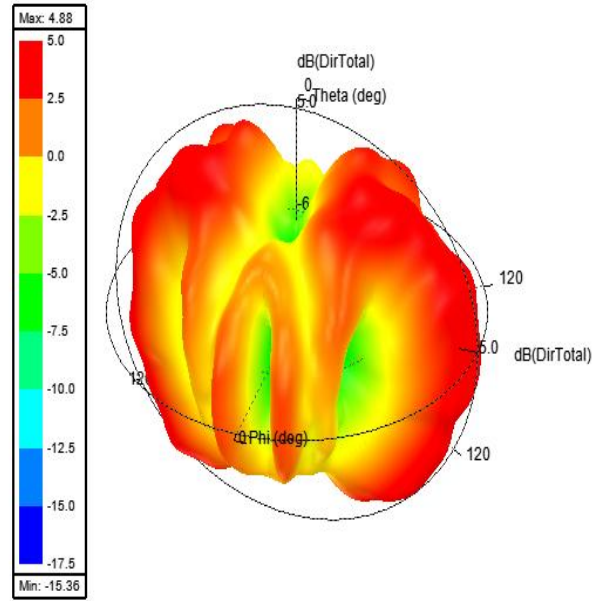
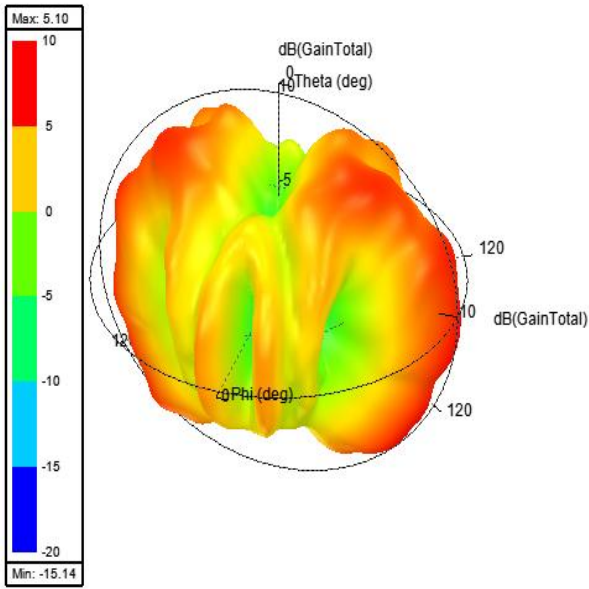
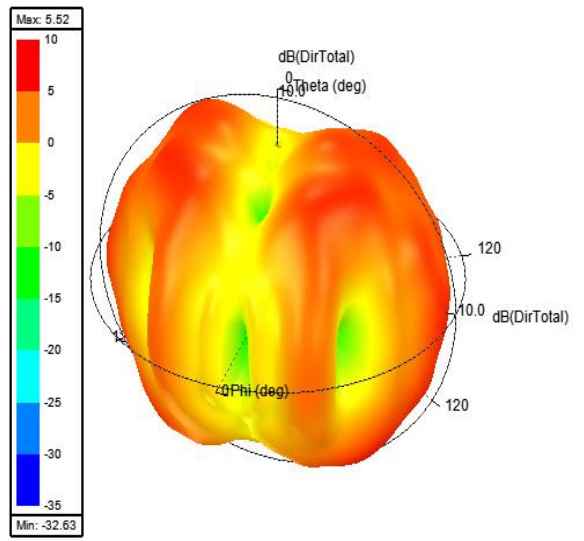
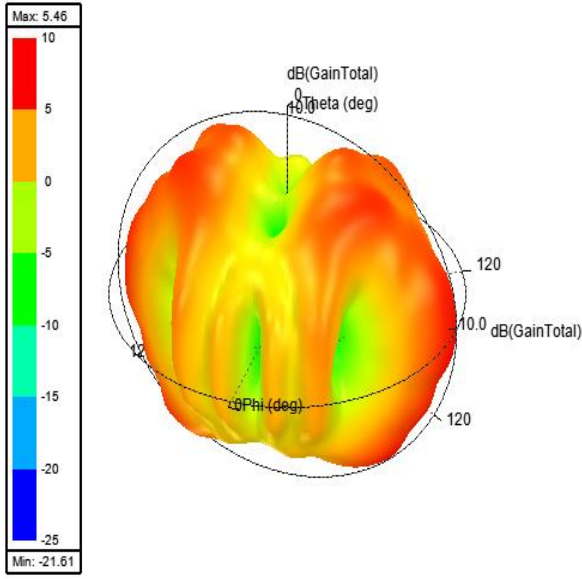


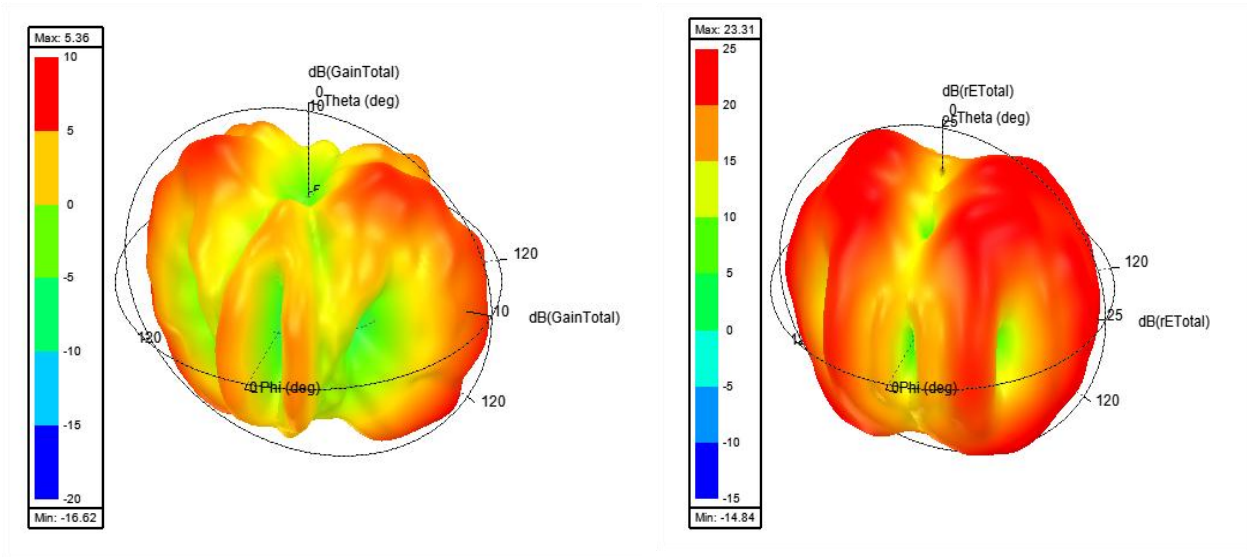
(e) Directivity at 24 GHz



(f) Radiation Efficiency at 24 GHz

Figure 6.8: 2D Gain, Directivity and Radiation Efficiency (H-Plane and E-Plane plots)





(a) 3D Total Gain Plots

(b) 3D Directivity Plots

Figure 6.9: 3D Gain and Directivity plots at 24 GHz, 26 GHz and 27 GHz frequencies

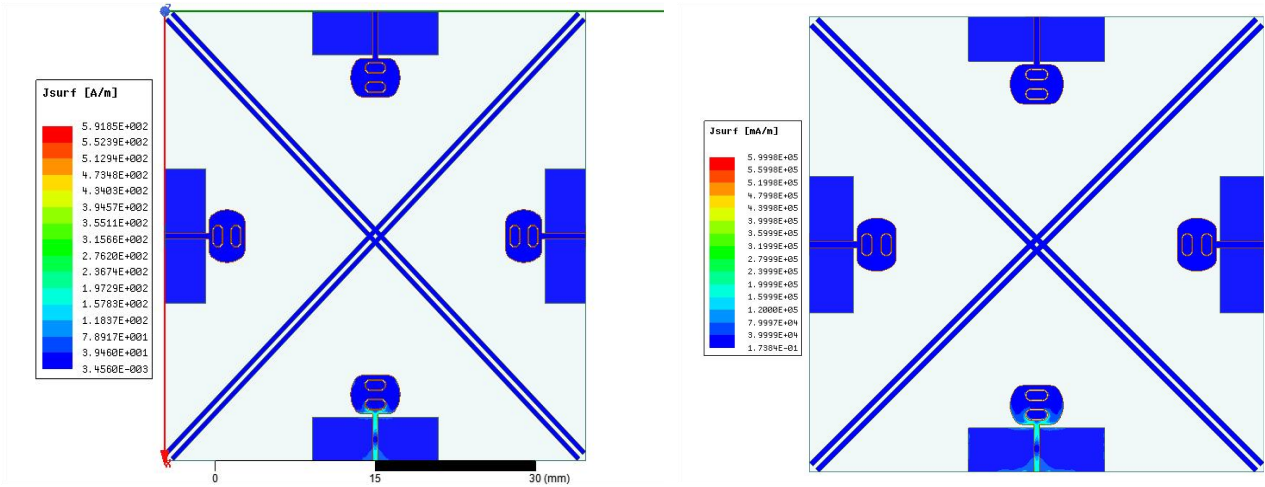
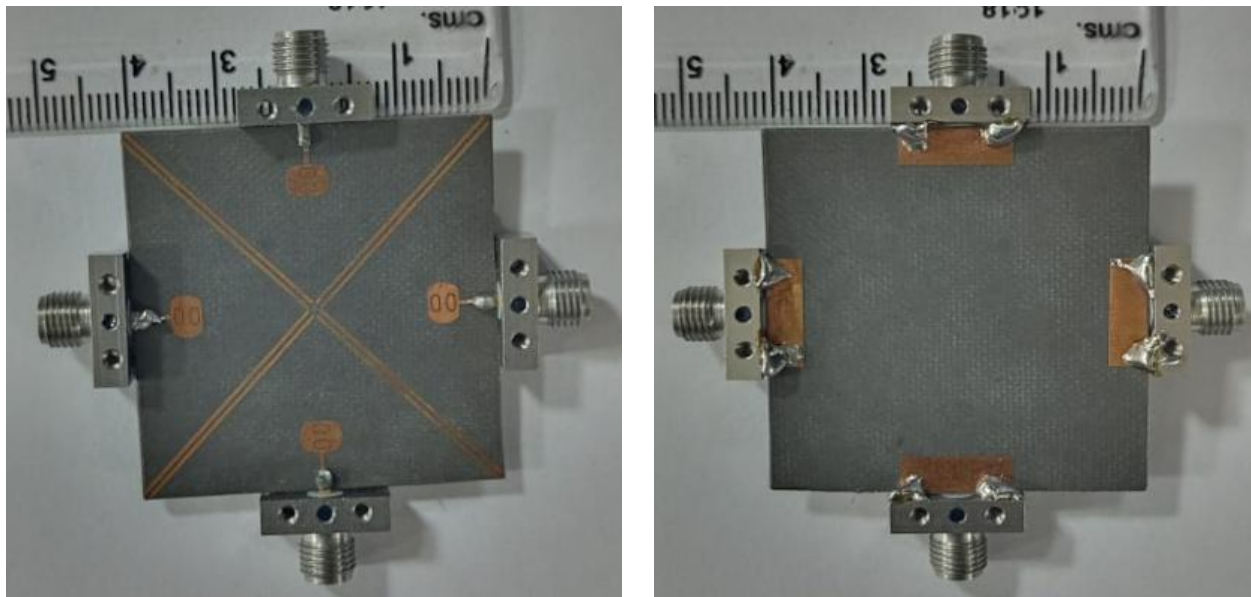


Figure 6.10: The Surface Current Distribution of the proposed UWB MIMO antenna

Figure 6.10 shows the simulated SCD (surface current distribution) at 24 GHz frequency for two configurations: 0-degree and 5-degree angles, employing partially ground planes. Partial ground plane allows for the distribution of surface current across all four antenna elements. To decrease the surface current, an X-shaped structure is introduced amidst the antenna elements.

6.4. MEASUREMENT RESULTS AND DISCUSSION

The experimental antenna in this study was crafted using the MITS- Eleven Lab printed circuit board machine, employing a Roger RT Duriod 5880 substrate. It comprises four antenna elements situated on a compact 40 mm x 40 mm substrate, as shown in Figure 6.11. The substrate had a dielectric constant of 2.2, a loss tangent of 0.0009, a thickness of 0.8 mm. An Agilent N5230A vector network analyzer (VNA) was employed to validate the accuracy of the simulated results through measurements. Additionally, radiation characteristics were assessed in an anechoic chamber, as depicted in Figure 6.12 and Figure 6.13.



(a)

(b)

Figure 6.11: Fabricated prototype (a) Top View (b) Bottom View



(a)

(b)

Figure 6.12: Measurement setup with VNA (a), & (b).

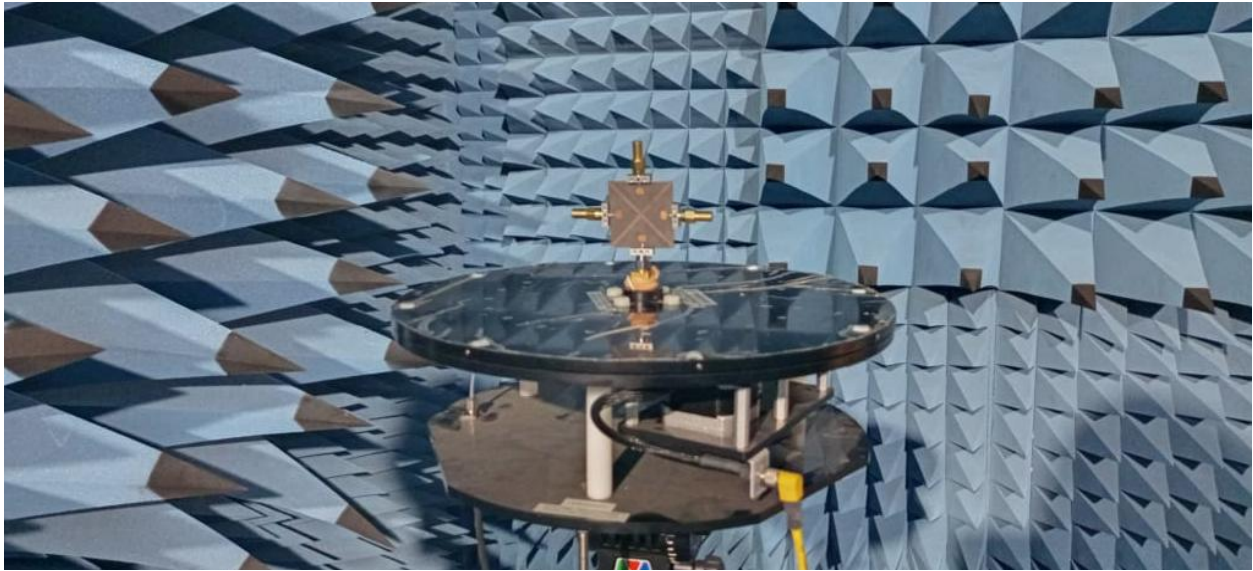


Figure 6.13: Measurement setup inside the anechoic chamber

Both simulated and measured results are compared to confirm the antenna's performance. Figure 6.14 illustrates the S-parameter outcomes, providing a side-by-side comparison of the measured and simulated data. The measured Reflection coefficient indicated an impedance bandwidth spanning from 21.92 to 26.3 GHz, meeting the UWB requirement specified by the FCC. The measured and simulated results from HFSS demonstrated robust agreement.

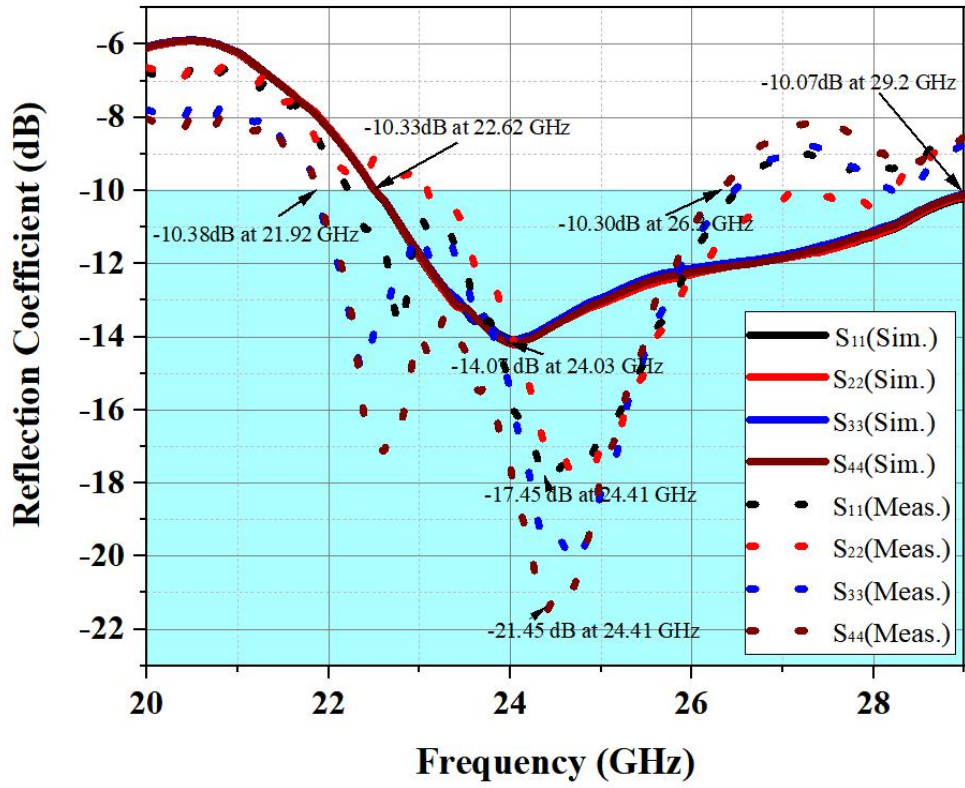


Figure 6.14: Simulated and measured Reflection Coefficients in dB

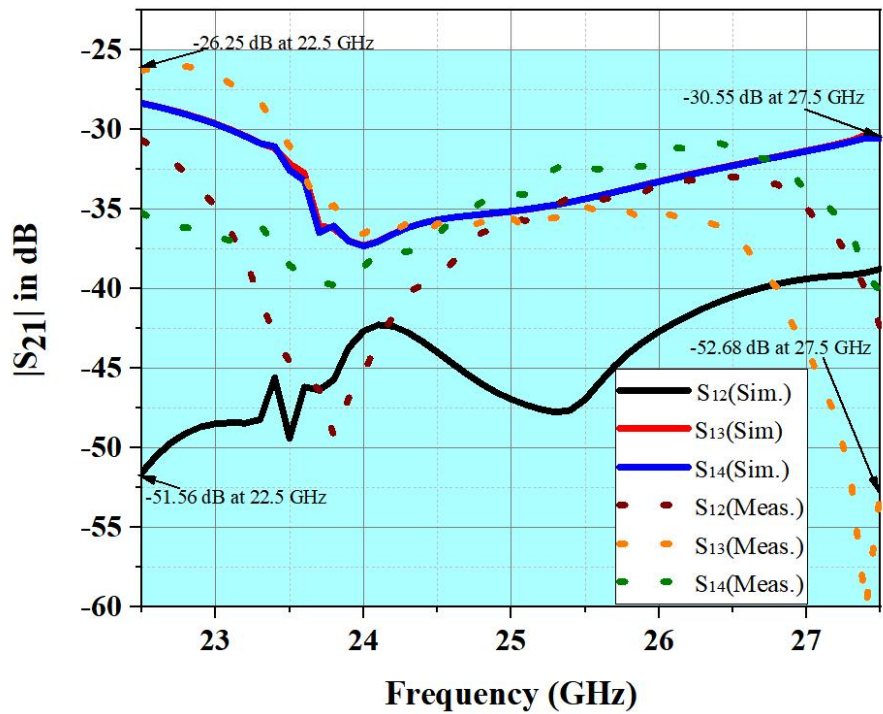


Figure 6.15: Simulated and measured $|S_{21}|$ in dB

In Figure 6.15, the simulation and the measurement results of the isolation parameters are depicted. The analysis reveals that the values for S_{12} , S_{13} , S_{14} , and so on, were consistently below -26 dB across the entire UWB range. This finding suggests that the proposed prototype exhibits minimal interference or coupling between its ports. The range of gain is sustained between 1.3 to 2.25 dBi across a entire frequency range as shown in the Figure 6.16.

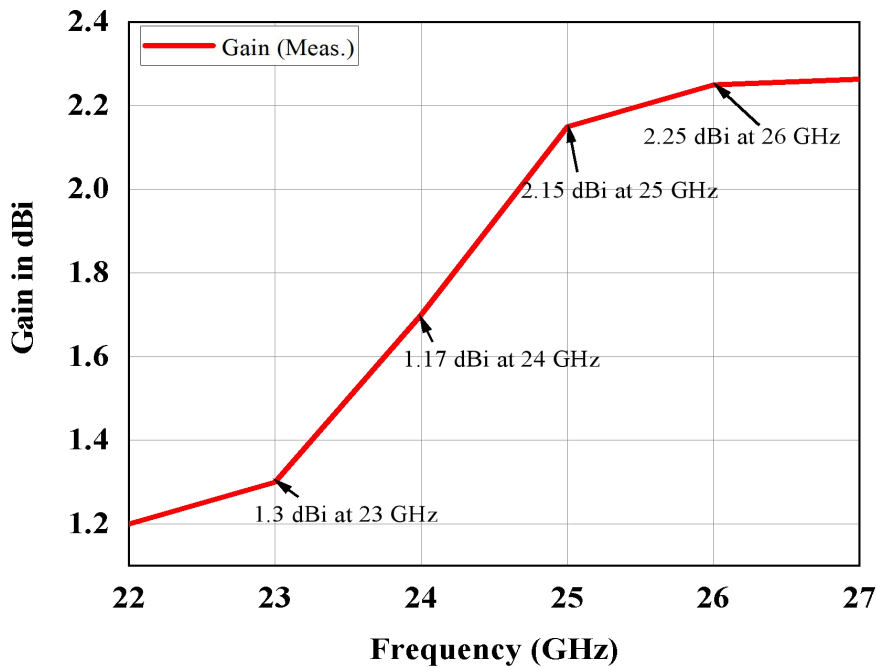


Figure 6.16: The Measured Gain Plot in dBi

6.5. DIVERSITY PARAMETERS

Examining the MIMO antenna's effectiveness extends beyond merely scrutinizing Reflection coefficient and isolation factors. To thoroughly gauge its performance, one must consider supplementary parameters such as ECC, diversity gain, TARC, and mean effective gain etc.

6.5.1. Envelope correlation coefficient (ECC):

The mutual coupling between antenna elements is significantly influenced by the diversity parameter, making it a crucial factor. The evaluation of ECC can be done in two ways - by

analyzing the far-field radiation pattern and by assessing the S-parameter and its calculation is given in equation (6.9);

$$ECC(k, m) = \rho_e(k, m, N) = \frac{|\sum_{n=1}^N S_{k,n}^* S_{m,j}|^2}{|\prod_{l=k,m} (1 - \sum_{n=1}^N S_{l,n}^* S_{n,l})|} \quad (6.9)$$

Where N = number of antenna elements and i and j are the port numbers.

By inserting N = 4 in equation (1); the ECC between antenna elements for a quad-port MIMO antenna may be calculated. The permissible value of ECC should be less than 0.5 for devices.

$$ECC_{12} = \rho_e(1,2,4) = \frac{|S_{11}^* S_{12} + S_{21}^* S_{22} + S_{13}^* S_{32} + S_{14}^* S_{42}|^2}{(1 - |S_{11}|^2 - |S_{21}|^2 - |S_{31}|^2 - |S_{41}|^2)(1 - |S_{12}|^2 - |S_{22}|^2 - |S_{32}|^2 - |S_{42}|^2)} \quad (6.9a)$$

Where ECC_{12} represents the mutual coupling on port-1 because of port-2. Similarly, can evaluate ECC_{13} , ECC_{14} , ECC_{23} , ECC_{24} , ...etc. from equation (6.9).

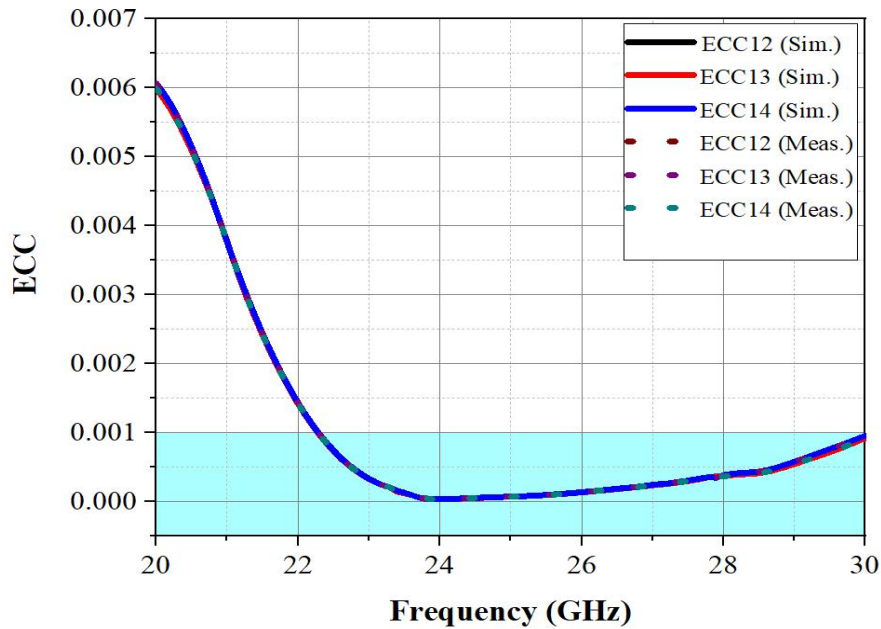


Figure 6.17: Simulated and measured ECC Plots

Figure 6.17 illustrates that the ECC value remains consistently below 0.005 across the entire operational range. The measured value is significantly lower than practical value of 0.001.

6.5.2. Diversity Gain (DG):

An established metric employed to evaluate the efficiency of diversity is the antenna Diversity Gain (DG) [48]. It is defined as the ratio of the Signal-to-Noise Ratio (SNR) of a single antenna in the system to the enhancement in SNR achieved by combining signals from multiple antennas. For proper functioning of the MIMO antenna, the diversity gain, directly calculable from the Envelope Correlation Coefficient (ECC) value, should approach 10 dB. The assessment of Diversity Gain (DG) for the suggested antenna is performed using the formula:

$$DG_{12} = 10\sqrt{1 - |ECC_{12}|^2} \quad (6.10)$$

Similarly, can evaluate DG_{13} , DG_{14} , DG_{23} , DG_{24} , ...etc. from equation (6.10).

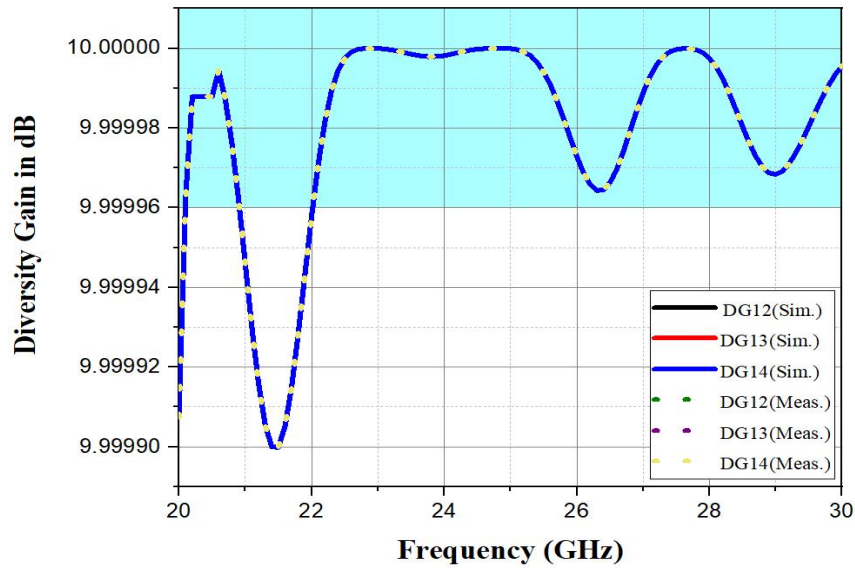


Figure 6.18: The Simulated and the measured DG Plots

The UWB-MIMO antenna is capable of achieving 10 dB of diversity gain. Figure 6.18, it is evident that even when port 1 is active and the other port is inactive, the diversity gain consistently remains at 10 dB for all three cases. This exceeds the widely accepted threshold of 9.5 dB, signifying excellent diversity performance. Furthermore, the value of 10 dB represents the optimal level of diversity gain, underscoring the exceptional capabilities of the prototype antenna in terms of diversity.

6.5.3. Mean effective gain (MEG):

The MEG is a crucial parameter for assessing MIMO diversity performance. It quantifies the ratio between the average power of the outgoing signal and the incoming signal. Equation (6.11) allows for the evaluation of MEG at each port.

$$MEG_k = 0.5 \times \left[1 - \sum_{m=1}^N |S_{k,m}|^2 \right] \quad (6.11)$$

$$MEG_1 = 0.5 \times [1 - |S_{11}|^2 - |S_{12}|^2 - |S_{13}|^2 - |S_{14}|^2] \quad (6.11a)$$

$$MEG_2 = 0.5 \times [1 - |S_{24}|^2 - |S_{23}|^2 - |S_{22}|^2 - |S_{21}|^2] \quad (6.11b)$$

$$MEG_3 = 0.5 \times [1 - |S_{34}|^2 - |S_{33}|^2 - |S_{32}|^2 - |S_{31}|^2] \quad (6.11c)$$

$$MEG_4 = 0.5 \times [1 - |S_{44}|^2 - |S_{43}|^2 - |S_{42}|^2 - |S_{41}|^2] \quad (6.11d)$$

In order to ensure optimal functionality of the UWB-MIMO antenna, it is important that the average effective gain of each individual antenna element is lower than < -3 dB, while the discrepancy in average effective gain between any two elements should not exceed > 3 dB.

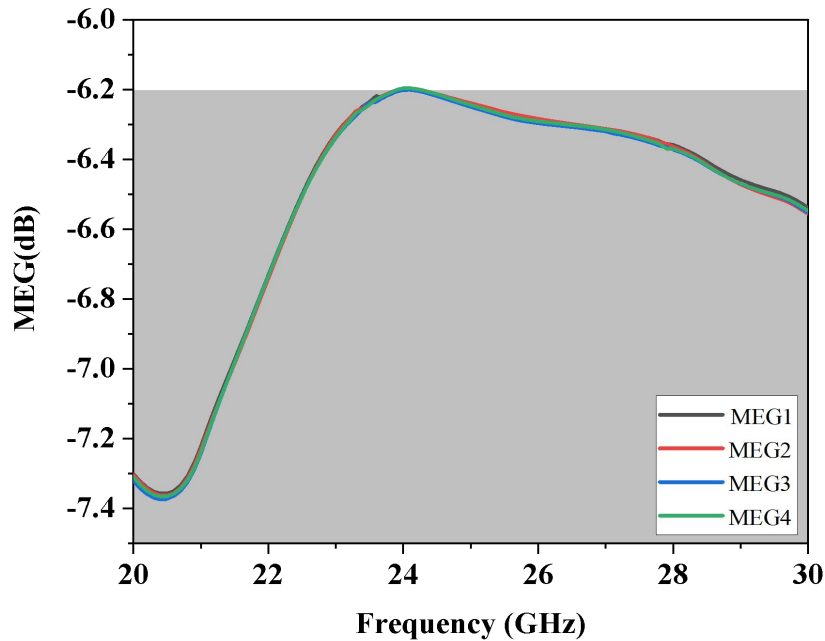


Figure 6.19: The Simulated MEG Plots

Figure 6.19 demonstrates that the MEG value remains below the practical threshold at every port within the frequency range and that the MEG values are below -6 dB across the entire frequency range.

6.5.4. Total Active Reflection Coefficient (TARC):

Operating bandwidth and efficiency in the MIMO system will be impacted when all antenna elements are active at once. As a result, S-parametric data are insufficient to determine how effective the antenna is, thus we used TARC, another crucial parameter, to assess the antenna's performance. The formula can be used to measure TARC [146] is given below,

$$TARC = \frac{\sqrt{\sum_{k=1}^4 (|R_k|^2)}}{\sum_{k=1}^4 (|I_k|^2)} \quad (6.12)$$

Where, R_k - Reflected Signal and I_k - incident signal.

Provided that all incoming signals at every port exhibit identical amplitude and phase (with a phase difference of 0 degrees) in the proposed MIMO antenna, the equation for Total Active Reflection Coefficient (TARC) is outlined below.

$$TARC = \sqrt{\frac{|S_{31}+S_{32}+S_{33}+S_{34}|^2+|S_{21}+S_{22}+S_{23}+S_{24}|^2+|S_{11}+S_{12}+S_{13}+S_{14}|^2+|S_{41}+S_{42}+S_{43}+S_{44}|^2}{4}} \quad (6.13)$$

6.5.5. Channel Capacity Loss (CCL):

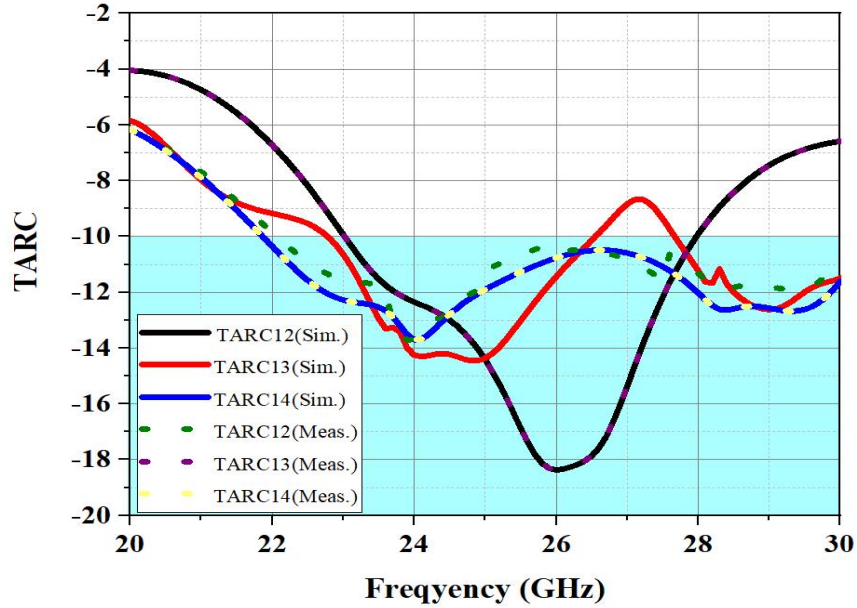
The channel capacity loss can be understood as the maximum amount of data that can reliably transmitted through a transmission channel. In MIMO systems, the accepted limit for practical purposes is usually below 0.4 bits per second per hertz across the entire frequency range used. The evaluation of CCL can be performed by following these steps.

$$C_{Loss} = -\log_2 \det(\varphi^R) \quad (6.14)$$

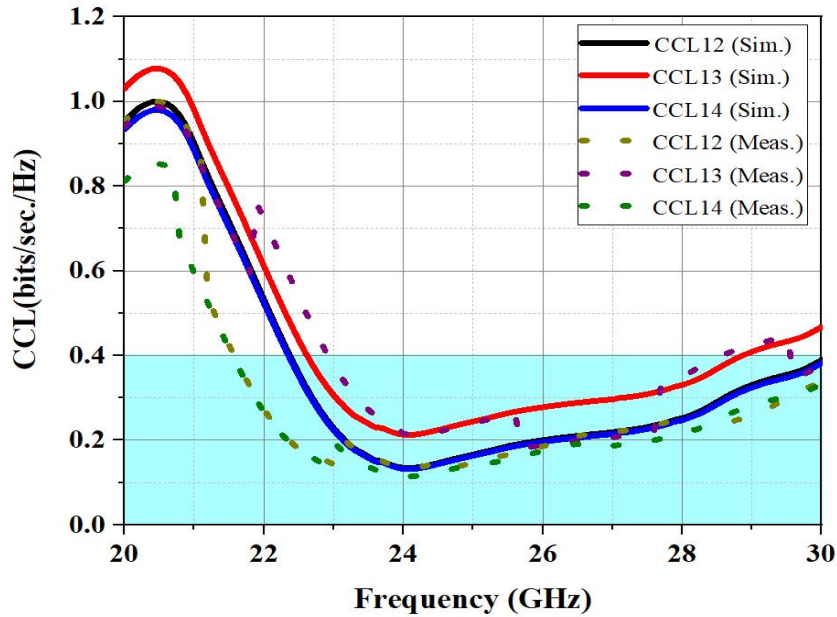
$$\varphi^R = \begin{bmatrix} \partial_{11} & \partial_{12} & \partial_{13} & \partial_{14} \\ \partial_{21} & \partial_{22} & \partial_{23} & \partial_{24} \\ \partial_{31} & \partial_{32} & \partial_{33} & \partial_{34} \\ \partial_{41} & \partial_{42} & \partial_{43} & \partial_{44} \end{bmatrix} \quad (6.14a)$$

$$\partial_{ii} = \left(1 - |S_{ii}|^2 - |S_{ij}|^2\right) \text{ and } \partial_{ij} = -\left(S_{ii}^* S_{ij} + S_{ji}^* S_{ij}\right) \text{ for } i, j=1,2,3, \text{ and } 4$$

The correlation matrix for the receiving antenna is denoted as φ^R . In the case of an N port MIMO system, this matrix can be calculated using the following method.



(a)



(b)

Figure 6.20: Simulated and Measured (a) TARC and (b) CCL Plots

In Figure 6.20, the simulated TARC and channel capacity loss (CCL) are depicted, demonstrating that the channel capacity loss remains below < 0.4 bits/s/Hz and the TARC remains below -10 dB across the entire frequency range.

Table 6.2: The performance comparison in relation to prior studies published literature

Ref. No./ Year	Size of Antenna	No. of Elements	Substrate	BW (GHz)	Isolation (dB)	Gain (dBi)	ECC	DG	CCL	Radiation Efficiency %
[146]/ 2017	$40 \times 40 \times 1.6$	4	FR4	3.1 to 11	< -20	3	< 0.004	---	---	---
[147]/ 2019	$40 \times 43 \times 1$	4	FR4	3.1 to 10.6	< -20	4	< 0.2	---	0.3	92
[148]/ 2019	$40 \times 40 \times 1.6$	4	FR4	3 to 12	< -17	2.9	< 0.06	---	---	---
[149]/ 2021	$40 \times 40 \times 1.6$	4	FR4	11 to 13	< -15	6	< 0.4	---	< 0.4	---
[150]/ 2021	$40 \times 40 \times 1.6$	4	FR4	3 to 3.5	< -15	3	< 0.4	> 9.95	---	89
[151]/ 2021	$40 \times 40 \times 1.524$	4	FR4 laminate	3.1 to 10.6	< -16	2.9	< 0.13	---	0.25	90
[152]/ 2022	$40 \times 40 \times 1.6$	4	FR4	3.1 to 13.75	< -18	8	< 0.012	---	< 0.3	> 89
[153]/ 2022	$28 \times 40 \times 1.6$	4	FR4	3.1 to 13.75	< -25	8.1	< 0.004	> 9.92	< 0.39	> 90

[154]/ 2023	40 × 40 × 1.6	4	FR4	2.8 to 11.4	<-26	8.5	<0.00 1	>9. 99	0.28	90
Prop. Work	40 × 40 × 0.8	4	Roger RT/Durio d 5880	22.5 to 29.3	<-27	6.8	<0.00 5	9.9 99	0.4	>97

In Table 6.2, the designed antenna is compared to similar size of antennas previously discussed in the literature. This proposed antenna has the advantage of being newly designed with new substrate material as well as with new frequency range, distinguishing it from existing models. Upon assessment of ECC, DG, Isolation, frequency range, gain, and other relevant parameters, it is evident that this antenna excels in these aspects. Given these outstanding characteristics, the antenna is considered a strong contender for 5G wireless communication systems.

There are some limitations of Millimeter wave frequencies used in 5G applications that necessitate one of them is Smaller antenna elements, which might limit the efficiency and radiation characteristics of the quad-port antenna, are one of the limits of Millimetre wave frequencies employed in 5G applications. Compact designs with optimal performance remain a considerable issue, as size concessions may result in reduced antenna gain and coverage.

The second is Millimetre waves have larger propagation losses and are frequently impeded by objects such as buildings and trees. MIMO quad-port antennas may require assistance in sustaining reliable connections in non-line-of-sight settings, limiting the promised coverage and capacity increases.

The last and very important one is that MIMO quad-port antennas are sensitive to interference and crosstalk due to their many ports and closely spaced antenna elements. It is critical to manage the interactions between antenna parts to minimize mutual coupling and ensure signal integrity. It may reduce the achievable data rates and overall system performance in certain instances.

6.6. SUMMARY

The UWB MIMO antenna design, which integrates a decoupling structure, shows potential for improving MIMO system performance by addressing mutual coupling issues among radiating elements. The effective design and analysis of the decoupling structure are crucial for achieving the desired isolation levels and optimizing the antenna's overall performance in ultra-wide band applications. This study presents a proficient four-element UWB MIMO antenna that achieves compactness and desired performance through a symmetric layout, multi-slit techniques orthogonal structure, multi-slot, and well-separated X-shaped decoupling.

The antenna's performance undergoes thorough evaluation through simulations and measurements, encompassing S-parameters, MIMO diversity, gain, radiation patterns, and isolation. Both prototype measurements and simulation results confirm that the S11 of the antenna remains below -10.0 dB across the entire UWB frequency band, accompanied by a very small VSWR (< 2). The close agreement between measurements and simulations provides evidence of the antenna's broad impedance bandwidth within the UWB range, consistent high gain, comprehensive radiation patterns, robust isolation, and commendable diversity performance.

Covering a broad frequency range from 22.6 GHz to 29.2 GHz, the proposed antenna proves compatible with the K-band used in satellite communication (for TV broadcasting) and mobile communication. Additionally, the antenna exhibits an average mutual coupling of < -27 dB, a maximum gain of 4.38 dB (6.88 dBi), ECC of less than 0.004, Omni-directional radiation across its entire impedance bandwidth. In conclusion, the proposed antenna is well-suited for upcoming UWB MIMO 5G wireless communication applications, including portable systems and satellite communication systems. The results of all the designs developed in this thesis demonstrate its suitability for various hand-held wireless devices in the UWB higher frequency range and its effective performance in multipath channel environments.

CHAPTER-7

CONCLUSION AND FUTURE SCOPE

7.1. INTRODUCTION

A comprehensive look into the design and analysis of an ultra-wide band MIMO antenna is carried out in this study. The Ansys HFSS V.15.0 software was used to design and simulate two versions of the four-element antenna structure, one with isolation techniques and one without. Several parameters were studied in depth, including Reflection coefficient, isolation parameter, gain, radiation efficiency, surface current distribution, TARC, ECC, MEG, DG, CCL and etc. The antenna was then built, and the results were measured with a VNA and an anechoic chamber. A comparison of the simulated and the measured findings found a close match, with slight deviations due to cable effects, SMA connector soldering, and ambient factors. This chapter provides a concise summary of the final outputs, as well as justification for the work done.

The third chapter describes the design and development of a unique microstrip patch antenna for 5G wireless communication applications using millimeter-wave frequencies. This antenna features a streamlined capsule-shaped design, employing a slot-loading technique to enhance its performance. The compact size of the antenna facilitates easy integration into limited spaces around microwave electronics, especially at higher frequencies. To further improve the antenna design, two elliptical slots have been introduced, leading to heightened current density. The proposed antenna showcases optimal dimensions of $(12 \times 15 \times 0.8)$ mm³, emphasizing its compact and straightforward design.

The suggested design presents numerous benefits compared to other UWB microstrip antennas, such as diminished radiation loss, decreased dispersion, an innovative configuration, and notable gain without requiring supplementary techniques. The antenna displays favorable attributes, featuring a low VSWR (< 2), a wide bandwidth (10 GHz covering the range from 20 to 30 GHz), and satisfactory gain (3.53 dB). Furthermore, the article provides detailed insights into radiation patterns in both the E and H planes at various frequencies.

The suggestion is to introduce a UWB antenna with a capsule-shaped structure and elliptical slots to attain an extensive bandwidth within the SHF range. A notable feature of this design is its compact size, rendering it well-suited for applications in both 5G and UWB at millimeter (mm) -wave frequencies. This is attributed to its apt geometry and uncomplicated structure.

A concise quad-port UWB MIMO antenna, measuring $(36 \times 24 \times 0.8)$ mm³ and situated on an RT Duroid 5880 substrate, is proposed. The substrate possesses sub-values for dielectric constant, loss tangent (0.0009), and thickness ($h=0.8$ mm), eliminating the need for any external decoupling structure that could unnecessarily complicate and enlarge the antenna. The design incorporates four similar antenna elements arranged in a capsule shape on the radiator, featuring two elliptical slits that play a crucial role in achieving substantial isolation, thereby reducing interference through diversity. Alterations to the ground plane, including the strategic placement of elliptical slots, modify the dispersion of the surface current, consequently enhancing the antenna's bandwidth.

The prototype antenna proves to be well-suited for contemporary 5G wireless systems, particularly in indoor UWB-MIMO devices, showcasing a broad bandwidth ranging from 22 to 30 GHz. It has strong isolation and enhanced gain, and measures such as total Active Reflection Coefficient, gain, Envelope Correlation Coefficient, Diversity Gain, and Mean Effective Gain confirm the antenna's MIMO performance. Comparisons with recent works in connected applications underscore the suggested antenna's superiority, offering a compact size alongside high-performance MIMO specifications.

When developing a MIMO antenna with diverse isolation techniques, it is critical to thoroughly examine the antenna type, design characteristics, and the desired level of isolation. This meticulous assessment is vital for optimizing the overall performance of the antenna. Each isolation technique type presents distinct features tailored to specific wireless communication systems, ranging from cost-effective traditional methods to more intricate signal cancellation approaches. Consequently, the choice of the most suitable isolation technique for a particular MIMO antenna design relies on the specific goals and requirements of the system. The proposed MIMO antenna is made up of four pieces and features a decoupling structure (an X-shaped wall between the radiating elements), making it an effective solution for 5G communications. The

antenna operates at frequencies ranging from 22.5 GHz to 29.1 GHz, with an isolation level of 27.63 dB and a gain increase of 6.39 dBi. Through the application of the hybrid technique, the isolation is further enhanced to 28.84 dB, and the bandwidth is expanded from 6.6 GHz to 7.5 GHz, all while maintaining the gain. Simulations using HFSS software showcase a noteworthy alignment between the anticipated and observed parameters, including Reflection coefficient, Voltage standing wave ratio (VSWR), isolation level, and Peak Gain, across the operational band. These results confirm the antenna's reliable suitability for 5G communications. In this context, the Hybrid Technique stands out as the most fitting isolation technique for the proposed MIMO antenna design.

The UWB MIMO antenna design, which integrates a decoupling structure, shows potential for improving MIMO system performance by addressing mutual coupling issues among radiating elements. The effective design and analysis of the decoupling structure are crucial for achieving the desired isolation levels and optimizing the antenna's overall performance in ultra-wideband applications. This study presents a proficient four-element UWB MIMO antenna that achieves compactness and desired performance through a multi-slot, orthogonal structure, symmetric layout, well-separated X-shaped decoupling, and multi-slit techniques.

The antenna's performance undergoes thorough evaluation through simulations and measurements, encompassing S-parameters, MIMO diversity, gain, isolation, and radiation patterns. Both prototype tests and modelling results demonstrate that the antenna's S11 remains below -10.0 dB across the full UWB frequency band, with a very minimal VSWR (<2). The close agreement between calculations and tests demonstrates the antenna's wide impedance bandwidth in the UWB region, persistent high gain, comprehensive radiation patterns, strong isolation, and outstanding diversity performance.

The suggested antenna covers a wide frequency range of 22.6 GHz to 29.2 GHz and is compatible with the K-band used in satellite communication (for TV broadcasting) and mobile communication. The antenna has a maximum gain of 4.38 dB (6.88 dBi), average mutual coupling of < -27 dB, envelope correlation coefficient of less than 0.004, and Omni-directional radiation across its impedance bandwidth. To summaries, the suggested antenna is well-suited for future UWB MIMO 5G wireless communication applications, such as portable and satellite

communication systems. The results of all the designs developed in this thesis demonstrate its suitability for various hand-held wireless devices in the UWB higher frequency range and its effective performance in multipath channel environments.

The proposed MIMO antenna designs incorporating different isolation techniques face several limitations. These include increased design complexity and larger physical size due to the addition of decoupling structures, which can be problematic in space-constrained applications. The introduction of isolation methods, such as slots or decoupling elements, may also narrow the operational bandwidth, limiting performance in broadband systems like 5G. Moreover, complex structure like defected ground structures (DGS) can pose manufacturing challenges, increasing costs and introducing variability. Additionally, improving isolation can result in reduced radiation efficiency and performance sensitivity to environmental conditions, potentially leading to real-world performance degradation. Design trade-offs are also a concern, as enhancing isolation may compromise other parameters such as gain and beam width. Finally, scaling these techniques to larger MIMO systems, such as in massive MIMO configurations, can be difficult, leading to reduced isolation effectiveness as the array size grows.

7.2. FUTURE SCOPE

It is customary to say that for any technology there will saturation points due to the demand or may be the evolution of some other technology which is more efficient than this. Keeping that one in mind we can suggest some of the clue which may be implemented to this existing work to fulfil the future demand. The following are possible solutions which are listed below:

1. For high channel capacity more the number of the antenna elements are required. So new technique massive MIMO can be implemented to enhance the channel capacity.
2. The size of antenna can be further reduced by adding metamaterial, metasurface or combination of both or by adopting any other suitable method.
3. Recently 5G is in growing state, so in future extension of this work could be quite handy.
4. In this thesis, the entire antenna measured inside anechoic chamber. In future, performance of designed antenna can be evaluated after embedded in to device like mobile or laptop or other wireless portable device.

5. Though we have design antenna here which is suitable for MIMO application but we have not tested, what is its radiation effect on environment. One can further extend this work to estimate radiation effect.
6. Research can be further extended to have multiple band notch characteristics to avoid any kind of interference in UWB system.
7. By adding something to this design mutual coupling can further be reduced.

Research Publications

Published Papers:

1. Suverna Sengar, Praveen Kumar Malik, “A comprehensive survey of Massive-MIMO Based on 5G Antennas”, International Journal of RF and Microwave Computer-Aided Engineering, **published-2022**. DOI: [10.1002/MMCE.23496](https://doi.org/10.1002/MMCE.23496).
2. Suverna Sengar, Praveen Kumar Malik, Subba Reddy V. and Sudipta Das, “Design a Novel Capsule Shape UWB Antenna for 5G Wireless Applications”, Journal of Nano- and Electronic Physics- **Published-13 Oct,23**. [https://doi.org/10.21272/jnep.15\(4\).04031](https://doi.org/10.21272/jnep.15(4).04031).
3. Suverna Sengar, Praveen Kumar Malik, Puneet Chandra Srivastava, Kiran Srivastava and Anita Gehlot, “Performance Analysis of MIMO Antenna Design with High Isolation Techniques for 5G Wireless Systems”, International Journal of Antennas and Propagation, **published-2023**.
4. Suverna Sengar, Praveen Kumar Malik, Sudipta Das, Tanvir Islam, Rajesh Singh, Sivaji Asha, Saad Aldosary, “A Quad Port MIMO Antenna Designed with an X-Shaped Decoupling Structure for Wideband Millimeter-Wave (mm-Wave) 5G FR2 New Radio (N258/N261) Bands Applications”, in Wireless personal communications, springer (**published-2024**).
5. Suverna Sengar and Praveen Kumar Malik, “A Compact Tri-band Microstrip Patch Antenna Design for 5G millimetre waves applications” *14th INTERNATIONAL CONFERENCE ON COMPUTING, COMMUNICATION AND NETWORKING TECHNOLOGIES (ICCCNT)-2023, Presented and Published- 23 Nov, 23*. DOI: [10.1109/ICCCNT56998.2023.10308282](https://doi.org/10.1109/ICCCNT56998.2023.10308282).
6. Suverna Sengar and Praveen Kumar Malik, “Performance Evaluation of Compact Microstrip Antenna Design for 5G Wireless Applications.” International Conference on Contemporary Trends in Multidisciplinary Research and Innovation (ICCTMRI – 2023), **Presented**.

Papers Communicated:

1. Suverna Sengar, Praveen Kumar Malik and Rajesh Singh, “A Novel Design and Analysis of Compact Size Quad Port UWB MIMO Antenna for 5G Millimeter Wave Applications”, International Journal of Antennas and Propagation (**Under Revision**).
2. Suverna Sengar, Praveen Kumar Malik, “A Small Size and Novel Design Microstrip Patch Antenna for 5G Millimeter wave Applications”, International Conference on Artificial Intelligence and its Application (ICAIA - 2023) (**Communicated**).

Patent Published:

1. Multi-Port UWB-MIMO Antenna, application number IN202311062392 .

Book Chapter:

1. Suverna Sengar, Praveen Kumar Malik and Monika Agarwal, “Artificial intelligence-based communication systems used in Industry 4.0: For Multiple Input and Multiple Output antenna 5G Wireless Devices,” in book Artificial Intelligence and Blockchain in Industry 4.0, Taylor & Francis Group, CRC Press, e-book: 9781003452591, **Published-2023**.
2. Suverna Sengar, Praveen Kumar Malik and Prashant Kumar , “Design and Analysis of UWB Patch Antenna for 5G Millimeter Wave Applications.” Taylor & Francis Group, LLC, **(Published-2024)**.

Bibliography

- [1] Alhayani, B. and Abdallah, A.A. (2021), "Manufacturing intelligent Corvus corone module for a secured two way image transmission under WSN", *Engineering Computations*, Vol. 38 No. 4, pp. 1751-1788. <https://doi.org/10.1108/EC-02-2020-0107>
- [2] A. A. R. Alsaedy and E. K. P. Chong, "Mobility Management for 5G IoT Devices: Improving Power Consumption With Lightweight Signaling Overhead," in *IEEE Internet of Things Journal*, vol. 6, no. 5, pp. 8237-8247, Oct. 2019, doi: 10.1109/JIOT.2019.2920628.
- [3] Wang, J., Weitzen, J., Bayat, O. et al. Interference coordination for millimeter wave communications in 5G networks for performance optimization. *J Wireless Com Network* 2019, 46 (2019). <https://doi.org/10.1186/s13638-019-1368-6>
- [4] Gao X, Dai L, Chen Z, Wang Z, Zhang Z (2015) Near-Optimal Beam Selection for BeamSpace MmWave Massive MIMO Systems, 2015 IEEE
- [5] Alhayani, B., Kwekha-Rashid, A.S., Mahajan, H.B. et al. 5G standards for the Industry 4.0 enabled communication systems using artificial intelligence: perspective of smart healthcare system. *Appl Nanosci* (2022). <https://doi.org/10.1007/s13204-021-02152-4>
- [6] Balevi, Eren, Andrews, Jeffrey G., "Wideband Channel Estimation with A Generative Adversarial Network", *IEEE Transactions on Wireless Communications*, 2021.
- [7] Balevi, Eren, Doshi, Akash, Andrews, Jeffrey G., "Massive MIMO channel estimation with an untrained deep neural network", *IEEE Transactions on Wireless Communications*, 2020.
- [8] Zheng, Kan, Zhao, Long, Mei, Jie, Shao, Bin, Xiang, Wei, Hanzo, Lajos, "Survey of Large-Scale MIMO Systems", *IEEE Communications Surveys and Tutorials*, 2015.
- [9] Gupta, Akhil, Jha, Rakesh Kumar, "Power optimization using massive MIMO and small cells approach in different deployment scenarios", *Wireless Networks*, 2017.
- [10] Abd El-Hameed, Anwer S., Wahab, Mohamed G., Elshafey, Nashwa A., Elpeltagy, Marwa S., "Quad-Port UWB MIMO antenna based on LPF with vast rejection band" , *AEU - International Journal of Electronics and Communications*, 2021.
- [11] Ahmad, Ashfaq, Choi, Dong you, Ullah, Sadiq, "A compact two elements MIMO antenna for 5G communication" , *Scientific Reports*, 2022.
- [12] Khan, Aqeel Ahmed, Naqvi, Syed Aftab, Khan, Muhammad Saeed Ijaz, Bilal, "Quad port miniaturized MIMO antenna for UWB 11 GHz and 13 GHz frequency bands" , *AEU - International Journal of Electronics and Communications*, 2021.
- [13] Mahmood, Sarmad Nozad, Ishak, Asnor Juraiza, Ismail, Alyani, Soh, Azura Che, Zakaria, Zahriladha, Alani, Sameer, "ON-OFF Body Ultra-Wideband (UWB) Antenna for Wireless Body Area Networks (WBAN): A Review" , *IEEE Access*, 2020.
- [14] Ramesh, R., Kommuri, Usha Kiran, "Isolation enhancement for dual-band MIMO antenna system using multiple slots loading technique" , *International Journal of Communication Systems*, 2020.

- [15] Saxena, Gaurav Jain, Priyanka Awasthi, Yogendra Kumar, “High Diversity Gain MIMO-Antenna for UWB Application with WLAN Notch Band Characteristic Including Human Interface Devices” , Wireless Personal Communications, 2020.
- [16] Naktong, Watcharaphon, Ruengwaree, Amnoi, “Four-Port Rectangular Monopole Antenna for UWB-MIMO Applications”, Progress In Electromagnetics Research B, 2020.
- [17] Tirado-Méndez, José Alfredo, Jardón-Aguilar, Hildeberto, Rangel-Merino, Arturo, Vasquez-Toledo, Luis Alberto, Gómez-Villanueva, Ricardo, “Four ports wideband drop-shaped slot antenna for MIMO applications”, Taylor and Francis Ltd., Journal of Electromagnetic Waves and Applications, 2020.
- [18] Kiem, Nguyen Khac, Phuong, Huynh Nguyen Bao, Chien, Dao Ngoc, “Design of compact 4×4 UWB-MIMO antenna with WLAN band rejection” , International Journal of Antennas and Propagation, 2014.
- [19] Zhao, Xiongwen, Riaz, Sharjeel, “A Dual-Band Frequency Reconfigurable MIMO Patch-Slot Antenna Based on Reconfigurable Microstrip Feedline”, Institute of Electrical and Electronics Engineers Inc., IEEE Access, 2018.
- [20] Kumar, Pawan Urooj, Shabana Alrowais, Fadwa, “Design and implementation of quad-port MIMO antenna with dual-band elimination characteristics for ultra-wideband applications”, Applied Sciences (Switzerland), 2020.
- [21] W. L. Stutzman, Polarization in Electromagnetic Systems, MA: Artech House, 1993.
- [22] James, J. R., and P. S. Hall, Handbook of Microstrip Antennas, Vol. 1, London: Peter Peregrinus Ltd., 1989.
- [23] K.D Prasad, “Antenna wave and propagation”, Satya Parkashan, 1983.
- [24] Bhattacharya, A. K., and R. Garg, “Generalized Transmission Line Model for Microstrip Patches”, IEE Proceedings Microwaves, Antennas and Propagation, Pt. H, Vol. 132, No. 2, pp(s): 93–98, 1985.
- [25] Mahnoor Khalid, Syeda Iffat Naqvi, Niamat Hussain, MuhibUr Rahman, Fawad, Seyed Sajad Mirjavadi, Muhammad Jamil Khan and Yasar Amin, “4-Port MIMO Antenna with Defected Ground Structure for 5G Millimeter Wave Applications”, Nov 15 2022.
- [26] Philip Ayiku Dzagbletey and Young-Bae Jung, “Stacked Microstrip Linear Array for Millimeter-Wave 5G Baseband Communication”, 1536-1225 (c) 2018 IEEE.
- [27] Mian Muhammad Kamal, Shouyi Yang, Xin-cheng Ren, Ahsan Altaf, Saad Hassan Kiani, Muhammad Rizwan Anjum, Amjad Iqbal, “Infinity Shell Shaped MIMO Antenna Array for mm-Wave 5G Applications”, Electronics 2021, *10*(2), 165.
- [28] Ajay Kumar Dwivedi, Anand Sharma, Akhilesh Kumar Pandey, Vivek Singh, “Circularly Polarized Two Port MIMO Cylindrical DRA for 5G Applications”, October 03,2020 IEEE Xplore.
- [29] Evizal Abdul Kadir, “A Reconfigurable MIMO Antenna System for Wireless Communications”, 19-21 September 2017.
- [30] Smart Antennas: Latest Trends in Design and Application, “Springer” Malik, P., Lu, J., Madhav, B.T.P., Kalkhambkar, G., Amit, S. (Eds.), ISBN 978-3-030-76636-8, DOI: 10.1007/978-3-030-76636-8

- [31] Roges, R, Malik, PK. Planar and printed antennas for Internet of Things-enabled environment: Opportunities and challenges. *Int J Commun Syst.* 2021; 34 (15): e4940. <https://doi.org/10.1002/dac.4940> (IF: 2.047) ISSN: 1099-1131, Sep 2021
- [32] Abdul Rahim, Praveen Kumar Malik, Analysis and design of fractal antenna for efficient communication network in vehicular model, *Sustainable Computing: Informatics and Systems*, Elsevier, Volume 31, 2021, 100586, ISSN 2210-5379, <https://doi.org/10.1016/j.suscom.2021.100586>
- [33] Shaik, N., Malik, P.K. A comprehensive survey 5G wireless communication systems: open issues, research challenges, channel estimation, multi carrier modulation and 5G applications. *Multimed Tools Appl* (2021). <https://doi.org/10.1007/s11042-021-11128-z>
- [34] Malik, P.K., Wadhwa, D.S. & Khinda, J.S. A Survey of Device to Device and Cooperative Communication for the Future Cellular Networks. *International Journal of Wireless Information Networks*, Springer 27, 411–432 (2020). <https://doi.org/10.1007/s10776-020-00482-8>
- [35] Tiwari, P., & Malik, P. K. (2021). Wide Band Micro-Strip Antenna Design for Higher “X” Band. *International Journal of e-Collaboration (IJeC)*, 17(4), 60-74. <http://doi.org/10.4018/IJeC.2021100105> (ISSN: 1548-3673) Oct 2021
- [36] Wadhwa, D.S., Malik, P.K. and Khinda, J.S. (2021), "High gain antenna for n260- & n261-bands and augmentation in bandwidth for mm-wave range by patch current diversions", *World Journal of Engineering*, Vol. ahead-of-print No. ahead-of-print. <https://doi.org/10.1108/WJE-03-2021-0133> (ISSN: 1708-5284)
- [37] Amandeep Kaur and Praveen Kumar Malik, "Multiband Elliptical Patch Fractal and Defected Ground Structures Microstrip Patch Antenna for Wireless Applications," *Progress In Electromagnetics Research B*, Vol. 91, 157-173, 2021. doi:10.2528/PIERB20102704 (ISSN: 1937-6472)
- [38] Raheel, Kiran, et al. "E-shaped H-slotted dual band mmWave antenna for 5G technology." *Electronics* 10.9 (2021): 1019.
- [39] Awan, Irtiza Abbas, et al. "Single Patch Fractal-Shaped Antenna with Small footprint Area and High Radiation Properties for Wide Operation Over 5G Region." 2021 46th International Conference on Infrared, Millimeter and Terahertz Waves (IRMMW-THz). IEEE, 2021.
- [40] Zahra, Hijab, et al. "A 28 GHz broadband helical inspired end-fire antenna and its MIMO configuration for 5G pattern diversity applications." *Electronics* 10.4 (2021): 405.
- [41] Ta, Son Xuat, Hosung Choo, and Ikmo Park. "Broadband printed-dipole antenna and its arrays for 5G applications." *IEEE Antennas and Wireless Propagation Letters* 16 (2017): 2183-2186.
- [42] Dwivedi, Ajay Kumar, et al. "Two port circularly polarized MIMO antenna design and investigation for 5G communication systems." *Wireless Personal Communications* 120.3 (2021): 2085-2099.
- [43] T. Itoh, and W. Menzel, "A Full-Wave Analysis Method for Open Microstrip Structure", *IEEE Transactions Antennas Propagation*, Vol. 29, pp(s): 63–68, January 1981.
- [44] Young-Bae Jung, Soon-Young Eom, and Soon-Ik Jeon, "Novel Antenna System Design for Satellite Mobile Multimedia Service", *IEEE transactions on Vehicular technology*, Vol-59, pp(s): 4237-4247, Issue-9, 2010.

- [45] Yikai Chen, Shiwen Yang, and Zaiping Nie, "Bandwidth Enhancement Method for Low Profile E-Shaped Microstrip Patch Antennas", *IEEE Transactions on Antennas and Propagation*, Vol.58, Issue- 7, pp(s):2442-2247, 2010.
- [46] Hussein Attia, Leila Yousefi, Omar Ramahi, "High-Gain Patch Antennas Loaded with High Characteristic Impedance Superstrates", *IEEE Letters on Antenna and Wireless propagation*, Vol.10, pp(s): 858-861, 2011.
- [47] Ramona Cosmina Hadarig, María Elena de Cos, Fernando Las-Heras, "On the Bandwidth Enhancement of Patch Antenna Using EBG/AMC Structures", *IEEE 6th European Conference on Antennas and Propagation (EUCAP)*, pp(s): 2853-2857, 2011.
- [48] Soumyojit Sinha, Anjumanara Begam, "Design of Probe Feed Micro-strip Patch Antenna in S-Band", *International Journal of Electronics and Communication Engineering*, Vol.5, Issue-4, pp(s): 417-423, 2012.
- [49] Y. Sung, "Bandwidth Enhancement of a Microstrip Line-Fed Printed Wide-Slot Antenna With a Parasitic Center Patch", *IEEE Transactions on Antennas and Propagation*, Vol.60, Issue-4, pp(s): 1712-1716, 2012.
- [50] S. T. Fan, Y. Z. Yin, B. Lee, W.Hu, X. Yang, "Bandwidth Enhancement of a Printed Slot Antenna With a Pair of Parasitic Patches", *IEEE letters on Antennas and Wireless Propagation*, Vol.11, pp(s): 1230-1233, 2012.
- [51] P. A. Ambresh, G. M. Pushpanjali, A. A. Sujata, P. M. Hadalgi, P. V. Hunagund, "S-Band compact microstrip antenna with slots", *National conference on Challenges in research & Technology in the coming Decades(CRT 2013)*, pp(s): 1-3, 2013.
- [52] Syeda Fizzah Jilani, Hamood-Ur-Rahman, Muhammad Naeem Iqbal, "Novel Star-shaped Fractal Design of Rectangular Patch Antenna for Improved Gain and Bandwidth", *IEEE International Symposium on Antenna and Propagation Society (APSURSI)*, pp(s): 1486-1487, 2013.
- [53] Nitin Saluja, Rajesh Khanna, "Design, analysis, and fabrication of a novel multi band folded edge compact size fractal PIFA for Wifi/LTE/Wimax/ Wlan application", *IEEE Letters on Antennas and Wireless propagation*, Vol.56, pp(s):2836-2841, 2014.
- [54] Swaraj Panusa, Mithilesh Kumar, "Quad Band H-slot Microstrip Patch Antenna for WiMAX Application", *International Journal of Computer Applications*, Vol.103, Issue -12, pp(s):14-16, 2014.
- [55] Lei Chen, Tian-Ling Zhang, Chao Wang, Xiao-Wei Shi, "Wideband Circularly Polarized Microstrip Antenna With Wide Beamwidth," *IEEE Letters on Antennas and Wireless propagation*, Vol.13, pp(s):1577-1580, 2014.
- [56] Eun-cheol Choi, JaeW. Lee, Taek-Kyung Lee, Woo-Kyung Lee, "Circularly Polarized S-Band Satellite Antenna with Parasitic Elements and Its Arrays", *IEEE Letters on Antennas and Wireless propagation*, Vol.13, pp(s):1689-1692, 2014.
- [57] N Jayarenjini, A.N Ali Fathima, S.Megha, C.Unni, "Dual Polarized Microstrip Fractal patch antenna for S-band applications", *International Conference on Control Communication & Computing India*, 2015.
- [58] Liu, X., Zhao, Z., & Wang, Y. (2022). Reconfigurable intelligent surfaces for massive MIMO: Enhancing signal quality and reducing interference. *IEEE Transactions on Wireless Communications*, 21(4), 3207-

3219.

- [59] Wang, X., Zhao, L., & Chen, P. (2023). Metamaterial-based reconfigurable antennas for tunable 5G mm-wave systems. *IEEE Transactions on Antennas and Propagation*, 71(5), 1123-1130.
- [60] Zhang, L., Li, H., & Wang, J. (2024). Dual-polarized MIMO UWB antenna with enhanced isolation for 5G applications. *IEEE Antennas and Wireless Propagation Letters*, 22(2), 435-440.
- [61] Lee, S., Park, D., & Kim, J. (2024). Reconfigurable UWB antennas using metamaterials for mm-wave 5G systems. *IEEE Transactions on Antennas and Propagation*, 72(1), 58-66.
- [62] Sanjukta Nej and Anumoy Ghosh, "Design of a Wideband mm Wave Massive MIMO Antenna for 5G Communication." Asian Conference on Innovation in Technology (ASIANCON), Pune, India. Aug 28-29, 2021.
- [63] Rakesh N. Tiwari, Prabhakar Singh, Binod Kumar Kanaujia, Sachin Kumar & Surendra Kumar Gupta, "A low profile dual band MIMO antenna for LTE/Bluetooth/Wi-Fi/WLAN applications." JOURNAL OF ELECTROMAGNETIC WAVES AND APPLICATIONS, 9 January 2020.
- [64] S. Chouhan, D. K. Panda, V. S. Kushwah, and S. Singhal, "Spider-shaped fractal MIMO antenna for WLAN/WiMAX/Wi-Fi/Bluetooth/C-band applications," *AEU - Int. J. Electron. Commun.*, vol. 110, p. 152871, 2019, doi: 10.1016/j.aeue.2019.152871.
- [65] Tathababu Addepalli and Vaddinuri R. Anitha, "Design and Parametric Analysis of Hexagonal Shaped MIMO Patch Antenna for S-Band, WLAN, UWB and X-Band Applications." *Progress In Electromagnetics Research C*, Vol. 97, 2019.
- [66] Haitham AL-Saif, Muhammad Usman, Muhammad Tajammal Chughtai, and Jamal Nasir, "Compact Ultra-Wide Band MIMO Antenna System for Lower 5G Bands." *Hindawi Wireless Communications and Mobile Computing*, Volume 2018.
- [67] Y. F. Cao, S. W. Cheung and T. I. Yuk, "A Multi-band Slot Antenna for GPS/WiMAX/WLAN Systems." *IEEE Transactions on Antennas and Propagation*, 2015.
- [68] NAVEEN JAGLAN, SAMIR DEV GUPTA, AND MOHAMMAD S. SHARAWI, "18 Element Massive MIMO/Diversity 5G Smartphones Antenna Design for Sub-6 GHz LTE Bands 42/43 Applications." *IEEE Open Journal of Antennas and Propagation*, VOLUME 2, 2021.
- [69] Surendra Loya and Habibulla Khan, "Complementary Split Ring Resonator Based Massive MIMO Antenna System for 5G Wireless Applications." *Progress In Electromagnetics Research C*, Vol. 116, 81-93, 2021.
- [70] Botao Feng, Tao Luo, Tian Zhou, Chow-Yen-Desmond Sim, "A dual-polarized antenna with low cross polarization, high gain, and isolation for the fifth-generation array/ multiple-input multiple-output communications." *Int J RF Microw Comput Aided Eng*. 2020.
- [71] Naveen Kumar and Rajesh Khanna, "A two element MIMO antenna for sub-6 GHz and mmWave 5G systems using characteristics mode analysis." *Microw Opt Technol Lett*. 2020.
- [72] Srinivasa Naik Kethavathu, Aruna Singam, Pachiyannan Muthusamy, "Compact symmetrical slot coupled linearly polarized two/four/eight element MIMO bowtie DRA for WLAN applications." *International Journal of Electronics and Communications*, 2021.

- [73] Wenfei Yin, Shaoxiang Chen, Junjie Chang, Chunhua Li and Salam K. Khamas, "CPW Fed Compact UWB 4-Element MIMO Antenna with High Isolation." MDPI Sensors 2021, 21, 2688.
- [74] Daniyal Ali Sehrai, Mujeeb Abdullah, Ahsan Altaf, Saad Hassan Kiani, Fazal Muhammad, Muhammad Tufail, Muhammad Irfan, Adam Glowacz and Saifur Rahman, "A Novel High Gain Wideband MIMO Antenna for 5G Millimeter Wave Applications." MDPI Electronics 2020, 9, 1031.
- [75] CHENYIN YU, SHUHUI YANG, YINCHAO CHEN, WENSONG WANG, LI ZHANG1, BIN LI, AND LING WANG, "A Super-Wideband and High Isolation MIMO Antenna System Using a Windmill-Shaped Decoupling Structure." IEEE ACCESS, 2020.
- [76] Yufeng Zhu, Yikai Chen and Shiwen Yang, "Decoupling and Low-Profile Design of Dual-Band Dual-Polarized Base-Station Antennas Using Frequency Selective Surface." IEEE, 2019.
- [77] NASER OJAROUDI PARCHIN, YASIR ISMAEL ABDULRAHEEM AL-YASIR, AMMAR H. ALI, ISSA ELFERGANI, JAMES M. NORAS, JONATHAN RODRIGUEZ, and RAED A. ABD-ALHAMEED, "Eight-Element Dual-Polarized MIMO Slot Antenna System for 5G Smartphone Applications." IEEE ACCESS, 2019.
- [78] BOTAO FENG1, JIEXIN LAI, QINGSHENG ZENG and KWOK L. CHUNG, "A Dual-Wideband and High Gain Magneto-Electric Dipole Antenna and Its 3D MIMO System with Metasurface for 5G/WiMAX/WLAN/X-Band Applications." IEEE. Translations, VOLUME 4, 2018, 2169-3536.
- [79] Naser Ojaroudi Parchin, Haleh Jahanbakhsh Basherlou2, Yasir I. A. Al-Yasir, Maryam Sajedin, Jonathan Rodriguez, and Raed A. Abd-Alhameed, "Multi-Mode Smartphone Antenna Array for 5G Massive MIMO Applications." IEEE Xplore, July 19, 2020.
- [80] Kiran Raheel, Ahsan Altaf, Arbab Waheed, Saad Hassan Kiani, Daniyal Ali Sehrai, Faisal Tubbal and Raad Raad, "E-Shaped H-Slotted Dual Band mmWave Antenna for 5G Technology." MDPI Electronics 2021, 10, 1019.
- [81] Mustapha El Halaoui, Laurent Canale, Adel Asselman and Georges Zisis, "Dual-Band 28/38 GHz Inverted-F Array Antenna for Fifth Generation Mobile Applications." MDPI Proceedings 2020.
- [82] Hijab Zahra, Wahaj Abbas Awan, Wael Abd Ellatif Ali, Niamat Hussain, Syed Muzahir Abbas and Subhas Mukhopadhyay, "A 28 GHz Broadband Helical Inspired End-Fire Antenna and Its MIMO Configuration for 5G Pattern Diversity Applications." MDPI Electronics 2021, 10, 405.
- [83] Mahnoor Khalid, Syeda Iffat Naqvi, Niamat Hussain, MuhibUr Rahman, Fawad, Seyed Sajad Mirjavadi, Muhammad Jamil Khan and Yasar Amin, "4-Port MIMO Antenna with Defected Ground Structure for 5G Millimeter Wave Applications." MDPI Electronics 2020, 9, 71.
- [84] Son Xuat Ta, Hosung Choo, and Ikmo Park, "Broadband Printed-Dipole Antenna and Its Arrays for 5G Applications." IEEE, 1536-1225, 2016.
- [85] Philip Ayiku Dzagbletey and Young-Bae Jung, "Stacked Microstrip Linear Array for Millimeter-Wave 5G Baseband Communication." IEEE, 1536-1225, 2018.
- [86] Bin Yu , Kang Yang, Chow-Yen-Desmond Sim , and Guangli Yang, "A Novel 28 GHz Beam Steering Array for 5G Mobile Device With Metallic Casing Application." IEEE TRANSACTIONS ON ANTENNAS

AND PROPAGATION, VOL. 66, NO. 1, JANUARY 2018.

- [87] Mian Muhammad Kamal, Shouyi Yang, Xin-cheng Ren, Ahsan Altaf, Saad Hassan Kiani, Muhammad Rizwan Anjum, Amjad Iqbal, Muhammad Asif and Sohail Imran Saeed, "Infinity Shell Shaped MIMO Antenna Array for mm-Wave 5G Applications." *MDPI Electronics* 2021, 10, 165.
- [88] Ajay Kumar Dwivedi, Anand Sharma, Akhilesh Kumar Pandey, Vivek Singh, "Two Port Circularly Polarized MIMO Antenna Design and Investigation for 5G Communication Systems." *Wireless Personal Communications (2021)* 120:2085–2099.
- [89] Evizal Abdul Kadir, "A Reconfigurable MIMO Antenna System for Wireless Communications." *Proc. EECISI 2017, Yogyakarta, Indonesia, 19-21 September 2017*.
- [90] ETSI, "Electromagnetic Compatibility and Radio Spectrum Matters (ERM); Short Range Devices; Ultra Wide Band Devices (UWB); Harmonized EN covering essential requirements under article 3.2 of the R&TTE Directive," ETSI EN 302 065, 2011.
- [91] Volakis, John, Chi-Chih Chen, and Kyohei Fujimoto. *Small antennas: miniaturization techniques & applications*. McGraw Hill Professional, 2009.
- [92] C.A.Balanis, *Antenna Theory: analysis and design* 2nd edition, John Willey & sons, Inc., 1997.
- [93] M. Ayyappan and Pragati Patel, "On Design of a Triple Elliptical Super Wideband Antenna for 5G Applications" , *IEEE Access*, Received 18 May 2022, accepted 13 June 2022, date of publication 22 June 2022, date of current version 25 July 2022. Digital Object Identifier 10.1109/ACCESS.2022.3185241
- [94] *Smart Antennas: Latest Trends in Design and Application*, "Springer" Malik, P., Lu, J., Madhav, B.T.P., Kalkhambkar, G., Amit, S. (Eds.), ISBN 978-3-030-76636-8, DOI: 10.1007/978-3-030-76636-8
- [95] Roges, R, Malik, PK. Planar and printed antennas for Internet of Things-enabled environment: Opportunities and challenges. *Int J Commun Syst.* 2021; 34 (15): e4940. <https://doi.org/10.1002/dac.4940> (IF: 2.047) ISSN: 1099-1131, Sep 2021
- [96] Abdul Rahim, Praveen Kumar Malik, *Analysis and design of fractal antenna for efficient communication network in vehicular model*, *Sustainable Computing: Informatics and Systems*, Elsevier, Volume 31, 2021, 100586, ISSN 2210-5379, <https://doi.org/10.1016/j.suscom.2021.100586>
- [97] Shaik, N., Malik, P.K. A comprehensive survey 5G wireless communication systems: open issues, research challenges, channel estimation, multi carrier modulation and 5G applications. *Multimed Tools Appl* (2021). <https://doi.org/10.1007/s11042-021-11128-z>
- [98] Malik, P.K., Wadhwa, D.S. & Khinda, J.S. A Survey of Device to Device and Cooperative Communication for the Future Cellular Networks. *International Journal of Wireless Information Networks*, Springer 27, 411–432 (2020). <https://doi.org/10.1007/s10776-020-00482-8>
- [99] Tiwari, P., & Malik, P. K. (2021). Wide Band Micro-Strip Antenna Design for Higher "X" Band. *International Journal of e-Collaboration (IJeC)*, 17(4), 60-74. <http://doi.org/10.4018/IJeC.2021100105> (ISSN: 1548-3673) Oct 2021
- [100] Amandeep Kaur and Praveen Kumar Malik, "Multiband Elliptical Patch Fractal and Defected Ground Structures Microstrip Patch Antenna for Wireless Applications," *Progress In Electromagnetics Research B*,

Vol. 91, 157-173, 2021. doi:10.2528/PIERB20102704 (ISSN: 1937-6472)

- [101] Nilofer Shaik, Praveen Kumar Malik. (2020). A Retrospection of Channel Estimation Techniques for 5G Wireless Communications: Opportunities and Challenges. *International Journal of Advanced Science and Technology*, 29(05), 8469-8479. ISSN: 2005-4238, June 2020
- [102] Praveen Kumar Malik, Madam Singh "Multiple Bandwidth Design of Micro strip Antenna for Future Wireless Communication", *International Journal of Recent Technology and Engineering*. ISSN: 2277-3878, Volume-8 Issue-2, pp 5135-5138, July 2019 DOI: 10.35940/ijrte.B2871.078219
- [103] Senger, S, Malik, PK. A comprehensive survey of massive-MIMO based on 5G antennas. *Int J RF Microw Comput Aided Eng*. 2022; 32(12):e23496. doi:10.1002/mmce.23496
- [104] P. Tamil Manoj Prasanth and G. Velmathi, "Design and development of cylindrical dielectric resonator (CDR) MIMO antenna for multiband applications," *Proc. 2016 IEEE International Conference of Wireless Communication Signal Processing Networking, WiSPNET 2016*, pp. 670–673, 2016, doi: 10.1109/WiSPNET.2016.7566217.
- [105] Kumar, J. P., & Karunakar, G., "Ultra Wideband MIMO Notched Antenna for WLAN and Mobile Applications", *International Journal of Pure and Applied Mathematics*, 2018. 118(9), 929-934.
- [106] Y. F. Cao, S. W. Cheung and T. I. Yuk, "A Multiband Slot Antenna for GPS/WiMAX/WLAN Systems", *IEEE Transactions on Antennas and Propagation*, vol. 63, no. 3, pp. 952-958, March 2015.
- [107] Tewary, T., Maity, S., Mukherjee, S., Roy, A., Sarkar, P.P., Bhunia, S.: Design of high gain broadband microstrip patch antenna for UWB/X/Ku band applications. *AEU Int. J. Electron. Commun.* 139, 1–13 (2021).
- [108] Darwin, R., and P. Sampath. "Sub-6 GHz band massive MIMO antenna system for variable deployment scenarios in 5G base stations." *Microsystem Technologies* 28.9 (2022): 2047-2059.
- [109] Abdullah, Mujeeb, et al. "Future smartphone: MIMO antenna system for 5G mobile terminals." *IEEE Access* 9 (2021): 91593-91603.
- [110] Tiwari, Rakesh N., et al. "A low profile dual band MIMO antenna for LTE/Bluetooth/Wi-Fi/WLAN applications." *Journal of Electromagnetic Waves and Applications* 34.9 (2020): 1239-1253.
- [111] Ahmad, Aqsa, and Farooq A. Tahir. "Multiband Reconfigurable MIMO Antenna for GSM/GPS/GLONASS/LTE/WWAN Wireless Terminals." *2020 International Conference on UK-China Emerging Technologies (UCET)*. IEEE, 2020.
- [112] Sharma, Manish, et al. "An ultra-compact four-port 4×4 superwideband MIMO antenna including mitigation of dual notched bands characteristics designed for wireless network applications." *AEU-International Journal of Electronics and Communications* 123 (2020): 153332.
- [113] Kumar, Naveen, and Rajesh Khanna. "A two element MIMO antenna for sub-6 GHz and mmWave 5G systems using characteristics mode analysis." *Microwave and Optical Technology Letters* 63.2 (2021): 587-595.
- [114] Zhao, Anping, and Zhouyou Ren. "Size reduction of self-isolated MIMO antenna system for 5G mobile phone applications." *IEEE Antennas and Wireless Propagation Letters* 18.1 (2018): 152-156.

- [115] Zhu, Yufeng, Yikai Chen, and Shiwen Yang. "Decoupling and low-profile design of dual-band dual-polarized base station antennas using frequency-selective surface." *IEEE Transactions on Antennas and Propagation* 67.8 (2019): 5272-5281.
- [116] Yu, Chenyin, et al. "A super-wideband and high isolation MIMO antenna system using a windmill-shaped decoupling structure." *IEEE Access* 8 (2020): 115767-115777.
- [117] Fatah, Sara Yehia Abdel, et al. "Design of compact 4-port MIMO antenna based on Minkowski fractal shape DGS for 5G applications." *PIER C* 113 (2021): 123-136.
- [118] Ali, Wael AE, and Ahmed A. Ibrahim. "A compact double-sided MIMO antenna with an improved isolation for UWB applications." *AEU-International Journal of Electronics and Communications* 82 (2017): 7-13.
- [119] S.F. Jilani, A. Alomainy, "Millimetre-wave t-shaped mimo antenna with defected ground structures for 5g cellular networks". *IET Microw Antennas Propag* 12(5), 672–677 (2018). <https://doi.org/10.1049/iet-map.2017.0467>
- [120] Bilal, Muhammad, et al. "High-Isolation MIMO antenna for 5G millimeter-wave communication systems." *Electronics* 11.6 (2022): 962.
- [121] Hussain, Musa, et al. "Isolation Improvement of Parasitic Element-Loaded Dual-Band MIMO Antenna for Mm-Wave Applications." *Micromachines* 13.11 (2022): 1918.
- [122] Abbas, Mohamed Atef, et al. "Compact UWB MIMO Antenna for 5G Millimeter-Wave Applications." *Sensors* 23.5 (2023): 2702.
- [123] Sehrai, Daniyal Ali, et al. "A novel high gain wideband MIMO antenna for 5G millimeter wave applications." *Electronics* 9.6 (2020): 1031.
- [124] Khalid, Mahnoor, et al. "4-Port MIMO antenna with defected ground structure for 5G millimeter wave applications." *Electronics* 9.1 (2020): 71.
- [125] Hussain, Musa, et al. "Design and characterization of compact broadband antenna and its MIMO configuration for 28 GHz 5G applications." *Electronics* 11.4 (2022): 523.
- [126] Marzouk, Hala M., Mohamed Ismail Ahmed, and Abdel Hamied Abdel Shaalan. "Novel dual-band 28/38 GHz MIMO antennas for 5G mobile applications." *Progress In Electromagnetics Research C* 93 (2019): 103-117.
- [127] Muttair, Karrar Shakir, et al. "A new design of mm-Wave MIMO antenna with high isolation for 5G applications." *International Journal of Microwave and Optical Technology* 16.4 (2021): 370-379.
- [128] Hussain, Sayed Aqib, et al. "Wideband, High-Gain, and Compact Four-Port MIMO Antenna for Future 5G Devices Operating over Ka-Band Spectrum." *Applied Sciences* 13.7 (2023): 4380.
- [129] Alnemr, Fadwa, Mai Foua'ad Ahmed, and Abdulhamed Abdulmonem Shaalan. "A compact 28/38 GHz MIMO circularly polarized antenna for 5 G applications." *Journal of Infrared, Millimeter, and Terahertz Waves* 42 (2021): 338-355.
- [130] Chang, Rui, et al. "CPW Compact Ultra-Wideband MIMO Antenna for 5G Millimeter Wave Applications." (2022).
- [131] Munir, Mehr E., et al. "A Four Element mm-Wave MIMO Antenna System with Wide-Band and High

- Isolation Characteristics for 5G Applications." Micromachines* 14.4 (2023): 776.
- [132] Sehrai, D.A.; Asif, M.; Shoaib, N.; Ibrar, M.; Jan S.; Alibakhshikenari, M.; Lalbakhsh, A.; Limiti, E., "Compact quad-element high-isolation wideband MIMO antenna for mm-wave applications." *Electronics* 2021, 10, 1300.
- [133] Roh, W.; Seol, J.Y.; Park, J.; Lee, B.; Lee, J.; Kim, Y.; Cho, J.; Cheun, K.; Aryanfar, F. Millimeter-wave beamforming as an enabling technology for 5G cellular communications: Theoretical feasibility and prototype results. *IEEE Commun. Mag.* 2014, 52, 106–113.
- [134] Khalily, M.; Tafazolli, R.; Xiao, P.; Kishk, A.A. Broadband mm-Wave microstrip array antenna with improved radiation characteristics for different 5G applications. *IEEE Trans. Antennas Propag.* 2018, 66, 4641–4647
- [135] Winters, J., On the capacity of radio communication systems with diversity in a Rayleigh fading environment, *IEEE Journal on Selected Areas in Communications*, Vol. 5, No. 5, 871-878, Jun. 1987.
- [136] Foschini, G. J. and M. J. Gans, On limits of wireless communications in a fading environment when using multiple antennas, *Wireless Personal Communication*, Vol. 6, No. 3, 311-335, Mar. 1998
- [137] Sharma Y, Sarkar D, Saurav K and Srivastava KV (2016) Three element MIMO antenna system with pattern and polarization diversity for WLAN application. *IEEE Antennas and Wireless Propagation Letters* 16, 1163–1166.
- [138] Goldsmith A, Jafar SA, Jindal N and Vishwanath S (2003) Capacity limits of MIMO channels. *IEEE Journal on Selected Areas in Communications* 21, 684–702.
- [139] Khan MS, Shafique MF, Naqvi A, Capobianco AD, Ijaz B and Braaten BD (2015) A miniaturized dual band MIMO antenna for WLAN applications. *IEEE Antennas and Wireless Propagation Letters* 14, 958–961.
- [140] Mark, Robert, et al. "Metamaterial based superstrate towards the isolation and gain enhancement of MIMO antenna for WLAN application." *AEU-International Journal of Electronics and Communications* 100 (2019): 144-152.
- [141] Ibrahim,A.A.; Ali,W.A.E.; Alathbah,M.; Sabek,A.R. "Four-Port 38 GHz MIMO Antenna with High Gain and Isolation for 5G Wireless Networks". *Sensors-2023*,23,3557. <https://doi.org/10.3390/s23073557>.
- [142] Khalid M, Iffat Naqvi S, Hussain N, Rahman M, Fawad, Mirjavadi SS, Khan MJ, Amin Y. 4-Port MIMO Antenna with Defected Ground Structure for 5G Millimeter Wave Applications. *Electronics*. 2020; 9(1):71. <https://doi.org/10.3390/electronics9010071>
- [143] Yoon, N.; Seo, C., "A 28-GHz Wideband 2×2 U Slot Patch Array Antenna." *J. Electro magn. Eng. Sci.* 2017, 17, 133–137.
- [144] Chang, Rui, et al. "*CPW Compact Ultra-Wideband MIMO Antenna for 5G Millimeter Wave Applications.*" (2022).
- [145] Munir, Mehr E., et al. "*A Four Element mm-Wave MIMO Antenna System with Wide-Band and High Isolation Characteristics for 5G Applications.*" *Micromachines* 14.4 (2023): 776.
- [146] Ali, Wael AE, and Ahmed A. Ibrahim. "A compact double-sided MIMO antenna with an improved isolation for UWB applications." *AEU-International Journal of Electronics and Communications* 82 (2017): 7-13.

- [147] Amin, F.; Saleem, R.; Shabbir, T.; Rehman, S.u.; Bilal, M.; Shafique, M.F. A Compact Quad-Element UWB-MIMO Antenna System with Parasitic Decoupling Mechanism. *Appl. Sci.* 2019, 9, 2371. <https://doi.org/10.3390/app9112371>.
- [148] Rajkumar, S., A. Anto Amala, and Krishnasamy T. Selvan. "Isolation improvement of UWB MIMO antenna utilising molecule fractal structure." *Electronics Letters* 55.10 (2019): 576-579.
- [149] Khan, Aqeel Ahmed, et al. "Quad port miniaturized MIMO antenna for UWB 11 GHz and 13 GHz frequency bands." *AEU-International Journal of Electronics and Communications* 131 (2021): 153618.
- [150] Raheja, D.K.; Kanaujia, B.K.; Kumar, S. Compact four-port MIMO antenna on slottededge substrate with dual-band rejection characteristics. *Int. J. RF Microw. Comput.-Aided Eng.* 2019, 29, e21756.
- [151] Singh, Dharmendra, et al. "Inverted-c ground MIMO antenna for compact UWB applications." *Journal of Electromagnetic Waves and Applications* 35.15 (2021): 2078-2091.
- [152] Suresh, Ankireddy C., and Thatiparthi Sreenivasulu Reddy. "A flower shaped miniaturized 4× 4 MIMO antenna for UWB applications using characteristic mode analysis." *Prog. Electromagn. Res. C* 119 (2022): 219-233.
- [153] Suresh, Ankireddy Chandra, et al. "Investigations on Stub-Based UWB-MIMO Antennas to Enhance Isolation Using Characteristic Mode Analysis." *Micromachines* 13.12 (2022): 2088.
- [154] Suresh, Ankireddy Chandra, Thatiparthi Reddy, and SV SVUCE. "Experimental Investigation of Novel Frock-Shaped Miniaturized 4× 4 UWB MIMO Antenna Using Characteristic Mode Analysis." *Progress In Electromagnetics Research B* 101 (2023): 45-61.